

Dissertation
submitted to the
Combined Faculties for the Natural Sciences and for Mathematics
of the Ruperto-Carola University of Heidelberg, Germany

For the degree of
Doctor of Natural Sciences

Presented by
M.Phil - Rashda Abbasi
Born in Karachi, Pakistan

Oral-examination:.....

Nucleotide excision repair pathway modulating both cancer risk and therapy

Referees:

Prof. Dr. Thomas Efferth

PD Dr. Rajiv Kumar

Division: Epigenomics and Cancer Risk Factors

Head of the division: Prof. Dr. Christoph Plass

Deutsches Krebsforschungszentrum (DKFZ) in the Helmholtz

Association

Heidelberg

DECLARATION

This thesis is a presentation of my original research work and that it has not been submitted anywhere for any award. Wherever contributions of others are involved, every effort is made to indicate this clearly, with due reference to the literature.

Heidelberg, 1st December, 2009

Rashda Abbasi

بِسْمِ اللَّهِ الرَّحْمَنِ الرَّحِيمِ

In The Name Of Allah, The Most Beneficent, The Most Merciful

Summary

Nucleotide excision repair (NER) plays a key role in repairing a wide variety of DNA damage including bulky DNA adducts caused by ultraviolet radiation and exposure to harmful substances like tobacco smoke and alcohol. Genetic variations and somatic mutations in NER genes might affect cancer risk and therapy. However, both these aspects are not well understood.

The first part of the thesis deals with the role of NER in modulation of laryngeal cancer risk. The major risk factors for laryngeal cancer are smoking and high alcohol consumption. Polymorphisms in NER genes might therefore affect laryngeal cancer susceptibility. In a population-based case-control study including 248 cases and 647 controls, the association of laryngeal cancer with 11 single nucleotide polymorphisms (SNPs) in 7 NER genes (*XPC*, *ERCC1*, *ERCC2*, *ERCC4*, *ERCC5*, *ERCC6* and *RAD23B*) was analyzed with respect to smoking and alcohol exposure. For genotyping, sequence specific hybridization probes were used. Data were evaluated by conditional logistic regression analysis, stratified for age and gender, and adjusted for smoking, alcohol consumption and education. Pro-carriers of *ERCC6* Arg1230Pro showed a decreased risk for laryngeal cancer (OR=0.53, 95% CI 0.34-0.85), being most protective in heavy smokers and high alcohol consumers. *ERCC5* Asp1104His was associated with risk in heavy smokers (OR=1.70, 95% CI 1.1-2.5). Val-carriers of *RAD23B* Ala249Val had an increased cancer risk in heavy smokers (OR=1.6, 95% CI 1.1-2.5) and high alcohol consumers (OR=2.0, 95% CI 1.1-3.4). The combined effect of smoking and alcohol intake affected risk, at high exposure level, for *ERCC6* 1230Pro carriers (OR=0.47, 95% CI 0.22-0.98) and *RAD23B* 249Val carriers (OR=2.6, 95% CI 1.3-4.9). When tested for gene-gene interaction, presence of 3 risk alleles in the *XPC RAD23B* complex increased the risk 2.1 fold. SNPs in the other genes did not show a significant association with laryngeal cancer risk. We conclude that common genetic variations in NER genes can significantly modify laryngeal cancer risk.

The second part of the thesis deals with the question how NER affects cancer therapy. NER genes become deficient in many cancer types. By employing methods to target these deficiencies, tumor cells can be killed more effectively. Two NER deficient cell lines i.e., XP3BE (*XPC* deficient cells) and GM10902 (*ERCC6* deficient cells) and a normal cell line GM01310 were exposed to 72 traditional Chinese medicine (TCM) drugs. Cytotoxicity screening revealed that 13 of the drugs killed NER deficient cells more efficiently compared to normal cells. Depending on the effect and available amount, 6 drugs were selected for further analysis and their IC_{50} values, effects on cell cycle distribution and DNA damage induction were measured. Ascaridol was found to be the most effective compound with a difference of more than 1000 fold in resistance between normal and NER deficient cells (IC_{50} for GM10902 0.025 $\mu\text{g/ml}$, XP3BE 0.03 $\mu\text{g/ml}$ and GM01310 > 30 $\mu\text{g/ml}$). The drug had a strong and differential effect on cell cycle distribution of the three cell lines. Ascaridol produced around three times more DNA damage in NER deficient cells compared to normal cells. Results obtained for ascaridol were validated in a second set of cell lines having isogenic background. *XPC* deficient (XP4PA; IC_{50} 0.013 $\mu\text{g/ml}$) and *ERCC6* silenced (IC_{50} 0.095 $\mu\text{g/ml}$) cells were more sensitive to the drug than *XPC* proficient (XP4PA-SE2; IC_{50} 2.19 $\mu\text{g/ml}$) and Luciferase siRNA treated (IC_{50} 3.0 $\mu\text{g/ml}$) cells. Following ascaridol exposure, *XPC* deficient and *ERCC6* silenced cells gathered around 1.5 to 3 times more DNA damage than repair competent cells. Ascaridol was also characterized for its ability to generate oxidative DNA damage. A dose-dependent increase in intracellular peroxide levels was observed in ascaridol treated cells. Ascaridol (1 $\mu\text{g/ml}$) treated *XPC* deficient (Fpg sensitive lesions 13.78 ± 1.72) and *ERCC6* silenced (Fpg sensitive lesions 19.33 ± 1.2) cells also had a strong increase in the amount of oxidized bases (8-oxodG sites). Both *XPC* proficient and Luciferase siRNA cells did not show such an increase. Thus we showed, for the first time that ascaridol is mediating DNA damage by reactive oxidative intermediates. We identified that ascaridol is specifically affecting NER deficient cells and this might provide a new therapeutic option for differentially killing tumor and normal cells.





Zusammenfassung

Nukleotid Exzisions Reparatur (NER) spielt eine wichtige Rolle bei der Reparatur vieler verschiedener Arten von DNA-Schäden, dazu gehören auch DNA-Addukte, die durch ultraviolette Strahlung und durch Exposition gegenüber schädlichen Substanzen wie Tabakrauch und Alkohol entstehen. Genetische Variationen und somatische Mutationen in NER-Genen können möglicherweise Auswirkungen auf Krebsrisiko und Therapie haben. Der Kenntnisstand hierüber ist jedoch gering.

Der erste Teil der Arbeit untersucht die Rolle von genetischer Variation in NER-Genen bei der Modulation des Kehlkopfkrebs-Risikos. Die wichtigsten Risikofaktoren für Kehlkopfkrebs sind Rauchen und hoher Alkoholkonsum. Polymorphismen in NER-Genen könnten sich daher auf die Anfälligkeit für Kehlkopfkrebs auswirken. In einer populationsbezogenen Fall-Kontroll-Studie mit 248 Fällen und 647 Kontrollen wurden die Assoziationen von Kehlkopfkrebs mit 11 Einzel-Nukleotid-Polymorphismen (SNPs) in 7 NER-Genen (*XPC*, *ERCC1*, *ERCC2*, *ERCC4*, *ERCC5*, *ERCC6* und *RAD23B*) unter Berücksichtigung von Rauchen und Alkoholkonsum analysiert. Für die Genotypisierung wurden Sequenz-spezifische Hybridisierungssonden verwendet. Die für Alter und Geschlecht, sowie Rauchen, Alkoholkonsum und Bildung adjustierten Daten wurden mittels logistischer Regressionsanalyse ausgewertet. Träger der Pro-Allele in *ERCC6* Arg1230Pro zeigten ein vermindertes Risiko für Kehlkopfkrebs (OR=0,53, 95% KI 0,34 - 0,85), welches bei starken Rauchern und Pro-Allel-Trägern mit hohem Alkoholkonsum am stärksten reduziert war. *ERCC5* Asp1104His war mit dem Risiko bei starken Rauchern assoziiert (OR=1,70, 95% KI 1,1 - 2,5). Val-Allel-Träger von *RAD23B* Ala249Val hatten ein erhöhtes Krebsrisiko, wenn sie starke Raucher waren (OR=1,6, 95% KI 1,1 - 2,5) oder viel Alkohol konsumierten (OR=2,0, 95% KI 1,1 - 3,4). Die kombinierte Wirkung von Rauchen und Alkoholkonsum beeinflusste das Risiko bei starker Exposition und zwar für *ERCC6* 1230Pro (OR = 0,47, 95% KI 0,22 - 0,98) und *RAD23B* 249Val (OR=2,6, 95% KI 1,3 - 4,9). Bei der Untersuchung von Gen-Gen-Interaktionen erhöhte die Anwesenheit von 3 Risikoallelen im *XPC-RAD23B*-

komplex das Risiko um das 2,1-fache. SNPs in den anderen Genen zeigten keine signifikante Assoziation mit dem Risiko für Kehlkopfkrebs. Wir schließen daraus, dass häufige genetische Variationen in NER-Genen das Kehlkopfkrebs-Risiko erheblich beeinflussen können.

Der zweite Teil der Arbeit hat die Frage zum Thema, wie sich NER-Defizite auf den Erfolg einer Krebstherapie auswirken. NER Gene sind in vielen Krebszellen mutiert. Der Einsatz von Substanzen, die diese Zellen gezielt angreifen, könnte die Therapiewirkung bei gleichzeitiger Schonung des Reparatur-kompetenten Normalgewebes verstärken. Zwei NER-defiziente Zelllinien, XP3BE (*XPC*-defiziente Zellen) und GM10902 (*ERCC6*-defiziente Zellen) sowie eine normale Zelllinie GM01310 wurden mit 72 Substanzen aus der traditionellen chinesischen Medizin (TCM) behandelt. Ein Screening ergab, dass 13 dieser Substanzen in NER-defizienten Zellen deutlich zytotoxischer wirken als in normalen Zellen. Abhängig von ihrer Wirkung sowie der verfügbaren Menge wurden 6 dieser Substanzen zur weiteren Analyse ausgewählt, um ihre IC_{50} Werte, Auswirkungen auf den Zellzyklus und ihre Fähigkeit zur Induktion von DNA-Schäden zu bestimmen. Die wirksamste Substanz war Ascaridol, mit einer über 1000-fach höheren Resistenz von normalen gegenüber NER-defizienten Zellen (IC_{50} für GM10902 0,025 $\mu\text{g} / \text{ml}$, XP3BE 0,03 $\mu\text{g} / \text{ml}$ und GM01310 > 30 $\mu\text{g} / \text{ml}$). Diese Substanz hatte starke und unterschiedliche Auswirkungen auf die Zellzyklus Verteilung der drei Zelllinien. Ascaridol verursachte etwa drei mal mehr DNA-Schäden in NER-defizienten Zellen im Vergleich zu normalen Zellen. Die Ergebnisse für Ascaridol wurden in einem zweiten Set von isogenen Zelllinien validiert. *XPC*-defiziente (XP4PA; IC_{50} 0,013 $\mu\text{g} / \text{ml}$) und mit *ERCC6*-siRNA-behandelte Zellen (IC_{50} 0,095 $\mu\text{g} / \text{ml}$) waren empfindlicher gegenüber diesem Wirkstoff als *XPC*-kompetente (XP4PA-SE2; IC_{50} 2,19 $\mu\text{g} / \text{ml}$) und Luciferase-siRNA-behandelte Kontroll-Zellen (IC_{50} 3,0 $\mu\text{g} / \text{ml}$). Nach Ascaridolexposition zeigten *XPC*-defiziente und *ERCC6*-siRNA-behandelte Zellen 1,5 bis drei mal mehr DNA-Schäden als Reparatur-kompetente Zellen. Außerdem wurde eine dosisabhängige Erhöhung der intrazellulären Peroxidmenge durch Ascaridol in den Zellen beobachtet. Mit Ascaridol (1 $\mu\text{g} / \text{ml}$) behandelte *XPC*-

defiziente und *ERCC6*-siRNA-behandelte Zellen zeigten auch einen starken Anstieg in der Menge der oxidierten Basen, der weder in *XPC*-kompetenten noch in Luciferase-siRNA-behandelten Kontroll-Zellen sichtbar war. Diese Ergebnisse zeigen zum ersten Mal, dass Ascaridol DNA-Schäden über reaktive oxidative Zwischenprodukte verursacht, und dass Ascaridol besonders NER-defiziente Zellen angreift. Dies könnte eine neue therapeutische Option für das selektive Abtöten von Tumorzellen darstellen.



Table of Contents

Summary	XI
Zusammenfassung	XV
Abbreviations	XXV
1. Introduction	1
1. 1. Nucleotide excision repair (NER)	1
1. 1. 1. Molecular mechanisms of NER	1
1. 1. 2. Syndromes caused by defects in NER	4
1. 2. NER and cancer risk	6
1. 2. 1. Laryngeal cancer	9
1. 2. 1. 1. Larynx	9
1. 2. 1. 2. Facts about larynx cancer	10
1. 2. 1. 3. Larynx cancer risk factors	10
1. 2. 2. NER and larynx cancer risks	11
1. 2. 3. The Rhein-Necker study	12
1. 3. NER and cancer therapy	13
1. 3. 1. Targeted Cancer therapy	13
1. 3. 2. NER deficiencies in tumors	15
1. 3. 3. Traditional Chinese medicine (中医, 中醫)	17
1. 3. 3. 1. Importance of TCM	17
1. 3. 3. 2. TCM drugs as cancer therapeutics	18
1. 3. 4. Our investigations on TCM drugs	19
1. 4. Aim of the present thesis	19
2. Materials and Methods	23
2. 1. Materials	23
2. 1. 1. Equipment	23
2. 1. 2. Chemicals	26
2. 1. 3. Primers	29
2. 1. 4. LC TM Hybridization probes	31
2. 1. 5. Restriction enzymes	32
2. 1. 6. Cell lines	33
2. 1. 7. Traditional Chinese medicine compounds	33

Table of contents

2. 1. 8. Computer Softwares and Databases	34
2. 2. Methods	35
2. 2. 1. NER and cancer risk	35
2. 2. 1. 1. Study population	35
2. 2. 1. 2. DNA extraction	37
2. 2. 1. 3. Genotyping analysis	37
2. 2. 1. 3. 1. Single nucleotide polymorphisms (SNPs)	37
2. 2. 1. 3. 2. Optimization of PCR conditions	37
2. 2. 1. 3. 3. Optimization of real time PCR	39
2. 2. 1. 3. 4. Validation of optimized conditions	41
2. 2. 1. 3. 5. Genotyping by Fluorescence-based Real time PCR	41
2. 2. 1. 3. 6. Color compensation	44
2. 2. 1. 3. 7. Validation of genotyping data	45
2. 2. 2. NER and cancer therapy	46
2. 2. 2. 1. Cell culture	46
2. 2. 2. 1. 1. Culture conditions	46
2. 2. 2. 1. 2. Contamination check	46
2. 2. 2. 1. 3. Freezing	47
2. 2. 2. 1. 4. Thawing	47
2. 2. 2. 1. 5. Doubling time	47
2. 2. 2. 2. Mutation confirmation	48
2. 2. 2. 2. 1. XP3BE	48
2. 2. 2. 2. 2. GM10902	49
2. 2. 2. 2. 3. XP4PA and XP4PA-SE2	49
2. 2. 2. 3. Knockdown experiments	49
2. 2. 2. 3. 1. Optimization of conditions for transfection	49
2. 2. 2. 3. 2. General protocol for ERCC6 gene silencing	50
2. 2. 2. 4. UV sensitivity	52
2. 2. 2. 5. Live / Dead assay	52
2. 2. 2. 5. 1. Optimization of dye concentration	54
2. 2. 2. 5. 2. Calibration of the assay	54
2. 2. 2. 6. Screening of the traditional Chinese medicine (TCM) compounds	54
2. 2. 2. 6. 1. Determination of a suitable time for drug exposure – an experiment with arsenic trioxide	54
2. 2. 2. 6. 2. Cytotoxicity screening of the TCM drugs	55
2. 2. 2. 7. IC ₅₀ values	55

2. 2. 2. 8. Cell cycle analysis by flow cytometry	56
2. 2. 2. 8. 1. Determination of a suitable time for drug exposure – an experiment with arsenic trioxide	57
2. 2. 2. 8. 2. Effect of TCM drugs on cell cycle distribution	57
2. 2. 2. 9. Single cell gel electrophoresis (Alkaline Comet assay)	58
2. 2. 2. 10. Formamidopyrimidine DNA glycosylase (Fpg)-modified comet assay	59
2. 2. 2. 11. Reactive oxygen species (ROS) production	61
2. 2. 2. 12. Aldehyde reactive probe (ARP) assay	61
2. 2. 2. 13. Determination of gene expression	62
2. 2. 2. 13. 1. RNA extraction and quantification	62
2. 2. 2. 13. 2. Reverse Transcription and cDNA amplification (RT-PCR)	63
2. 2. 2. 13. 3. RNA/cDNA Quality check assay	64
2. 2. 2. 13. 4. Relative quantification of ERCC6 and GAPDH by real time PCR	65
2. 2. 2. 14. Protein extraction	68
2. 2. 2. 14. 1. Quantification of protein samples	68
2. 2. 2. 14. 2. Sodium dodecyl sulfate polyacrylamide gel electrophoresis (SDS-PAGE)	68
2. 2. 2. 14. 3. Western blotting	69
2. 2. 2. 14. 4. Stripping antibodies off the PVDF membranes	70
2. 2. 2. 15. Statistical analysis	71
2. 2. 2. 15. 1. Genotype frequencies	71
2. 2. 2. 15. 2. Hardy-Weinberg equilibrium	71
2. 2. 2. 15. 3. Logistic regression analysis	72
2. 2. 2. 15. 4. Gene-environment interaction	72
2. 2. 2. 15. 5. Linkage disequilibrium	73
2. 2. 2. 15. 6. Haplotype analysis	73
2. 2. 2. 15. 7. Gene-gene interaction	73
2. 2. 2. 15. 8. NER and cancer therapy	73
3. Results, NER and cancer risk	75
3. 1. Quality control of genotyping data	75
3. 1. 1. Optimization of conditions for genotyping	75
3. 1. 2. Genotyping by fluorescence-based real time PCR	76
3. 1. 2. 1. Multiplex Hybprobe assay	76
3. 1. 3. Color compensation	77
3. 1. 4. Validation of genotyping data	77
3. 1. 4. 1. Restriction fragment length polymorphism (RFLP)	77
3. 1. 4. 2. Sequencing	77

3. 2. Genotype analysis	80
3. 2. 1. Genotype frequency	80
3. 2. 2. Genotype distribution	81
3. 2. 3. Larynx cancer risk	82
3. 2. 3. 1. Overall effect of genotype	82
3. 2. 3. 2. Gene-environment interactions	86
3. 2. 3. 2. 1. Effect of smoking and genotype on larynx cancer risk	86
3. 2. 3. 2. 2. Effect of alcohol intake and genotype on larynx cancer risk	89
3. 2. 3. 2. 3. Combined effect of smoking and alcohol intake and genotype on larynx cancer risk	91
3. 2. 3. 3. Gene-Gene interactions	93
3. 2. 3. 4. Linkage analysis	93
3. 2. 3. 5. Haplotype analysis	93
4. Results, NER and cancer therapy	95
4. 1. Cell models	95
4. 1. 1. Mutation confirmation	96
4. 1. 2. P53 status of the cell lines	98
4. 1. 3. Sensitivity to UV exposure	98
4. 2. Silencing of ERCC6 gene in XP4PA-SE2 cells	100
4. 2. 1. Optimized conditions for transfection	100
4. 2. 2. ERCC6 knockdown	102
4. 2. 3. Gene expression at mRNA level	102
4. 2. 4. Gene expression at protein level	102
4. 3. Viability / Cytotoxicity assay	105
4. 3. 1. Calibration of the assay	106
4. 4. Screening of TCM drugs for their differential cytotoxic effect on NER deficient cell lines	106
4. 4. 1. Determination of a suitable time for drug exposure – an experiment with arsenic trioxide	107
4. 4. 2. Screening of TCM drugs	108
4. 5. Analysis of the selected drugs	111
4. 5. 1. Determination of IC ₅₀ values	112
4. 5. 2. Cell cycle analysis	114

4. 5. 2. 1. Determination of a suitable time for observation of TCM effects on cell cycle distribution – an experiment with arsenic trioxide	114
4. 5. 2. 2. Effect of the selected TCM drugs on cell cycle progression	115
4. 5. 2. 2. 1. Ascaridol	116
4. 5. 2. 2. 2. Arsenic trioxide	116
4. 5. 2. 2. 3. Other drugs	117
4. 5. 3. Single cell gel electrophoresis	122
4. 5. 3. 1. Ascaridol	122
4. 5. 3. 2. Arsenic trioxide	123
4. 5. 3. 3. TCM-25-RAB	124
4. 5. 3. 4. Quercetin, Scopoletin and isonardosinon	126
4. 5. 4. Quantification of AP sites (Arp assay)	126
4. 6. Validation of results obtained for ascaridol	128
4. 6. 1. Determination of IC ₅₀ values	128
4. 6. 1. 1. Effect of ascaridol on paired XPC cell lines	129
4. 6. 1. 2. Effect of ascaridol on ERCC6 silenced cells	130
4. 6. 2. Single cell gel electrophoresis	131
4. 6. 2. 1. Genotoxic effects of Ascaridol on paired XPC cell lines	131
4. 6. 2. 2. Genotoxic effects of Ascaridol on ERCC6 silenced cells	132
4. 7. Mode of action of Ascaridol	133
4. 7. 1. 2',7'-dichlorofluorescein diacetate (H ₂ DCFDA) assay	133
4. 7. 2. Quantification of 8-oxodG sites by Fpg-modified comet assay	136
4. 7. 2. 1. Effect of ascaridol on XPC deficient and proficient cell line	136
4. 7. 2. 2. Effect of ascaridol on ERCC6 silenced and Luciferase siRNA exposed (repair competent control) cells	136
5. Discussion, NER and cancer Risk	139
5. 1. Genotype analysis	139
5. 2. ERCC6	139
5. 3. ERCC5	140
5. 4. Exogenic risk factors for larynx cancer and NER genotypes	140
5. 5. Limitations of our study	142
5. 6. Conclusion	143

6. Discussion, NER and cancer therapy	145
6. 1. Cell models	145
6. 2. Ascaridol	146
6. 3. Arsenic trioxide	148
6. 4. Other TCM drugs	149
6. 5. Validation of results	150
6. 6. Mode of action of ascaridol	150
6. 7. Role of NER proteins in the repair of oxidative damage	151
6. 8. Other possible mechanisms	152
6. 8. 1. Formation of DNA adducts	152
6. 8. 2. Synthetic lethal interactions	152
6. 9. Limitations of the study	153
6. 10. Conclusion	153
7. Reference List	155
8. Appendix	177
8.1. Genotypes of the larynx cancer case-control study participants	177
8. 2. Traditional Chinese medicine compounds	199
Acknowledgements	209
Curriculum Vitae	211
Publications from thesis	215

Abbreviations

8-oxoA	8-oxo-7,8-dihydroxyadenosine
8-oxodG	8-oxo-7,8-dihydro-2'-deoxyguanosine
95% CI	95% confidence intervals
<i>ADH1B</i> and <i>ADH1C</i>	Alcohol dehydrogenase 1B and 1C
AFU	Arbitrary fluorescence units
AP sites	Apurinic / apyrimidinic site
BER	Base excision repair
<i>BRCA1/2</i>	Breast cancer gene 1/2
BSA	Bovine serum albumin
Cal AM	Calcein AM
CC Object	Color compensation object
CDKs	Cyclin-dependent kinases
Cp values	Crossing point
CS	Cockayne syndrome
DCF	dichlorofluorescein
DCFH	2', 7'-dichlorofluorescein
DF4	DharmaFECT-4
DKFZ	Deutsches Krebsforschungszentrum
DME	Dulbecco's modified Eagle's medium
DMSO	Dimethylsulfoxid
EDTA	Ethylenediaminetetraacetic acid
EDTA-Na ₂	Ethylendiamintetraessigsäure-Dinatriumsalz-solution
EH	Estimating Haplotypes
ELISA	Enzyme immunosorbant assay
<i>ERCC1 to 8</i>	Excision repair cross complementing gene 1 to 8
Eth HD	Ethidium homodimer
EtOH	Ethanol
Ex	Exon
Exp	Expected
FACs	Fluorescence activated cell sorter
FCS	Fetal Calf Serum

Abbreviations

FL	Fluorescein
FL2	Fluorescence 2
Fpg	Formamidopyrimidine-DNA Glycosylase
FRET	Fluorescence resonance energy transfer
FSC	Forward Scatter
<i>GAPDH</i>	Glyceraldehyde-3-phosphate dehydrogenase
GGR	Global genome repair
GLM	Generalized linear model
GSTM1	Glutathione S-transferase mu-1
GSTT1	Glutathione S-transferase Theta-1
H ₂ DCFDA	2',7'-dichlorodihydrofluorescein diacetate
<i>HPRT</i>	Hypoxanthine Phosphoribosyltransferase
HRP	Horseradish peroxidase
Husar	Heidelberg Unix Sequence Analysis Resources
IC ₅₀	Inhibition Concentration 50
LC-480	Light cycler 480
LC-Red610 to Red670	light cycler Red610 to Red670
LOH	Loss of heterozygosity
N	Number
NCBI	National Center for Biotechnology Information .
NER	Nucleotide excision repair
NTC	Non transfected cells
Obs	Observed
OR	Odds ratios
OTM	Olive tail moment
OX	Oxidized bases
PAH	Polycyclic aromatic hydrocarbons
<i>PARP</i>	Poly ADP adenosine diphosphate-ribose polymerase
PBS	Phosphate buffered saline
PCR	Polymerase chain reaction
PI	Propidium iodide
PVDF membrane	Polyvinylidene fluoride membrane
py	Pack-year

<i>RAD23B</i>	DNA damage repair and recombination protein-23B
RFLP	Restriction fragment length polymorphism
ROS	Reactive oxygen species
<i>RPA</i>	Human replication protein A
RPMI-1430	Roswell park memorial institute-1430
R _{ROS}	Rate of ROS production
RR _{ROS}	Relative rate of ROS production
RT-PCR	Reverse Transcription and cDNA amplification
SB	Strand breaks
SDS	Sodium dodecyl sulfate
SDS-PAGE	Sodium dodecyl sulfate polyacrylamide gel electrophoresis
siRNA	Small inhibitory RNA
SNPs	Single nucleotide polymorphisms
SSC	Side scatter
Std. error	Standard error
Std. dev	Standard deviation
TAE	Tris-acetate EDTA
TBST	Tris-buffered saline Tween
TCM	Traditional Chinese medicine
TCR	Transcription coupled repair
TE	Tris-EDTA
TFIIH	Basal transcription factor IIH
T _m	Melting temperature
TTD	Trichothiodystrophy
<i>UV-DDB</i>	UV-damaged DNA-binding factor
XP	Xeroderma pigmentosum
<i>XPA to XPG</i>	Xeroderma pigmentosum group A to group G
χ^2	Chi-square



1. Introduction

DNA repair is of fundamental importance in maintaining (Cheng *et al.*, 2000) genomic stability after exogenous exposures such as smoking and protects against cancer (Hoeijmakers, 2001a; Wu *et al.*, 2007a). Impaired DNA repair contributes to tumorigenesis and its overexpression is a mechanism for tumor resistance to chemotherapy (Brabec & Kasparkova, 2002). More than 160 human DNA repair genes are known (Wood *et al.*, 2001). These can be sub-grouped into genes associated with DNA damage signaling and regulation of the repair system and genes working with distinct repair pathways such as mismatch repair, base excision repair, nucleotide excision repair (NER), direct damage reversal and DNA double-strand break repair. This thesis is concentrating on NER.

1. 1. Nucleotide excision repair (NER)

NER eliminates a wide variety of different forms of DNA damage. It eliminates mainly the bulky or helix-distorting DNA adducts (Buschta-Hedayat *et al.*, 1999) such as those caused by ultraviolet (UV) radiation (Lindahl *et al.*, 1997) and polycyclic aromatic hydrocarbons (PAH) (Platt *et al.*, 2008). PAHs are commonly present in tobacco smoke (Ding *et al.*, 2008), coal tar, pesticides and herbicides (Becher *et al.*, 2005). NER also removes lesions caused by DNA crosslinking agents e.g., cisplatin (Furuta *et al.*, 2002). There are around 30 proteins involved in NER (Andressoo *et al.*, 2006).

1. 1. 1. Molecular mechanisms of NER

NER consists of two sub-pathways, **Global genome repair (GGR)** and **Transcription coupled repair (TCR)**. GGR mainly repairs DNA lesions arising in non-transcribing regions of the genome (Fousteri & Mullenders, 2008; Shuck *et al.*, 2008). TCR is involved in damage repair at actively transcribing sites (Fousteri & Mullenders, 2008).

Figure.1.1 is a schematic representation of NER. The complex interaction of NER proteins in the pathway is not completely known yet, but damage recognition is specific for each of the sub-pathways. In GGR, two heterodimers *XPC-RAD23B* and *UV-DDB* (heterodimer of *DDB1-DDB2*) recognize DNA distortion and bind to the damaged site (Fousteri & Mullenders, 2008; Shuck *et al.*, 2008). In TCR, RNA polymerase II gets blocked at the damaged site. This blockade is recognized and removed by the proteins *ERCC6 (CSB)* and *ERCC8 (CSA)* (Fousteri & Mullenders, 2008). In the next step, the basal transcription factor IIH (TFIIH) complex unwinds the DNA duplex. TFIIH comprises up to 10 subunits (Volker *et al.*, 2001) including the ATP dependent helicases *ERCC2 (XPD)* and *ERCC3 (XPB)* which unwind the duplex DNA in 3' - 5' and 5' - 3' direction, respectively. This generates an open DNA structure around the lesion making place for the *RPA-XPA* complex which stabilizes the open DNA structure and assembles the pre-incision complex (Sugasawa, 2008). *ERCC5 (XPG)* and the *ERCC1-ERCC4 (XPF)* heterodimer are structure specific endonucleases that incise the DNA at the 3' and 5' junctions between single-stranded and double-stranded DNA thus releasing a 24 to 32 bases long DNA piece creating a single-strand gap in the DNA. This gap is filled by DNA polymerases δ and ϵ , and ligase I (Shuck *et al.*, 2008; Fousteri & Mullenders, 2008) which use the undamaged strand as a template for DNA resynthesis.

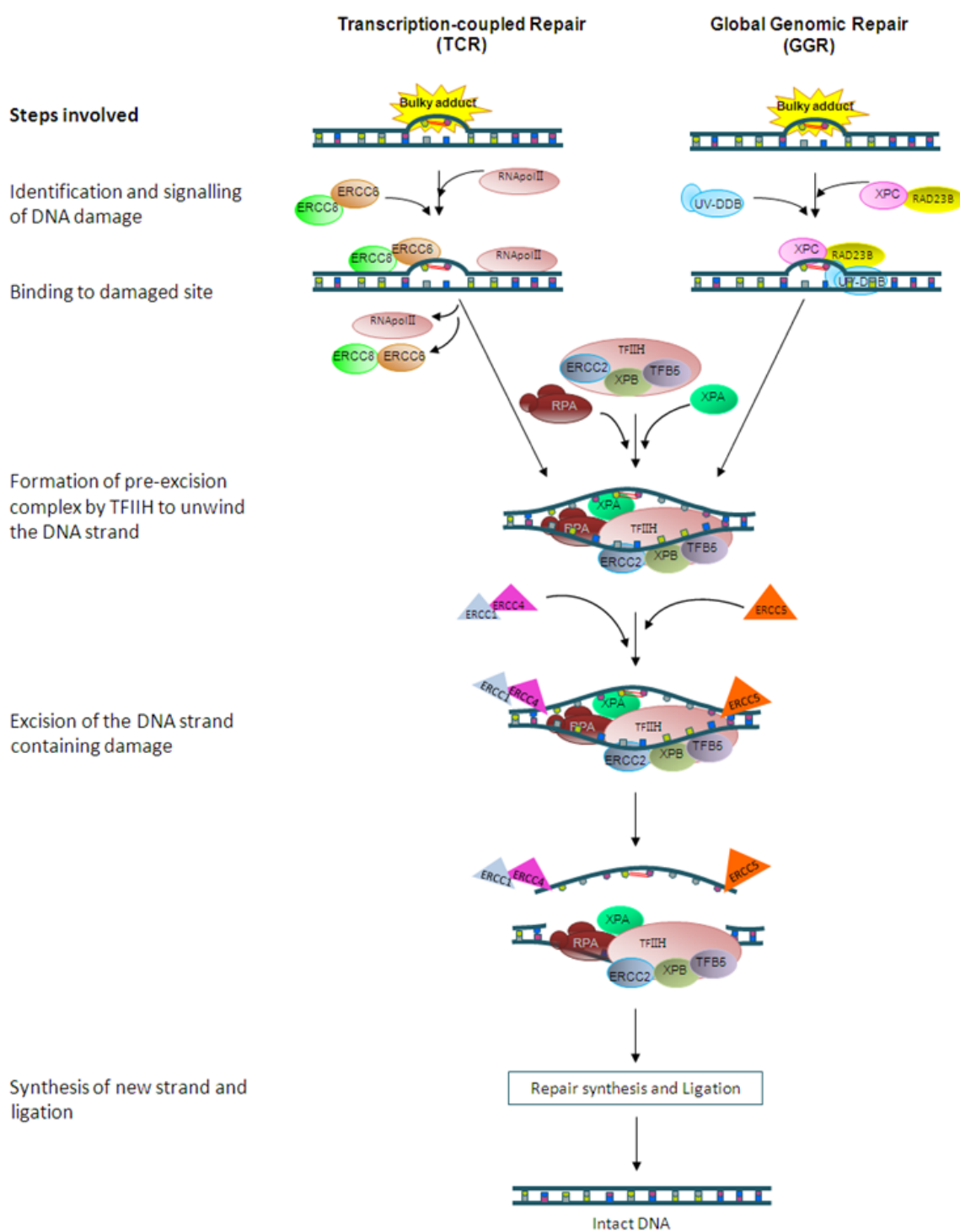


Figure.1.1. Nucleotide excision repair (NER) pathway. Modified from Fousteri & Mullenders, (2008).

1. 1. 2. Syndromes caused by defects in NER

Mutations in NER genes cause distinct disorders including Xeroderma pigmentosum (XP), Cockayne syndrome (CS) and Trichothiodystrophy (TTD). Table.1.1 outlines important NER genes, their implication in the pathway and diseases associated with the genes.

Xeroderma pigmentosum is the first disorder where, in 1968, a direct link between DNA repair and carcinogenesis was found (Cleaver, 1968). It is a rare autosomal recessive disorder, characterized by severe photosensitivity and predisposition to skin cancer at very young age (reviewed in Sugawara, 2008; Leibel *et al.*, 2006). Cells from XP patients are extremely sensitive to UV light and have a defect in NER. Eight NER genes are involved in XP (*XPA* to *XPG*, *XPV*).

Cockayne syndrome is a rare disorder associated with many clinical symptoms including dwarfism, mental retardation and photosensitivity. CS is not associated with enhanced incidence of skin cancer. Cells from CS patients are hypersensitive to UV exposure. Defects in two NER genes, *ERCC6* (*CSB*) and *ERCC8* (*CSA*) lead to CS (Leibling *et al.*, 2006; Foustari and Mullenders, 2008). A third group comprises patients exhibiting both XP and CS symptoms. They have been associated with mutations in three NER genes, *ERCC2* (*XPD*), *ERCC3* (*XPB*) and *ERCC5* (*XPG*).

Individuals suffering from Trichothiodystrophy exhibit photosensitivity, Ichthyosis, brittle hair, impaired intelligence, decreased fertility and short stature (Itin *et al.*, 2001). TTD is also not associated with predisposition to cancer. Certain mutations in *ERCC2* (*XPD*), *ERCC3* (*XPB*) and *ERCC5* (*XPG*) genes have been linked to TTD.

Table.1.1. Genes implicated in NER

Gene	location	Gene function ^a	Involved in ^b		Associated syndrome ^c
			GGR	TCR	
<i>XPC</i>	3p25.1	Damage detection In GGR.	Y	N	XP
<i>RAD23B</i>	9q31.2	<i>RAD23B</i> and <i>XPC</i> work as a complex	Y	N	-
<i>UV-DDB2</i>	11p12-p11	Damage detection In GGR.	Y	N	XP
<i>ERCC6 / CSB</i>	10q11.23	Damage detection and removal of RNA polymerase II blockade in TCR	N	Y	CS
<i>ERCC8 / CSA</i>	5q12.1	Damage detection and removal of RNA polymerase II blockade in TCR	N	Y	CS
<i>XPA</i>	9q22.3	stabilizes the open DNA structure	Y	Y	XP
<i>ERCC1</i>	19q13.32	5' Endonuclease, works as a complex with <i>ERCC4 / XPF</i>	Y	Y	-
<i>ERCC2 / XPD</i>	19q13.32	3' - 5' Helicase	Y	Y	XP, CS, TTD
<i>ERCC3 / XPB</i>	2q21	5' - 3' Helicase	Y	Y	XP, CS, TTD
<i>ERCC4 / XPF</i>	16p13.12	works as a complex with <i>ERCC1</i>	Y	Y	XP
<i>ERCC5 / XPG</i>	13q33.1	3' Endonuclease	Y	Y	XP, CS, TTD

^a GGR, global genome repair; TCR, transcription coupled repair.

^b Y, Yes; N, No.

^c XP, xeroderma pigmentosum; CS, Cockayne syndrome; TTD, Trichothiodystrophy.

1. 2. NER and cancer risk

Cancer is a complex disease manifested by genetic and epigenetic changes in cells, accumulating over a period of time (Frank, 2004; Heng *et al.*, 2009). Individuals vary in their ability to develop cancer. Age, genes and environmental factors like eating habits and life style play a major role in defining this ability (Bartsch & Hietanen, 1996; Brose *et al.*, 2003). The cross-talk between genetics and environment does not directly cause cancer but greatly affects the risk of developing it in future.

Genetic factors like highly penetrant mutations cause strong predisposition to nearly every cancer type (Mohandas, 2001). Major mutations in several NER genes (Table.1.1) cause XP syndrome with predisposition to skin cancer. As these mutations are an evolutionary disadvantage they are rare. On the other hand, low-penetrance genetic variations, also known as polymorphisms, might also influence cancer susceptibility (Frank, 2004). Genetic polymorphisms generally have a higher frequency, appearing in at least 1% of a population. Single nucleotide polymorphisms (SNPs) are genetic variations that occur when a single nucleotide in a DNA sequence is altered (Au, 2006; Orr & Chanock, 2008). SNPs are usually considered point mutations having evolutionarily success to recur in a significant proportion of the population.

Many SNPs have been associated with higher cancer risk. Table.1.2 lists some of the SNPs present in NER genes associated with increased cancer risk. The mechanism by which these SNPs could impact cancer risk is still unclear. Variations in DNA repair genes suggest variation in the ability to repair. Decrease in DNA repair capacity results in increased mutation rates and genetic instability that leads to cancer development (Matakidou *et al.*, 2007). This hypothesis is firmly supported by the presence of breast-ovarian cancer syndrome, XP syndrome and many other heredity cancer types (Brose *et al.*, 2003). With the advances in technology and increasing knowledge, the hypothesis has also been applied to the general population to ascertain cancer risk (Shuck *et al.*, 2008).

Table.I.2 summarizes common SNPs present in NER genes which were reported to be associated with increased risk of head and neck, lung, breast, bladder or other cancer types. A good example is *ERCC2*. Three most common SNPs in the gene, Arg156Arg, Asp312Asn and Lys751Gln, have been the center of many studies. A meta-analysis by Manuguerra *et al.*, (2006) revealed that Arg156Arg, which is a synonymous polymorphism, is important in skin cancer whereas Asp312Asn and Lys751Gln are linked with breast and lung cancer. Peripheral blood lymphocytes from individuals with 312Asn and 751Gln had higher UV sensitivity compared with 312Asp and 751Lys (Au, 2006). The finding was consistent with decreased NER capacity. *XPC* Lys939Gln has been associated with lung cancer, bladder cancer and advanced colorectal adenoma (Huang *et al.*, 2006; Sanyal *et al.*, 2004; Shen *et al.*, 2005). The SNP maps to C-terminal domain of *XPC*, which is essential for interaction with TFIIH through *ERCC3* and *p62* subunits, and crucial for NER (Uchida *et al.*, 2002). This might explain the significance of the SNP in decreased repair capacity and increased cancer risk.

Table.1.2. Cancer associated SNPs in NER genes.

Gene	Polymorphism ^a		Associations reported for Cancer
	Nucleic acid	amino acid	
XPC	A/C, Lys939Gln		Advanced Colorectal Adenoma (Huang <i>et al.</i> , 2006), lung cancer (Shen <i>et al.</i> , 2005), bladder cancer (Sanyal <i>et al.</i> , 2004)
	C/T, Ala499Val		Squamous cell carcinoma of the head and neck (An <i>et al.</i> , 2007)
RAD23B	C/T, Ala249Val		Lung cancer (Shen <i>et al.</i> , 2005)
XPA	G/A, G23A		Lung cancer (Popanda <i>et al.</i> , 2004)
ERCC1	T/C, Asn118Asn		Lung cancer (Kiyohara & Yoshimasu, 2007; Zienolddiny <i>et al.</i> , 2006), bladder Cancer (Matullo <i>et al.</i> , 2005)
	C/A, C8092A		Squamous Cell Carcinoma of the Head and Neck (Sturgis <i>et al.</i> , 2002), adult-Onset Glioma (Chen <i>et al.</i> , 2000)
	C/A, IVS5+33		Bladder Cancer (Garcia-Closas <i>et al.</i> , 2006)
ERCC2	A/C, Arg156Arg		Lung Cancer (Yin <i>et al.</i> , 2007; Shen <i>et al.</i> , 2005; Yin <i>et al.</i> , 2005), Bladder Cancer (Garcia-Closas <i>et al.</i> , 2006), basal cell carcinoma (Vogel <i>et al.</i> , 2001)
	A/C, Lys751Gln		Lung cancer (Kiyohara & Yoshimasu, 2007; Zienolddiny <i>et al.</i> , 2006; Zhou <i>et al.</i> , 2002), esophageal adenocarcinoma (Liu <i>et al.</i> , 2007), multiple primary melanoma (Millikan <i>et al.</i> , 2006), basal cell carcinoma (Vogel <i>et al.</i> , 2001)
	G/A, Asp312Asn		Lung cancer (Kiyohara & Yoshimasu, 2007; Zhou <i>et al.</i> , 2002), multiple primary melanoma (Millikan <i>et al.</i> , 2006), basal cell carcinoma (Vogel <i>et al.</i> , 2001)
ERCC4	G/A, Arg415Gln		Smoking and breast cancer (Mechanic <i>et al.</i> , 2006), prostate cancer (Lockett <i>et al.</i> , 2005)
ERCC5	G/C, Asp1104His		Lung cancer (Kiyohara & Yoshimasu, 2007), lung cancer and SCC of the oropharynx, larynx and esophagus (Cui <i>et al.</i> , 2006), Smoking and breast cancer (Mechanic <i>et al.</i> , 2006), bladder cancer (Sanyal <i>et al.</i> , 2004), breast cancer (Kumar <i>et al.</i> , 2003)
	T/C, His46His		Lung cancer (Kiyohara & Yoshimasu, 2007; Zienolddiny <i>et al.</i> , 2006)
ERCC6	A/G, Arg1213Gly		Colorectal cancer (Berndt <i>et al.</i> , 2006), Smoking and breast cancer (Mechanic <i>et al.</i> , 2006)

^a SNP500Cancer Database and NCBI; For each polymorphism nucleotide, codon number and amino acid change, if adequate, is provided.

1. 2. 1. Laryngeal cancer

1. 2. 1. 1. Larynx

The larynx (Figure.1.2), also known as the 'voice box', is located in the neck and is visible as 'Adam's apple', just below the chin (Schnke *et al.*, 2005). It is the top part of trachea (windpipe). During inhalation, air passes into the larynx and down the trachea towards the lungs. Larynx comprises vocal cords and epiglottis. Vocal cords are 'V' shaped ridges of muscle tissue on the inside lining of the larynx. They vibrate when air passes between them to produce speech. Epiglottis is a flap of cartilage tissue at the back of the tongue. During the swallowing process, epiglottis closes over the entrance to the larynx, making sure that food goes down the esophagus and not down the trachea.

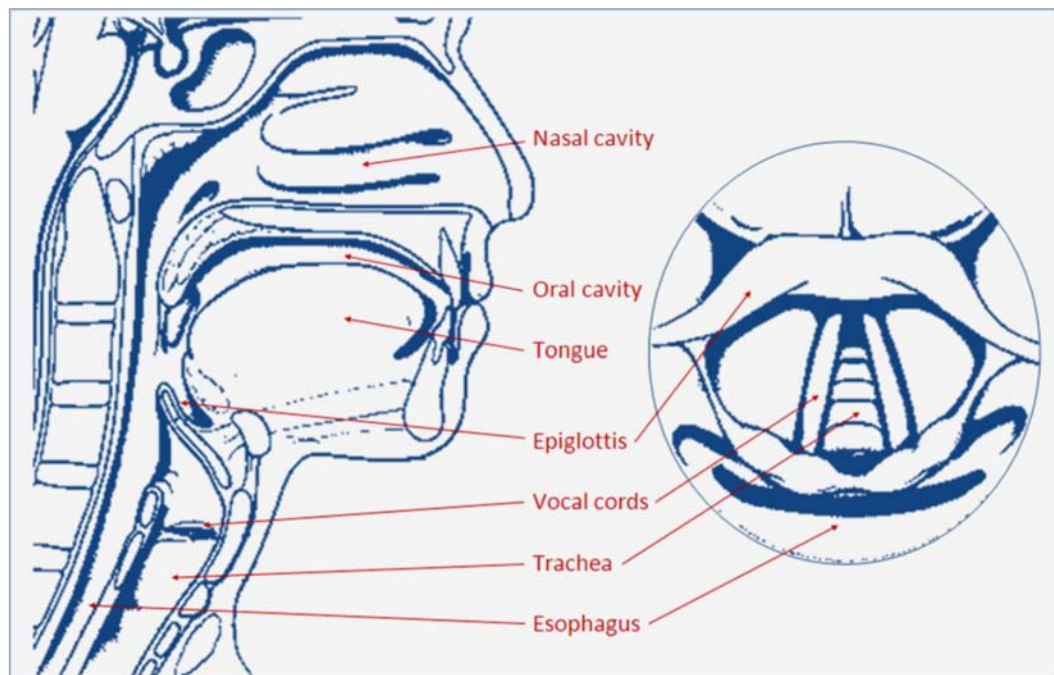


Figure.1.2. Human Larynx. Larynx comprises epiglottis and vocal cords. Inset: cross section of larynx. Taken and modified from <http://www.taxotere.com>

1. 2. 1. 2. Facts about larynx cancer

Laryngeal cancer is the most frequent form of head and neck cancers in Germany (Batzler *et al.*, 2008) and the second most common form of respiratory tract cancers in the US (American Cancer Society, 2006). The average age of onset of the disease is 64 years and it is more common in males than in females (6:1 ratio).

Nevertheless, laryngeal cancer is listed as a "rare disease" by the Office of Rare Diseases (ORD) of the National Institutes of Health (NIH) (Beenken *et al.*, 2009). In Germany, an estimated 3000 men and 400 women are diagnosed with this disease each year (Batzler *et al.*, 2008). The 5 years survival rate is around 61%. It is however to be noted that quality of life is strongly affected by this disease as it effects the speaking and swallowing abilities of the patients (Starmer *et al.*, 2008).

1. 2. 1. 3. Larynx cancer risk factors

Age and gender

As with most cancers, larynx cancer is more common in older people than in younger. Half of the patients are above 65 years of age. The disease is 6 to 7 times more common in men. The higher incidence in males can be attributed to their smoking and drinking habits (Batzler *et al.*, 2008; American Cancer Society, 2006).

Smoking and alcohol consumption

Cigarette smoking and alcohol consumption are well acknowledged risk factors for laryngeal cancer (Hashibe *et al.*, 2007; IARC, 2002; La *et al.*, 2008; Ramroth *et al.*, 2004; Talamini *et al.*, 2002). Cancer risk is directly related with duration and number of cigarettes smoked, and considerably increased in individuals consuming more than 50 g of alcohol per day. Tobacco smoke contains many carcinogens including a group of *N*-nitrosamines that produce carcinogenic methyl and pyridyloxobutyl DNA adducts (Hecht, 2001). A further constituent of tobacco smoke is the highly toxic acetaldehyde (Stein *et al.*, 2006; Smith *et al.*, 2000) which produces genotoxic 1,*N*²-propano-2'-deoxyguanosine DNA adducts (Stein *et al.*, 2006; Brooks & Theruvathu, 2005). Acetaldehyde is also an intermediate product of ethanol metabolism and its concentration increases in a multiplicative manner in

individuals who are simultaneously smoking and drinking alcohol (Salaspuro & Salaspuro, 2004). This observation might explain the synergistic and multiplicative effect found for alcohol and smoking in laryngeal cancer risk (Talamini *et al.*, 2002; Hashibe *et al.*, 2007).

Occupational exposure

Workers in construction industry are exposed to polyaromatic hydrocarbons (Becher *et al.*, 2005). Exposure to chemicals e.g., paint fumes, soot or coal dust over a period of time increases the risk of larynx cancer. Exposure to coal and wood as a fuel source in household over many years has also been linked to a higher risk of laryngeal cancer (Sapkota *et al.*, 2008).

Eating habits and physical health

A weak Immune system and poor eating patterns increase larynx cancer risk (American Cancer Society, 2006). Intake of fresh or salt-preserved meat and fish increases the risk whereas whole grains, fruits and vegetables protect against larynx cancer (Garavello *et al.*, 2009; Kasum *et al.*, 2002; Zheng *et al.*, 1992).

Other risk factors

Racial variations and some gastro esophageal reflux problems like heartburn are also linked to increased risk of larynx cancer (Qadeer *et al.*, 2005).

1. 2. 2. NER and larynx cancer risks

Although development of laryngeal cancer can widely be attributed to exogenous exposures by smoking and alcohol consumption, only a small portion of exposed individuals develop cancer, suggesting the involvement of genetic predisposition (Brose *et al.*, 2003; Bartsch & Hietanen, 1996).

Few studies report association between SNPs in NER genes and laryngeal cancer risk. Wen *et al.*, (2006) reported that individuals heterozygous for *ERCC5* Asp1104His have an increased risk for larynx cancer. Cui *et al.*, (2006) reported that individuals carrying at least one copy of *ERCC5* 1104His allele have an increased risk

for oropharyngeal, laryngeal and esophageal cancer, this risk increased in heavy smokers and high alcohol consumers.

SNPs in important NER genes are hypothesized to modulate an individual's ability to repair tobacco smoke-induced DNA damage thus contributing to cancer susceptibility (Shuck *et al.*, 2008). Genetic profiling helps to identify high-risk individuals who then can be enrolled in preventive measures or treated by personalized therapies (Bartsch *et al.*, 2007). The current study is aimed to contribute to such risk profiles for larynx cancer by analyzing SNPs in NER pathway.

1. 2. 3. The Rhein-Necker study

Our project is in collaboration with Prof. Heiko Becher and Dr. Heribert Ramroth, Department of Tropical Hygiene and Public Health, University of Heidelberg, Germany, and Prof. Andreas Dietz, Department of Otolaryngology, Plastic Surgery, University of Leipzig, Germany. A population-based laryngeal cancer case-control study is being carried out in the Rhein-Necker-Odenwald region southwest of Germany (Becher *et al.*, 2005). A total of 257 patients and 769 randomly selected population-based controls were recruited (n = 1026; case-control ratio of 1:3, matched for age and gender). Personal and job specific data were collected by well-trained interviewers using specific questionnaires. A strong affect of cigarette smoking, alcohol consumption (Ramroth *et al.*, 2004) and exposure to polycyclic aromatic hydrocarbons (Becher *et al.*, 2005) on the laryngeal cancer risk was observed. Rajae-Bebahani *et al.*, (2002) found a reduced Poly (ADP-ribose) polymerase activity in peripheral blood lymphocytes from the laryngeal cancer patients. Genetic polymorphisms in *ADH1B*, *ADH1C*, *GSTM1* and *GSTT1*, the ethanol and tobacco carcinogen metabolizing enzymes, did not show any significant association with larynx cancer risk (Risch *et al.*, 2003).

1. 3. NER and cancer therapy

Cancer therapy means exposing the body to agents that selectively kill cancer cells but produce less harm to normal cells (Helleday *et al.*, 2008). Chemotherapy has become a valuable tool for the control of cancer. In chemotherapy, chemical compounds are used to damage cancer cells and stop them from growing and dividing. The treatment has proven remarkably effective at treating many cancers, especially in combination with radiotherapy, but is plagued with toxic side effects. Most established chemotherapy drugs show insufficient specificity towards tumor cells, they kill healthy cells as well as cancerous ones (Liang *et al.*, 2009). Therefore we need improved antitumor drugs with higher recognition for cancer cells.

1. 3. 1. Targeted Cancer therapy

Tumors develop multiple genetic deficiencies e.g., in DNA damage response, that differentiate them from normal cells. Knowing the molecular defect in tumors has opened up the possibility to design the treatment of cancer, with a potential increase of the therapeutic index. In particular, by defining a sub-set of tumors carrying specific defects in DNA repair pathways allows to differentially treat the patients whose tumors harbor such defects (Damia & D'Incalci, 2007; Martin *et al.*, 2008). Several cancer chemotherapy drugs work by producing excessive DNA damage that causes cell death directly or following DNA replication (Helleday *et al.*, 2008).

As highlighted in Figure.1.3 tumors with DNA repair defects can be treated systemically by DNA damaging anticancer drugs. Examples of targeted therapy include the treatment of testicular cancer. NER is compromised in testicular cancer and 80% of the patients suffering with this disease respond to cisplatin therapy (Welsh *et al.*, 2004). Patients with completely resected non-small cell lung *ERCC1*-negative tumors appear to benefit from adjuvant cisplatin-based chemotherapy expressed as longer survival, whereas patients with *ERCC1*-positive tumor do not (Olaussen *et al.*, 2006). NER deficient cell lines are sensitive to several alkylating agents used in cancer chemotherapy, including cisplatin and melphalan

(Selvakumaran *et al.*, 2003). Ongoing clinical studies test *PARP* inhibitors as single agents in *BRCA1/2* deficient tumors (Farmer *et al.*, 2005).

In addition to the examples discussed, many new drugs can be developed to target cancer based on the concept of targeted therapy, particularly in the context of NER deficiency.

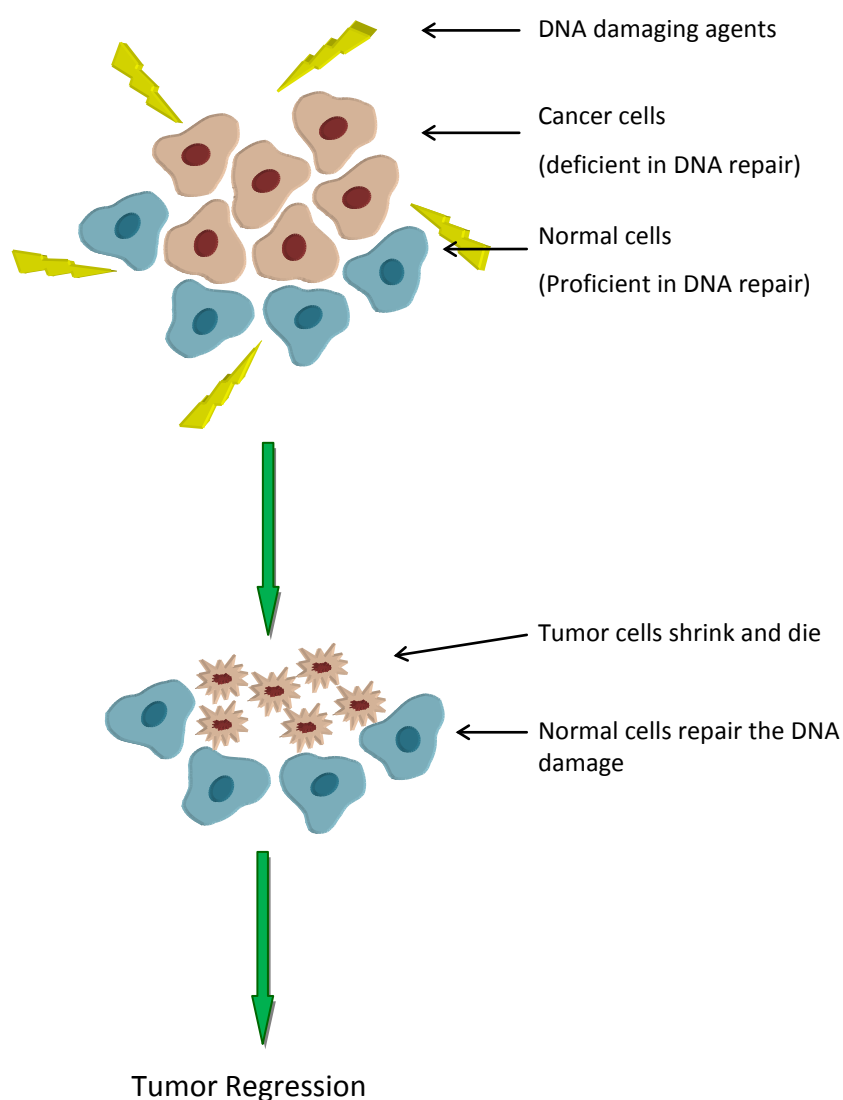


Figure.1.3. Targeted therapy of tumor cells deficient in DNA repair.

Because of great genetic variations between tumors, targeted cancer therapy cannot be pursued in all cancer patients and using the same regimes, but it should

be tailored according to the specific tumor DNA repair pattern. The efficacy and tolerability of a specific treatment can be predicted by genetic analysis of the tumors (Damia & D'Incalci, 2007; Di *et al.*, 2004). By tailoring chemotherapy regimens for specific predictive markers, one will improve response and survival in subgroups of patients, hence in the management of cancer (Rosell *et al.*, 2007). There is a need to find new truly disease related and target oriented drugs. It will help in achieving stronger effects at lower doses of the drugs, reducing side effects and economic burden.

1. 3. 2. NER deficiencies in tumors

NER pathway is defective in many cancer types. Table.1.3 shows that NER genes exhibit loss of heterozygosity (LOH) in ovarian, colon, lung, oral and breast cancer. Genes involved in the pathway also show a reduced expression and loss of normal co-ordination in several tumor types.

An important NER regulator is *p53*. It effects both dependent and independent transactivation of NER (Rubbi & Milner, 2003; SenGupta & Harris, 2005) especially by mediating expression of the GGR-specific damage recognition genes, *XPC* and *DDB2* (Adimoolam & Ford, 2003). Thus, cells mutant in *p53* are also deficient in GGR. *p53* defects are the most common event in human cancer and occur in at least 50% of all malignancies (Hoogervorst *et al.*, 2005). This suggests that a high percentage of tumors are devoid of GGR.

In short, NER deficiencies are common in tumors and these can be exploited for therapeutic purpose. By employing methods to target these deficiencies, tumor cells can be killed more effectively.

Table.1.3. Somatic NER deficiencies reported in different tumor types

NER genes	Type of impairment	Cancer type	Reference
Genetic defects in NER genes			
<i>XPA, XPC, ERCC2, XPE, ERCC4, ERCC5</i> and <i>ERCC6</i>	Loss of heterozygosity (LOH)	ovarian tumors (62.1 %), of colon (16.7%) and lung (22.2%) carcinomas	(Takebayashi <i>et al.</i> , 2001)
<i>ERCC2, ERCC3, ERCC4</i>	LOH	30% of oral carcinoma patients	(Miyashita <i>et al.</i> , 2001)
<i>XPA</i>	LOH promoter hypermethylation	20% of breast carcinoma Late-onset breast carcinoma	(Sinha <i>et al.</i> , 2008)
Reduced expression of NER genes.			
NER gene network	Most impaired and highly reduced gene expression	Brain, breast, cerebellum, stomach and many other sporadic solid tumors.	(Castro <i>et al.</i> , 2007)
<i>ERCC1</i> and <i>ERCC2</i>	Lose of normal co-ordination at mRNA level	glioma	(Dabholkar <i>et al.</i> , 1995)
<i>ERCC3</i> with <i>ERCC1, XPA</i> and both. <i>ERCC6</i> with <i>ERCC1</i> and <i>ERCC2</i>	Degree of disorder in co-ordination at mRNA level increases with advancing cancer stage	glioma	(Dabholkar <i>et al.</i> , 1996)
<i>XPC</i>	Reduced gene expression	bladder cancer	(Chen <i>et al.</i> , 2007)
<i>XPA, ERCC1</i> and <i>ERCC4</i>	Highly reduced expression	testicular cancer	(Welsh <i>et al.</i> , 2004)
<i>ERCC1</i>	Highly reduced expression	ovarian cancer	(Dabholkar <i>et al.</i> , 1994)
<i>XPC</i>	<i>XPC</i> promoter hypermethylation reduced its expression and caused <i>p53</i> mutations	non-smokers with lung cancer	(Wu <i>et al.</i> , 2007c)
<i>XPA</i>	Reduced expression	Colorectal cancer	(Yu <i>et al.</i> , 2006b)
<i>XPC</i>	Reduced expression	Non-small cell lung cancer in 1. Nonsmokers 2. advanced cancer stage (stage III)	(Wu <i>et al.</i> , 2007b)

1. 3. 3. Traditional Chinese medicine (中医, 中醫)



Figure.1.4. Some ingredients of traditional Chinese medicine

Traditional Chinese medicine (TCM) is a 2000 to 3000 years old unique medical care system developed in China to diagnose and cure illness (Han, 1988; Yu *et al.*, 2006a). It is a complete system of healing and includes herbal and dried animal medicine (Figure.1.4), acupuncture, moxibustion and massage, etc. In the western world, TCM is considered an alternative medical system (Yu *et al.*, 2006a).

1. 3. 3. 1. Importance of TCM

With increased understanding of therapeutic benefits, the demand for natural products has also increased. Knowledge gained over centuries is becoming the center of active search for new medicines. The evolution from traditional to empirical and to molecular screening has increased the chances of discovering new drug candidates from natural sources (Wang *et al.*, 2007) esp. the traditional folk medicines (Lobo *et al.*, 2009).

TCM has a very ancient history and a lot of experience has been gathered. The medicinal value of some of the herbs used in TCM has already been confirmed by modern scientific research. TCM is also a vast source of fascinating novel chemical structures which could be used as a rational for designing more ideal synthetic or semisynthetic new drugs (Han, 1988). In recent decades, many pharmacological functions have been suggested by experimental research.

More than 3000 single chemical compounds with novel structures have been identified from TCM since the 1950s and several of them are now used as medicines, including artemether, salvicine, huperzine A and depside salts (Wang *et al.*, 2007).

1. 3. 3. 2. TCM drugs as cancer therapeutics

TCM are a rich source of potential anticancer agents (Han, 1988). Several powerful anticancer drugs have been found including arsenic trioxide, indirubin, camptothecin, vinblastine, vincristine and etoposide (VP-16).

Tan *et al.*, (2008) claimed TCM has been used to treat colorectal cancer for around 6000 years. Currently several TCM remedies are being used in clinics in China during perioperative period to relieve the patients of surgical stress, intestinal obstruction and urinary retention after rectal surgery in combination with western medicine.

Arsenic trioxide has been a component of TCM for more than 2000 years. Currently it is sold under the trade name Trisenox (manufacturer: Cephalon). Arsenic trioxide is a chemotherapeutic agent of idiopathic function used to treat leukemia that is unresponsive to "first line" agents. It kills cancer cells by inducing apoptosis, shows antiproliferative activity, and inhibits angiogenesis (Miller, Jr. *et al.*, 2002).

Indirubin is the active ingredient of *Danggui Longhui Wan*, a mixture of plants that is used in traditional Chinese medicine to treat chronic diseases including myelogenous leukemia. Indirubin inhibits cyclin-dependent kinases (CDKs) and induces cell cycle arrest and apoptosis in human colorectal cancer cells (Kim *et al.*, 2009).

Camptothecin is a cytotoxic quinoline alkaloid which inhibits the DNA enzyme topoisomerase I (topo I). It was discovered in 1958 by M. E. Wall and M. C. Wani in systematic screening of natural products for anticancer drugs (Wall & Wani, 1996). Currently two Camptothecin analogues Camptosar (irinotecan) and Hycamtin (topotecan) are used in chemotherapy of lung, ovarian, cervix and advanced colorectal cancer (Lorence & Nessler, 2004).

Salvianolic acid B, Oxymatrine and Tetrandrine are undergoing clinical trials in China for the treatment of liver fibrosis and cancer. Glycyrrhizin, triptolide, celastrol and berberine show anti-inflammatory and antineoplastic activity both in *in vitro* and *in vivo* studies (Luk *et al.*, 2007).

1. 3. 4. Our investigations on TCM drugs

Our project is in collaboration with Prof. Xiaojiang Hao, Kunming Institute of Botany, the Chinese Academy of Sciences, Kunming, China. Two hundred and fifty three extracts from 76 TCM plants were tested for antitumor activity against leukemia cells and 23 (9%) of these reduced the cell growth significantly (Efferth *et al.*, 2008). Further analysis lead to the identification of 25-O-acetyl-23,24-dihydro-cucurbitacin F (*Quisqualis indica*) and miltirone as the most promising compounds. In another study 22 TCM compounds were tested for their activity against leukemia cell lines. Homoharringtonine, artesunate and bufalin showed potent anticancer activity. Artesunate and bufalin also increased uptake of daunorubicin (chemotherapeutic agent) in multidrug-resistant leukemia cells (Efferth *et al.*, 2002a). Cantharidin, an active principle ingredient of *Mylabris*, was found to cause oxidative stress that provoked DNA damage and p53-dependent apoptosis in leukemia and lymphoma cell lines (Efferth *et al.*, 2005). Recently, 734 TCM compounds were screened for their specific activity against 60 cell lines of different tumor origin. 531 of these were cytotoxic to tumor cells. A database for these compounds was also established (Konkimalla & Efferth, 2008).

1. 4. Aim of the present thesis

The role of NER in modulation of cancer risk and therapy is not well understood. Therefore, **the first part of this thesis** focuses on the role of NER in modulation of laryngeal cancer risk. A major reason for our study is that reports on NER and laryngeal cancer risk are rare (Hall *et al.*, 2007; An *et al.*, 2007). Recent studies mainly focused on lung, bladder or breast cancer (Table.1.2). The table summarizes SNPs present in NER genes which were reported to be associated with increased cancer risk, their position in the gene and their reported risk allele. We suggested

that individuals carrying these repair gene SNPs are generally at higher cancer risk for cancers with an etiology strongly related to external carcinogen exposure such as smoking, as it is the case for laryngeal cancer. To increase our knowledge on this type of cancer, we established a population-based case-control study with 257 laryngeal cancer patients and 769 population-based controls recruited in the Rhein-Necker-Odenwald region southwest of Germany. We measured 11 SNPs (Table.1.4) present in seven NER genes (*XPC*, *RAD23B*, *ERCC1*, *ERCC2*, *ERCC4*, *ERCC5* and *ERCC6*), and evaluated that three of these SNPs located in *ERCC5*, *ERCC6* and *RAD23B* modified laryngeal cancer risk.

The second part of the thesis deals with the question how NER affects cancer therapy. As NER deficiencies are frequent in different tumor types (Table.1.3), and we aim to target NER deficient tumor cells to improve the therapeutic response. To deal with the question, two key NER genes i.e., *XPC* and *ERCC6* were selected. In the light of increased demand for new therapies, the precious source of TCM drugs is being explored for compounds specifically targeting *XPC* and *ERCC6* deficient cells. Both these genes become active at a very early stage of damage recognition. Table.1.1 shows *XPC* is involved only in GGR whereas *ERCC6* is involved only in TCR. Selection of these genes enables to screen for TCM drugs specifically effecting one or both sub-pathways. Appropriate cell lines deficient in *XPC* and *ERCC6* genes were used. A total of 72 TCM drugs (pure compounds; saturated solutions) were analyzed for their cytotoxic activity against two NER deficient cell lines i.e., XP3BE and GM10902 and a normal cell line GM01310. Depending on the effect and available amount, 6 drugs were selected for further analysis and their IC₅₀ values (by dose-response curves), effects on cell cycle distribution (FACs) and DNA damage induction were measured. Results obtained for the most promising compound 'Ascaridol' were validated in a second cellular model. Ascaridol was also characterized for its ability to generate oxidative DNA damage.

Introduction

Table.1.4. Cancer associated SNPs in NER genes which were analyzed in the Rhein-Neckar Odenwald larynx cancer study.

Gene ^a	db SNP cluster ID ^b	Polymorphism ^b Nucleic acid, amino acid	Exon ^b	Rare allele frequency ^c (published)	Risk Allele	Cancer Associations reported for head and neck, lung and other cancer types
XPC	rs2228001	A/C, Lys939Gln	Ex16	0.41	C	Huang <i>et al.</i> , 2006; Shen <i>et al.</i> , 2005; Sanyal <i>et al.</i> , 2004
RAD23B	rs1805329	C/T, Ala249Val	Ex.8	0.15	T	Shen <i>et al.</i> , 2005
ERCC6	rs4253211	G/C, Arg1230Pro	Ex.19	0.11	-	no associations reported
	rs2228527	A/G, Arg1213Gly	Ex.19	0.20	G	Berndt <i>et al.</i> , 2006; Mechanic <i>et al.</i> , 2006
ERCC2	rs238406	A/C, Arg156Arg	Ex.6	0.49	AA	Shen <i>et al.</i> , 2005; Yin <i>et al.</i> , 2005; Yin <i>et al.</i> , 2007; Garcia-Closas <i>et al.</i> , 2006; Vogel <i>et al.</i> , 2001
ERCC1	rs11615	T/C, Asn118Asn	Ex4	0.35	TT	Kiyohara & Yoshimasu, 2007; Zienolddiny <i>et al.</i> , 2006; Matullo <i>et al.</i> , 2005
	rs3212986	C/A, C8092A	196bp 3' of STP	0.23	CC	Sturgis <i>et al.</i> , 2002; Chen <i>et al.</i> , 2000
	rs3212961	C/A, IVS5+33	Intron 5	0.13	AA	Garcia-Closas <i>et al.</i> , 2006
ERCC4	rs1800067	G/A, Arg415Gln	Ex8	0.074	A	Mechanic <i>et al.</i> , 2006; Lockett <i>et al.</i> , 2005
ERCC5	rs17655	G/C, Asp1104His	Ex.15	0.27	GG	Kiyohara & Yoshimasu, 2007; Cui <i>et al.</i> , 2006; Mechanic <i>et al.</i> , 2006; Sanyal <i>et al.</i> , 2004
	rs1047768	T/C, His46His	Ex2	0.45	CC	Kiyohara & Yoshimasu, 2007; Zienolddiny <i>et al.</i> , 2006

^a Genes are arranged according to their position in NER pathway.

^b SNP500Cancer Database and NCBI; For each polymorphism nucleotide, codon number and amino acid change, if adequate, is provided.

^c NCBI. European Caucasian population NCBI Reference Assembly, CEU_GENO_PANEL. 2007; Available from: URL: www.ncbi.nlm.nih.gov



2. Materials and Methods

2. 1. *Materials*

2. 1. 1. Equipment

Name	Manufacturer
384 well plates (PCR)	Steinbrenner Laborsystems GmbH
96 well plates (PCR)	Becton Dickinson
Agilent 2100 bioanalyzer	Agilent Technologies, Inc., Palo Alto, USA
Biophotometer	Eppendorf AG, Hamburg
Blunt 20-gauge needle (BD Microlance™ 3)	Becton Dickinson
Cell culture plates (6, 24, 96 well)	Greiner Bio-One GmbH, Frickenhausen
Cellcoat - Collagen Type 1 coated plates (6, 24, 96 well)	Greiner Bio-One GmbH, Frickenhausen
Cellstar cell culture flasks, 50 ml (T25), 250 ml (T75)	Greiner Bio.One GmbH, Frickenhausen
Centrifuge 5402	Eppendorf AG, Hamburg
Centrifuge 5415C	Eppendorf AG, Hamburg
Classic E.O.S. (Type 5270/100)	AGFA
CO ₂ Incubator Jouan IG 150	Astel SA, Chateau Gontier, Frankreich
Color printer with cartridge	Migge, Heidelberg
Combitips plus (0.2, 0.5, 1.0, 10 ml)	Eppendorf AG, Hamburg
Comet Slides	Trevigen/AMS, Wiesbaden
Cover slips (24 x 70 mm)	Menzel, Braunschweig
Cryo 1°C Freezing Container	Nalge Europe Ltd., Neerijse, Belgium
Cryovials (2 ml, 5 ml)	Greiner Bio-One GmbH, Frickenhausen
CytoFlour multi well plate reader, series 4000	

Name	Manufacturer
Digital camera (NV8, Samsung)	Staurn, Mannheim
Disposable cuvettes	Brand GmbH, Wertheim
Electrophoresis power supply EPS 300	Amersham Pharmacia Biotech GmbH, Freiburg
Electrophoresis power supply EPS 3500	Amersham Pharmacia Biotech GmbH, Freiburg
FACSCalibur flow cytometer	Becton Dickinson Biosciences
Filter tips, sterile (10, 20, 100, 200, 1000 µl)	Nerbe Plus GmbH, Winsen/Luhe
Fluorescent microscope (Laborlux 11)	Leica
Horizontal electrophoreses gel chamber	Renner GmbH, Dannstadt- Schauernheim
HP Scanjet 8290	Hewlett-Packard GmbH, Böblingen
Hypercassette Amersham GE	Healthcare, Munich
Hyperfilm Amersham Biosciences,	Little Chalfont, UK
Invitrolon PVDF membrane	Invitrogen GmbH, Karlsruhe
Light microscope (Diavert)	Leica
LightCycler 480	Roche Diagnostics GmbH, Mannheim
Mastercycler ep	Eppendorf AG, Hamburg
Micro wave MT 832C	Robert Bosch GmbH, Stuttgart
Minifuge T	Heraeus, Hanau
Minifuge Universal	Hettich, Tuttlingen
Multi dispencer - Multipette® Stream	Eppendorf AG, Hamburg
Multi-channel pipettes (0.5 – 10, 10 – 100 µl)	Eppendorf AG, Hamburg
Nanodrop spectrophotometer (ND1000)	PeQlab biotechnologie GmbH
Neubauer-counting chamber	Migge, Heidelberg
NuPAGE Novex Bis-Tris Gels	Invitrogen GmbH, Karlsruhe
pH-Meter pH 211	Hanna Instruments Deutschland

Name	Manufacturer
	GmbH. Kehl am Rhein
Pipette aid	TecNoMara, Ruhberg
Pipette tips (unsterile, without filter; 10, 20, 200, 1000 µl)	Starlab GmbH, Attrensburg
Pipettes (0.1 - 2.5, 0.5 – 10, 2 – 20, 10 – 100, 20 – 200 and 100 - 1000 µl)	Eppendorf AG, Hamburg
Powerpack 25	Whatman Biometra GmbH, Göttingen
Reaction tubes (0.2, 0.5, 1.5 and 2.0 ml)	Eppendorf AG, Hamburg
RNase-free syringe (BD Discardit™ II)	Becton Dickinson Labware, Heidelberg
Round bottom tubes (5, 14 ml)	Becton Dickinson Labware, Heidelberg
Serological pipettes (2, 5 and 10 ml)	Corning B.V. Life Sciences, Schiphol-Rijk, Niederlande
Shaker Duomax 1030	Heidolph Instruments GmbH, Schwabach
Single use weighing boats (7 ml, 100 ml)	Neolab, Heidelberg
SpectraMax: GEMINIXS microplate	Molecular devices
Fluorometer	
Sterile filter (0.2 µM, 0.45 µM)	Millipore, Molsheim
Sterile Werkbank Biogard Hood KL II	Baker, Stanford, USA
Thermomixer Comfort	Eppendorf AG, Hamburg
UV-Densitometer	Herolab, Wiesloch
UV-Kuvettes	mikro Brand GmbH, Wertheim
Vertical electrophoresis gel chamber 'X Cell Sure Lock'	Invitrogen, Karlsruhe
Vortex Genie 2	Bender & Hobein, Zürich, Schweiz
Water bath WG	Neolab, Heidelberg
Weighing machine A200S	Sartorius AG Göttingen
Weighing machine Typ 1518	Sartorius AG, Göttingen

Name	Manufacturer
Wide bore Tips (200 µl)	Stratagene, La Jolla, USA

2. 1. 2. Chemicals

Name	Manufacturer
0.5 X LightCycler480 genotyping master mix	Roche Applied Sciences
10 X PCR buffer	Qiagen, Hilden, Germany
10% NuPAGE precast Bis-Tris polyacrylamide mini-gels (1.5 mm X 10 well)	Invitrogen GmbH, Karlsruhe
6 X DNA gel loading dye	MBI Fermentas GmbH, St. Leon
Absolute Ethanol	Sigma Aldrich Chemie GmbH, Munich
Agarose, low melting (SeaPlaque®GTG® agarose)	Biozym Diagnostics, Hameln
Agarose, PeqGold Universal Agarose	PeqLab, Erlangen
BD FACS Flow	Becton Dickinson Labware, Heidelberg
BD FACS Rinse	Becton Dickinson Labware, Heidelberg
Benzonase nuclease	Merck, Darmstadt
BioRad protein assay	Bio-Rad Laboratories, Munich
BSA	New England biolabs
Complete Mini, Protease Inhibitor Cocktail Tablets	Roche Diagnostics GmbH, Mannheim
DharmaFECT-4 (DF4)	Dharmacon
Diethylpyrocarbonat (DEPC)	Sigma-Aldrich Chemie GmbH, Munich
Dimethylsulfoxid (DMSO)	Merck, Darmstadt
DL-Dithiothreitol (DTT)	Sigma-Aldrich Chemie GmbH, Munich
DNA damage quantification assay-AP site counting kit	DOJINDO molecular technologies, Inc.
dNTP mixture	MBI Fermentas GmbH, St. Leon-Rot

Name	Manufacturer
(dTTPs, dATPs, dCTPs, dGTPs) 10 mM	
Dulbecco's modified Eagle's medium (DME)	Sigma-Aldrich Chemie GmbH, Munich
Ethidium bromide (1 mg/ml),	Bio-Rad Laboratories GmbH, Munich
Ethylene diamine tetraacetic acid	Sigma-Aldrich Chemie GmbH, Munich
Disodium-solution (EDTA-Na ₂), 0,5 M	
Fetal calf serum (FCS)	PAA, Pasching, Österreich
Flare buffer	Trevigen
Fluorescein-siRNA	New England Biolabs
Fpg solution	New England Biolabs
<i>GAPDH</i> siRNA (nM)	Dharmacon
Hyromycin B (1g)	GERBU biotechnik GmbH, Gaiberg
Isopropanol	Sigma-Aldrich Chemie GmbH, Munich
L-Glutamin 200 mM	Invitrogen GmbH, Karlsruhe
LightCycler FastStart DNA Master SYBR Green I Kit	Roche Diagnostics GmbH, Mannheim
LIVE/DEAD® Viability/Cytotoxicity assay	Invitrogen
Magic Mark XP, Western protein standard	Invitrogen GmbH, Karlsruhe
Methanol	Sigma-Aldrich Chemie GmbH, Munich
MgCl ₂	Qiagen, Hilden, Germany
Milk powder	Carl Roth GmbH, Karlsruhe
NEBuffer-1	New England Biolabs
NuPAGE antioxidant	Invitrogen GmbH, Karlsruhe
NuPAGE LDS sample buffer (4 x)	Invitrogen GmbH, Karlsruhe
NuPAGE MOPS SDS buffer (20 x)	Invitrogen GmbH, Karlsruhe
NuPAGE sample reducing agent (10 x)	Invitrogen GmbH, Karlsruhe
NuPAGE transfer buffer (20 x)	Invitrogen GmbH, Karlsruhe
ON-TARGETplus <i>ERCC6</i> SMARTpool	Dharmacon
Penicillin-Streptomycin-solution (10.000 units/μl)	Invitrogen GmbH, Karlsruhe

Name	Manufacturer
Phenyl methyl sulfonyl fluorid (PMSF)	Sigma-Aldrich Chemie GmbH, Munich
Phosphate buffered saline (PBS)	Invitrogen GmbH, Karlsruhe
Propidium iodide (PI)	Sigma-Aldrich Chemie GmbH, Munich
pUC19 DNA/MspI (HpaII) Marker, 23	MBI Fermentas, St. Leon
Q solution	Qiagen, Hilden, Germany
QIAamp DNA blood Midi kit	Qiagen GmbH, Hilden
QIAquick Gel extraction kit	Qiagen GmbH, Hilden
QIAquick PCR purification kit	Qiagen GmbH, Hilden
QuantiTect SYBR Green PCR kit	Qiagen GmbH, Hilden
Random hexamer primers	Thermo Fisher Scientific GmbH, Ulm, Germany
Ribonuclease (RNase)	Sigma-Aldrich Chem. GmbH, Munich
RNasin Ribonuclease inhibitor 40 units/ μ l	Promega GmbH, Mannheim
RNeasy Mini Kit	Qiagen GmbH, Hilden
Roswell Park Memorial Institute medium (RPMI) 1640	PAA Laboratories GmbH, Pasching, Austria
Sodium chloride (NaCl)	Sigma-Aldrich Chemie GmbH, Munich
Sodium dodecyl Sulfate (SDS)	Sigma-Aldrich Chemie GmbH, Munich
Sodium hydroxide (NaOH)	Sigma-Aldrich Chemie GmbH, Munich
β -Mercaptoethanol	Sigma-Aldrich Chemie GmbH, Munich
Superscript III - Reverse Transcriptase (200 units/ μ l)	Invitrogen GmbH, Karlsruhe
SYBR-Green I	Molecular Probes, Leiden
Taq DNA polymerase (5 units/ μ l)	Qiagen GmbH, Hilden
Trishydroxymethylaminomethan (Trizma base)	Sigma-Aldrich Chemie GmbH, Munich
Triton X-100	Sigma-Aldrich Chemie GmbH, Munich
Trypsin-EDTA	Invitrogen GmbH, Karlsruhe
Tween 20	Sigma-Aldrich Chemie GmbH, Munich

Name	Manufacturer
ultraPURE™ Water, DNase, RNase frei	Invitrogen GmbH, Karlsruhe
Western Lightning Chemiluminescence Reagent Plus	Perkin Elmer, Life Sciences, Inc., Boston, USA

2. 1. 3. Primers

Primers for genotype analysis were obtained from TIB MOLBIOL GmbH, Berlin. Other primers were obtained from Thermo Fisher Scientific Inc.

Table.2.1. Primers for genotype analysis

Gene	Polymorphism	Sequence (5' - 3')	Annealing temp. (°C)	Primer ratio for real time PCR
<i>XPC</i>	Lys939Gln	GCC TCA AAA CCG AGA AGA TGA CTC GTC TCC CCT GAC CC	61	5:1
<i>RAD23B</i>	Ala249Val	TTA CAG GGA ATC CCT GGA GAT AGA TCC CCA TCC AGA AGA TTC C	60	1:1
<i>ERCC6</i>	Arg1230Pro	GCA CAA GTC AAA AAC AAA ACA TCA	60	1:1
<i>ERCC6</i>	Arg1213Gly	ATC CCT GTG GCA AAC GTA TC		
<i>ERCC2</i>	Arg156Arg	CAC AGC CTC ACA GCC TCC TAT GT TCA TCC AGG TTG TAG ATG CCA	59	1:1
<i>ERCC1</i>	Asn118Asn	GGC CCT GTG GTT ATC AAG G TTC CTG AAG TCT GGG GTG G	57	1:1
<i>ERCC1</i>	C8092A	CCT GAA GCC AGG GCA ACT AGC TGC CAA GGA AAC CC	60	1:5
<i>ERCC1^a</i>	IVS5+33	GCT GCT CCC TAG CCA G XT C ^{LC-RED640-3'} CCA TGT CAT CTC AGA TGT GAA AAA C	59	3:1
<i>ERCC4</i>	Arg415Gln	CTT CGG GTG AAG GAA TAA G TTC TCA AAG GTT TTC CTG TAG	58	1:1
<i>ERCC5</i>	Asp1104His	TTT CAG ATT CTA AAC GAA AGA ATA GAG TTC TGC GAA TCT GAA GCA C	56	1:1
<i>ERCC5</i>	His46His	AAC AAT TCT CCC AGA TAT TAG C GAA AAA ATA AGA GTT TGC AGA G	59	1:1

^a For *ERCC1* IVS5+33 forward primer was labeled with LC-Red640 at 3' position.

Table.2.2. Primers used for confirmation of XPC and ERCC6 mutation reported in XP3BE and GM10902

Gene	Sequence (5' - 3')	Amplicon size [bp]	Annealing temperature (°C)
<i>XPC</i>	GGC GAA GAC AAG AGA AAG AAG GGT TTG AGA GGT AGT AGG TGT CC	254	57
<i>ERCC6</i>	ATC TGG CAA AGA AAG GCT CA TTG CAA TCA TTT CCC ACT GA	245	61

Table.2.3. Gene specific primers used for relative quantification

Name	Sequence (5' - 3')	Amplicon size [bp]	Annealing temperature (°C)
<i>ERCC6</i>	AAG GAA CAG AGC AAT GAC GAT T CTT CTG CCT CCA CCA GTA CAT	130	60
<i>GAPDH</i>	GAG TCC ACT GGC GTC TTC AC GTT CAC ACC CAT GAC GAA CA	120	60
<i>HPRT1</i>	TGA CCT TGA TTT ATT TTG CAT ACC CGA GCA AGA CGT TCA GTC CT	102	60

Table.2.4. *Clathrin* Primer Sequence

Name	Sequence (5' - 3')	Amplicon size [bp]	Annealing temperature (°C)
5' -<i>Clathrin</i>	GAC AGT GCC ATC ATG AAT CC TTT GTG CTT CTG GAG GAA AAG AA	570	56
3' -<i>Clathrin</i>	GCT CAC ARG GGA ATG TTC AC ATG TTG TCA AAG TTG TCA TAA	550	56

2. 1. 4. LCTM Hybridization probes

LCTM Hybridization probes (Hybprobes) were obtained from TIB MOLBIOL GmbH, Berlin.

Table.2.5. Hybprobes for genotype analysis

Gene	Polymorphism	Probe Sequence (5'-3') ^a
<i>XPC</i>	Lys939Gln	CTC AGC TCA CAG CTT CTC AAA TGG GAA CA ^{FL-3'} 5'LC-RED640-GTG GGA AGC TGC TGC TTT CTT TTC CCT TTT GG p
<i>RAD23B</i>	Ala249Val	TGA AGA CTG AGG A <u>A</u> C CCC A ^{FL-3'} 5'LC-RED640-CTA GCT GCT TGA GGG GGG TCA p
<i>ERCC6</i>	Arg1230Pro	CCT TGG CCT CAC TCT TGT TTT CAC TGT C ^{FL-3'} 5'LC-RED610-GCT TCT GGT A <u>A</u> G GCC TTT TCT TC p
<i>ERCC6</i>	Arg1213Gly	TGG CGT CTC <u>C</u> GC AAT GCT T ^{FL-3'} 5'LC-RED640-GAG TTC TTA GGC TTT TGC TTT GGT CTC AGA T p
<i>ERCC2</i>	Arg156Arg	CGC AGT ACC AGC ATG ACA CCA GCC T ^{FL-3'} 5'LC-RED640-CCC CAC TGC C <u>G</u> C TTC TAT p
<i>ERCC1</i>	Asn118Asn	CGC A <u>A</u> C GTG CCC TGG GAA T ^{FL-3'} 5'LC-RED640-TGG CGA CGT AAT TCC CGA CTA TGT GCT G p
<i>ERCC1</i>	C8092A	GAC AAG AAG CGG AAG <u>C</u> AG CAG C ^{FL-3'} 5'LC-RED640-GCA GCA GCC TGT GTA GTC TGC CCC C p
<i>ERCC1^b</i>	IVS5+33	CCA CTG CAC AAC CTC AAA GCC C <u>I</u> G TGA GA ^{FL-3'}
<i>ERCC4</i>	Arg415Gln	CAT GTT <u>C</u> GG TCA TCA CTT GC ^{FL-3'} 5'LC-RED610-CAA ATC AGT ACT TGA CCT GAA AAT AGA AAA CA p
<i>ERCC5</i>	Asp1104His	TCA AGT GAA <u>G</u> AT GCT GAA AGT TC ^{FL-3'} 5'LC-RED640-CTT TAA TGA ATG TAC AAA GGA GAA CAG CTG p
<i>ERCC5</i>	His46His	TCG CCA <u>C</u> GG GAA CTC AAT ^{FL-3'} 5'LC-RED670-GAA AAT CCT CAT CTT CTC ACT TTG TTT CAT CG p

^a FL-3: probe is labeled with fluorescence at 3' position; 5'LC- RED**: probe is labeled with LightCycler-RedTM at 5' position; the position of polymorphism is underlined.

^b For *ERCC1* IVS5+33 forward primer was labeled with LC-Red640 at 3' position.

2. 1. 5. Restriction enzymes

Restriction enzymes were obtained from New England Biolabs.

Table.2.6. Restriction enzymes for genotype analysis

Gene	Polymorphism	Restriction enzyme	Restriction site	Sequence around SNP	
				Wild type allele	Variant allele
<i>RAD23B</i>	Ala249Val	<i>Ban11</i>	5'...G R G C Y* C ...3' 3'...C _↓ Y C G R G...5'	5'..... TGGGGCT* CCT....3'	5'..... TGGGGIT* CCT.....3'
<i>ERCC6</i>	Arg1230Pro	<i>Hae111</i>	5'...G G* C C...3' 3'...CC _↓ G G...5'	5'.....AGG*CGTTA.....3'	5'.....AGG*CCTTA.....3'
<i>ERCC6</i>	Arg1213Gly	<i>HpyCH4V</i>	5'...T G* C A...3' 3'...A C _↓ G T...5'	5'.....CATG*CA GAGA.....3'	5'.....CATG*CG GAGA.....3'
<i>ERCC2</i>	Arg156Arg	<i>Fnu4H1</i>	5'...G C* N G C...3' 3'...CG N _↓ C G...5'	5'.....ACTGC*CGA TTC.....3'	5'.....ACTGC*CGC TTC.....3'
<i>ERCC1</i>	IVS5+33	<i>Msp1</i>	5'... C* C G G ...3' 3'... G G C _↓ C ...5'	5'.....GCCTCA C* CGG GCTT.... .3'	5'.....GCCTCA C* A GG GCTT.... .3'
<i>ERCC4</i>	Arg415Gln	<i>Xmn1</i>	5'...GAANN*NNTTC...3' 3'... CTTNN _↓ NNAAG...5'	5'..ACC GAACA* TGTTCCCA.. 3'	5'..ACC AAACA* TGTTCCCA.. 3'
<i>ERCC5</i>	Asp1104His	<i>Nla111</i>	5'... C A T G* ...3' 3'... _↓ G T A C ...5'	5'.....GAA GATG* CTG3'	5'.....GAA CATG* CTG.....3'
<i>ERCC5</i>	His46His	<i>Nla111</i>	5'... C A T G* ...3' 3'... _↓ G T A C ...5'	5'.....CGC CATG* GGA.....3'	5'.....CGC CAG* GGA.....3'

2. 1. 6. Cell lines

The cell lines were obtained from Coriell Cell Repositories.

Table.2.7. Cell lines analyzed for TCM sensitivity

Cell line / Coriell code	Cell type	Gene defect
GM01310	B lymphocytes	Normal
GM10902	B lymphocytes	<i>ERCC6</i> deficient cell line, carries a point mutation (C2282T) generating a premature stop codon and a truncated protein (734 amino acids) (Colella <i>et al.</i> , 2000).
XP3BE / GM02248	B lymphocytes	<i>XPC</i> deficient cell line, carrying an 83bp insertion following codon Lys90, causing a frame shift mutation and generating a pre-mature stop codon (Li <i>et al.</i> , 1993).
XP4PA / GM15983	Fibroblast	<i>XPC</i> deficient cell line, harbours a dinucleotide (TG) deletion at position 1483-1484 causing a frameshift at codon Val431 and a premature stop codon (Li <i>et al.</i> , 1993).
XP4PA-SE2 / GM16248	Fibroblast	Fully corrected form of XP4PA by stable transfection using pXPC-3 plasmid (Emmert <i>et al.</i> , 2000; Legerski & Peterson, 1992).

2. 1. 7. Traditional Chinese medicine compounds

Seventy-two drugs (saturated solutions) derived from traditional Chinese medicine (TCM) and their solvents are given in Table.8.2.

2. 1. 8. Computer Softwares and Databases

Name	Link / Provider
Adobe Photoshop 7.0	Adobe Systems Inc., San Jose, USA
CellQuestPro Software	Becton Dickinson Biosciences
Ensembl Genome Browser	http://www.ensembl.org
Estimating Haplotypes EH (Version 1.2)	Rockefeller University, New York
Heidelberg Unix Sequence Analysis Resources	http://husar.dkfz-heidelberg.de
Image J (version 1.41o)	Rasband, NIH, USA
Komet 4 Software	Kinetic Imaging Ltd., Liverpool, UK
LightCycler Software (version 1.5.0)	Roche Diagnostics GmbH, Mannheim
Microsoft Office 2007	Microsoft Corporation
National Center for Biotechnology Information (NCBI)	http://www.ncbi.nlm.nih.gov
PHASE v 2.2.1.1 Software	Code by M Stephens, http://www.stat.washington.edu/stephens/phase/download.html
SAS (version 9.2)	SAS Institute, Inc., Cary, North Carolina, USA
Sequencing - bi-directional 'single run - Run24'	GATC Biotech AG

2. 2. Methods

2. 2. 1. NER and cancer risk

2. 2. 1. 1. Study population

Study population (Table.2.8) was collected by our collaborators in this project and has been published as Becher et al., (2005). This population-based case control study was carried out in the Rhein-Neckar-Odenwald region, south west of Germany comprising the cities of Heidelberg, Mannheim, Ludwigshafen, Darmstadt and Heilbronn, with a population of about 2.7 million. Treatment of laryngeal cancer is only done in the clinics of these cities. Larynx cancer patients coming to these clinics between 1998 and 2000 were obtained. Local practitioners were additionally contacted to check for possible cases sent to other more distant clinics and to verify complete case ascertainment. Incidence rates in districts within the study were calculated and compared internally and with incidence rates from a cancer registry in a neighbouring state (Saarland). Cases and controls were restricted to German Caucasians aged up to 80 who were registered as citizen in the study region.

Histologically-confirmed cases (n = 257; 236 males, 21 females; ages: 36 – 80 years) effected with squamous cell cancer of larynx were contacted through their physician. Eleven cases refused participation, and 20 patients could not be interviewed because of speaking impairment or poor health status (response rate 89.2 %). Ethical clearance was received by the ethical committee of the University of Heidelberg and informed consent was obtained from the participants through collaborating physicians.

Randomly selected population controls (n = 1233; case-control ratio of 1:3, matched for age and gender) with no previous or present record of head and neck, esophageal or lung cancer were contacted. 769 controls completed interviews (response rate 62.4 %). All interviews were conducted by five well-trained interviewers under standardized conditions, who interviewed both cases and controls at similar proportions. Information on smoking, alcohol consumption,

occupational exposure, family history of cancer and nutrition was collected with a comprehensive, standardized questionnaire. Overall 253 of 257 cases and 664 of 769 controls provided blood samples. A complete data set and DNA was finally available for 248 (96.4%) cases and 647 (84.1%) controls. A profile of non-responders has not been created. However, the fact of non-participation can be assumed to be independent from the genotypes, thus, a non-responder bias is not expected. Blood buffy coats were stored at -80°C until DNA extraction.

Table.2.8. Characteristics of larynx cancer cases and controls

Characteristics	Cases				Controls			
	Male		Female		Male		Female	
	n	(%)	n	(%)	n	(%)	n	(%)
<u>Age (years)</u>								
36-45	8	3.4	2	9.5	22	3.1	8	11.9
46-55	40	16.9	4	19.0	122	17.4	17	25.4
56-65	93	39.4	8	38.1	277	39.5	19	28.4
66-75	81	34.3	5	23.8	225	32.1	16	23.9
76-80	14	5.9	2	9.5	56	8.0	7	10.4
<u>Smoking (pack-years)</u>								
≤20	34	14.4	9	42.9	446	63.5	58	86.6
>20	202	85.6	12	57.1	256	36.5	9	13.4
<u>Alcohol consumption (g ethanol/day)</u>								
≤25	57	24.2	12	57.1	303	43.2	51	76.1
>25-50	51	21.6	4	19.0	169	24.1	9	13.4
>50	128	54.2	5	23.8	230	32.8	7	10.4
<u>Educational level (years of school education)</u>								
9 or less	206	87.3	18	85.7	436	62.1	43	64.2
10	16	6.8	2	9.5	105	15	15	22.4
More than 10	14	5.9	1	4.8	161	22.9	9	13.4
Total	236	100	21	100	702	100	67	100

2. 2. 1. 2. DNA extraction

Genomic DNA was extracted using QIAamp DNA blood midi kit (Qiagen, Hilden, Germany) by our technician. Optical densities of DNA samples were measured on a Biophotometer (version 1.35, eppendorf) and concentration of the stock solutions was set to 40 ng/ml. For genotyping, DNA dilutions (10 ng/ml) were prepared in 96 well plates, making it easy to work with 96 well plate format of light cycle 480 (LC-480). Three negative control (dH₂O) samples were placed in every fourth column of each plate. Samples were stored at 4°C until genotyping.

2. 2. 1. 3. Genotyping analysis

2. 2. 1. 3. 1. Single nucleotide polymorphisms (SNPs)

For genotyping, 11 SNPs in 7 NER genes *XPC*, *Rad23B*, *ERCC1*, *ERCC2*, *ERCC4*, *ERCC5* and *ERCC6* (Table.1.4.) were selected. The SNPs had a reported rare allele frequency of > 10% in Caucasians, with exception of *ERCC4* Arg415Gln with a rare allele frequency of 7.4 %. Among the selected SNPs, seven are non-synonymous, three are synonymous and one intronic. Selection favored SNPs with evidence for association with cancer risk reported for head and neck and lung cancer, or any type of cancer.

2. 2. 1. 3. 2. Optimization of PCR conditions

The PCR protocol for three SNPs *XPC* Lys939Gln, *ERCC1* Asn118Asn and C8092A was already set in the Lab. Methodology for all other SNPs was established during the present study. A generalized starting recipe of the PCR reaction mixture and cycling conditions used for optimization is given in Table.2.9 and 2.10. PCR was performed at a suitable annealing temperature gradient on Mastercycler (Eppendorf). The suitable temperature gradient was defined by the calculated melting temperature (T_m) of the primers ± 5 °C. T_m was calculated by the formula given below.

$$T_m = [(G + C) \times 4] + [(A + T) \times 2].$$

Amplified samples were checked for the expected sizes on 1.5 % Agarose gel in 1 X TAE buffer. pUC19 DNA/MspI M,23 (Fermentas) was used as a size reference. The best suited annealing temperature was selected. If there was need of further optimization varying concentrations of MgCl₂ (1.5mM, 2.0mM, 2.5mM) were used. The list of primers optimized for genotyping the SNPs is provided in Table.2.1.

Table.2.9. PCR reaction mixture

Reagent	Final concentration
DNA template	20 ng
10 X PCR buffer (Qiagen)	1 X PCR buffer
MgCl ₂	1.5 mM
10 μM dNTPs	0.2 μM dNTPs
5 μM Forward Primer	0.5 μM
5 μM Reverse Primer	0.5 μM
5U Taq polymerase (Qiagen)	0.5U
ultraPURE™ H ₂ O	To fill up the volume
Final reaction volume	20 μl

Table.2.10. PCR cycling conditions

	Step	Temperature	time
1 cycle	initial denaturation	95°C	3 min
35 cycles	i- denaturation	95°C	25 sec
	ii- Annealing	suitable temperature gradient	25 sec
	iii- extension	72°C	25 sec
1 cycle	elongation	72°C	5 min

2. 2. 1. 3. 3. Optimization of real time PCR

For optimization of real time PCR, different primer ratios (1:1, 1:5), suitable concentration of LC™ Hybridization probes (Hybprobes) to be detected on LC-480 and varying concentration of MgCl₂ were considered. A generalized starting recipe of the PCR reaction mixture and cycling conditions used for optimization is given in Table.2.11 and 2.12.

Table.2.11. PCR reaction mixture for real time PCR

Reagent	Final concentration
DNA template	10 ng
10 X PCR buffer (Qiagen)	1 X PCR buffer
MgCl ₂	1.5 mM
10 μM dNTPs	0.2 μM dNTPs
5 μM Forward Primer	0.5 μM
5 μM Reverse Primer	0.5 μM
2 μM sensor probe	0.2 μM
2 μM anchor probe	0.2 μM
5U Taq polymerase (Qiagen)	0.5U
ultraPURE™ H ₂ O	To fill up the volume
Final reaction volume	10 μl

¹ for XPC Lys939Gln, ERCC1 C8092A and IVS 5+33 2.5 mM MgCl₂ was used

Table.2.12. PCR cycling conditions for real time PCR

Program name	cycles	Analysis mode	Target temperature (°C)	Acquisition mode	Ramp rate (°C / sec)	acquisition rate (per °C)	Hold
Pre-incubation	1	None	95	None	4.4	-	3 min
amplification	44	Quantification	95	None	4.4	-	10 sec
			suitable temperature (Table.2.1)	Single	2.2	-	15 sec
			72	None	4.4	-	12 sec
Melting curve	1	Melting curves	95	None	4.4	-	1 min
			40	None	2	-	1 min
			80	Continuous	-	2.5	-
cooling	1	None	40	none	2.2	-	30 sec

2. 2. 1. 3. 4. Validation of optimized conditions

Optimized PCR conditions were validated by restriction fragment length polymorphism (RFLP). RFLP is a technique used to differentiate between homologous DNA samples having different restriction sites for a certain restriction enzyme. SNP specific restriction enzymes (Table.2.6) were searched at DKFZ HUSAR site using the Program MAPSORT. For each SNP, restriction enzymes were selected to cut specifically at the SNP site, so that differentiation between wild type, variant and heterozygous samples was possible. 20 to 25 samples were amplified by PCR (final reaction volume = 20 µl). Digestion mixture for the respective restriction enzymes was prepared according to the manufacturer protocol and samples were incubated with the mixture for 16 hours at 37 °C. The reaction was inactivated at 65 °C for 20 min. Digestion products were separated on 3% agarose gel at 100 volt for one hour. The selected samples were also genotyped on LC-480. Results obtained via both techniques were compared. A 100% concordance of the results validated the optimized conditions.

2. 2. 1. 3. 5. Genotyping by Fluorescence-based Real time PCR

SNP detection in all 895 samples was performed by real-time PCR on LightCycler 480 (Roche, Mannheim, Germany) using Hybprobes (Table.2.5). Either mono- or multiplex Hybprobe assays were used. Hybprobe detection format is based on melting curve analysis and uses fluorescence resonance energy transfer (FRET) for analysis of polymorphic sites. It comprises of two sequence-specific oligonucleotide probes known as donor and acceptor. Donor probe is labeled with fluorescein (excitation at 483 nm) at the 3'-end and acceptor with a LightCycler Red fluorophore at the 5'-end. The acceptor probe is also 3'-phosphorylated to prevent extension. The probes are specifically designed to bind the target sequences in a head-to-tail manner. The probe designed to bind across the SNP site is called "sensor" where as the probe designed to hybridize to an adjacent site is known as "anchor". During annealing phase of PCR, the HybProbe pair binds to the complementary template. This brings the probes in close proximity. The donor dye excites the acceptor fluorophore, hence, producing FRET. As temperature is raised,

the probes will melt at their corresponding Tms and no longer produce FRET. This melting coincides with a drop in fluorescence signal. The temperature at which the sensor probe melts depends on the underlying sequence. Thus, if sensor probe binding site carries a SNP, the complex is destabilized and melts at a lower temperature compared to the perfect match. Genotyping assays were done without knowledge of the clinical diagnosis.

2. 2. 1. 3. 5. 1. Monoplex Hybprobe assay

The SNPs *XPC* Lys939Gln, *RAD23B* Ala249Val, *ERCC1* Asn118Asn, *ERCC1* C8092A, *ERCC1* IVS5+33, *ERCC4* Arg415Gln and *ERCC5* Asp1104His were genotyped by monoplex Hybprobe assay. Table.2.11 and 2.12 gives the recipe for PCR reaction mixture and PCR conditions for the genotyping. For *XPC* Lys939Gln detection, 0.5 x Q solution and 0.1% BSA was additionally added to the reaction mixture. Table.2.1 and 2.5 provide the primer ratio and Hybprobe concentration used in the assays.

2. 2. 1. 3. 5. 2. ERCC1-IVS 5+33

The SNP lies in a region full of high binding stem loops. To overcome this problem an internally labeled primer (iLC mis; Table.2.1) containing a mismatch was designed. Furthermore the sensor probe used has a high Tm value. PCR products amplification for the SNP was carried out using 20 ng of DNA, 1 X buffer, 2.5 mM MgCl₂, 0.2 μM dNTPs, 1 X Q solution, 0.5U Taq polymerase (Qiagen, Hilden, Germany), 0.5 μM of iLC mis primer and 0.1 μM of reverse primer and the sensor probe, with a final reaction volume of 10 μl.

2. 2. 1. 3. 5. 3. Multiplex Hybprobe assay

In two cases, two SNPs were analyzed in one reaction using multiplex Hybprobes.

ERCC6 Arg1230Pro and ERCC6 Arg1213Gly

ERCC6 Arg1230Pro and *ERCC6* Arg1213Gly are located in the same exon therefore it was possible to detect both SNPs using a single pair of primers and two separate pairs of probes, labeled with different dyes (RED640 for Arg1230Pro and RED610 for Arg1213Gly). Recipe for PCR reaction mixture is provided in Table.2.13.

ERCC2 Arg156Arg and ERCC5 His46His

ERCC2 Arg156Arg and *ERCC5 His46His* are located on different chromosomes, so two separate pairs of primers and two differently labeled probe-pairs were used (RED640 for *ERCC2 Arg156Arg* and RED670 for *ERCC5 His46His*). Recipe for PCR reaction mixture is provided in Table.2.14. Cycling conditions were same as described earlier and the multiple peaks were resolved by color compensation for the respective probes.

Table.2.13. PCR reaction mixture For *ERCC6 Arg1230Pro* and *ERCC6 Arg1213Gly*

Reagent	Final concentration
DNA template	10 ng
10 X PCR buffer (Qiagen)	1 X
MgCl ₂	1.5 mM
dNTPs (10 µM)	0.2 µM
Primer Mix (5 µM)	0.5 µM
each probe (2 µM)	0.1 µM
Taq polymerase (5U / µl; Qiagen)	0.5U
ultraPURE TM H ₂ O	To fill up the volume
Final reaction volume	10 µl

Table.2.14. PCR reaction mixture for the detection of *ERCC2 Arg156Arg* and *ERCC5 His46His*

Reagent	Final concentration
DNA template	10 ng
5 X LightCycler480 genotyping master mix (Roche Applied Sciences)	0.5 X
MgCl ₂	2 mM
Primer Mix for <i>ERCC5 His46His</i> (5 µM)	0.5 µM
Primer Mix for <i>ERCC2 Arg156Arg</i> (5 µM)	0.5 µM
each probe (2 µM)	0.2 µM
Final reaction volume	10 µl

2. 2. 1. 3. 6. Color compensation

Color Compensation is a tool to calibrate the LightCycler® Instruments. It corrects for the spectral overlap of fluorescence channels in multiplex Hybprobe assays. Conditions for color compensation are provided in Table.2.15. Figure.2.1 provides the plate setup of the different reaction mixtures. The reaction was performed at an annealing temperature of 59°C. After the run, Color Compensation data were analyzed to generate a color compensation object 'CC Object'. The 'CC Object' was later used to resolve the complex peaks obtained during multiplex assays.

	1	2	3	4	5	6	7	8	9	10	11	12
A												
B		B L A N K		F L U O S		R E D 610		R E D 640		R E D 670		
C												
D												
E												
F												
G												
H												

Figure.2.1. PCR plate setup for color compensation

Table.2.15. PCR reaction mixture for color compensation

Reagent	Final concentration		
	Blank	Fluorescein-labeled probe	Acceptors dye-labeled probe
DNA template	10 ng	10 ng	10 ng
10 X PCR buffer (Qiagen)	1 X	1 X	1 X
MgCl ₂	1.5 mM	1.5 mM	1.5 mM
dNTPs (10 μM)	0.2 μM	0.2 μM	0.2 μM
Primer mix (5 μM)	0.5 μM	0.5 μM	0.5 μM
probe (2 μM)	-	0.3 μM	1.0 μM
Taq polymerase (5U / μl; Qiagen)	0.5U	0.5U	0.5U
ultraPURE™ H ₂ O			
Final reaction volume	10 μl	10 μl	10 μl

2. 2. 1. 3. 7. Validation of genotyping data

2. 2. 1. 3. 7. 1. Restriction fragment length polymorphism (RFLP)

10% of randomly selected samples were repeated and genotyping data was confirmed by RFLP. Results obtained were compared with the genotyping data by LC-480 by two investigators, independently. A 100% concordance was found.

2. 2. 1. 3. 7. 2. Sequencing

As *ERCC2* Arg156Arg and *ERCC5* His46His were genotyped in multiplex Hybprobe assay, they were further validated by sequencing. Six samples were selected, two of these were homozygous for wild type allele, two were heterozygous and two homozygous for variant allele of each SNP. The samples were amplified following standardized PCR protocol and cycling conditions (Table.2.9 & 2.10) with a final reaction volume of 50 μ l. Samples were separated on 1.5 % TAE Agarose gels at 90 volts for 1.5 hrs. DNA bands were cut from the gel using a sharp razor and were extracted with a QIAquick® Gel extraction kit (Qiagen, Hilden, Germany). Figure.2.2 shows two samples amplified for *ERCC2* Arg156Arg (PCR product size = 221 bp) and *ERCC5* His46His (PCR product size = 131 bp) in multiplex PCR before (Lane 1, 2) and after (Lane 3, 4, 5, 6) agarose gel extraction. Optical densities of the extracted samples were measured on a Biophotometer (version 1.35, eppendorf) and their concentration was set between 20 to 30 ng / μ l. Quality of the extracted samples was checked on 1.5 % TAE - Agarose gel (90 volts for 45 min). Samples were sent to GATC Biotech AG for sequencing 'single run - Run24'. Samples were sequenced bi-directional i.e., by both forward and reverse primers. Results obtained were 100% concordant.

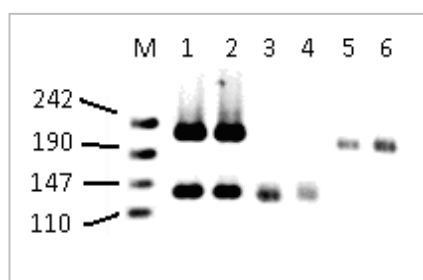


Figure.2.2. Lane 1 and 2 represent two samples amplified for *ERCC2* Arg156Arg (PCR product size = 221 bp) and *ERCC5* His46His (PCR product size = 131 bp). Lane 3, 4, 5 and 6 represent the same samples after being cut out of the Agarose gel and extracted with a QIAquick® Gel extraction kit. M = pUC19 DNA/Mspl M,23 (Fermentas) was used as size reference.

2. 2. 1. 3. 7. 3. *RAD23B Ala249Val*

As genotyping data for *RAD23B Ala249Val* deviated from Hardy-Weinberg principle ($\chi^2 = 6.28$), all the genotyping data for this SNP was rechecked, additional 5% samples were genotyped by RFLP, and some of the samples were also sequenced.

2. 2. 2. **NER and cancer therapy**

2. 2. 2. 1. *Cell culture*

2. 2. 2. 1. 1. *Culture conditions*

GM01310, XP3BE and GM10902 were maintained as suspension cultures in RPMI-1430 supplemented with 15% FCS and 1% Penicillin (100 units/ml) and Streptomycin (100 g/ml) at 37°C in a humidified 5% CO₂ atmosphere. Cultures were passaged twice a week at 2.5×10^5 cells/ml and grown in T75 culture flasks (250 ml, Greiner Bio-One) in vertical posture.

XP4PA and XP4PA-SE2 were maintained as monolayer cultures in DME (high glucose) supplemented with 10% not inactivated FCS, 2mM L-glutamine and 1% Penicillin (100 units/ml) and Streptomycin (100 g/ml) at 37 °C in a humidified 8% CO₂-atmosphere. For XP4PA-SE2 Hyromycin B (0.2 mg/ml) was also added. Cultures with 70 to 90% confluency were passaged at 3×10^4 to 3.5×10^4 cells/ml every five days by trypsinization with 1 ml 0.5 mM trypsin/EDTA for 1 min at room temperature.

9 to 10 weeks old cultures were discarded and new cells were grown.

2. 2. 2. 1. 2. *Contamination check*

All cultures were controlled for contaminations by multiplex cell contamination test through Genomics and Proteomics Core Facility at DKFZ. Samples were tested before starting any experiments and after six weeks. Multiplex cell contamination test is a high-throughput test and can detect 37 contamination markers for viral contamination, mycoplasma, and Cross-contamination by other cell lines in a single PCR reaction.

2. 2. 2. 1. 3. Freezing

Cells were collected and counted. The culture media was removed by centrifugation (1200 rpm, 5 min, 4 °C) and cell pellets were resuspended in an appropriate volume of pre-cooled freezing medium (respective culture medium + 10% DMSO) to yield approximately ten million viable cells/ml for suspension cell culture and 5×10^5 viable cells/ml for adherent cell culture. The cell suspension was dispensed in 1-ml aliquots into cryovials (Greiner Bio-One). Samples were frozen passively in a pre-cooled (4 °C) isopropanol bath at the rate of $-1 \text{ }^\circ\text{C} / \text{min}$ to $-80 \text{ }^\circ\text{C}$ placed in a -80°C freezer overnight and subsequently stored in liquid nitrogen.

2. 2. 2. 1. 4. Thawing

Cells were recovered by thawing at room temperature and quickly re-suspending the vial contents in culture medium. Samples were centrifuged at 1200 rpm for 5 min at room temperature. Suspension cells were re-suspended in 10 ml medium and placed in T25 culture flask (50 ml, Greiner Bio-One) in standing position. Adherent cells were resuspended in 5 ml of culture media and placed in horizontal position. Samples were allowed to grow at respective culturing conditions. After two days 5 to 7 ml of the old media were removed and fresh medium was added. Samples were allowed to grow for another two days before being handled as normal cell culture.

2. 2. 2. 1. 5. Doubling time

Cultures (> 90% viability), 5×10^5 cells/ml for suspension cells and 6×10^4 cells/ml for adherent cells, were grown in Petri dishes (35 x 10 mm, Becton Dickinson). Number of viable cells was counted on Neubauer-counting chamber via Trypanblue staining (Lindl 2002) every 24hrs for seven days. Each time half of the old culture medium was also replaced with fresh media. Experiment was repeated three times. Growth curves were generated. Number of generations and the doubling time for each cell line were calculated using the following formulas

$$\text{No. of generations} = (\log N - \log N_0) / \text{Log } 2$$

N_0 is the number of viable cells at time point '0'

N is the number of viable cells at the end of experiment

$$\text{Doubling time} = (t_x - t_0) \times \log 2 / (\log N_x - \log N_0)$$

N_0 is the no. of viable cell at the start of Log phase of cell growth

N_x is the no. of viable cells at the end of Log phase of cell growth

2. 2. 2. 2. Mutation confirmation

Mutations reported for the cell lines used in this project were confirmed. GM01310 was included as normal control. In addition, the cell lines were checked for their p53 protein expression.

2. 2. 2. 2. 1. XP3BE

The cell line and has an insertion of 83bp at position 462 in the cDNA of *XPC* leading to a frame-shift mutation and generating a pre-mature stop codon (Li *et al.*, 1993). Insertion was checked in cDNA by PCR using gene specific primers (Table.2.2) and standard PCR protocol (Table.2.16). PCR products were separated on 2% agarose gel (90 volts, 45 min). The protein was analyzed by western blotting.

Table.2.16. Reaction mixture used for confirmation of XPC and ERCC6 mutations

Reagent	Final concentration
Qiagen 10 x PCR buffer	1 X
MgCl ₂ [25mM]	2.0 mM (for ERCC6 only)
dNTPs (10 mM)	0.2 mM
Forward Primer (10 μM)	0.5 μM
Reverse Primer (10 μM)	0.5 μM
Qiagen Taq DNA Polymerase (5 U/μl)	0.05 U/μl
ultraPURE™ H ₂ O	To fill up the volume
DNA / H ₂ O	0.1 μl/μl of reaction mix
Total volume	50 μl

2. 2. 2. 2. 2. GM10902

It is an *ERCC6* deficient cell line and harbors a point mutation at position C2282T in cDNA (Colella *et al.*, 2000). To confirm the mutation, genomic DNA of the cell line was sequenced and compared with the sequence of the normal cell line. DNA samples were amplified using gene specific primers (Table.2.2) following standardized PCR protocol (Table.2.16) with a final reaction volume of 50 μ l. Amplification was checked on 1.5% Agarose gels (90 volts, 45min). Optical densities of the amplified samples were measured on a Biophotometer (version 1.35, eppendorf) and final concentration was set to 30 ng/ μ l. Samples were sent to GATC Biotech AG for bi-directional 'single run - Run24' sequencing. The protein was analyzed by western blotting.

2. 2. 2. 2. 3. XP4PA and XP4PA-SE2

The cell lines were checked for presence of XPC and ERCC6 protein by western blotting (see 2. 2. 2. 14. 3).

2. 2. 2. 3. Knockdown experiments

ERCC6 gene was silenced in XP4PA-SE2 cells using ON-TARGETplus SMARTpool (Dharmacon). It is a pool of four individual duplexes and under optimized conditions it is guaranteed to silence ERCC6 gene by 75% or more.

2. 2. 2. 3. 1. Optimization of conditions for transfection

For effective silencing of the gene following experimental parameters were determined: a suitable plating density (cells/ml), a suitable transfection reagent, its concentration needed to deliver enough siRNA into the cells to silence the gene and the plating effect. The best combination of these parameters was picked for the silencing experiments.

2. 2. 2. 3. 1. 1. Plating density

As in our experimental setup we need to transfect cells for upto 96hrs after transfection, an optimum plating density is required that yields enough cells after 24hrs for mRNA extraction and after 96hrs cells are still growing in monolayer.

Three plating densities were tested for the cell line (2×10^4 , 4×10^4 , 6×10^4 cells/ml) and samples were checked for confluency after every 24hr for 96hrs. 6×10^4 cells/ml was considered as a suitable cell density.

2. 2. 2. 3. 1. 2. Suitable transfection reagent, its transfection efficiency and plating effect

DharmaFECT-4 (DF4) was suggested by Dharmacon as suitable to deliver siRNA into the fibroblast cells. In addition polyFECT (Qiagen) was tested for its efficiency in our cells. Exponentially growing XP4PA-SE2 cells (> 90% viability, 6×10^4 cells/ml) were incubated with different volumes of DF4 and polyFECT in normal and collagen coated plates (Cellcoat, Greiner Bio-One) for 4 and 24 hrs. 15 nM Fluorescein-siRNA was used as transfection control (New England Biolabs). Untreated cells were included as control. Table.2.17 provides the conditions for the transfection media used. The experiment was performed once with five replicates of each treatment.

After 4 hrs of incubation (37°C, 8% CO₂) samples were observed by fluorescent microscope (Laborlux 11, Leica) in blue (wavelength 390 to 490 nm) and white light. The number of cells visible in both lights was counted and transfection efficiency was calculated as follows.

$\text{Transfection efficiency} = \frac{\text{Number of cells visible in blue light}}{\text{Number of cells visible in white light}} \times 100$
--

For plating effects, cells were grown for 24hrs, cultures were observed under a light microscope (Diavert, Leica) and cellular viability was measured by trypan blue staining.

2. 2. 2. 3. 2. General protocol for ERCC6 gene silencing

ERCC6 gene silencing was performed using the general protocol provided by the company. Table.2.18 provides the transfection media used in the experiment. Each experiment included the following samples in quadruplicates: 1) ERCC6 siRNA

(100nM) at two different ratios of DF4 / siRNA (DF4/*ERCC6* siRNA – 0.88, DF4/*ERCC6* siRNA – 1.76), 2) *GAPDH* siRNA (100nM) as positive control siRNA, 3) Luciferase siRNA (100nM) as negative control siRNA, 4) DF4 control and 5) Untreated cells. In separate tubes the appropriate volume of siRNA and DF4 were mixed gently with serum-free culture medium and incubated for 5min at room temperature. The two solutions were mixed and incubated for another 20min at room temperature and the required volume of antibiotic-free complete medium was added to the mixture. In exponentially growing cells (> 90% viability, 6×10^4 cells / ml) culture medium was replaced with appropriate volume of transfection medium and samples were incubated at 37°C in 8% CO₂ for 24 to 96 hrs for both mRNA and protein analysis. To avoid cytotoxicity caused by DF4, transfection medium was replaced with complete medium after 24 hours.

Table.2.17. Transfection media used for optimizing transfection efficiency.

Transfection reagent	Ratio of Transfection reagent / siRNA	Tube 1		Tube 2		Medium (μl) to be added	Transfection Medium (μl)
		10 μM Fluorescein siRNA (μl)	serum-free Medium (μl)	Transfection reagent (μl)	serum-free Medium (μl)		
DharmaFECT-4	5:1	0.75	49.25	0.54	49.5	400	500
	10:1	0.75	49.25	1.08	48.9	400	500
PolyFECT	8:1	0.75	49.25	0.87	49.1	400	500
	16:1	0.75	49.25	1.74	48.3	400	500

Note: Antibiotics were not added to medium used in transfection experiments.

Table.2.18. Transfection medium used for *ERCC6* knockdown.

	Ratio of DF 4 / siRNA ¹	Tube 1		Tube 2		Culture Medium (μ L) to be added	Transfection Medium (μ L)
		2 μ M siRNA (μ l)	serum-free Medium (μ L)	DF 4 ¹ (μ L)	serum-free Medium (μ L)		
<i>ERCC6</i> siRNA	0.88	25	25	0.59	49.4	400	500
<i>ERCC6</i> siRNA	1.76	25	25	1.18	48.8	400	500
<i>GAPDH</i> siRNA	1.77	25	25	1.18	48.8	400	500
Luciferase siRNA	1.77	2.5	47.5	1.18	48.8	400	500
DharmaFECT 4 control	-	0	50	1.18	48.8	400	500
Untreated cells	-	0	50	0	50	400	500

¹DF 4, DharmaFECT-4

Note: Antibiotics were not added to the medium used in transfection experiments.

2. 2. 2. 4. UV sensitivity

In exponentially growing cells (> 90% viability) culture media was replaced with PBS and cells were exposed to varying intensities of UVC (J/m^2) by Stratagene UV-StratalinkerTM 2400 and cells were allowed to grow for 48 hrs at normal culture conditions. Each experiment included an unexposed sample as a control. Relative growth was measured by Calcein assay and growth curves were generated against UVC intensity. The experiment was performed twice with three replicates for each treatment.

2. 2. 2. 5. Live / Dead assay

Fluorescence based 'LIVE/DEAD[®] Viability/Cytotoxicity assay' (Invitrogen) was used to measure live and dead cells in the cultures simultaneously. The assay comprises two fluorescent dyes, Calcein AM (Cal AM) and Ethidium homodimer (Eth HD). Cal AM enters live cells freely and is cleaved by nonspecific cellular esterases into a fluorescent product i.e., Calcein (excitation: 485nm, emission: 520nm), which is

retained by intact cells. When excited the dye gives a green fluorescence. Eth HD (Ex: 520nm, Em: 620nm) intercalates into nucleic acids and produces a red fluorescence. It is a large molecule and can only enter cells with ruptured membranes therefore it is ideal for measuring dead cells. The assay allows high-throughput (microtiter plates) screening and is a basic research tool for studying apoptosis and cell proliferation. It is also useful for screening compounds that induce cytotoxicity.

A typical experiment included 100% live culture, 100% dead culture and experimental samples. Cells not exposed to any treatment were considered as '100% live culture'. '100% dead culture' was prepared by treating cells with 70% methanol for 45min. Samples were taken in triplicates on a 96 well plate (Becton Dickinson). Cells were washed once with PBS and incubated with the dyes at 37 °C for 30 min. As controls, 'mix dye', 'Cal AM only', and 'Eth HD only' solutions were included. Fluorescence was measured on SpectraMax: GEMINIXS microplate Fluorometer (Molecular devices). Before calculations, fluorescence from the dyes was subtracted from respective sample readings. Percentage viability was calculated relative to unexposed sample and percentage of dead cells was calculated relative to 100% dead culture. Calculations were done by using following formulas.

$$\% \text{ Live cells} = \frac{F(520)_{\text{sam}} - F(520)_{\text{min}}}{F(520)_{\text{max}} - F(520)_{\text{min}}} \times 100\%$$

$$\% \text{ Dead cells} = \frac{F(620)_{\text{sam}} - F(620)_{\text{min}}}{F(620)_{\text{max}} - F(620)_{\text{min}}} \times 100\%$$

F(520)max: Reading for 100% live culture + mix dye

F(520)min: Reading from 100% dead sample + mix dye

F(520)sam: Reading from experimental sample + mix dye

F(620)max: Reading for 100% dead culture + mix dye

F(620)min: Reading from 100% live culture + mix dye

F(620)sam: Reading from experimental sample + mix dye

2. 2. 2. 5. 1. Optimization of dye concentration

Optimal dye concentrations for each cell line were determined according to the user's manual provided with the kit. Briefly, exponentially growing cultures (> 90% viability) were exposed to different concentrations of dye (0.1, 1.0, 2.0, 3.0, 4.0, 5.0 μ M). No cells + 5.0 μ M dye and no cells + no dye (PBS only) were included as controls. Fluorescence was measured after every five min for 45 min. The minimum dye concentration and a suitable time producing the highest signal were considered as optimum for a given cell line. The experiment included samples in triplicates.

2. 2. 2. 5. 2. Calibration of the assay

Calibration curves for the cell lines were generated by mixing live and dead cells in different proportions (live/dead ratio: 10:0, 9:1, 8:2, 7:3, 6:4, 5:5, 4:6, 3:7, 2:8, 1:9, 0:10). Samples, in triplicates, were incubated with optimized dye concentrations for 30 min at 37 °C, readings were taken and relative percentage viability and relative percent of dead cells was calculated. Calibration curves were generated by plotting relative percentage of the cells against proportions of live/dead cells.

2. 2. 2. 6. Screening of the traditional Chinese medicine (TCM) compounds

2. 2. 2. 6. 1. Determination of a suitable time for drug exposure – an experiment with arsenic trioxide

In order to select the time points when we can see maximum effect of the drugs, a time-line experiment was performed with Arsenic trioxide. Exponentially growing cells (> 90% viability, 7.5×10^5 cells/ml) of the three cell lines (GM01310, XP3BE, GM10902) were exposed to 10 μ g/ml of arsenic trioxide for 10 min, 3 hrs, 6 hrs and 24 hrs. Relative percentage viability and relative percent of dead cells was calculated by 'LIVE/DEAD® Viability/Cytotoxicity assay' (Invitrogen) and viability curves over a time period were designed.

2. 2. 2. 6. 2. Cytotoxicity screening of the TCM drugs

All TCM drugs and their solvents were screened for cytotoxicity against three cell lines GM01310, XP3BE and GM10902. Healthy cultures (> 90% viability; 7.5×10^5 cells/ml) were seeded in 96 well plates (Becton Dickinson) a day before the actual experiment. Just before treatment with the drugs, culture media was carefully replaced with fresh media. Cultures were incubated with saturated solutions of the drugs (1 μ l/ 100 μ l of the cell suspension) for **10 min**; to observe an early effect and **24 hrs**; to observe a later effect at 37 °C. Unexposed samples were included as experimental controls. The relative percentage of viable and dead cells was measured by 'LIVE/DEAD® Viability/Cytotoxicity assay' (Invitrogen). The experiment was performed twice with three replicates of each sample.

2. 2. 2. 7. IC₅₀ values

IC₅₀ (Inhibition Concentration 50, IC₅₀) is the concentration of a drug required to inhibit 50% of cell growth. IC₅₀ values of the selected TCM drugs were determined through dose-response curves. Exponentially growing cultures (> 90% viability; 7.5×10^5 cells/ml) were exposed to serial dilutions of the selected TCM drugs for 24 hrs at 37 °C. Unexposed and solvent exposed samples were included as experimental controls. The relative percentage of viable and dead cells was calculated by 'LIVE/DEAD® Viability/Cytotoxicity assay' (Invitrogen) and dose-response curves for viable cells were generated. Experiment included four replicates of each sample.

IC₅₀ values of the drugs were calculated by the formula given below.

$$IC_{50} = b - \frac{[(b - a)(50\% - d)]}{(c - d)}$$

'a' and 'b' are the drug concentrations producing 'just more than 50%' and 'just less than 50%' viable cells, respectively and 'c' is the percent viability produced by drug concentration 'a', and 'd' is the percent viability produced by drug concentration 'b'.

2. 2. 2. 8. Cell cycle analysis by flow cytometry

Cell cycle analysis is an important tool for testing new drugs e.g., for cancer therapy (Jayat & Ratinaud, 1993). It helps in understanding drug cytotoxicity and its influence on a specific cell cycle phase, where it arrests and kills the cells. As an increased SubG1 fraction depicts cell killing by apoptosis (Kong *et al.*, 2005), the technique allows emphasizing the portion of cells undergoing apoptosis after drug

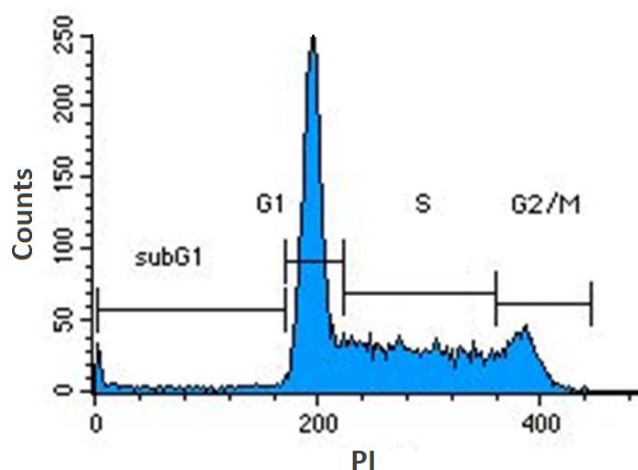


Figure.2.3. Different phases of cell cycle as observed with flow cytometry using PI (Propidium iodite) staining.

treatment. *In vitro* characterization of a potential drug helps forecast its activity *in vivo* (Jayat & Ratinaud, 1993).

Flow cytometry follows the principle of hydrodynamic focusing. During the process, samples are injected into the center of a liquid sheath flow, forcing them in a way that single cells are presented to a light excitation source e.g., a laser. As cells pass through the laser they scatter light. The Forward Scatter (FSC) and Side Scatter (SSC) represent the size and structure of the particles. Information is collected on light scattering, light excitation, and emission of fluorochrome molecules using specific detectors to generate specific multi-parameter data.

If cells are stained with a DNA staining dye e.g., Propidium iodide (PI), the emitted fluorescence will be proportional to DNA content present in cells (Jayat & Ratinaud, 1993). For a particular sample it will give a picture of different cell cycle phases.

Cells (Figure.2.3) with a single DNA content (diploid cells) are in G1 phase, cells with doubled DNA content (tetraploid cells) are in G2/M phase and cells with an intermediate DNA content lie in S phase of cell cycle. The apoptotic cells have less DNA than diploid cells and come in subG1 phase.

2. 2. 2. 8. 1. Determination of a suitable time for drug exposure – an experiment with arsenic trioxide

In order to determine a suitable time for TCM drug exposure to see a clear effect on cell cycle distribution, exponentially growing cells (> 90% viability; 7.5×10^5 cells/ml) of GM01310 were exposed to 0.73 and 2.2 $\mu\text{g/ml}$ (IC_{50} value for the cell line) of arsenic trioxide for 4 hrs, 8 hrs and 24 hrs. Cells were harvested by centrifugation (1000 rpm, 5 min, 4°C) and washed (2 X) with PBS. Cells were fixed by ice-cold fixative (70% Ethanol, 20% deionized H_2O , 10% PBS) added drop wise while vortexing. Fixed samples remained at -20°C for overnight followed by centrifugation (1000 rpm, 5 min, 4°C). Cell pellets were washed with PBS and samples were incubated with staining solution (100 $\mu\text{g/ml}$ RNaseA, 50 $\mu\text{g/ml}$ PI) for 30 min in dark. DNA content of the samples was measured by flow cytometry on a FACSCalibur flow cytometer (Becton Dickinson Biosciences) with the help of 'CellQuestPro' (Becton Dickinson Biosciences) software. 10,000 cells per sample were gated as single cells and three readings per sample were recorded. The parameters recorded were Forward Scatter (FSC), Side Scatter (SSC), FL2-Height, FL2-Area und FL2-Width (FL2 stands for Fluorescence 2 and represents PI fluorescence). Gating out of doublet cells or clumps and boundaries of different cell cycle phases (sub G1, G1, S, G2/M) in the samples was based on the unexposed samples.

2. 2. 2. 8. 2. Effect of TCM drugs on cell cycle distribution

To analyze the effect of selected drugs and their solvents on cell cycle distribution in NER deficient and proficient cells, exponentially growing cultures (> 90% viability; 7.5×10^5 cells/ml) of GM01310, XP3BE and GM10902 were treated with different doses of the drugs for 24 hrs. The drug concentrations were picked from dose-response curves generated during IC_{50} calculations. As control, unexposed samples

were included in each experiment. Samples were handled as explained above and experiments were performed twice with three replicates for each treatment.

2. 2. 2. 9. Single cell gel electrophoresis (Alkaline Comet assay)

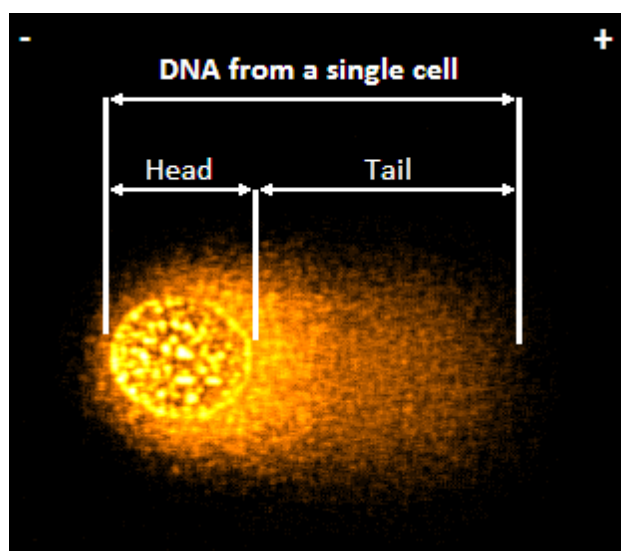


Figure.2.4. Comet from a damaged cell.

The single cell gel electrophoresis or 'Alkaline Comet assay' was performed to quantify the genotoxic effects of the selected TCM drugs and their solvents on repair deficient and repair proficient cell lines. The assay was carried out as described by Singh *et al.*, (1988) with some modifications (Popanda *et al.*, 2003). Briefly exponentially growing cells (> 90% viability) were exposed to different concentrations of the selected drugs and their solvents for one hour. As control, unexposed samples were included. Cells were collected and kept on ice to minimize repair processes. Samples were centrifuged (1000 rpm, 5 min, 4°C) to wash out the drugs and resuspended (2.7×10^5 cells/ml) in basic culture medium (RPMI1430 + Penicillin / Streptomycin). To prevent additional DNA damage, further steps were performed under red light. 25 μ l of sample were embedded in 175 μ l of 0.7% low-melting agarose (SeaPlaque®GTG® agarose; Biozym, Oldendorf, Germany) and spotted on 20 spot comet assay slides (Trevigen) in triplicates. Cells were incubated in lysis buffer (2.5 M NaCl, 10 mM Trizma-Base at pH 10.0, 100 mM Na₂ EDTA, 1 % sodium sarcosinate, 1 % Triton X-100, 10 % DMSO) for overnight at 4°C. Slides were

kept in a pre-chilled alkaline solution (NaOH 0.3 M, EDTA-Na₂ 1.0 M; pH 13.1) for 20 min to allow unwinding of DNA followed by electrophoresis (25 V, 300 Amp, 20 min). Larger DNA molecules will stay in the nuclei whereas smaller fragments will move out towards anode forming a tail and give a comet like shape (Figure.2.4) to the cells. If the amount of damaged DNA is high, more fragments will move out. The slides were then immersed two to three times in absolute ethanol and air dried. Slides were stained with SYBR-green (Biozol; 0.2 µl/ml TE buffer) for 30 min and analyzed with the software 'Komet 4' (semi automated system; Kinetic Imaging Ltd., Liverpool, UK). The program is designed to differentiate comet head from tail and to measure a variety of parameters including tail length, percentage of total fluorescence in head and tail, and 'tail moment'. Fifty one cells per replicate (153 cells per treatment) were scored and olive tail moment was determined. Olive Tail Moment (Olive *et al.*, 1990) is defined as the product of the tail length and the fraction of total DNA in the tail.

$$\text{Olive tail moment} = \text{tail length} \times \% \text{ DNA in tail}$$

Note: Tail length is the distance of DNA migration from the body of the nuclear core and it is used to evaluate the extent of DNA damage.

As Olive tail moment has a skew distribution, median values of the three replicates were taken and means \pm standard deviation was calculated for each treatment. Tail moment relative to unexposed sample was determined. For the data, back ground damage, drug induced damage, and effect of the solvent were estimated. The analysis did not include the edges and damaged parts of the gel as well as debris, superimposed comets and ghost cells.

2. 2. 2. 10. Formamidopyrimidine DNA glycosylase (Fpg)-modified comet assay

Fpg is a repair glycosylase that detects primarily 8-oxo-7,8-dihydro-2'-deoxyguanosine (Dianov *et al.*, 1999) sites in DNA samples (Azqueta *et al.*, 2009). The Fpg-modified comet assay was performed to quantify the oxidative DNA

damage potentially caused by Ascaridol in repair-deficient and repair-proficient cell lines. The assay was performed as described previously (Collins *et al.*, 1993, Collins *et al.*, 2001, Domijan *et al.*, 2006, Eiberger *et al.*, 2008) and its procedure was essentially similar to the alkaline comet assay. Exponentially growing cells (> 90% viability) were treated with the drug for one hour. Cells were harvested and centrifuged (1000 rpm, 5 min, 4°C) to wash out the drugs. Cells were resuspended (2.7×10^5 cells/ml) in basic culture medium (RPMI1430 + Penicillin / Streptomycin) and embedded in 0.7% agarose gel (SeaPlaque®GTG® agarose; Biozym, Oldendorf, Germany) and spotted on 20 spot comet assay slides (Trevigen) in quadruplicates. Two identical slides were prepared for each cell line. Cells were lysed for overnight and slides were immersed thrice in 1X Flare buffer (Trevigen) for 15 min. One of the slides was incubated with freshly prepared Fpg solution (New England Biolabs; 8U/ml 1X NEBuffer-1) for 50 min at 37°C. The second slide was incubated with 1X NEBuffer-1 (New England Biolabs) at the same conditions. Afterwards, they were placed on ice for 40 min to solidify the agarose gel again. Slides were then immersed in a pre-chilled alkaline solution (NaOH 0.3 M, EDTA-Na₂ 1.0 M; pH 13.1) three times for 15 min each. To allow unwinding of DNA they were kept in this pre-chilled alkaline solution for 20 min followed by electrophoresis (25V, 300Amp, 20 min). The slides were immersed two to three times in absolute ethanol and air dried. Staining was performed by SYBR-green (Biozol; 0.2 µl/ml TE buffer) for 30 min and slides were analyzed the software 'Komet 4' (Kinetic Imaging Ltd., Liverpool, UK). One hundred and fifty-three cells per treatment were scored and olive tail moment was determined.

The NEBuffer-1 treated slides provide an estimate of the background of DNA strand breaks (SB). The Fpg-treated slides reveal strand breaks and oxidized bases (SB + OX). Assuming a linear dose-response of either % DNA in tail or in arbitrary units, subtraction of (SB) from (SB + OX) gives a measure of oxidised pyrimidines/purines in the samples. Therefore

$$\text{Fpg sensitive lesions} = \text{OTM}_{\text{Fpg}} - \text{OTM}_{\text{Buffer}}$$

OTM_{Fpg}: Olive tail moment of Fpg treated samples

OTM_{Buffer}: Olive tail moment of buffer treated samples

For each treatment the Fpg sensitive lesions (mean \pm standard error) were considered as a measure of oxidative DNA damage. For the data, back ground damage, drug induced damage, and effect of the solvent were estimated.

2. 2. 2. 11. Reactive oxygen species (ROS) production

Intracellular ROS was detected by the fluorescent dye 2',7'-dichlorodihydrofluorescein diacetate (H₂DCFDA). The dye enters the cells where it gets cleaved by intracellular esterases forming a nonfluorescent molecule, 2', 7'-dichlorofluorescein (DCFH). In the presence of H₂O₂, DCFH gets oxidized to the fluorescent compound dichlorofluorescein (DCF). XP4PA and XP4PA-SE2 cells were seeded (6 X 10⁴ / ml) in 96 well plates for overnight. Cultures were washed once with PBS and wells were loaded with 25 μ M H₂DCFDA. Immediately before starting the measurement, cells were exposed to different ascaridol concentrations, DMSO (solvent) and different H₂O₂ concentrations as a positive control. Unexposed samples and samples without cells were also included as control. Fluorescence in the samples was measured by CytoFlour multi well plate reader, series 4000 at Ex / Em : 485 / 520 nm for 40 min. The rate of ROS production was generated in terms of arbitrary fluorescence units per min (Rate_{ROS} = AFU/min) and rate of ROS production relative to the unexposed sample (RR_{ROS}) was calculated for each cell line.

2. 2. 2. 12. Aldehyde reactive probe (ARP) assay

Apurinic / apyrimidinic site (AP) sites are one of the major type of lesions in DNA. AP sites can be formed by spontaneous depurination. They also occur as an intermediate in base excision repair (Boiteux & Guillet, 2004). In this process, a damaged base is recognized and cleaved by a DNA glycosylase, leaving an AP site.

The AP site can then be cleaved either by an AP endonuclease or by bifunctional glycosylase-lyases. Both mechanisms form a single-strand break, which is then repaired by base excision repair. Detection of AP sites can be a measure of oxidative damage.

AP sites were counted using the DNA damage quantification assay-AP site counting (DOJINDO molecular technologies, Inc.). The assay constitutes of aldehyde reactive probe (ARP), a biotinylated alkoxyamine that reacts specifically with the aldehyde group in the ring opened AP site. AP sites are thus tagged with a biotin residue. These sites can then be quantified with an ELISA-like assay, using avidin-biotin complex conjugated with horseradish peroxidase (HRP) as an indicator enzyme. Cells were incubated with drugs for 24 hours, harvested and DNA was extracted using QIAamp DNA blood mini kit (Qiagen). DNA samples (100 µg/ml) were coupled with 10 mM biotinylated ARP solution for 1hr at 37 °C, than diluted in TE buffer, and filtered twice to purify the ARP-tagged DNA. The tagged DNA was bound to the wells of a 96-well microtiter plate in the dark at room temperature overnight. The samples were washed thoroughly and incubated with HRP-streptavidin solution (1 in 4000 dilution) for 1hr at 37 °C, washed again and incubated with HRP substrate for 1hr at 37 °C. The absorbance was measured at 650 nm using SpectraMax: GEMINIXS microplate Fluorometer (Molecular devices). The number of AP sites in the treatment group was measured relative to the solvent control and was quantified by using standard ARP labeled DNA solution (Dojindo Molecular Technologies, Inc.). Standard ARP labeled DNA solution has a known amount of AP sites, ranging from 0 to 40 per 1×10^5 base pairs of calf thymus DNA.

2. 2. 2. 13. Determination of gene expression

2. 2. 2. 13. 1. RNA extraction and quantification

Total RNA was extracted using RNeasy mini kit (Qiagen, Hilden, Germany) and spin technology according to the protocol provided by the company. The following options were used during the extraction. After lyses samples were homogenized by passing at least 5 times through a blunt 20-gauge needle (BD Microlance™ 3) fitted to an RNase-free syringe (BD Discardit™ II). Final elution of RNA was performed

twice to increase the yield, first with 30µl, then with 10µl RNase-free water. Optical densities of RNA samples were measured on nanodrop spectrophotometer (ND 1000, PeQlab biotechnologie GmbH). The samples were handled on ice and stored at -80°C.

2. 2. 2. 13. 2. Reverse Transcription and cDNA amplification (RT-PCR)

Using the total RNA samples, first-strand cDNA was synthesized using Random Hexamer primers (Thermo Fisher Scientific GmbH, Ulm, Germany) and superscript III reverse transcription (Invitrogen). Random hexamers are random oligo deoxyribonucleotides. They have higher sensitivity and can amplify short and fragmented mRNA with or without a poly-A tail. Random hexamers are ideal for mRNA samples having low concentration as they provide higher yields.

As cDNA was later to be used for gene expression studies, same amount of RNA (1 µg) was taken for all samples. Reverse transcription comprised two steps. Table.2.19 gives the reaction mixtures for both steps. First the Mini mix (12 µl) was incubated at 65°C for 5 min following incubation on ice for 1 min. Next Master mix (8 µl) was added and samples were incubated at 25°C for 5 min, at 42°C for 50 min.

Table.2.19. Reaction mixture for the two step RT-PCR

Reagents	Final concentration
Mini mix (volume = 12 µl)	
Total RNA	1µg
Random primer (200 ng/ml)	0.025 µg/µl
dNTPs (10 mM)	0.5 mM
ultraPURE™ H ₂ O	To fill the volume
Master mix (volume = 8 µl)	
5 x first strand buffer	1 x
DTT (0.1 M)	0.01M
SuperScript™ III RT (200 U/µl)	10 U/µl
Rnasin (40 u/µl)	2 u/µl
Final reaction volume	20 µl

The reaction was inactivated at 70°C for 15 min. 2 µl of the cDNA was aliquoted to check reverse transcription and the remaining samples were diluted to 1:10 and stored at -80°C till further experiments.

2. 2. 2. 13. 3. RNA/cDNA Quality check assay

To check quality of RNA and resultant cDNA, *Clathrin* gene was amplified at 5'- and 3'-ends. Clathrin is a large gene with mRNA around 6000 bp. The gene was amplified by specific primers (Table.2.4) to yield a 570 bp fragment at 5'- end and a 550 bp fragment at 3'- end. In case of complete conversion of mRNA into cDNA, the amount of both PCR products will be same. Table.2.20 and 2.21 provided PCR conditions for the reactions. PCR products (Fig.2.5) were separated on a 1.5% agarose gel (300 mA, 100 V, 30 min).

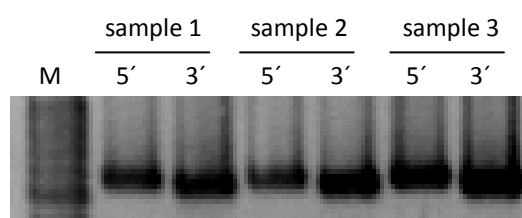


Figure.2.5. Amplification of *Clathrin* gene

Table.2.20. Clathrin-PCR program

	Step	Temperature (°C)	time
1 cycle	initial denaturation	95	15 min
30 cycles	i- denaturation	94	30 sec
	ii- Annealing	56	30 sec
	iii- extension	72	60 sec
1 cycle	elongation	72	7 min

Table.2.21. Clathrin-PCR reaction mixture

Reagents	Final concentration
ultraPURE™ H2O	To fill up the volume
Qiagen 10 x PCR buffer	1 x
Forward Primer (50 µM)	0.5 µM
Reverse Primer (50 µM)	0.5 µM
dNTPs (10 mM)	0.2 mM
Qiagen Taq DNA Polymerase (5 U/µl)	0.05 U/µl
cDNA	0.05 µl/µl of reaction mix

2. 2. 2. 13. 4. Relative quantification of ERCC6 and GAPDH by real time PCR

Relative quantification was done by real time PCR using gene specific primers and QuantiTect SYBR Green PCR master mix (Qiagen) on a lightcycler480 (Roche, Mannheim, Germany). Samples were analyzed by LightCycler®480 software (version 1.5.0). QuantiTect SYBR Green PCR master mix contains HotStarTaq DNA polymerase, PCR buffer, dNTPs and fluorescent dyes (SYBR Green I and ROX). In solution, the unbound SYBR Green I exhibits very little fluorescence; however, fluorescence (wavelength, 530 nm) is greatly enhanced upon intercalation to double stranded DNA. During PCR, a laser excites the dye and signal is measured after every cycle (real time) by specific detectors. The increase in SYBR Green I fluorescence is directly proportional to the amount of double-stranded DNA generated. The software plots the measured fluorescence against the no. of cycles and generates a sigmoid curve (Figure.2.6). From these plots it automatically calculates the *Crossing Point* (Cp) values. The Cp values represent the PCR cycle when the signal raises from the threshold. The quantity of target gene is compared with the reference sequence in the same samples and final result is expressed as a ratio of these targets. This step corrects for the differences in starting RNA/cDNA quantity, and RNA quality.

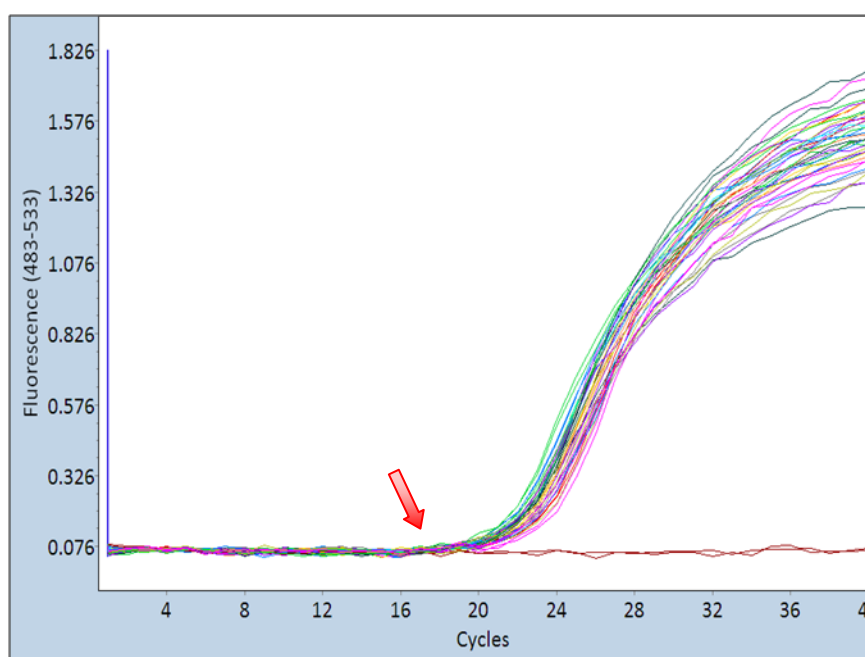


Fig.2.6. A typical sigmoid plot obtained by fluorescence measurement during mRNA quantification. Arrow represents the Cp value of the gene.

2. 2. 2. 13. 4. 1. Establishing and optimization of real time PCR

For each gene three primer pairs were designed and PCR conditions were optimized as described previously (2.2.1.2.3 Optimization of PCR conditions). The best performing primer pair was selected for real time quantification. Real time PCR was established in 384 well plate (Steinbrenner Laborsystems GmbH). This format allowed keeping target and reference genes in the same run therefore calibrators were not needed. The target gene was quantified in samples with two different cDNA concentrations (undiluted, 1:10). The Cp values for both concentrations were calculated by the software. As PCR product doubles after every cycle, the PCR efficiency was automatically picked by the software as 2. The dilution of cDNA, and number of cycles required to produce enough signal were plotted. PCR program and conditions followed are given in Table.2.22 and 2.23.

Samples were measured in triplicates and for calculations mean Cp values were taken. As a check for cross contamination negative control (no cDNA) samples were placed at different positions on the plate. The cDNA dilution allowing easier detection of the target genes was considered as suitable and annealing

temperature producing least difference among replicates was considered as optimum.

2. 2. 2. 13. 4. 2. Relative quantification of *ERCC6* and *GAPDH*

ERCC6 and *GAPDH* were quantified using gene specific primers (Table.2.3) and standardized PCR conditions (Table.2.22 and 2.23). *HPRT* (mean Cp value = 22.8) was included as housekeeping gene and quantification of *ERCC6* and *GAPDH* was done relative to *HPRT* (Relative quantity of target gene = Target Cp /Reference Cp).

Table.2.22. Reaction mix for quantitative PCR

Reagents	Final concentration
cDNA	
Quantitect (2 X)	1 X
Gene specific primer mix (10 μ M)	0.5 μ M
ultraPURE TM H ₂ O	to fill the volume
Final reaction volume	7 μl

Table.2.23. Cycling conditions for real time quantification PCR.

Program name	Cycles	Analysis mode	Target temperature (°C)	Acquisition mode	Ramp rate (°C / sec)	Acquisition rate (per °C)	Hold
Pre-incubation	1	None	95	None	4.4	-	15 min
Amplification	44	Quantification	95	None	2.2	-	30 sec
			60	None	2.2	-	30 sec
			72	Single	4.4	-	30 sec
Melting curve	1	Melting curves	95	None	4.4	-	1 min
			40	None	2.2	-	1 min
			80	Continuous	-	2	-
Cooling	1	None	40	none	2.2	-	10 min

2. 2. 2. 14. Protein extraction

Depending on the cell type, cells were harvested either by centrifugation or by trypsinization. Samples were washed with PBS, centrifuged (1000 rpm, 5 min, 4°C) and cell pellets were resuspended in 100 µl per 1×10^6 cells of lysis buffer (20mM Tris, 7 M urea, 100mM DDT, 1% Triton-X 100, Roche Complete Mini Tabs as Protease inhibitor, 1 mM $MgCl_2$ and 1 mM Phenylmethylsulfonyl fluoride). Samples were incubated on ice for 30 min followed by Benzonase (1 µl / 100µl lysis buffer) addition and incubation at 37°C for 30 min. Samples were centrifuged (13000 rpm, 5 min, 4°C) to settle the cell debris down, supernatant was carefully collected in clean tubes and samples were stored at -80°C.

2. 2. 2. 14. 1. Quantification of protein samples

Protein samples were quantified by Bio-Rad protein assay, based on the method of Bradford, which is a spectroscopic analytical procedure (Bradford, 1976; Compton & Jones, 1985). The assay comprises of an acidic solution of Coomassie® Brilliant Blue G-250 dye which binds to proteins causing a spectral shift from 465nm - 595nm. A subsequent measurement at 595 nm with a spectrophotometer and comparison to a standard curve provides a relative measurement of protein concentration.

Briefly, protein samples (2 µl) were incubated with H₂O (798 µl) and Bradford reagent (200 µl, protein assay, Bio-Rad) for 5 min at room temperature. Lysis buffer was used as a blank sample. Absorbance was measured on Biophotometer (version 1.35, eppendorf). Protein concentration was calculated as follow.

$$\text{Total conc. } (\mu\text{g} / \text{ml}) = \text{measured protein reading} \times 400$$

400 is the dilution factor for the protein sample.

2. 2. 2. 14. 2. Sodium dodecyl sulfate polyacrylamide gel electrophoresis (SDS-PAGE)

Under denaturing conditions, protein samples can be separated according to their size on polyacrylamide gels (Goldenberg & Creighton, 1984; Laemmli, 1970). Mixing

protein solutions with anionic detergents like sodium dodecyl sulfate (SDS) denatures secondary and non-disulfide-linked tertiary structures, giving nearly a uniform negative charge along the length of the polypeptide. As voltage is applied, the anions migrate toward the anode (positive electrode) allowing protein fractionation by size.

Protein samples were denatured in the presence of LDS-sample buffer (1:4 ratio, Invitrogen) and 'NuPAGE sample reducing agent' (1:10 ratio, Invitrogen) at 70°C for 10 min and were placed quickly on ice. Samples were loaded on 10% NuPAGE precast Bis-Tris polyacrylamide mini-gels (1.5 mm X 10 well, Invitrogen) in SDS running buffer (1 X NuPAGE MOPS, Invitrogen), set in a vertical electrophoresis chamber (X Cell Sure Lock System, Invitrogen). Proteins were separated at 200 volts for one hour. MagicMark XP molecular weight marker (Invitrogen) was used as a size reference.

2. 2. 2. 14. 3. Western blotting

The proteins separated by SDS-PAGE were blotted on Polyvinylidene flouride (PVDF) membrane (0.45 μm , Invitrolon, Invitrogen). The PVDF membranes were soaked in 100% methanol for 30 sec, washed with dH_2O and equilibrated in transfer buffer (Table.2.24) for at least 5 min. Separately 2 filter papers and 4 to 6 foam pads were soaked in the transfer buffer. For blotting, foam pads, gel, PVDF membrane and filter papers were arranged, as shown in Figure.2.7, carefully so

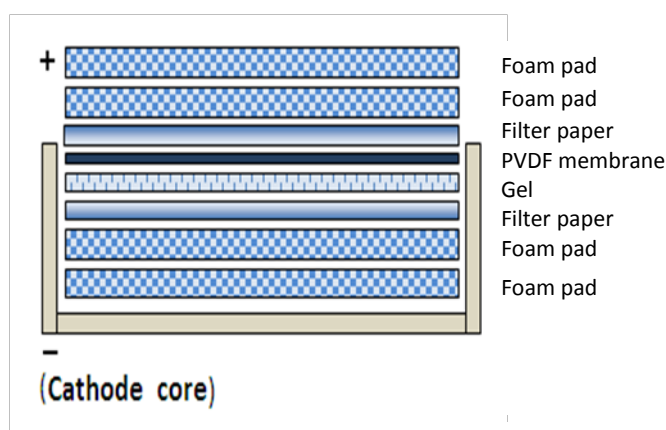


Figure.2.7. Arrangement of blotting apparatus

that no air bubbles are present. Blotting apparatus was filled with chilled transfer buffer and running chamber filled with chilled ddH₂O. Blotting was performed at 30 Volts for 70 min at room temperature.

Further steps were performed carefully with gentle shaking on a shaker (DuoMax 1030, Heidolph). The PVDF membrane was briefly washed twice with dH₂O and blocked with 5% milk solution in Tris Buffered Saline-Tween (TBST; 10 mM Tris pH 8.0, 150 mM NaCl, 0.05% Tween 20) at 4°C for overnight. Membrane was washed (3 x 5 min) with TBST and incubated with protein specific primary antibody (Table.2.25) for one hour at room temperature. Membrane was washed (4 x 10 min) again and incubated with secondary antibody solution for one hour at room temperature. Membrane was washed (3 x 15 min) again and incubated with 'Western Lightning Chemiluminescence reagent plus' system (Perkin Elmer) for 3 min. Extra solution was removed and membrane was placed in a transparent plastic bag. Under red light the membranes were exposed to Hyperfilm (Amersham) films and developed on Classic E.O.S. (Type 5270/100, AGFA). Developed films were photographed with digital camera (NV8, Samsung) and target protein bands were quantified with the help of Image J (version 1.41o; Rasband, NIH, USA). Quantification was relative to β -actin band.

Table.2.24. Transfer buffer for western blotting.

Reagents	Volume (for one gel)	Volume (for two gels)
20 x Transfer buffer	50 ml	50 ml
Methanol	100 ml	200 ml
dd H ₂ O	850 ml	750 ml

Note: Before use add 1ml Antioxidant

2. 2. 2. 14. 4. Stripping antibodies off the PVDF membranes

In order to quantify more than one protein on one blot, the membranes were stripped off of the antibodies. The membranes were incubated with 50 ml strip buffer (1 mM Tris pH 6.8, 10% SDS, 0.08% β -Mercaptoethanol) at 50°C for 15 min in a rotating oven (Biometra OV2) followed by washing with TBST. The membranes were again blocked and immunostained.

Table.2.25. Primary and secondary antibodies used during the course of study.

Primary antibody (santa cruz)	Company code	product size (kDa)	dilution used	type	secondary antibody (santa cruz)	dilution used
anti-XPC	sc-30156 (H-300)	125	1:500	rabbit polyclonal	goat anti-rabbit	1:2000
anti-p53	sc-55476 (C-11)	53	1:500	mouse monoclonal	goat anti-mouse	1:5000
anti-CSB	sc-10459 (E-18)	168	1:500	goat polyclonal	donkey anti-goat	1:2000
anti-β actin	sc-47778 (C4)	43	1:3000	mouse monoclonal	goat anti-mouse	1:5000

2. 2. 2. 15. Statistical analysis

2. 2. 2. 15. 1. Genotype frequencies

Allele frequencies were calculated by following formulas.

$$\text{Rare allele frequency (q)} = \frac{(aa*2) + Aa}{N*2}$$

$$\text{Wild type allele frequency (p)} = 1 - q$$

‘aa’ is the no. of individuals homozygous for variant allele

‘Aa’ is the no. of heterozygous individuals

‘N’ is the total no. of individuals

2. 2. 2. 15. 2. Hardy-Weinberg equilibrium

Allele and genotype frequencies were tested for Hardy-Weinberg equilibrium using the Chi-square test of goodness of fit with one degree of freedom. The formula used is given below. The $T_{\text{critical}} = 3.84$ for 1 degree of freedom. A chi-square value larger than this means that the genotype distribution deviates significantly from Hardy-Weinberg equilibrium.

$$\chi^2 = \sum \frac{(\text{Obs}_{AA} - \text{Exp}_{AA})^2}{\text{Exp}_{AA}} + \frac{(\text{Obs}_{Aa} - \text{Exp}_{Aa})^2}{\text{Exp}_{Aa}} + \frac{(\text{Obs}_{aa} - \text{Exp}_{aa})^2}{\text{Exp}_{aa}}$$

'Obs' is the observed no. of individuals

'Exp' is the expected no. of individuals and is calculated by $\text{Exp}_{AA} = n \cdot p \cdot p$,

$\text{Exp}_{Aa} = 2n \cdot p \cdot q$, $\text{Exp}_{aa} = n \cdot q \cdot q$, (p ; is the wild type allele frequency, q ; is the rare allele frequency)

2. 2. 2. 15. 3. Logistic regression analysis

Statistical analysis of the data was performed by using the statistical software package SAS (version 9.2). Odds ratios (OR) with 95% confidence intervals (CI) were computed by multivariate conditional logistic regression analysis, conditioned on age and gender and adjusted for smoking behavior, alcohol consumption and education. These potential confounders were differently distributed among cases and controls. The high frequency allele was taken as the reference genotype.

2. 2. 2. 15. 4. Gene-environment interaction

For estimating gene-environment interaction, the population was divided into subgroups. Smoking was quantified by the degree of tobacco consumption as pack-year (py) groups with ≤ 20 py and > 20 py (1 py = 20 cigarettes/day for 1 year). Regarding alcohol consumption population was subgrouped as: less than 25 g of alcohol intake/day, between 25–50 g of alcohol intake/day and above 50 g of alcohol consumed/day. For estimating a possible combined effect of smoking and alcohol intake on genotype and cancer risk, the study population was divided in the following three groups, (i) a group with a low exposure level included individuals with ≤ 20 py of smoking and ≤ 50 g of alcohol intake/day, (ii) a group with a medium exposure level included persons with ≤ 20 py of smoking and > 50 g alcohol consumption/day or > 20 py but ≤ 50 g of alcohol intake/day, whereas individuals with high exposure level had > 20 py and > 50 g of alcohol intake/day.

2. 2. 2. 15. 5. Linkage disequilibrium

Linkage disequilibrium values for SNPs present in the same gene and for genes located on the same chromosome were calculated using the EH program (Ott, 2006).

2. 2. 2. 15. 6. Haplotype analysis

Phase v 2.2.1.1 was used to estimate haplotype frequencies in cases and controls (Stephens & Donnelly, 2003). To test for haplotype-trait association, a generalized linear model (GLM) framework was used (haplo.glm). This model applies an iterative two-step expectation-maximization algorithm to estimate haplotype frequencies (Lake *et al.*, 2003). The GLM framework was adjusted for age, gender, smoking and alcohol consumption.

2. 2. 2. 15. 7. Gene-gene interaction

Gene-gene interaction was computed for the genes working as a complex in the NER pathway. For those SNPs that exhibit association with cancer risk in the present study, a 'risk score' was assigned to each group thereby increasing the score with each additional risk allele. Correction for multiple testing was considered according to Bonferroni (Silicon Genetics, 2003).

2. 2. 2. 15. 8. NER and cancer therapy

Data were statistically analyzed in Excel 2007. ANOVA and t-test (two tailed) were used to investigate statistical differences between unexposed, solvent exposed and drug treated samples within cell lines. Furthermore NER proficient cell lines were compared to NER deficient cell lines using these tests.



3. Results, NER and cancer risk

3.1. Quality control of genotyping data

3.1.1. Optimization of conditions for genotyping

Conditions for genotyping were carefully optimized. Suitable annealing temperature for the primers was selected by performing PCR with a temperature gradient and analyzing the samples on agarose gel. Samples were genotyped in high throughput by real time PCR using SNP specific LCTM Hybridization probes (Hybprobes). Suitable concentration of primers and probes used for real time PCR are provided in Table.2.1 & 2.5.

Optimized conditions were validated by genotyping 20 to 25 samples both by real time PCR on LC-480 and RFLP using SNP specific restriction enzymes. Genotypes obtained via both techniques were compared and a 100% concordance was found. Figure.3.1 presents an example for validation of optimized conditions for *ERCC5 Asp1104His* of three samples (318, 319 and 320). Figure.3.1-a shows the melting peaks of the samples obtained by real time PCR. Probes having a matched underlying sequence melt at 60.5°C and represent the 'G' allele whereas the probes having an unmatched underlying sequence melt at 55°C and represent the 'C' allele. The heterozygous samples carry a peak at both these temperatures. As the figure shows, the genotype of sample 318 is 'GG', sample 319 is 'CC' and sample 320 is 'GC'. For RFLP (Figure.3.1-b) the samples (PCR product size = 172 bp) were digested using the restriction enzyme *Nla111* (restriction site 5'...CATG^v...3'). The expected sizes after digestion were **GG** = 144, 28 bp, **CC** = 82, 62, 28 bp and **GC** = 144, 82, 62, 28 bp. As shown in the figure, sample 318 has a genotype 'GG', sample 319 is 'CC' and sample 320 is 'GC', validating the results obtained by real time PCR.

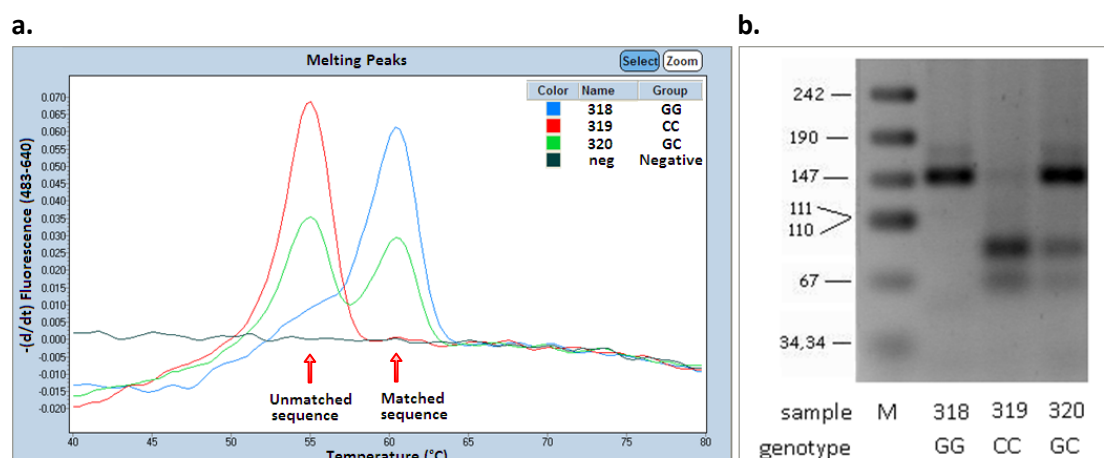


Figure.3.1. Genotyping results for *ERCC5* Asp1104His of three samples (318, 319 and 320).

a. Melting peaks obtained via real time PCR on LC-480. Matched sequence (60.5°C) represents the genotype 'G' and unmatched sequence (55°C) represents 'C'. **b.** RFLP of the samples (PCR product size = 172 bp) using the restriction enzyme *Nla*111. Expected sizes after digestion were **GG** = 144, 28 bp, **CC** = 82, 62, 28 bp and **GC** = 144, 82, 62, 28 bp. M = pUC19 DNA/MspI M,23 (Fermentas) was used as size reference.

3. 1. 2. Genotyping by fluorescence-based real time PCR

Genotyping assays were performed without knowledge of the clinical status. Genotyping data was checked by two investigators independently. Samples having ambiguous peaks were repeated. Melting temperatures (Table.3.1) of the probes were specific for matched and unmatched sequences and standards were used to analyze the melting peaks.

3. 1. 2. 1. Multiplex Hybprobe assay

In situations where two SNPs were analyzed in one reaction using multiplex Hybprobes, probes were labeled with different dyes. In case of *ERCC6* SNPs, RED640 was used for Arg1230Pro and RED610 was used for Arg1213Gly. For the detection of *ERCC2* Arg156Arg and *ERCC5* His46His, Hybprobes were labeled with RED640 and RED670, respectively. Additionally, for *ERCC2* Arg156Arg and *ERCC5* His46His, two separate pairs of primers having same annealing temperature and

PCR conditions were used. The complex peaks obtained by multiplex assays were resolved by color compensation.

3. 1. 3. Color compensation

Color Compensation was used as a tool to calibrate the LightCycler® Instruments. It corrected for the spectral overlap of fluorescence channels in multiplex Hybprobe assays. During a calibration run, the LightCycler® Instrument measured the fluorescence of each dye in all channels and generated an instrument-specific color compensation object 'CC Object'. In multiplex Hybprobe assays the CC Object was used to reassign the fluorescence in each channel to the appropriate dye. The net result is detection of only one dye signal in each channel.

Figure.3.2 demonstrates the detection of *ERCC6* Arg1230Pro and Arg1213Gly by using RED610 and RED640 in multiplex Hybprobe assay, with (Figure.3.2-b, d, & f) or without (Figure.3.2-a, c, & e) color compensation. The melting peaks observed at a wavelength of 610 nm are simple (Figure.3.2-a) and are not affected by color compensation (Figure.3.2-b). The melting peaks observed at a wavelength of 640 nm are complex (Figure.3.2-c) and following color compensation they get simplified (Figure.3.2-d). A similar effect was observed for samples in a 96 well plate (Figure.3.2-e & f).

3. 1. 4. Validation of genotyping data

3. 1. 4. 1. Restriction fragment length polymorphism (RFLP)

10% of randomly selected samples were genotyped by a second method, RFLP. Results obtained were compared with the genotyping data by LC-480 by two investigators, independently. A 100% concordance was found.

3. 1. 4. 2. Sequencing

As *ERCC2* Arg156Arg and *ERCC5* His46His were genotyped in multiplex Hybprobe assay, they were further validated by sequencing. Six samples were selected, two of these were homozygous for wild type allele, two were heterozygous and two homozygous for variant allele of each SNP. The amplified PCR products of the two

genes were separated on agarose gel. DNA bands were cut out of the gel and samples were extracted. Samples were sequenced and results obtained were 100% concordant with the genotyping data.

Table.3.1. Melting temperatures for Hybprobes used for genotype analysis

Gene	Polymorphism	Probe Sequence (5' - 3') ^a	Melting temperature (°C)	
			Matched sequence	Unmatched sequence
XPC	Lys939Gln	CTC AGC TCA CAG CT <u>I</u> CTC AAA TGG GAA CA ^{FL-3'} 5'LC-RED640-GTG GGA AGC TGC TGC TTT CTT TTC CCT TTT GG p	67	62
RAD23B	Ala249Val	TGA AGA CTG AGG A <u>A</u> C CCC A ^{FL-3'} 5'LC-RED640-CTA GCT GCT TGA GGG GGG TCA p	58	51
ERCC6	Arg1230Pro	5'LC-RED610-GCT TCT GGT A <u>A</u> G GCC TTT TCT TC p CCT TGG CCT CAC TCT TGT TTT CAC TGT C ^{FL-3'}	65.5	60.5
ERCC6	Arg1213Gly	TGG CGT CTC <u>C</u> GC AAT GCT T ^{FL-3'} 5'LC-RED640-GAG TTC TTA GGC TTT TGC TTT GGT CTC AGA T p	64	55
ERCC2	Arg156Arg	CGC AGT ACC AGC ATG ACA CCA GCC T ^{FL-3'} 5'LC-RED640-CCC CAC TGC <u>C</u> G C TTC TAT p	65	54
ERCC1	Asn118Asn	CGC A <u>A</u> C GTG CCC TGG GAA T ^{FL-3'} 5'LC-RED640-TGG CGA CGT AAT TCC CGA CTA TGT GCT G p	66.5	56.5
ERCC1	C8092A	GAC AAG AAG CGG A <u>A</u> G <u>C</u> AG CAG C ^{FL-3'} 5'LC-RED640-GCA GCA GCC TGT GTA GTC TGC CCC C p	69	61
ERCC1^b	IVS5+33	CCA CTG CAC AAC CTC AAA GCC <u>C</u> TG TGA GA ^{FL-3'}	73	68.5
ERCC4	Arg415Gln	CAT GTT <u>C</u> GG TCA TCA CTT GC ^{FL-3'} 5'LC-RED610-CAA ATC AGT ACT TGA CCT GAA AAT AGA AAA CA p	65.5	58
ERCC5	Asp1104His	TCA AGT GAA <u>G</u> AT GCT GAA AGT TC ^{FL-3'} 5'LC-RED640-CTT TAA TGA ATG TAC AAA GGA GAA CAG CTG p	60.5	55
ERCC5	His46His	TCG CCA <u>C</u> GG GAA CTC AAT ^{FL-3'} 5'LC-RED670-GAA AAT CCT CAT CTT CTC ACT TTG TTT CAT CG p	61.5	52

^a FL-3: probe is labeled with fluorescein at 3' position; 5'LC- RED*: probe is labeled with LightCycler-RedTM at 5' position; the position of polymorphism is underlined.

^b For ERCC1 IVS5+33 forward primer was labeled with LC-Red640 at 3' position.

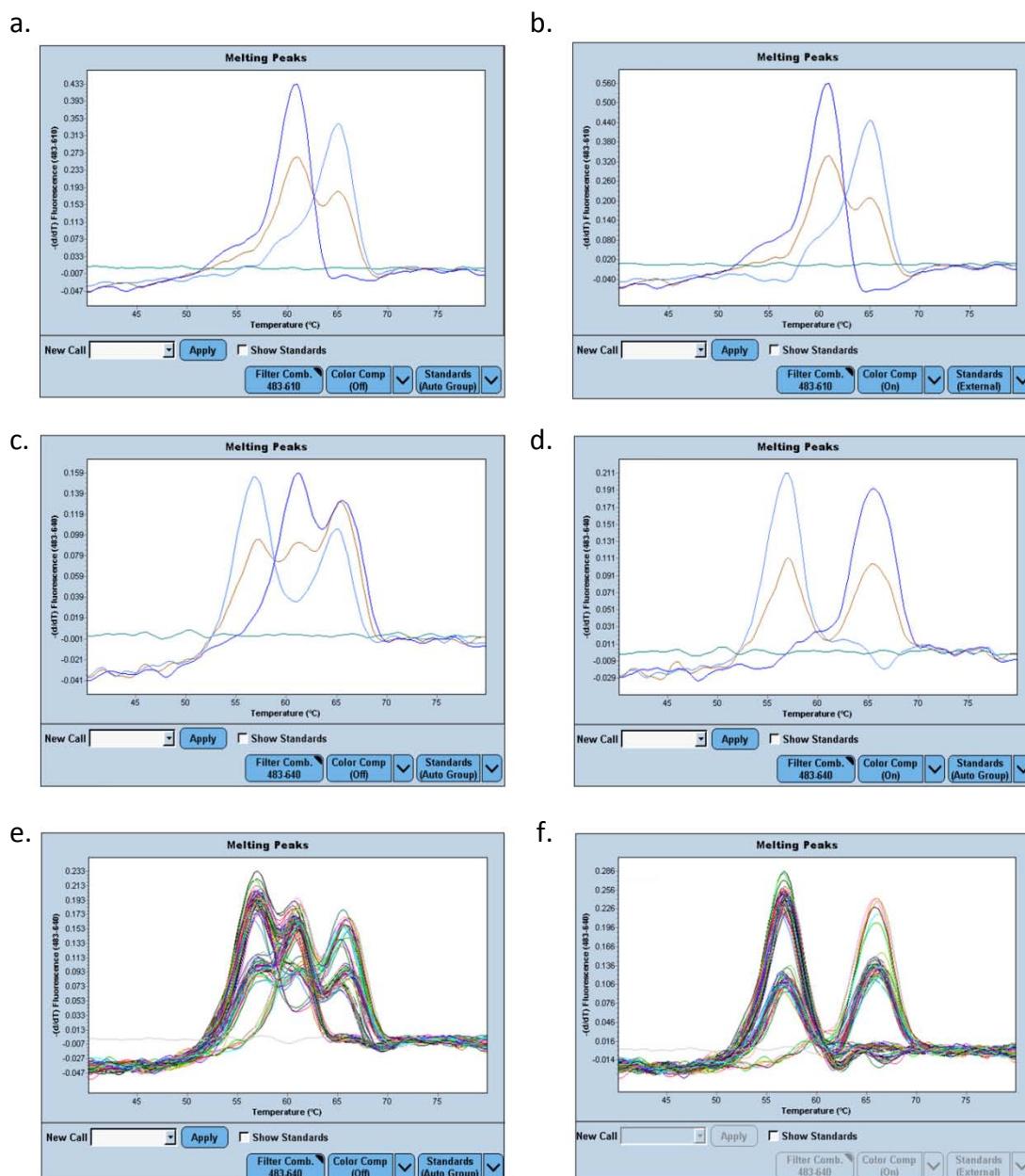


Figure.3.2 Effect of color compensation on melting peaks in multiplex Hybprobe experiments. a, c and e are samples without color compensation. b, d and f are the same samples with color compensation. a) melting peak of three samples at a wavelength of 610 nm, **b)** effect of color compensation on melting peak of the samples at a wavelength of 610 nm, **c)** complex melting peaks of the same three samples as in **a** and **b** at 640 nm, **d)** simplified melting peaks of the three samples at 640 nm after color compensation, **e)** melting peaks of samples in a 96 well plate at 640 nm without color compensation **f)** melting peaks of samples in the same 96 well plate as in ‘e’ after color compensation.

3. 2. Genotype analysis

In this study, a total of 11 SNPs in seven NER genes were investigated for their effect on larynx cancer risk. These included *XPC* (Lys939Gln), *RAD23B* (Ala249Val), *ERCC1* (Asn118Asn, C8092A and IVS5+33), *ERCC2* (Arg156Arg), *ERCC4* (Arg415Gln), *ERCC5* (Asp1104His and His46His) and *ERCC6* (Arg1230Pro and Arg1213Gly).

3. 2. 1. Genotype frequency

Figure.3.3 shows the rare allele frequencies of the SNPs in controls of the present study. For *all the SNPs* the allele frequencies were similar ($\leq \pm 5\%$) to those given for European Caucasian populations at the National Center for Biotechnology Information (NCBI).

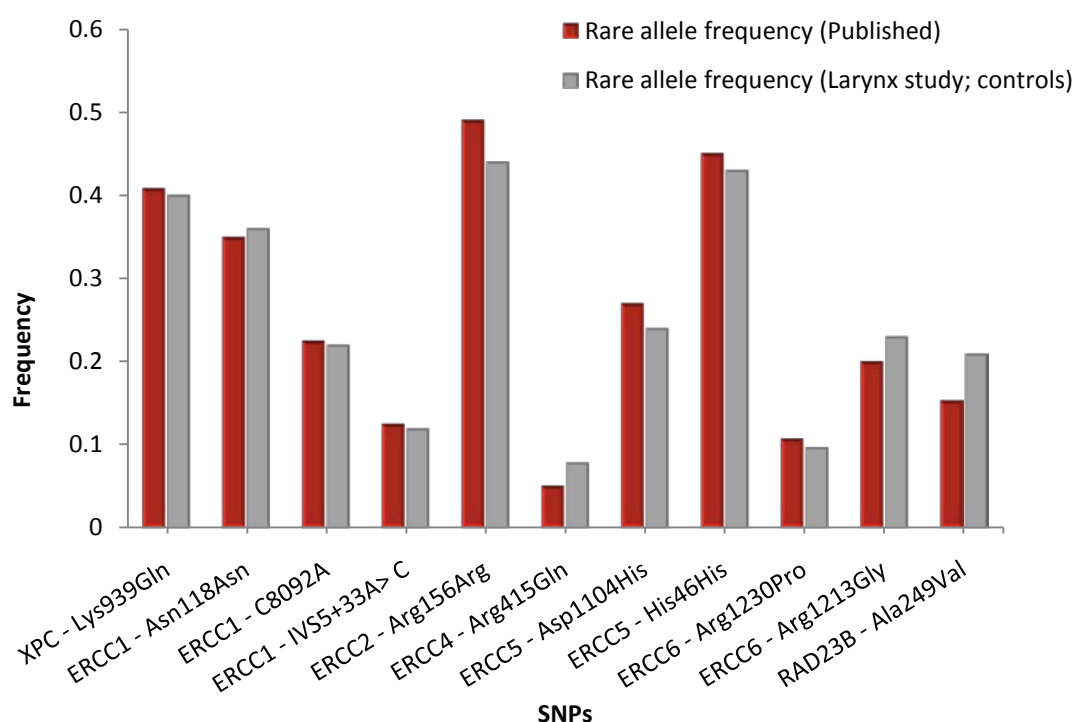


Figure.3.3. Rare allele frequency of each SNP in controls (red bars) compared with rare allele frequency of each SNP in European Caucasian population (gray bars) given at National Center for Biotechnology Information.

3. 2. 2. Genotype distribution

The allele and genotype frequencies were tested for Hardy-Weinberg equilibrium. The Hardy–Weinberg principle states that both allele and genotype frequencies in a population remain in equilibrium, from generation to generation unless specific disturbing influences like non-random mating, mutations, selection, limited population size, random genetic drift and gene flow are introduced (Campbell *et al.*, 2009). To test the allele and genotype frequencies for Hardy-Weinberg equilibrium, Chi-square test of goodness of fit with one degree of freedom was applied. The T_{critical} for one degree of freedom is 3.84. Figure.3.4 demonstrates that the genotype distributions of all the SNPs were consistent with Hardy-Weinberg equilibrium except for *RAD23B* Ala249Val ($\chi^2 = 6.28$). For this SNP, all the genotyping data was rechecked, additional 5% samples were genotyped by RFLP, and some of the samples were also sequenced. Results were compared with the genotyping data and 100% concordance was obtained, thus ruling out any technical discrepancies.

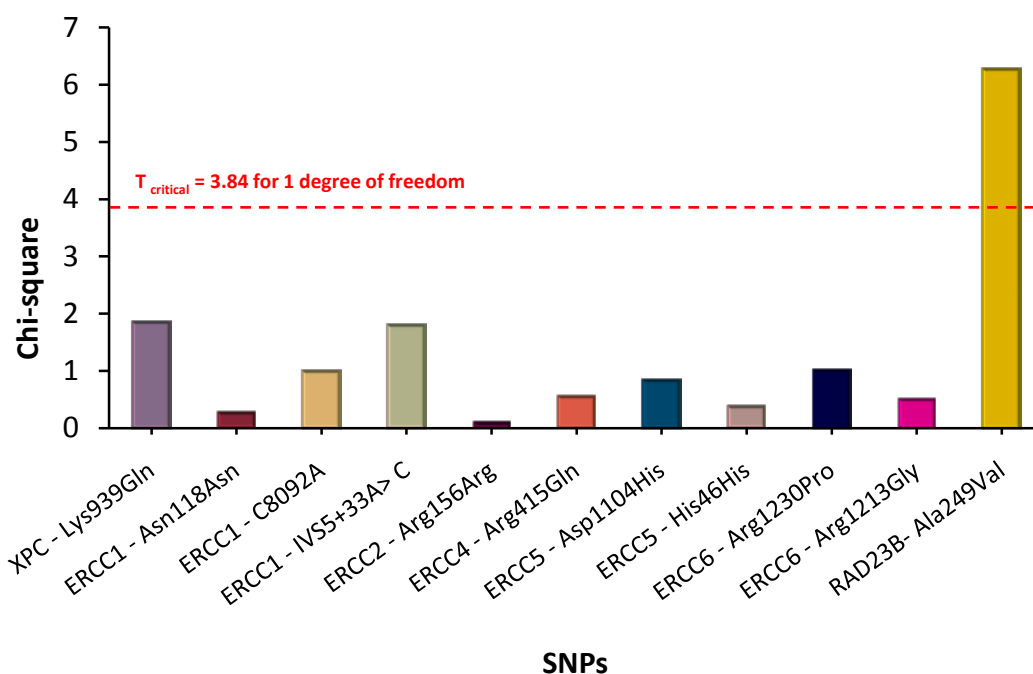


Figure.3.4. Chi-square values of whole population. Red line indicates the $T_{\text{critical}} = 3.84$ for 1 degree of freedom A chi-square value below this line shows that the genotype distribution does not deviate from Hardy-Weinberg equilibrium.

3. 2. 3. Larynx cancer risk

3. 2. 3. 1. Overall effect of genotype

To find the association between larynx cancer risk and the SNPs in NER genes, data were statistically analyzed by multivariate conditional logistic regression analysis and odds ratios (OR) with 95% confidence intervals (CI), conditioned on age and gender and adjusted for smoking behavior, alcohol consumption and education, were computed. The potential confounders were differently distributed among cases and controls. The high frequency allele was taken as the reference genotype. For each SNP, the distribution of gene variants in cases and controls, the crude and adjusted ORs and 95 % CI for laryngeal cancer risk are provided in Table.3.2.

An increased risk for larynx cancer was shown by the individuals homozygous for variant allele of *XPC* Lys939Gln (OR= 1.42, 95% CI 0.91 – 2.19), *RAD23B* Ala249Val (OR= 1.27, 95% CI 0.68 – 2.35) and *ERCC6* Arg1213Gly (OR= 1.37, 95% CI 0.75 – 2.51), where as individuals with at least one variant allele of *ERCC4* Arg415Gln and *ERCC5* His1104Asp exhibited an increased risk for the cancer (OR= 1.33, 95% CI 0.9 – 1.98) and (OR= 1.24, 95% CI 0.92 – 1.68) respectively. Also a decrease in risk for larynx cancer was found in individuals carrying variant allele of *ERCC2* Arg156Arg (OR= 0.74, 95% CI 0.48 – 1.15) and *ERCC6* Arg1230Pro (OR= 0.55, 95% CI 0.12 – 2.56), however these results did not reach a statistical significance. No change in OR was found for rest of the SNPs.

As the study population differs in educational status, smoking and alcohol intake, ORs were adjusted for these factors (Table.3.2). Figure.3.5 demonstrates a highly significant reduction in risk for larynx cancer was associated with the heterozygous group of *ERCC6* Arg1230Pro (OR=0.53, 95% CI 0.33 – 0.86) and in the Pro-allele carriers (OR=0.53, 95% CI 0.34 - 0.85). Heterozygote *ERCC5* Asp1104His carriers exhibited a significantly increased risk (OR=1.40, 95% CI 1.0 – 2.10). Risk association was not detected in the homozygous variant group for both SNPs largely due to the small number of samples. No statistically significant association was found between the other SNPs and laryngeal cancer risk in the current study.

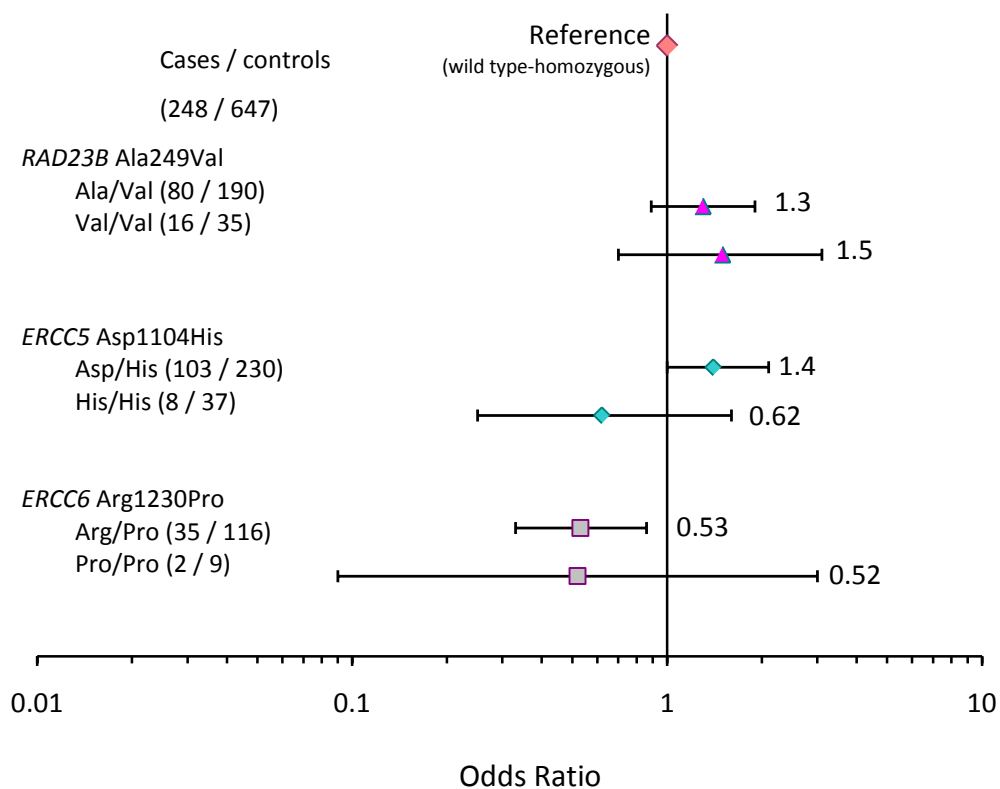


Figure.3.5. Overall effect of *RAD23B* Ala249Val, *ERCC5* Asp1104His and *ERCC6* Arg1230Pro on Laryngeal cancer risk. Wild type homozygous genotype was considered as reference. Bullets represent the 'OR', and whiskers show the respective '95% Confidence interval' obtained for the genotype. Results were stratified for age, gender and adjusted for education, smoking and alcohol intake.

Table.3.2. Genotype distribution and odds ratios (ORs) determined for larynx cancer cases and controls

Genotype	Cases		Controls		Crude odds ratio		Adjusted odds ratio ^a	
	n	(%)	n	(%)	OR	95% CI	OR	95% CI
Subjects analyzed	248	(100)	647	(100)				
XPC Lys939Gln								
Lys/Lys	83	(34)	230	(36)	1.0		1.0	
Lys/Gln	120	(48)	329	(51)	1.01	0.73 - 1.40	0.90	0.61 - 1.3
Gln/Gln	45	(18)	88	(14)	1.42	0.91 - 2.19	1.30	0.76 - 2.1
Gln carriers	165	(67)	417	(65)	1.10	0.80 - 1.49	0.98	0.68 - 1.4
RAD23B Ala249Val								
Ala/Ala	152	(61)	422	(65)	1.0		1.0	
Ala/Val	80	(32)	190	(29)	1.17	0.84 - 1.61	1.30	0.89 - 1.9
Val/Val	16	(7)	35	(5)	1.27	0.68 - 2.35	1.50	0.70 - 3.1
Val carriers	96	(39)	225	(35)	1.18	0.88 - 1.60	1.30	0.92 - 1.9
ERCC6 Arg1230Pro								
Arg/Arg	211	(85)	522	(81)	1.0		1.0	
Arg/Pro	35	(14)	116	(18)	0.75	0.49 - 1.12	0.53	0.33 - 0.86
Pro/Pro	2	(1)	9	(1)	0.55	0.12 - 2.56	0.52	0.09 - 3.0
Pro carriers	37	(15)	125	(19)	0.73	0.49 - 1.09	0.53	0.34 - 0.85
ERCC6 Arg1213Gly								
Arg/Arg	152	(61)	383	(59)	1.0		1.0	
Arg/Gly	78	(32)	231	(36)	0.85	0.61 - 1.16	0.82	0.57 - 1.2
Gly/Gly	18	(7)	33	(5)	1.37	0.75 - 2.51	1.20	0.59 - 2.5
Gly carriers	96	(39)	264	(41)	0.92	0.68 - 1.24	0.87	0.61 - 1.2
ERCC2 Arg156Arg								
CC	79	(32)	199	(31)	1.0		1.0	
CA	128	(52)	309	(48)	1.04	0.75 - 1.45	1.10	0.73 - 1.6
AA	41	(17)	139	(22)	0.74	0.48 - 1.15	0.79	0.48 - 1.3
A carriers	169	(68)	448	(69)	1.05	0.77 - 1.44	0.98	0.68 - 1.4
ERCC1 Asn118Asn								
TT	103	(42)	272	(42)	1.0		1.0	
TC	114	(46)	289	(45)	1.04	0.76 - 1.43	0.88	0.61 - 1.3
CC	31	(13)	86	(13)	0.95	0.59 - 1.52	0.65	0.37 - 1.1
C carriers	145	(59)	375	(58)	1.02	0.759-1.374	0.83	0.58 - 1.2

Table.3.2. Genotype distribution and odds ratios (ORs) determined for larynx cancer cases and controls

Genotype	Cases		Controls		Crude odds ratio		Adjusted odds ratio ^a	
	n	(%)	n	(%)	OR	95% CI	OR	95% CI
Subjects analyzed	248	(100)	647	(100)				
ERCC1 C8092A								
CC	146	(59)	392	(61)	1.0		1.0	
CA	87	(35)	218	(34)	1.07	0.78 - 1.46	0.91	0.63 - 1.3
AA	15	(6)	37	(6)	1.09	0.58 - 2.04	0.88	0.42 - 1.8
A carriers	102	(41)	255	(39)	1.07	0.78 - 1.45	0.90	0.64 - 1.3
ERCC1 IVS5+33A> C								
CC	194	(78)	498	(77)	1.0		1.0	
CA	50	(20)	135	(21)	0.95	0.66 - 1.37	0.78	0.51 - 1.2
AA	4	(2)	14	(2)	0.73	0.24 - 2.26	0.64	0.16 - 2.6
A carriers	54	(22)	149	(23)	0.93	0.65 - 1.32	0.77	0.51 - 1.2
ERCC4 Arg415Gln								
Arg/Arg	203	(82)	554	(86)	1.0		1.0	
Arg/Gln	44	(18)	90	(14)	1.33	0.9 - 1.98	1.50	0.92 - 2.3
Gln/Gln	1	(0)	3	(1)	0.91	0.09 - 8.79	0.60	0.05 - 6.7
Gln carriers	45	(18)	93	(14)	1.32	0.89 - 1.95	1.40	0.89 - 2.2
ERCC5 Asp1104His								
Asp/Asp	137	(55)	380	(59)	1.0		1.0	
Asp/His	103	(42)	230	(36)	1.24	0.92 - 1.68	1.40	1.0 - 2.1
His/His	8	(3)	37	(6)	0.60	0.27 - 1.32	0.62	0.25 - 1.6
His carriers	111	(45)	267	(41)	1.15	0.86 - 1.55	1.30	0.93 - 1.9
ERCC5 His46His								
CC	78	(32)	212	(33)	1.0		1.0	
CT	127	(51)	320	(50)	1.08	0.77 - 1.50	1.10	0.75 - 1.6
TT	43	(17)	115	(18)	1.02	0.66 - 1.57	1.30	0.80 - 2.2
T carriers	170	(69)	435	(67)	1.06	0.78 - 1.45	1.20	0.80 - 1.7

^a Stratified for age, gender and adjusted for education, smoking and alcohol intake.

3. 2. 3. 2. *Gene-environment interactions*

For evaluating gene-environment interactions by analysis of subgroups, the heterozygous individuals and the variant allele carriers (heterozygous + homozygous for variant allele) were regarded because for most SNPs the group of homozygous variants was too small for regression analysis.

3. 2. 3. 2. 1. *Effect of smoking and genotype on larynx cancer risk*

For estimating effect of smoking and genotype on larynx cancer risk, the population was divided into two subgroups, light smokers with ≤ 20 py and heavy smokers with > 20 py, where 1 py = 20 cigarettes/day for 1 year. Figure.3.6 and Table.3.3 demonstrate that the stratified results for smoking status presented a significantly reduced risk in heavy smokers (>20 py) for *ERCC6* Arg1230Pro heterozygous individuals (OR=0.59, 95% CI 0.35-0.98) and for *ERCC6* 1230Pro carriers (OR=0.56, 95% CI 0.34 – 0.93). The heterozygous group and the 249Val allele carriers of *RAD23B* displayed a significantly enhanced risk in heavy smokers (OR for heterozygosity = 1.70, 95% CI 1.1-2.7; OR for 249Val allele carriers = 1.60, 95% CI 1.10 – 2.50). In addition, cancer risk was increased in heavy smokers heterozygous for the *ERCC5* Asp1104His polymorphism (OR=1.7, 95% CI 1.1-2.5). There were no obvious effects of smoking on the association of other SNPs and larynx cancer risk (data not shown).

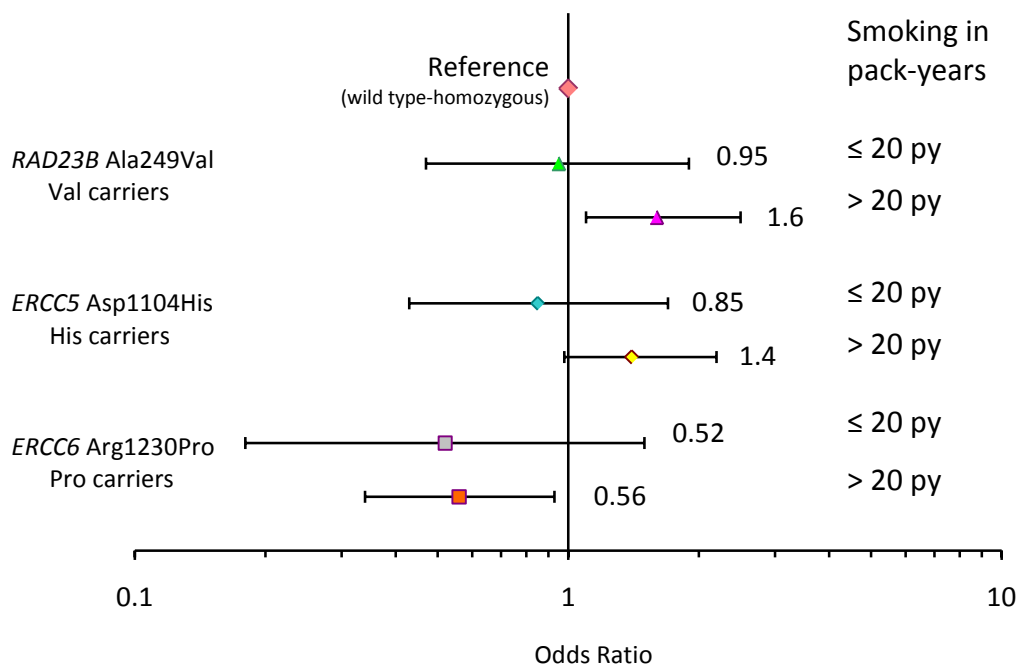


Figure.3.6. Smoking and different genotypes: Effect of *RAD23B* Ala249Val, *ERCC5* Asp1104His and *ERCC6* Arg1230Pro on Laryngeal cancer risk. Wild type homozygous genotype was considered as reference. Bullets represent the 'OR', and whiskers show the respective '95% Confidence interval' obtained for the genotype. Results were stratified for age, gender and adjusted for education, and alcohol intake.

Table.3.3. Larynx cancer risk: genotype distribution and odds ratios (ORs) for larynx cancer cases and controls after stratification for smoking

Genotype	Light smokers: ≤ 20 pack-years				Heavy smokers: > 20 pack-years			
	Cases	Controls	Adjusted odds ratio ^a		Cases	Controls	Adjusted odds ratio ^a	
	n (%)	n (%)	OR	95% CI	n (%)	n (%)	OR	95% CI
Subjects analyzed	42 (100)	429 (100)			206 (100)	218 (100)		
<i>RAD23B</i> Ala249Val								
Ala/Ala	28 (67)	270 (63)	1.0		124 (60)	152 (70)	1.0	
Ala/Val	9 (21)	136 (32)	0.70	0.31 - 1.6	71 (34)	54 (25)	1.70	1.1 - 2.7
Val carriers	14 (33)	159 (37)	0.95	0.47 - 1.9	82 (40)	66 (30)	1.60	1.1 - 2.5
<i>ERCC6</i> Arg1230Pro								
Arg/Arg	37 (88)	356 (83)	1.0		174 (84)	166 (76)	1.0	
Arg/Pro	4 (10)	68 (16)	0.43	0.14 - 1.3	31 (15)	48 (22)	0.59	0.35 - 0.98
Pro carriers	5 (12)	73 (17)	0.52	0.18 - 1.5	32 (16)	52 (24)	0.56	0.34 - 0.93
<i>ERCC5</i> Asp1104His								
Asp/Asp	25 (60)	243 (57)	1.0		112 (54)	137 (63)	1.0	
Asp/His	15 (36)	162 (38)	0.81	0.40 - 1.6	88 (43)	68 (31)	1.70	1.1 - 2.5
His carriers	17 (40)	186 (43)	0.85	0.43 - 1.7	94 (46)	81 (37)	1.40	0.97 - 2.2

^a Stratified for age, gender and adjusted for education and alcohol intake

3. 2. 3. 2. 2. Effect of alcohol intake and genotype on larynx cancer risk

For estimating effect of alcohol consumption and genotype on larynx cancer risk, the population was divided into three subgroups, less than 25 g of alcohol intake/day, between 25–50 g of alcohol intake/day and above 50 g of alcohol consumed/day. Figure.3.7 and Table.3.4 demonstrate, the heavy alcohol consumers (> 50g/day) exhibited a significantly reduced risk for the *ERCC6* 1230Pro carriers (OR=0.46, 95% CI 0.23 – 0.92). For *RAD23B* Ala249Val, a 2 fold significantly increased risk was observed with heterozygotes and with Val carriers in heavy alcohol consumers (> 50g/day; OR for heterozygosity = 2.00, 95% CI 1.1-3.6; OR for 249Val carriers=2.00, 95% CI 1.10 – 3.40). There were no obvious effects of alcohol intake on the association of other SNPs and larynx cancer risk (data not shown).

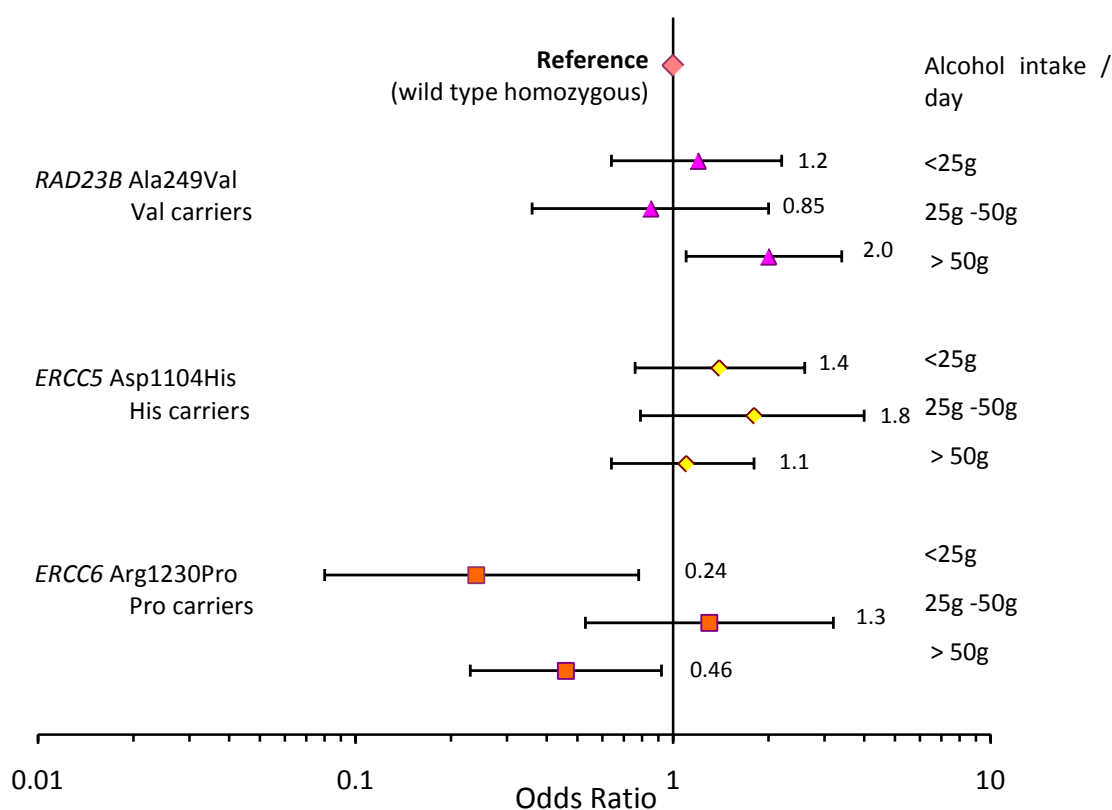


Figure.3.7. Effect of alcohol consumption and *RAD23B* Ala249Val, *ERCC5* Asp1104His and *ERCC6* Arg1230Pro on Laryngeal cancer risk. Wild type homozygous genotype was considered as reference. Bullets represent the 'OR', and whiskers show the respective '95% Confidence interval' obtained for the genotype. Results were stratified for age, gender and adjusted for education and smoking.

Table.3.4. Larynx cancer risk: genotype distribution and odds ratios (ORs) determined for larynx cancer cases and controls after stratification for alcohol consumption

Genotype	≤ 25g of ethanol / day				> 25g -50g of ethanol / day				> 50g of ethanol / day			
	Cases		Controls		Cases		Controls		Cases		Controls	
	Adjusted odds ratio ^a		Adjusted odds ratio ^a		Adjusted odds ratio ^a		Adjusted odds ratio ^a		Adjusted odds ratio ^a		Adjusted odds ratio ^a	
	n (%)	n (%)	OR	95% CI	n (%)	n (%)	OR	95% CI	n (%)	n (%)	OR	95% CI
Subjects analyzed	66 (100)	295 (100)			53 (100)	149 (100)			129 (100)	203 (100)		
RAD23B Ala249Val												
Ala/Ala	38 (58)	181 (61)	1.0		40 (75)	103 (69)	1.0		74 (57)	138 (68)	1.0	
Ala/Val	24 (36)	99 (34)	1.20	0.63 - 2.3	10 (19)	37 (25)	0.66	0.26 - 1.7	46 (36)	54 (27)	2.00	1.10 - 3.60
Val carriers	28 (42)	114 (39)	1.20	0.64 - 2.2	13 (25)	46 (31)	0.85	0.36 - 2.0	55 (43)	65 (32)	2.00	1.10 - 3.40
ERCC6 Arg1230Pro												
Arg/Arg	62 (94)	239 (81)	1.0		39 (74)	121 (81)	1.0		110 (85)	162 (80)	1.0	
Arg/Pro	3 (5)	52 (18)	0.18	0.05 - 0.69	13 (25)	27 (18)	1.20	0.48 - 3.1	19 (15)	37 (18)	0.50	0.25 - 1.0
Pro carriers	4 (6)	56 (19)	0.24	0.08 - 0.78	14 (26)	28 (19)	1.30	0.53 - 3.2	19 (15)	41 (20)	0.46	0.23 - 0.92
ERCC5 Asp1104His												
Asp/Asp	33 (50)	170 (58)	1.0		30 (57)	88 (59)	1.0		74 (57)	122 (60)	1.0	
Asp/His	29 (44)	112 (38)	1.40	0.72 - 2.6	21 (40)	48 (32)	2.20	0.96 - 5.3	53 (41)	70 (34)	1.20	0.71 - 2.1
His carriers	33 (50)	125 (42)	1.40	0.76 - 2.6	23 (43)	61 (41)	1.80	0.79 - 4.0	55 (43)	81 (40)	1.10	0.64 - 1.8

^aStratified for age, gender and adjusted for education and smoking.

3. 2. 3. 2. 3. Combined effect of smoking and alcohol intake and genotype on larynx cancer risk

For analyzing the combined effect of smoking and alcohol intake the study population was categorized into three groups, as shown by Figure.3.8 and Table.3.5. For Pro-carriers of *ERCC6* Arg1230Pro, a significant reduction in risk was observed at high exposure level (OR=0.47, 95% CI 0.22 - 0.98). His-heterozygotes for *ERCC5* Asp1104His exhibited a significant enhanced risk associated with the cancer in medium exposed group (OR=1.8, 95% CI 1.0 - 3.1). The Val-carriers in *RAD23B* Ala249Val had a 2.6-fold highly significant enhanced risk for larynx cancer at high exposure (OR=2.6, 95% CI 1.3 - 4.9). Risk increase was still stronger in subjects heterozygous for this SNP (OR=2.9, 95% CI 1.4-5.8). There were no obvious effects of smoking and alcohol intake on the association of other SNPs and larynx cancer risk (data not shown).

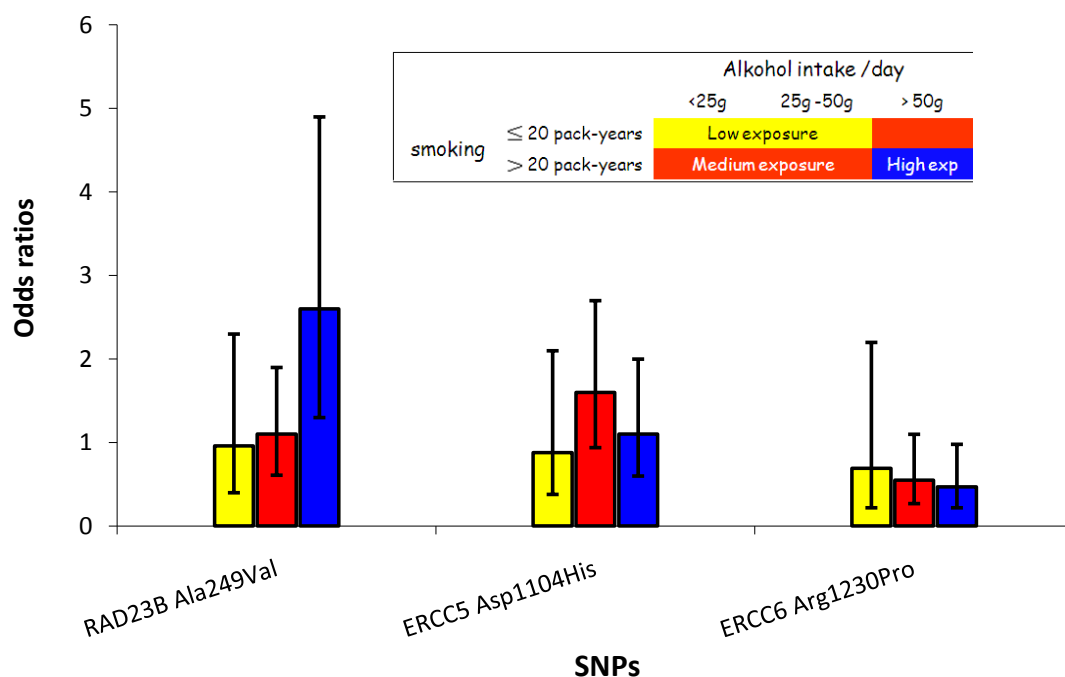


Figure.3.8. Combined effect of smoking and alcohol intake and different Genotypes, *RAD23B* Ala249Val, *ERCC5* Asp1104His and *ERCC6* Arg1230Pro on Larynx cancer risk. Wild type homozygous genotype was considered as reference and set to 1. Bars represent the 'OR', and whiskers show the respective '95% Confidence interval' obtained for the genotype. Results were stratified for age and gender, adjusted for education.

Table.3.5. Larynx cancer risk: genotype distribution and odds ratios (ORs) determined for combined effect of smoking and alcohol-intake in larynx cancer cases and controls

Genotype	Low exposure group ^a				Medium exposure group ^b				High exposure group ^c			
	Cases		Controls		Adjusted odds ratio ^d		Cases		Controls		Adjusted odds ratio ^d	
	n (%)	n (%)	OR	95% CI	n (%)	n (%)	OR	95% CI	n (%)	n (%)	OR	95% CI
Subjects analyzed	29 (100)	320 (100)			103 (100)	233 (100)			116 (100)	94 (100)		
<i>RAD23B</i> Ala249Val												
Ala/Ala	18 (62)	201 (63)	1.0		70 (68)	152 (65)	1.0		64 (55)	69 (73)	1.0	
Ala/Val	7 (24)	101 (32)	0.73	0.27 - 2.0	29 (28)	70 (30)	1.00	0.58 - 1.8	44 (38)	19 (20)	2.90	1.4 - 5.8
Val carriers	11 (38)	119 (37)	0.96	0.40 - 2.3	33 (32)	81 (35)	1.10	0.61 - 1.9	52 (45)	25 (27)	2.60	1.3 - 4.9
<i>ERCC6</i> Arg1230Pro												
Arg/Arg	25 (86)	265 (83)	1.0		88 (85)	186 (80)	1.0		98 (85)	71 (76)	1.0	
Arg/Pro	3 (10)	52 (16)	0.56	0.16 - 2.0	14 (14)	43 (19)	0.5	0.26 - 1.1	18 (16)	21 (22)	0.52	0.24 - 1.1
Pro carriers	4 (14)	55 (17)	0.69	0.22 - 2.2	15 (15)	47 (20)	0.6	0.27 - 1.1	18 (16)	23 (25)	0.47	0.22 - 0.98
<i>ERCC5</i> Asp1104His												
Asp/Asp	17 (59)	179 (56)	1.0		54 (52)	143 (61)	1.0		66 (57)	58 (62)	1.0	
Asp/His	10 (35)	122 (38)	0.79	0.32 - 1.9	45 (44)	78 (34)	1.80	1.0 - 3.1	48 (41)	30 (32)	1.30	0.68 - 2.3
His carriers	12 (41)	141 (44)	0.88	0.38 - 2.1	49 (48)	90 (39)	1.60	0.94 - 2.7	50 (43)	36 (38)	1.10	0.60 - 2.0

^a ≤ 20 pack-years of smoking & ≤ 50g ethanol per day,

^b ≤ 20 pack-years of smoking and >50g ethanol per day or > 20 pack-years of smoking and ≤ 50g ethanol per day,

^c > 20 pack-years of smoking and > 50g ethanol per day,

^d Stratified for age, gender and adjusted for education.

3. 2. 3. 3. Gene-Gene interactions

SNPs in genes working as a complex in NER pathway (*XPC-RAD23B* and *ERCC1-ERCC4*) and the genes showing an overall risk effect in the current study (*RAD23B-ERCC5-ERCC6*) were tested for a multiplicative effect associated with larynx cancer risk (Table.3.3). It was observed that presence of three risk alleles of *XPC* Lys939Gln and *RAD23B* Ala249Val increased the cancer risk by 2.1 fold (OR=2.1, 95% CI 1.0 - 4.3). Combined analysis of *ERCC1-ERCC4* SNPs did not reveal any significant effects. Carriers of more than one allele of genes showing an overall effect on risk were compared, risk increased up to 2 fold but the estimates were not statistically significant.

3. 2. 3. 4. Linkage analysis

SNPs present in the same gene and genes present on the same chromosome were analyzed for linkage. For SNPs in *ERCC1* (Asn118Asn, C8092A and IVS5+33), *ERCC2* (Arg156Arg, Lys751Gln and Asp312Asn) and *ERCC5* (Asp1104His and His46His), a highly significant allelic association was found ($P < 0.0001$ for both, larynx cancer cases and controls). The two SNPs present in *ERCC6* (Arg1213Gly and Arg1230Pro) presented a high association in larynx cancer cases ($P < 0.0001$), however weaker in controls ($P = 0.03$). *ERCC1* and *ERCC2* are located in close proximity on chromosome 19 and all the six SNPs from both these genes were strongly associated ($P < 0.0001$ for larynx cancer cases, controls). These results hint towards linkage disequilibrium.

3. 2. 3. 5. Haplotype analysis

Linked SNPs were analyzed for haplotype effects. For *ERCC6* (Arg1213Gly and Arg1230Pro) the carriers of the 1213Arg-1230Pro haplotype had a significant reduction in laryngeal cancer risk (OR=0.57, 95% CI 0.37 – 0.87). We did not find a statistically significant association between the other haplotypes and laryngeal cancer risk in the current study (data not shown).

Table.3.3. Larynx cancer risk and presence of more than one 'risk allele'. Combination of risk alleles from genes working as a complex in the NER pathway (*XPC + RAD23B* and *ERCC1 + ERCC4*) and the genes indicating larynx cancer risk when tested individually (*RAD23B + ERCC5 + ERCC6*)

No. of risk alleles	Cases	Controls	Crude odds ratio		Adjusted odds ratio ^a	
	n (%)	n (%)	OR	95% CI	OR	95% CI
Subjects analyzed	248 (100)	647 (100)				
<i>XPC - Rad23B</i>						
0	49 (20)	158 (24)	1.0		1.0	
1	105 (42)	263 (41)	1.30	0.87 - 1.9	1.30	0.81 - 2.1
2	69 (28)	181 (28)	1.23	0.80 - 1.9	1.30	0.76 - 2.1
3	25 (10)	45 (7)	1.80*	1.0 - 3.2	2.10*	1.0 - 4.3
<i>ERCC1 - ERCC4</i>						
0	14 (6)	31 (5)	1.0		1.0	
1	60 (24)	159 (25)	0.84	0.42 - 1.7	1.20	0.50 - 2.7
2	25 (10)	65 (10)	0.85	0.4 - 1.9	0.84	0.32 - 2.2
3	37 (15)	93 (14)	0.90	0.42 - 1.8	0.98	0.40 - 2.4
4	93 (37)	258 (40)	0.80	0.41 - 1.6	1.30	0.55 - 2.8
5	19 (8)	41 (6)	1.03	0.45 - 2.4	1.40	0.52 - 3.9
<i>Rad23B - ERCC5 - ERCC6</i>						
1	2 (1)	8 (1)	1.0		1.0	
2	11 (4)	27 (4)	1.63	0.3 - 8.9	1.60	0.19 - 13.7
3	41 (17)	118 (18)	1.39	0.28 - 6.8	2.10	0.28 - 14.8
4	55 (22)	144 (22)	1.53	0.31 - 7.4	2.40	0.34 - 17.6
5	46 (19)	122 (19)	1.51	0.31 - 7.4	2.10	0.29 - 15.2
6	50 (20)	113 (18)	1.77	0.36 - 8.6	2.50	0.35 - 18.2
7	28 (11)	74 (11)	1.51	0.30 - 7.6	2.00	0.28 - 15.2
8	15 (6)	41 (6)	1.46	0.28 - 7.7	2.40	0.30 - 18.4

^a Stratified for age, gender and adjusted for education, smoking and alcohol intake.

* $P < 0.05$ (two tailed t -test)

4. Results, NER and cancer therapy

In the current study 72 pure TCM compounds were screened for cytotoxicity against two NER deficient cell lines XP3BE (deficient in *XPC*) and GM10902 (deficient in *ERCC6*). As a control the normal cell line, GM01310 was included. Compounds differentially cytotoxic to NER deficient cells and not affecting normal cells were identified and selected ones were studied for their effects on cell cycle distribution and genotoxicity. The results obtained were validated for the strongest candidate in a second set of cell lines carrying *XPC* and *ERCC6* deficiencies.

4.1. Cell models

In our study, five cell lines were included (Table.2.7). Freshly grown cultures were tested for contaminations before starting any experiment and after six weeks. Table.4.1 provides the doubling times of the cell lines. 9 to 10 weeks old cultures were discarded and new cells were grown.

Table.4.1. Doubling time of the cell lines included in the study

Cell line / Coriell code	Gene defect	Doubling time (hrs) mean \pm std.dev
GM01310	Normal	48.4 \pm 0.43
GM10902	<i>ERCC6</i> deficient, point mutation at C2282T (Colella <i>et al.</i> , 2000)	43.7 \pm 1.44
XP3BE / GM02248	<i>XPC</i> deficient cell line, 83bp insertion following codon Lys90, (Li <i>et al.</i> , 1993).	37.1 \pm 3.38
XP4PA / GM15983	<i>XPC</i> deficient cell line, dinucleotide (TG) deletion at 1483-1484 bp (Li <i>et al.</i> , 1993)	31.8 \pm 2.01
XP4PA-SE2 / GM16248	Fully corrected form of XP4PA by stable transfection using pXPC-3 plasmid (Legerski & Peterson, 1992)	47.8 \pm 5.07

4. 1. 1. Mutation confirmation

As a control, mutations reported for the cell lines were checked either by PCR amplification or sequencing. Presence of ERCC6 and XPC proteins was checked by western blotting. For GM01310 (Figure.4.1) no mutations were found and normal sized XPC (125 kDa) and ERCC6 (168 kDa) proteins were present. XP3BE is heterozygous for an 83 bp insertion at position 462 in cDNA leading to a frameshift mutation (Li *et al.*, 1993). PCR amplification detected two PCR products (Figure.4.1-a) a normal 254 bp band and a second, lighter band with the insertion. The cell line had only a very small amount of XPC protein and a normal sized ERCC6 protein (Figure.4.1-d & e). GM10902 harbors a point mutation at position C2282T in the cDNA (Colella *et al.*, 2000). The region was sequenced and a G > A transition (Figure.4.1-b) was observed in the genomic DNA of GM10902. At protein level, only a weak band of ERCC6 (Figure.4.1-e) was observed. The cell line had a normal sized XPC protein. XP4PA had no visible XPC protein but had a normal sized ERCC6 (168 kDa) protein (Figure.4.1-c & e). XP4PA-SE2 is the fully corrected version of XP4PA, the cell line exhibits 90% of normal XPC expression and the protein is truncated by 53 amino acids (Emmert *et al.*, 2000). An XPC protein (Figure.4.1-c) slightly smaller in size than the normal XPC (125kDa; in GM01310) was detected. The cell line had normal sized ERCC6 protein (Figure.4.1-e).

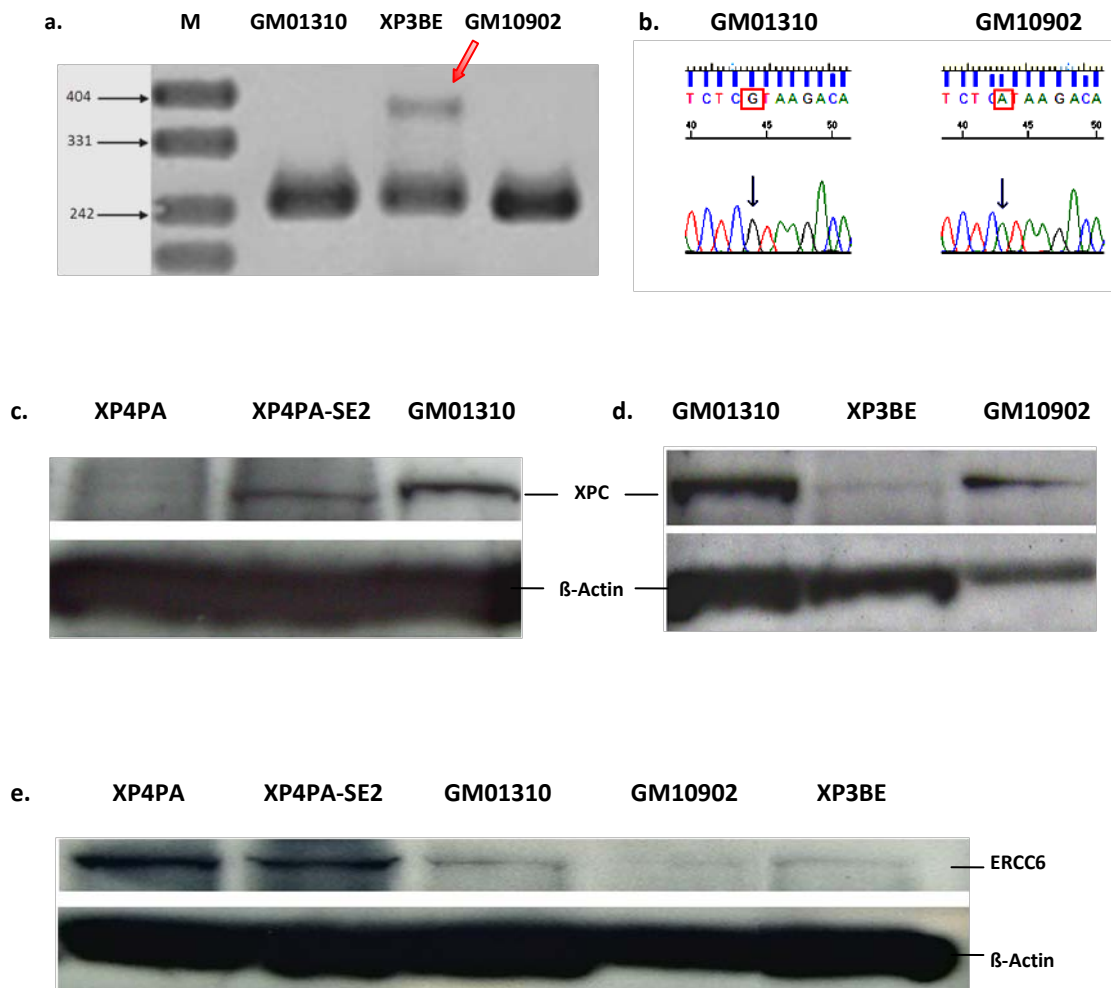
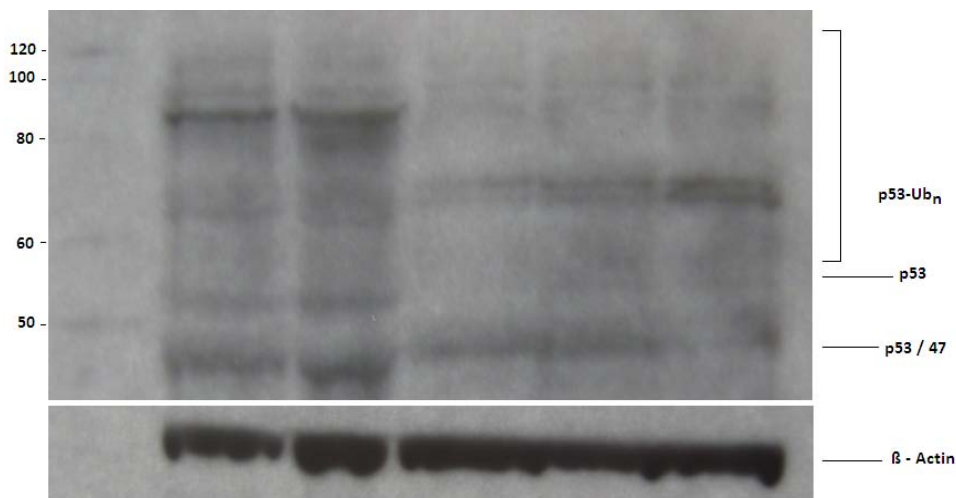


Figure.4.1. Confirmation of the mutations reported in the NER deficient cell lines. **a.** PCR amplification of *XPC* cDNA around position 462 (carrying mutation in XP3BE) in GM01310, XP3BE and GM10902. PCR products were separated on 2% Agarose gel. Arrow indicates 83bp insertion in XP3BE. **b.** Genomic DNA sequence of GM01310 and GM10902. Arrows indicate G > A transition at position C2282T. **c.** XPC protein in XP4PA, XP4PA-SE2 in comparison with GM01310. No protein is visible in XP4PA lane. XPC in XP4PA-SE2 is slightly smaller than GM01310. **d.** XPC protein in XP3BE and GM10902 in comparison with GM01310. A very weak band is visible in XP3BE lane. Varying amount of total cellular proteins was separated on the gel (see β-actin). **e.** ERCC6 protein in XP4PA, XP4PA-SE2, GM01310, GM10902 and XP3BE. GM10902 has a weak band. XPC (125kDa) and ERCC6 (168kDa) proteins were detected by western blotting using gene specific antibodies and β-actin (43kDa) was used as a reference.

4. 1. 2. P53 status of the cell lines

Expression of P53 in the cell lines was checked by western blotting. Figure.4.2 demonstrates that P53 expression was cell type specific. Overall the level of p53 in all cell lines was either undetectable or very low and p53/47 complex, and ubiquitinated forms of p53 were present. This profile is normal for resting cells (Yin *et al.*, 2002; Maki, 1999)



M	XP4PA	XP4PA-SE2	GM01310	XP3BE	GM10902
XPC	-	+	+	-	+
ERCC6	+	+	+	+	-

Figure.4.2. p53 expression in the cell lines included in the study. Proteins were detected by western blotting using gene specific antibodies and β-Actin was used as a reference. 150 μg of total cellular proteins were separated on the gel.

4. 1. 3. Sensitivity to UV exposure

NER pathway is involved in the repair of bulky lesions produced by UV light. In case of a deficient NER cells are more sensitive to UV exposure than the normal cells. To examine the response of our cell lines to UV light exposure, cultures were exposed to different intensities of UVC and grown for 48 hrs at normal cell culture

conditions. The percent viabilities relative to unexposed samples were measured by Calcein assay.

Figure.4.3 demonstrates that GM01310 and XP4PA-SE2, the NER proficient cell lines had a better relative percent viability with increased UVC intensity. The IC_{50} values for GM01310 and XP4PA-SE2 were 41.09 J/m^2 and 27.92 J/m^2 , respectively. NER deficient cell lines XP3BE, XP4PA and GM10902 had poor relative viabilities with increased UVC intensity. The IC_{50} value was 7.67 J/m^2 for XP3BE, 15.66 J/m^2 for XP4PA and 16.22 J/m^2 for GM10902. Exposure to 60 J/m^2 UVC killed almost all the cell lines.

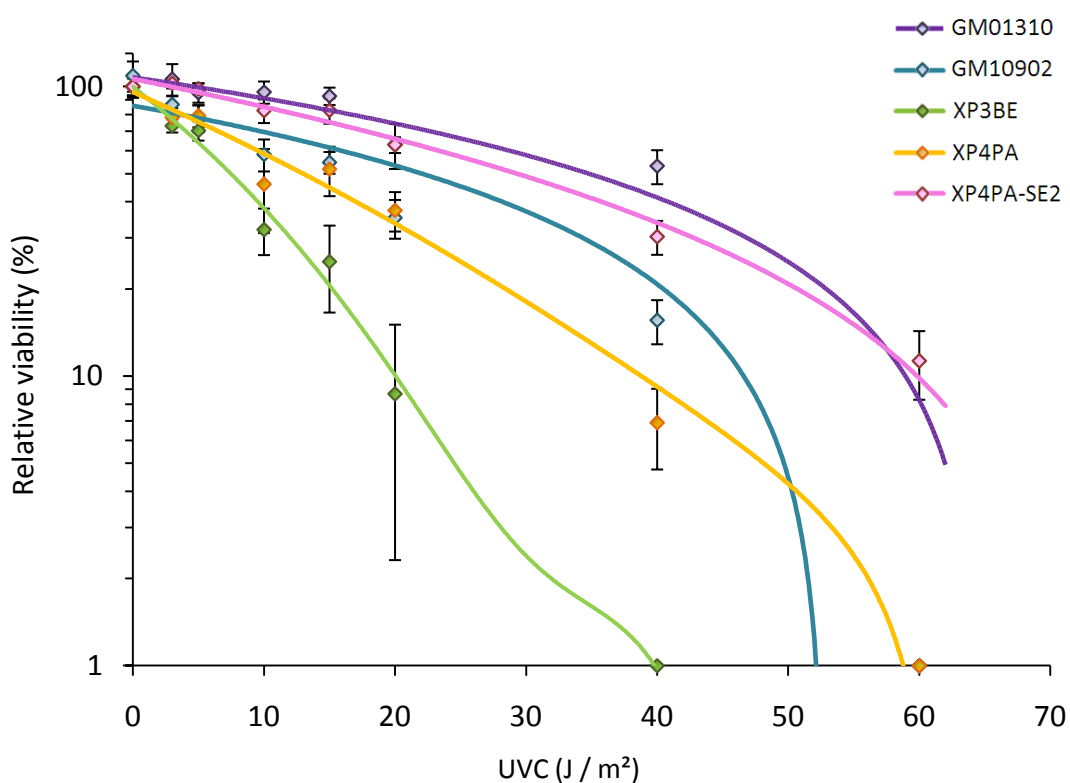


Figure.4.3. Viability curves. Sensitivity of the five cell lines to different dose of UVC (J/m^2) exposure. After exposure cultures were grown for 48hrs and their percent growth (mean \pm std.dev) relative to the unexposed samples was measured by Calcein assay. NER deficient cell lines (GM10902, XP3BE, XP4PA) are more sensitive to UVC. The results are from two experiments with three replicates each.

4. 2. Silencing of ERCC6 gene in XP4PA-SE2 cells

ERCC6 was silenced in XP4PA-SE2 cells using ON-TARGETplus SMARTpool siRNA. Luciferase and *GAPDH* siRNA were used as negative and positive controls for knockdown, respectively. Transfection reagent treated and non transfected cells (NTC) were included as experimental controls. Before starting the knockdown experiments, certain conditions like plating densities, plating effects and suitable ratios of transfection reagent/siRNA were optimized. A plating density of 6×10^4 cells/ml was considered as suitable for efficient gene silencing for up to 96hrs.

4. 2. 1. Optimized conditions for transfection

Two transfection reagents DharmaFECT-4 (DF4) and polyFECT were tested for their transfection efficiency. Exponentially growing cells were transfected with Fluorescein-siRNA (15 nM) by two concentrations of each reagent for 4 hrs. Cells (Figure.4.4-a) were counted using fluorescent microscope under blue (wavelength 390 to 490 nm) and white light and the transfection efficiency was calculated. At DF4/siRNA-5:1 the transfection efficiency was 96% and at DF4/siRNA-10:1 it was 75.76%. Both concentrations of polyFECT and the non treated cells did not show any fluorescent cells.

To check the effect of the transfection reagent on cell viability and plating efficiency, exponentially growing cultures were incubated with the reagents for 24 hrs in a normal 24-well plate and collagen coated plates which should offer better adhering. After 24 hrs, cells in the normal 24-well plate were floating whereas those incubated in collagen coated plates were still attached to the surface. When checked for cell viability (Figure.4.4-b) DF4 was cytotoxic to the cells. DF 4/siRNA-5:1 samples growing in collagen coated culture plates had around 76% viable cells and cultures in normal plates had around 60% viability. At higher DF4 concentration the viability was very low. PolyFECT did not show any cytotoxicity to the cells.

Clearly, DF4 transfected the cells with high efficiency but it was cytotoxic. This situation was not very ideal for experiments where we aim to see cytotoxicity and DNA damage caused by ascaridol in ERCC6-silenced cells. To reduce the cytotoxic

effects cells were grown in collagen-coated plates with lower concentrations of DF4. In addition, the transfection media was replaced by culture media after 24 hrs and cells were allowed to grow for another 48 hrs before any experiments were performed on them.

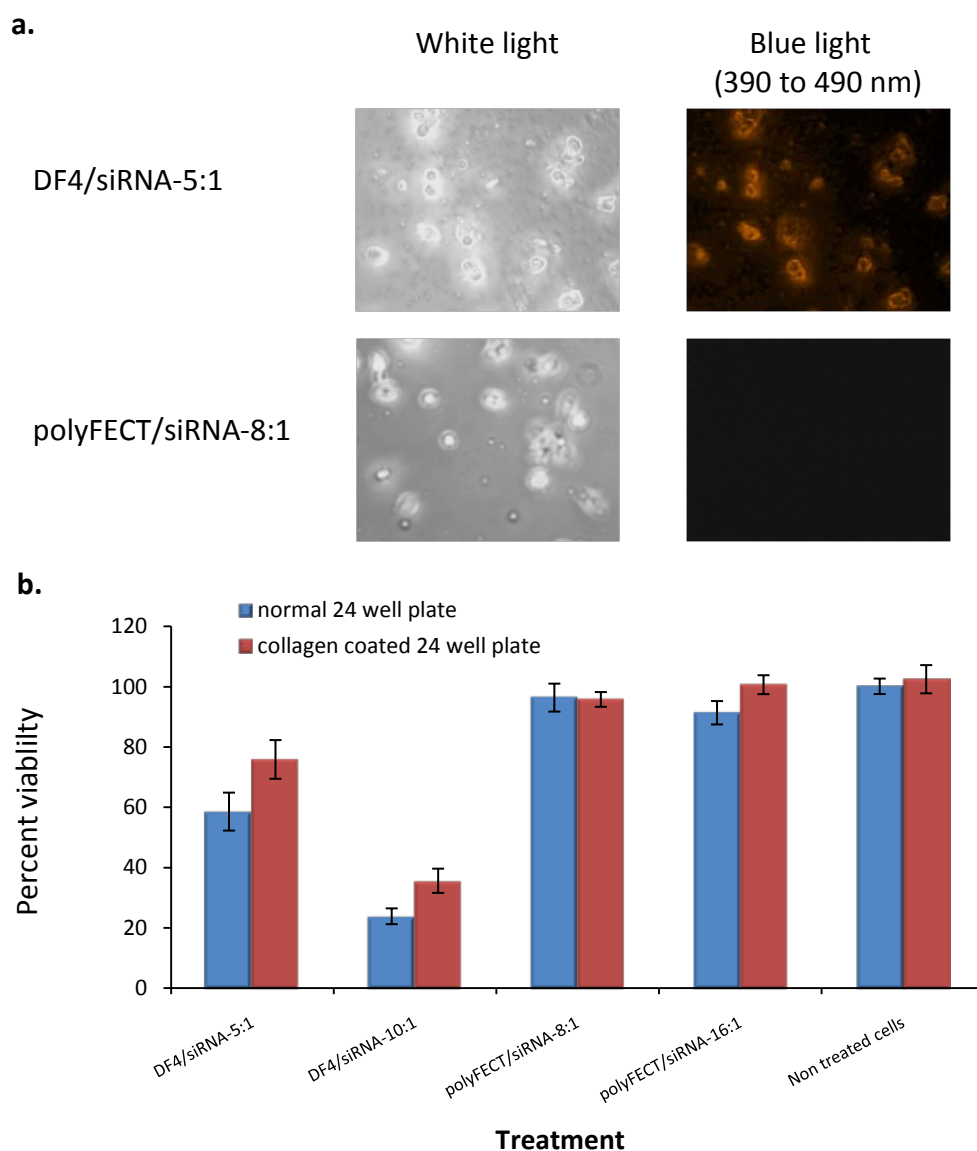


Figure.4.4. Optimization of conditions for transfection of XP4PA-SE2 cells with DF4/Fluorescein siRNA (5:1, 10:1) and polyFECT/Fluorescein siRNA (8:1, 16:1). **a.** Transfected cells (DF4/siRNA-5:1 and polyFECT/siRNA-8:1) observed under fluorescent microscope in blue (wavelength 390 to 490 nm) and white light after 4 hours of incubation. **b.** Percent viability of the cells grown in a normal 24-well plate and collagen coated 24-well plate after 24 hours of incubation. Viability (mean \pm std.dev) as measured with trypan blue staining. Experiment included 3 replicates per treatment.

4. 2. 2. *ERCC6* knockdown

The *ERCC6* gene was silenced in exponentially growing cultures of XP4PA-SE2 using the transfection conditions described above and ON-TARGETplus SMARTpool siRNA. The amount of DF4 is the same but the amount of siRNA was increased according to recommendations of manufacturer. Two concentrations of DF4/*ERCC6* siRNA (0.88, 1.76) were used to silence the gene. Luciferase and

GAPDH siRNA were included as negative and positive controls for knockdown, respectively. DF4 only and NTC were included as experimental controls. To analyze the knockdown, expression of *ERCC6* gene was checked both at mRNA and protein level after 24, 48, 72 and 96 hrs. Relative quantification of mRNA levels was done by real time PCR on LightCycler 480 after reverse transcription and protein expression was checked by western blotting. Each experiment was performed twice with two replicates for each treatment.

4. 2. 3. Gene expression at mRNA level

Total RNA was extracted using RNeasy mini kit and cDNA was prepared using random hexamer primers and superscript III RT. Gene expression was quantified relative to *HPRT* expression (housekeeping gene) by LightCycler 480. Gene expression was calculated relative to expression in luciferase siRNA treated samples. Figure.4.5-a shows that expression of *ERCC6* at DF4/siRNA-0.88 was reduced to 20% after 24 hrs but after 48 hrs expression levels resumed to normal. At DF4/siRNA-1.76 after 24 hrs expression levels were reduced to 18% and they remained below 50% even after 96 hrs of transfection. Silencing of *GAPDH* (positive control for knockdown) showed a gradual decrease in gene expression reaching to 14% after 72 hrs. DF4 only and non-transfect cells had normal or high expression of *ERCC6* gene.

4. 2. 4. Gene expression at protein level

Protein expression was analyzed by western blotting using gene specific antibodies, and compared to β -actin expression. Results are provided in Figure.4.2-b. After 24

hrs, ERCC6 protein is still visible in all samples. In the DF4/siRNA-0.88 sample, a weak ERCC6 band is visible after 48 hrs and 72 hrs whereas it disappears after 96 hrs (indicated by arrows). In DF4/siRNA-1.76 samples ERCC6 is not visible after 48, 72 and 96 hrs. The protein is present in negative control and NTC.

As DF4/siRNA-1.76 silenced the gene effectively, both at mRNA and protein level for longer periods of time, this concentration was used in further experiments.

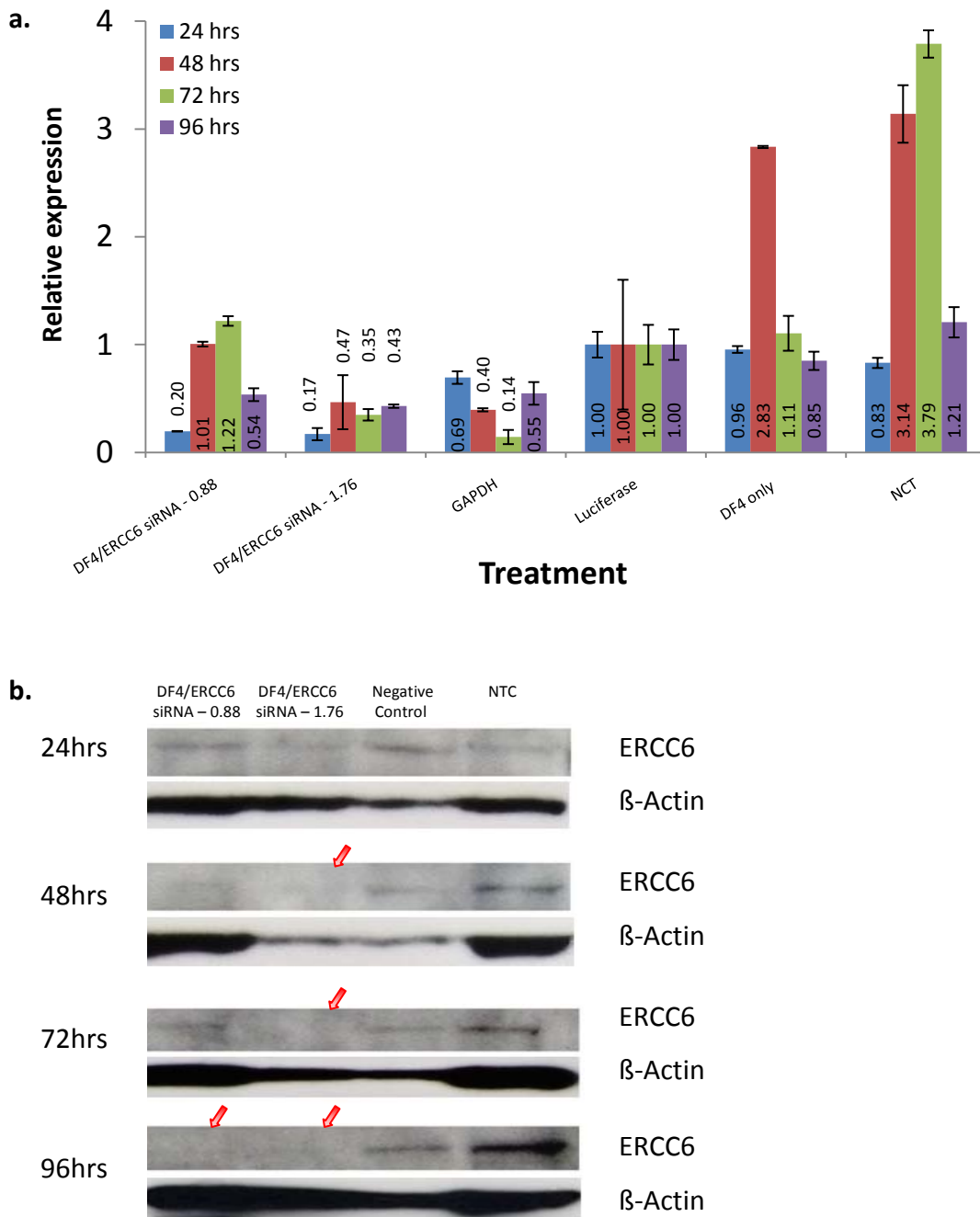


Figure.4.5. ERCC6 knockdown in XP4PA-SE2 cells using ON-TARGETplus SMARTpool siRNA (Dharmacon) after 24, 48, 72 and 96hrs. Two concentrations of DF4/ERCC6 siRNA (0.88, 1.76) were used to silence ERCC6. Luciferase and GAPDH siRNA were included as negative and positive controls for knockdown, respectively. DF4 only and NTC (non transfected cells) were included as experimental controls. **a.** Relative quantification of ERCC6 and GAPDH expression at mRNA level by real time PCR. HPRT was used as reference. GAPDH indicates knockdown of GAPDH and expression of GAPDH was measured for these samples. Results are relative to ERCC6 or GAPDH expression in negative control. **b.** ERCC6 expression at protein level. β -Actin was used as a reference. Arrows indicate no visible ERCC6 band. These are results of two experiments with two replicates each treatment.

4. 3. Viability / Cytotoxicity assay

In the present study fluorescence based ‘**The LIVE/DEAD® Viability/Cytotoxicity assay**’ (Invitrogen) was used to measure relative percentage of live and dead cells simultaneously. The assay comprises of two fluorescent dyes, Calcein AM (excitation: 485nm, emission: 520nm) for detecting live cells and Ethidium Homodimer (excitation: 520nm, emission: 620nm) for detection of dead cells. Table.4.2 gives the optimum concentrations of the dyes used for each cell line. Ethidium Homodimer could not be optimized for adherent cells (XP4PA and XP4PA-SE2). A possible explanation is that washing step removed all the dead cells. For these cell lines relative viabilities were measured by Calcein AM only (Calcein assay).

Table.4.2. Optimized concentrations of dyes used for each cell line in LIVE/DEAD® Viability/Cytotoxicity assay

Cell line	Dye concentration	
	Calcein AM (μM)	Ethidium Homodimer (μM)
GM01310	1	2
XP3BE	2	2
GM10902	3	2
XP4PA	5	-
XP4PA-SE2	5	-

4. 3. 1. Calibration of the assay

To calibrate the assay, live and dead cells were mixed in different proportions and relative percent viability and relative percentage of dead cells was calculated according to LIVE/DEAD® Viability/Cytotoxicity assay. Figure.4.6 shows the calibration curves for GM01310. The assay permits a wide range of measurements in cultures with varying proportions of live and dead cells. The simultaneous determination of live and dead cells allows a bidirectional check in cytotoxicity screening. An average variation of 10% was observed between replicates.

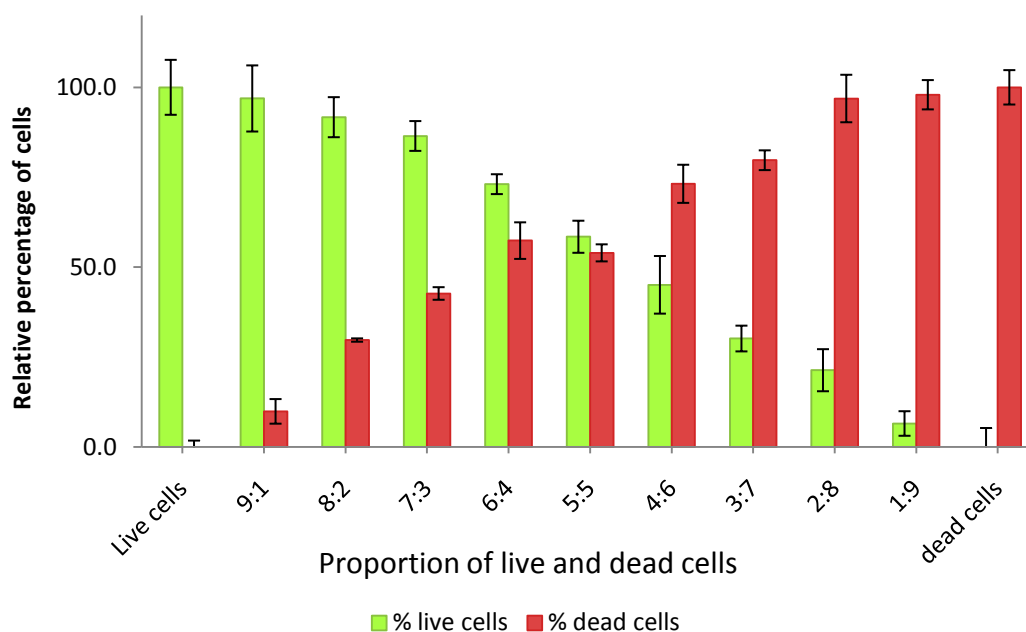


Figure.4.6. Relative percentage of live (■) and dead (■) cells of GM01310 measured in samples carrying different proportions of live and dead cells. Percentage of live cells was calculated relative to unexposed sample and percentage of dead cells was calculated relative to 100% dead culture.

4. 4. Screening of TCM drugs for their differential cytotoxic effect on NER deficient cell lines

In the current project a total of 72 drugs derived from TCM were screened for their activity against two NER deficient cell lines, XP3BE; an XPC deficient cell line and

GM10902; an *ERCC6/CSB* deficient cell line. As a control, the normal cell line GM01310 was used. After treatment with the drugs, relative percentage of live and dead cells was measured by LIVE/DEAD® Viability/Cytotoxicity assay and relative percent viabilities were considered as a measure of drug cytotoxicity.

4. 4. 1. Determination of a suitable time for drug exposure – an experiment with arsenic trioxide

To determine a suitable time for TCM exposure, exponentially growing cultures (> 90% viability) of XP3BE, GM10902 and GM01310 were exposed to arsenic trioxide (10 µg/ml) for different time periods (10 min, 3, 6, 24 hrs) and their relative percent viabilities were determined. Figure.4.7 depicts that after 10 min of exposure, relative percentage of viable cells decreased to around 75% for the three cell lines, which remained stable after 3 hrs. After 6 hrs of incubation with the drug around

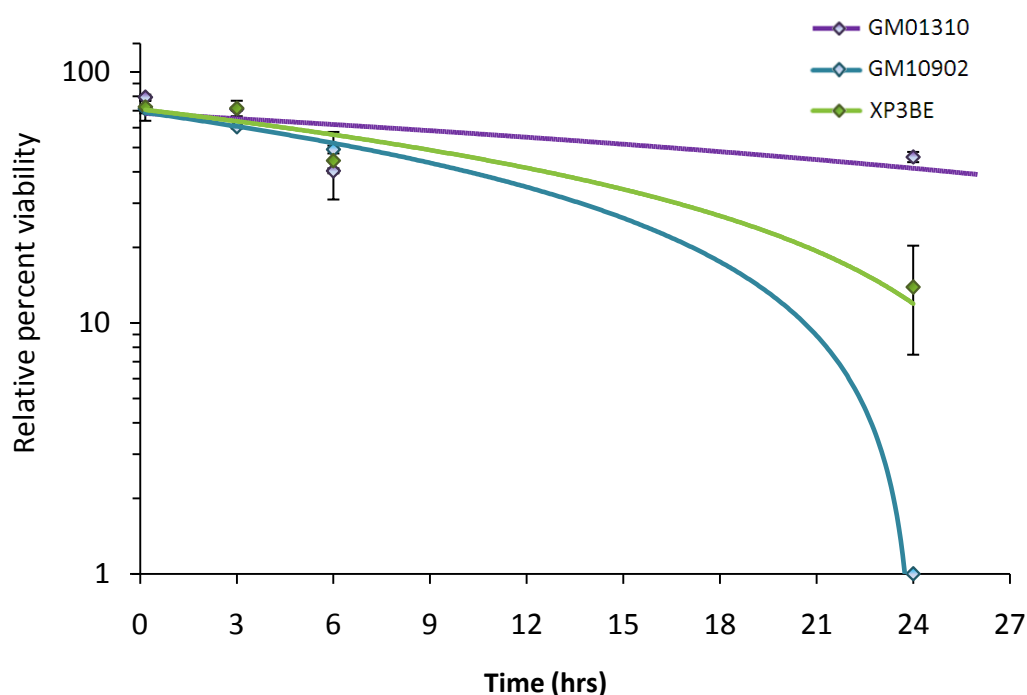


Figure.4.7. Effect of arsenic trioxide (10 µg/ml) on relative percent viability of GM01310, XP3BE and GM10902 cells over a time period of 24 hrs. Exponentially growing cultures of the three cell lines were exposed to arsenic trioxide for different time points and samples were analyzed by LIVE/DEAD® Viability / Cytotoxicity Assay. Results are relative to unexposed samples. An ‘early effect’ of the drug was observed after 10 min exposure and a ‘later effect’ after 24 hrs. The results are from a single experiment with three replicates each treatment.

55% of the cells from the three cell lines were dead and there was no significant difference between the cell lines. After 24 hrs, GM10902 had no viable cells, XP3BE had $13.9 \pm 6.4\%$ viable cells and the normal cells had a surviving proportion of $45.8 \pm 2.1\%$.

From these results '10 min exposure' was considered as ideal for observing an 'early effect' of the drug and '24 hrs exposure' as a time point where drugs show 'later effect' on the three cell lines. Based on this result we also found our first candidate drug differentially killing NER deficient cells.

4. 4. 2. Screening of TCM drugs

All the TCM compounds and their solvents were screened for cytotoxicity against GM01310, XP3BE and GM10902. Exponentially growing cultures ($> 90\%$ viability; 7.5×10^5 cells / ml) were exposed to the saturated solutions of the compounds ($1 \mu\text{l} / 100 \mu\text{l}$ of the cell suspension) for 10 min and 24 hours and grown at normal culture conditions. Relative percent viabilities, a measure of drug cytotoxicity, were measured by LIVE/DEAD® Viability/Cytotoxicity assay. The screening experiment was performed twice with three replicates of each treatment.

Drugs were categorized as having 'no effect' when the measured viability was $\geq 50\%$ after 10 min or 24 hrs, having 'Moderate effect' when viability was between $< 50\%$ to $\geq 25\%$, having 'Strong effect' when $< 25\%$ to $\geq 5\%$ viability and having 'Strongest effect' when $< 5\%$ viability was observed.

The cytotoxicity screening revealed that most of the TCM drugs were active after 24 hrs. Figure.4.8 demonstrates the overall results of the screening. Fifty three out of 72 drugs (74%) had either 'no' or 'comparable' effects on the three cell lines . 6 drugs were highly cytotoxic, with a 100% killing effect on all the three cell lines whereas 13 drugs (18%) showed a differential activity against at least one of the mutant cell lines. Of these, 2 drugs (quercetin and scopoletin) were specifically active against XP3BE only, 1 drug (TCM-25-RAB) was active against GM10902 only and 10 of the 72 TCM drugs (14%; arsenic trioxide, ascaridol, isonardosinon, TCM-22-RAB, TCM-23-RAB, TCM-44-RAB, TCM-47-RAB, TCM-48-RAB, TCM-50-RAB, TCM-

54-RAB) were killing the two NER deficient cell lines more efficiently when compared with the normal cells (Table.4.3).

Depending on the amount available, 6 of these drugs (Table.4.4; arsenic trioxide, ascaridol, isonardosinon, TCM-25-RAB, quercetin and scopoletin) were picked for further analyses.

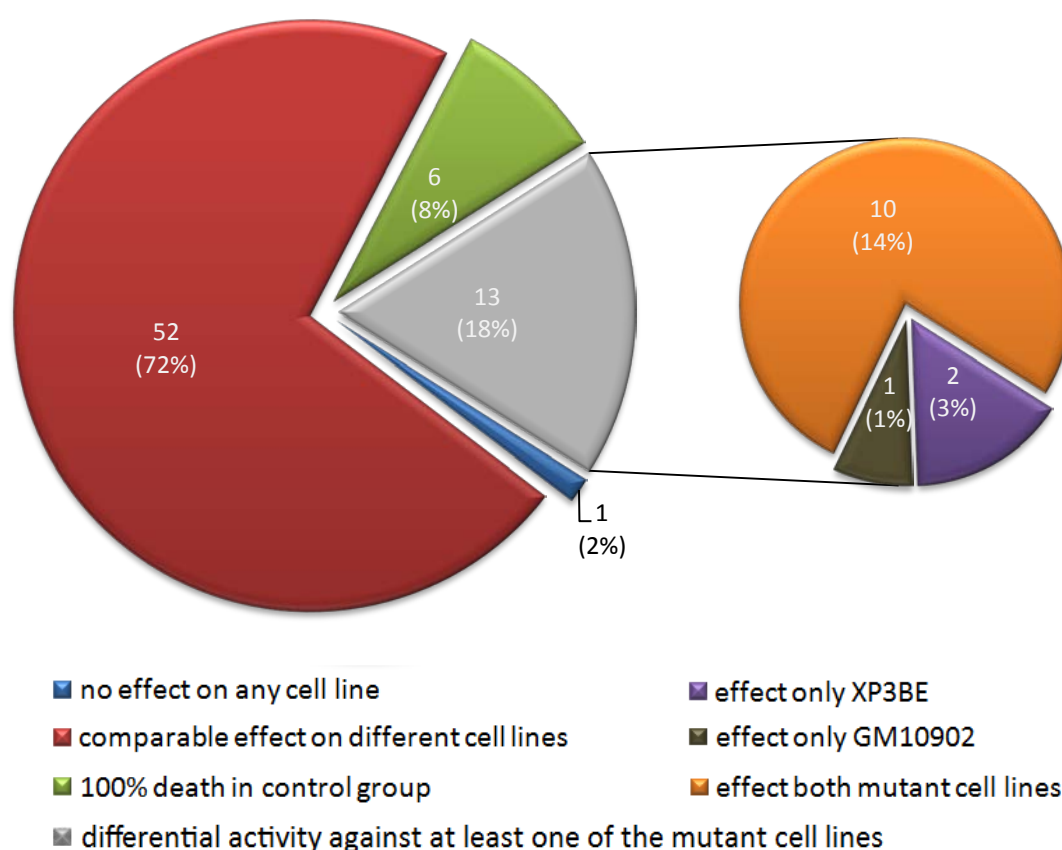


Figure.4.8. Screening for cytotoxicity of TCM drugs to GM01310, XP3BE and GM10902 cells. Exponentially growing cultures were exposed to 1% of stock solution of the drugs and analyzed by LIVE/DEAD® Viability / Cytotoxicity Assay after 24 hrs. Unexposed and solvent exposed samples were included as controls. The results are from two independent experiments with three replicates for each treatment.

Table.4.3. TCM drugs having differential cytotoxic effects on NER deficient cell lines.

no.	Effective compound	Cell lines					
		GM01310		GM10902		XP3BE	
		Early effect ²	Later effect ²	Early effect	Later effect	Early effect	Later effect
1	Arsenic trioxide ¹	-	-	-	+ ³	-	++
2	Ascaridol	-	-	-	++	-	++
3	Isonardosinon	-	-	-	++	-	++
4	TCM-22-RAB	-	-	-	++	-	++
5	TCM-25-RAB	-	-	-	+	-	-
6	TCM-23-RAB	-	+	-	++	-	++
7	TCM-44-RAB	-	+	-	++	-	++
8	TCM-47-RAB	-	+	-	+++	+	++
9	TCM-48-RAB	-	+	+	+++	++	+++
10	TCM-50-RAB	-	+	-	+++	-	+++
11	TCM-54-RAB	-	-	-	+++	-	+++
12	Quercetin	-	-	-	-	-	++
13	Scopoletin	-	-	-	-	-	++

¹ Red color indicates the drugs were selected for further analysis,

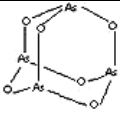
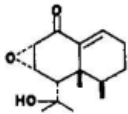
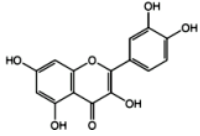
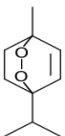
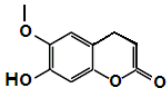
² Early effect; 10 min exposure to the compound, later effect; 24 hour exposure,

³ +, ≤ 50 % viability; ++, ≤ 25 %; +++, ≤ 5 % and -, no effect.

4. 5. Analysis of the selected drugs

Table.4.4 provides some details of the selected drugs. Arsenic trioxide and quercetin are established cytostatic drugs. Arsenic trioxide was selected as a positive control for our experiments as the drug is known to cause DNA damage and to effect cell cycle. Furthermore as we were blessed with plenty of this drug, it was also used to optimize conditions for different experiments.

Table.4.4. Details of the TCM drugs selected after screening experiments.

name	Structure	mole mass (g/mol)	CAS-no.	Information available
Arsenic trioxide		197.841	1327-53-3	Well studied compound (Gazitt & Akay, 2005; Miller <i>et al.</i> , 2002), used in treatment of acute promyelocytic leukemia (APL) (Shen <i>et al.</i> , 1997).
Isonardosinon		250.0	-	
Quercetin		338.0	117-39-5	Potential anti-cancer drug (van Erk <i>et al.</i> , 2005).
Ascaridol		168.23	512-85-6	It is an antihelmintic (Vanfleteren & Roets, 1972), has anti-malarial properties (Pollack <i>et al.</i> , 1990) and is a potential anti-cancer drug.
Scopoletin		192.6	92-61-5	Scopoletin is an antioxidant (Shaw <i>et al.</i> , 2003) and it induces apoptosis in promyelocytic cells (Kim <i>et al.</i> , 2005).
TCM-25-RAB	Under investigation			

4. 5. 1. Determination of IC₅₀ values

To determine IC₅₀ values of the selected drugs, exponentially growing cultures (> 90% viability; 7.5 X 10⁵ cells/ml) of GM01310, XP3BE and GM10902 were exposed to different concentrations of the drugs for 24 hrs and relative % viabilities were measured. Relative viability curves (Figure.4.9) were generated against drug concentrations and IC₅₀ values of the drugs for each cell line were calculated. As a control, solvent exposed and unexposed samples were included.

Ascaridol (Figure.4.9-a) did not kill 50% of GM01310 cells (IC₅₀ = > 30 µg/ml) at concentrations upto 30 µg/ml. As the drug was available only as a solution in DMSO, testing at higher concentrations would have increased DMSO to intolerable levels. NER deficient cell lines were very sensitive to the drug with an IC₅₀ of 0.025 µg/ml and 0.03 µg/ml for GM10902 and XP3BE, respectively. A difference of more than 1000 fold in resistance was observed between normal and NER deficient cells.

Arsenic trioxide (Figure.4.9-b) had an IC₅₀ of 2.2 µg/ml for GM01310, 0.4 µg/ml for GM10902 and 0.7 µg/ml for XP3BE. Normal cells were 3 to 5.5 times resistant to arsenic trioxide exposure when compared with NER deficient cells.

Isonardosinon (Figure.4.9-c) was active against both the NER deficient cell lines. It had an IC₅₀ of 30 µg/ml for the GM01310, 2.6 µg/ml for GM10902 and 1.6 µg/ml for XP3BE cells.

Quercetin (Figure.4.9-d) and Scopoletin (Figure.4.9-e) specifically affected XP3BE. For these cells quercetin and scopoletin had an IC₅₀ value of 0.5 µg/ml and 14.7 µg/ml, respectively. Quercetin exposure did not kill 50% of GM01310 and GM10902 cells even at highest concentrations (60 µg/ml) used in our experiments. Scopoletin had an IC₅₀ value of 24.9 µg/ml for GM01310 and 22.1 µg/ml for GM10902 cells.

TCM-25-RAB (Figure.4.9-f) was specifically active against GM10902 (IC₅₀ = 8.9 µg/ml). However it also showed toxicity to XP3BE cells (IC₅₀ = 15.4 µg/ml). Its IC₅₀ value for GM01310 was 21.3 µg/ml.

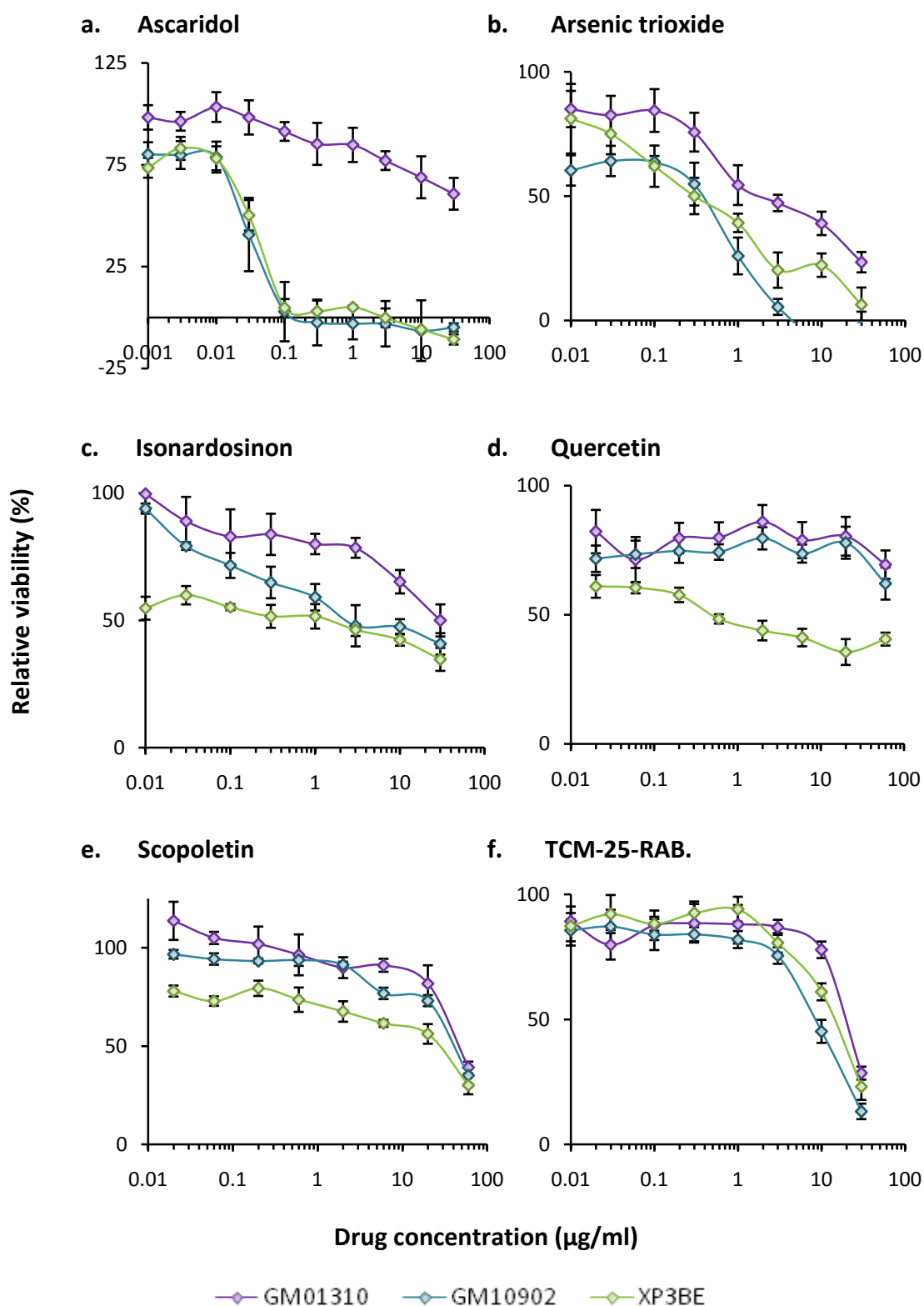


Figure.4.9. Determination of IC_{50} values for 6 TCM compounds in GM01310, GM10902 and XP3BE. Exponentially growing cultures were exposed to serial dilutions of the drugs ($\mu\text{g/ml}$) for 24hrs and relative % viabilities (mean \pm std.dev) were measured using LIVE/DEAD[®] Viability/Cytotoxicity Assay. **a.** Ascaridol, **b.** Arsenic trioxide, **c.** Isonardosinon, **d.** Quercetin, **e.** Scopoletin and **f.** TCM-25-RAB.

4. 5. 2. Cell cycle analysis

Analysis of cell cycle distribution by flow cytometry was used as a tool for characterization of the selected TCM drugs. In flow cytometry DNA content of cells was measured and propidium iodide (PI) was used as DNA dye. The DNA content of a cell can provide a great deal of information about the cell cycle and consequently the effect of external exposure e.g., drug treatment, on the cell cycle. Figure.2.3 demonstrates four different cell cycle phases as observed by flow cytometry. **G1 phase** comprises diploid (2n) cells, **S phase** is comprised of cells replicating their DNA content and generally lie between G1 and G2/M phase, **G2/M phase** consists of tetraploid (4n) cells, and **subG1 phase** includes apoptotic cells having DNA less than diploid cells.

The influence of the selected TCM drugs on a specific cell cycle phase, such as cell cycle arrests was studied. An increase in the SubG1 peak was considered as cell killing by apoptosis.

4. 5. 2. 1. Determination of a suitable time for observation of TCM effects on cell cycle distribution – an experiment with arsenic trioxide

Before starting experiments with the selected drugs, a suitable time to observe a clear effect of a given drug on cell cycle distribution was determined by exposing GM01310 cells to different arsenic trioxide (0.73, 2.2 µg/ml) concentrations for 4 hrs, 8 hrs and 24 hrs. Samples were fixed in 70% ice cold ethanol, stained with propidium iodide for 30 min and analyzed on a FACScalibur using the 'CellQuestPro' software.

The Figure.4.10 demonstrates that exposure to arsenic trioxide (0.73, 2.2 µg/ml) had no effect on the cells after 4 hrs. After 8 hrs exposure, minor effects of 0.73 µg/ml arsenic trioxide were observed and 2.2 µg/ml arsenic trioxide caused a decrease in G2/M peak and an increase in subG1 peak. Exposure to 0.73 µg/ml arsenic trioxide for 24 hrs increases the G2/M peak indicating G2/M arrest. At 2.2 µg/ml and after 24 hrs, a sharp decrease in G2/M peak and increase in subG1 peak is observed indicating that cells arrested in G2/M at lower arsenic trioxide

concentration undergo apoptosis at the higher concentration. As maximum drug effect for the concentrations used in the experiment was observed after 24 hrs, this time point was considered suitable for further experiments.

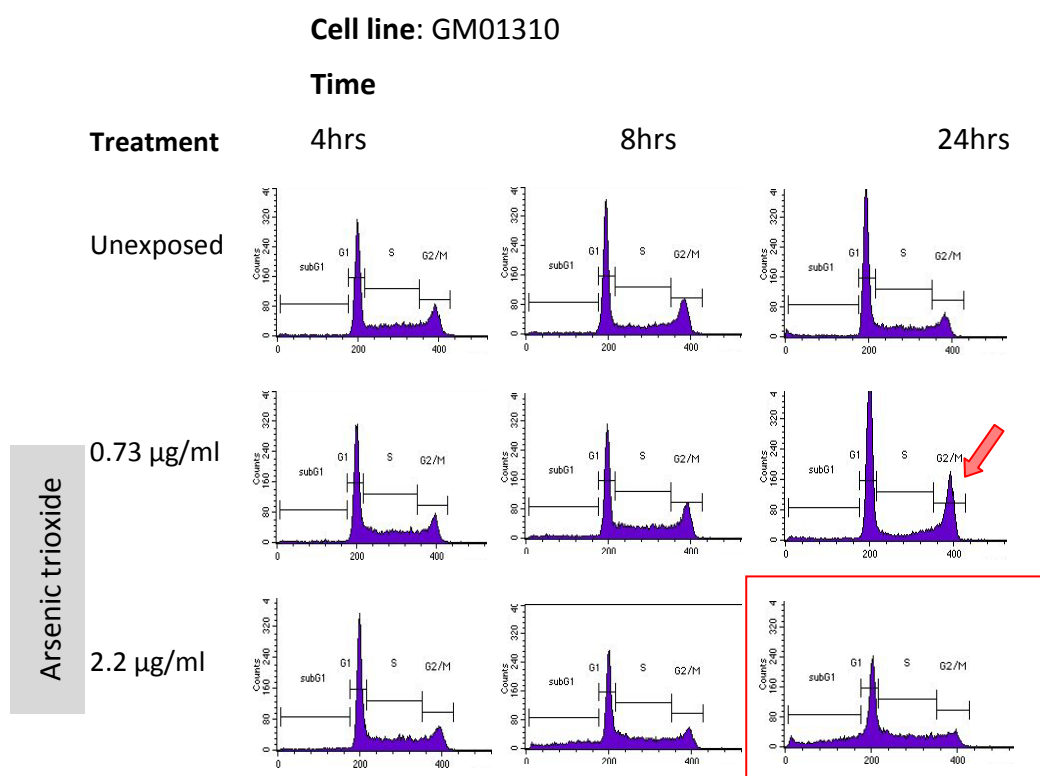


Figure.4.10. Cell cycle analysis of GM01310 cells after arsenic trioxide (0.73, 2.2 µg/ml) treatment after 4, 8 and 24 hours. Red arrow indicates increase in G2/M phase at 0.73 µg/ml arsenic trioxide and boxed data show a sharp decrease in G2/M and increase in subG1 at 2.2 µg/ml after 24 hrs indicating G2/M arrest at the lower arsenic trioxide concentration and cells arrested in G2/M undergoing apoptosis at higher concentration.

4. 5. 2. 2. Effect of the selected TCM drugs on cell cycle progression

To investigate the effect of the selected drugs on cell cycle distribution exponentially growing cells of XP3BE, GM10902 and GM01310 were exposed to

different concentrations of the drugs for 24 hrs and samples were handled as explained in the previous section.

4. 5. 2. 2. 1. *Ascaridol*

Ascaridol (Figure.4.11 and Table.4.5) caused a significant decrease of cells in G1 phase in all three cell lines at different concentrations (0.05, 0.1, 0.5 and 1.0 $\mu\text{g/ml}$) tested. In GM10902, an increase in G2/M peak was observed at 0.05 and 0.1 $\mu\text{g/ml}$. This peak decreased at higher concentrations (0.5, 1.0 $\mu\text{g/ml}$). In XP3BE cells, a decrease in G2/M phase was observed at 0.5 and 1.0 $\mu\text{g/ml}$ of ascaridol. In normal cells (GM01310), a decrease in height of G2/M peak was observed at 0.5 and 1.0 $\mu\text{g/ml}$ ascaridol but the overall percentage of cells in this phase remains unchanged. In GM01310, a significant increase in S phase was also observed at all concentrations of ascaridol.

At all the concentrations ascaridol produced 13 to 20% subG1 phase in GM01310. GM10902 showed a dose-dependent increase in subG1, reaching up to 28% at 1.0 $\mu\text{g/ml}$ and XP3BE had around 27% subG1 at all the concentrations. This indicates, in comparison to NER proficient cells, a higher number of NER deficient cells undergo apoptosis when exposed to same concentration of ascaridol.

4. 5. 2. 2. 2. *Arsenic trioxide*

Arsenic trioxide produced G2/M phase arrest in all three cell lines (Figure.4.12 and Table.4.5). This arrest was achieved in normal cells at 0.73 $\mu\text{g/ml}$ whereas 0.22 $\mu\text{g/ml}$ of arsenic trioxide produced the same effect in GM10902 and XP3BE cells. At 2.2 $\mu\text{g/ml}$ the G2/M phase peak disappears in GM10902 and XP3BE whereas it was still present in GM01310.

A significant increase in subG1 phase was observed in GM10902 and XP3BE cells at 0.73 $\mu\text{g/ml}$. At 2.2 $\mu\text{g/ml}$, $21.6 \pm 0.8 \%$ of GM01310, $49.1 \pm 3.0 \%$ of GM10902 and $36.2 \pm 0.8 \%$ of XP3BE cell were in subG1 phase, indicating, in comparison to NER proficient cells, a higher number of NER deficient cells undergo apoptosis when exposed to same concentration of arsenic trioxide.

4. 5. 2. 2. 3. Other drugs

Results for TCM-25-RAB, Quercetin, Scopoletin and Isonardosinon are given in Table.4.6. TCM-25-RAB (10 µg/ml) caused a slight increase in G1 phase in GM10902 cells. It also increased subG1 phase by 20%. Quercetin (10 µg/ml) decreased 'S phase' in XP3BE cells and significantly increased the subG1 phase, whereas Scopoletin (20 µg/ml) exposure caused an increase in G1 phase in GM01310 and XP3BE cells. Isonardosinon did not affect the cell cycle.

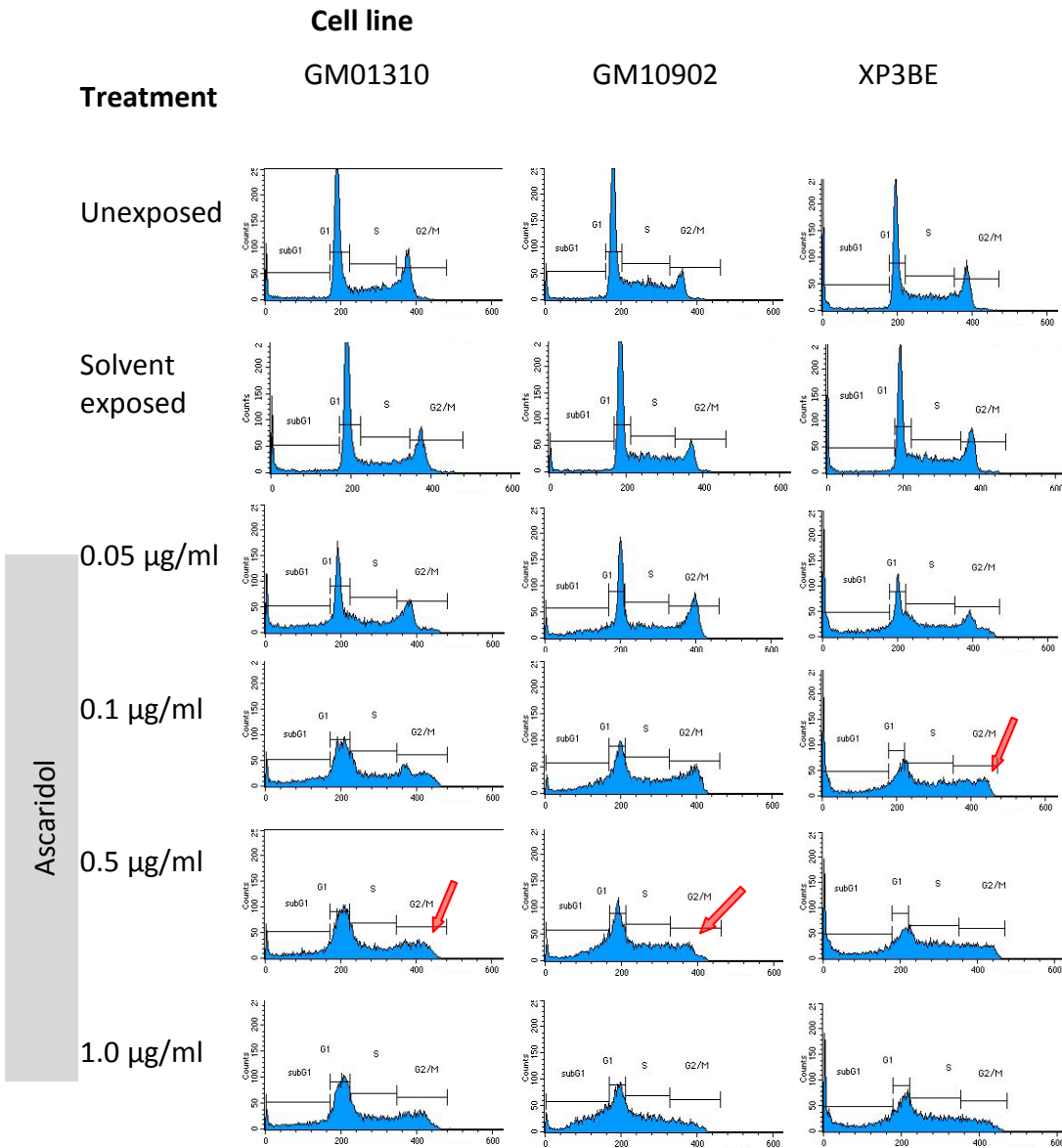


Figure.4.11. Cell cycle analysis of GM01310, GM10902 and XP3BE cells after Ascaridol (0.05, 0.1, 0.5, 1.0 µg/ml) treatment for 24 hours. The arrows indicate G2/M peak disappears in XP3BE (at 0.1 µg/ml), in GM10902 (at 0.5 µg/ml) and in GM01310 (at 0.5 µg/ml).

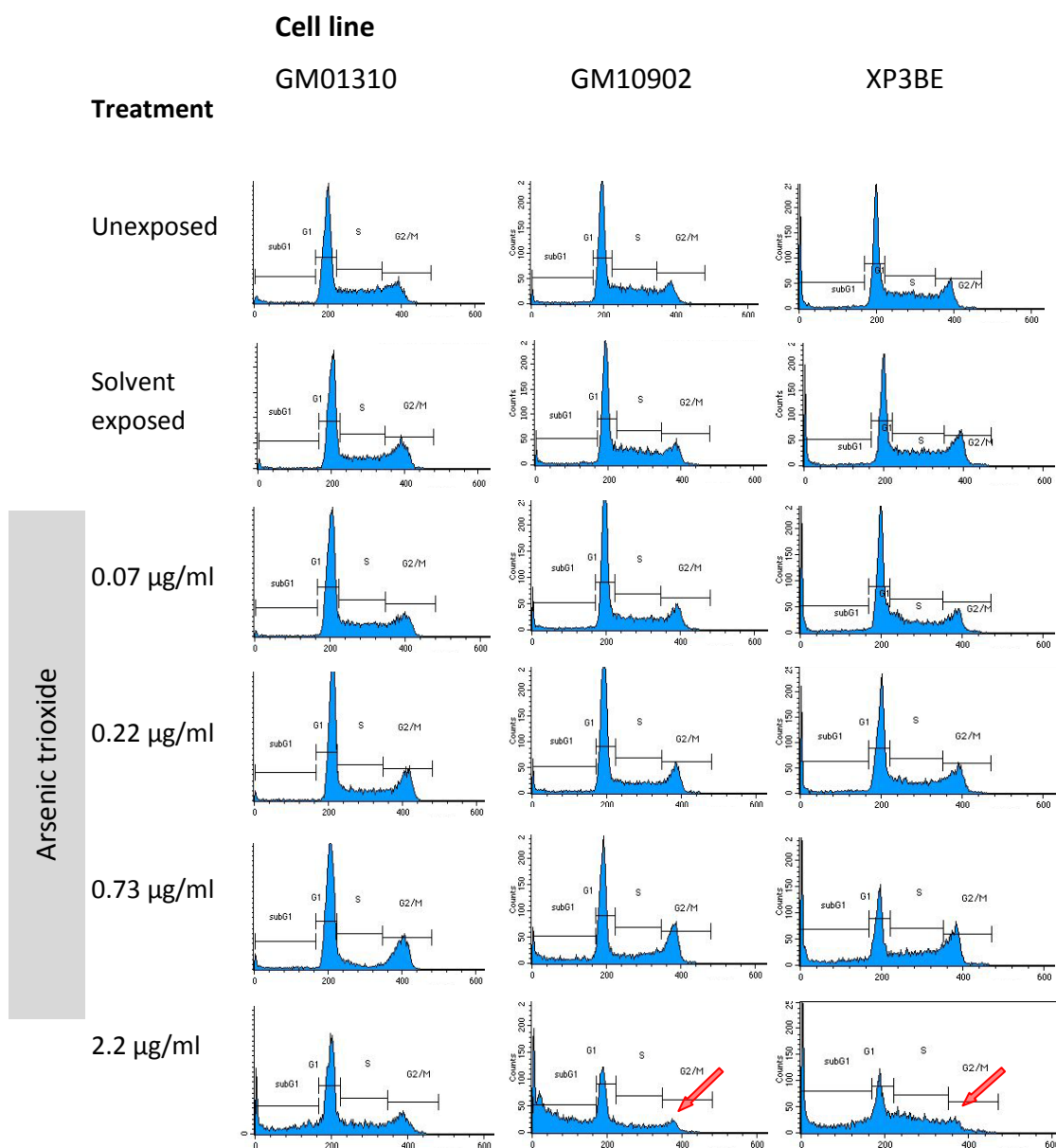


Figure.4.12. Cell cycle distribution of GM01310, GM10902 and XP3BE cells after arsenic trioxide (0.07, 0.22, 0.73, 2.2 µg/ml) treatment for 24 hours. Arrows indicate a clear reduction of G2/M peak at 2.2 µg/ml in GM10902 and XP3BE cells.

Table.4.5. Effect of Ascaridol and Arsenic trioxide on cell cycle distribution of GM01310, GM10902 and XP3BE.

Cell line	GM01310				GM10902				XP3BE			
	subG1	G1	S	G2/M	subG1	G1	S	G2/M	subG1	G1	S	G2/M
Un-exposed	4.5 ± 0.4	50.6 ± 0.7	23 ± 0.7	22.3 ± 0.9	3.5 ± 0.8	43.4 ± 1	34.7 ± 0.9	18.9 ± 1.1	9.4 ± 1.4	38.5 ± 0.6	32.3 ± 1.2	20 ± 1.3
Ascaridol												
0.05 µg/ml	20.5 ± 1.6 ²	34.4 ± 1.1 ²	25 ± 0.9 ²	20.9 ± 0.9	17.6 ± 1.6 ²	32.4 ± 1.1 ²	23.6 ± 0.4 ²	27.3 ± 2.2 ²	28.3 ± 1.6 ²	23.9 ± 1.1 ²	29.3 ± 0.5 ¹	19.3 ± 1.1
0.10 µg/ml	16.2 ± 1.3 ²	34.7 ± 1.3 ²	29.6 ± 1.8 ²	20.7 ± 1.1	19 ± 1.3 ²	26.9 ± 0.6 ²	27.9 ± 1.1 ¹	27.2 ± 0.6 ²	27.3 ± 1.1 ²	17.8 ± 0.7 ²	34.1 ± 1.4	21.9 ± 0.6
0.50 µg/ml	13.9 ± 0.6 ²	36.4 ± 1.2 ²	29.6 ± 1.7 ²	21.3 ± 0.4	24.2 ± 2.1 ²	29.8 ± 0.8 ²	30.8 ± 0.7	16.2 ± 1	27.9 ± 2.2 ²	21.9 ± 4.9 ²	34.5 ± 2.7	16.7 ± 4.5
1.00 µg/ml	15.4 ± 0.5 ²	37.8 ± 0.5 ²	27.8 ± 0.6 ²	20.1 ± 0.4	28.7 ± 0.7 ²	30.1 ± 1.2 ²	30.6 ± 0.5	11.8 ± 0.4 ²	26.4 ± 2 ²	25.1 ± 4.1 ¹	34.9 ± 1.3 ¹	14.7 ± 1.5 ¹
DMSO control	7.5 ± 1.3	51.3 ± 1	22.3 ± 1.2	19.6 ± 0.9	4 ± 0.4	51.2 ± 0.8	29.2 ± 1.3	16.3 ± 0.6	13.9 ± 4.8	37.4 ± 1.6	29.7 ± 1.4	19.7 ± 2
Arsenic trioxide												
0.07 µg/ml	1 ± 0.3	55.3 ± 0.8	26 ± 1.1 ¹	18.3 ± 1.7	4.9 ± 0.5 ¹	55.8 ± 0.9 ²	24.2 ± 0.9 ²	15.6 ± 1.3	11.1 ± 2	46.1 ± 0.6 ²	27.8 ± 1.2 ²	15.6 ± 1
0.22 µg/ml	1.1 ± 0.2	56.7 ± 2.4	21.6 ± 0.8 ²	21.2 ± 2.1	6 ± 0.6 ²	56.6 ± 0.7 ²	20.6 ± 0.7 ²	17.4 ± 0.7	10.7 ± 0.5 ²	45.6 ± 0.7 ²	25.2 ± 0.5 ²	19 ± 0.8
0.73 µg/ml	2.5 ± 0.4	60.9 ± 0.7 ²	10.7 ± 0.6 ²	26.5 ± 0.7 ²	13.5 ± 0.3 ²	46.1 ± 0.8 ²	17.1 ± 0.6 ²	23.7 ± 0.5 ²	19.2 ± 0.8 ²	30.6 ± 1.1 ²	27.1 ± 1.5 ²	23.7 ± 0.8 ¹
2.2 µg/ml	21.6 ± 0.8 ²	44.5 ± 1.3 ²	18.9 ± 0.9 ²	15.6 ± 0.5 ²	49.1 ± 3 ²	29.1 ± 1.1 ²	15.1 ± 1.8 ²	7.3 ± 0.6 ²	36.2 ± 0.8 ²	25.2 ± 0.8 ²	31.9 ± 0.5	7.4 ± 0.5 ²
PBS control	1.2 ± 0.3	50.5 ± 0.8	24.6 ± 0.5	24.2 ± 0.4	3.6 ± 0.4	50.3 ± 1.2	31.9 ± 1.3	14.8 ± 0.6	8.5 ± 1	39.1 ± 1.3	33.6 ± 1.3	19.4 ± 3

¹Significantly different from unexposed sample ($P < 0.05$, two tailed t -test)

²Significantly different from unexposed sample ($P < 0.001$, two tailed t -test)

Table.4.6. Effect of TCM-25-RAB, Quercetin, Scopoletin and Isonardosinon on cell cycle distribution of GM01310, GM10902 and XP3BE.

Cell line	GM01310				GM10902				XP3BE			
	subG1	G1	S	G2/M	subG1	G1	S	G2/M	subG1	G1	S	G2/M
Un-exposed	4.5 ± 0.4	50.6 ± 0.7	23 ± 0.7	22.3 ± 0.9	3.5 ± 0.8	43.4 ± 1	34.7 ± 0.9	18.9 ± 1.1	9.4 ± 1.4	38.5 ± 0.6	32.3 ± 1.2	20 ± 1.3
TCM-25-RAB												
10 µg/ml	15 ± 3.1	52.6 ± 3	15.6 ± 0.4	17.2 ± 0.9	18.7 ± 4 ¹	45.7 ± 5.4 ¹	24.6 ± 2.1	13.1 ± 1.1	16.7 ± 0.3	44.2 ± 0.3	23.7 ± 0.3	16 ± 0.4
DMSO (solvent)	7.5 ± 1.3	51.3 ± 1	22.3 ± 1.2	19.6 ± 0.9	4 ± 0.4	51.2 ± 0.8	29.2 ± 1.3	16.3 ± 0.6	13.9 ± 4.8	37.4 ± 1.6	29.7 ± 1.4	19.7 ± 2
Quercetin												
0.5 µg/ml	3.6 ± 0.4	51.8 ± 0.5	22.7 ± 0.4	22.4 ± 0.7	10.5 ± 2.3	48.1 ± 1.8	32.3 ± 1.1	9.8 ± 0.5	13.7 ± 1.6	37.6 ± 1.4	28.4 ± 0.6	20.8 ± 2.1
1.0 µg/ml	4.1 ± 0.9	52.1 ± 0.6	23.4 ± 1.4	21 ± 1.9	8.3 ± 2.8	48.6 ± 1.2	34.2 ± 2	9.6 ± 0.9	11.2 ± 1.8	37.7 ± 1.4	30.1 ± 0.9	21.5 ± 1.9
5 µg/ml	4.1 ± 0.8	52.8 ± 0.9	22.8 ± 0.4	20.7 ± 1.6	7.1 ± 0.6	48.3 ± 0.8	35 ± 0.8	10.2 ± 1.2	13.9 ± 2.2	37.6 ± 1	28.8 ± 1.3	20.3 ± 1.1
10 µg/ml	4.2 ± 0.4	51.4 ± 0.6	22.4 ± 0.6	22.5 ± 0.8	8.8 ± 1.3	47 ± 0.8	33.8 ± 1.3	11 ± 0.6	21.6 ± 1.4 ¹	36.7 ± 0.7	24.3 ± 1.2 ¹	17.8 ± 1.3
10% NaOH (solvent)	3.7 ± 0.5	53.5 ± 0.9	22.4 ± 0.7	20.9 ± 0.7	6.2 ± 1.6	46.8 ± 0.7	36.7 ± 1.4	10.9 ± 0.6	13 ± 1.6	38.1 ± 0.8	29.2 ± 1.3	20.2 ± 0.8
Scopoletin												
20 µg/ml	8.9 ± 4.2	61.4 ± 3.8 ¹	15 ± 3.5	15 ± 3	3.4 ± 0.4	51.6 ± 0.5	23.1 ± 0.7	22.4 ± 1.1	11.6 ± 1	42.3 ± 0.8 ¹	26.2 ± 0.7	20.4 ± 1.6
Isonardosinon												
5 µg/ml	6 ± 0.1	50 ± 0.8	22 ± 0.5	22 ± 0.9	1.9 ± 0.3	38.4 ± 1.1	35.2 ± 0.6	25.2 ± 1.5	9.7 ± 1.7	35.7 ± 1.5	31.1 ± 1.6	24 ± 2.1
10 µg/ml	8 ± 0.2	48 ± 1.1	23 ± 0.4	21 ± 1.1	1.8 ± 0.1	38.3 ± 0.6	34.1 ± 1.5	26.4 ± 1.3	10 ± 1.3	36.6 ± 1	30.1 ± 0.8	23.8 ± 1.8
10% EthOH (solvent)	1.1 ± 0.1	52.5 ± 0.5	24.3 ± 0.9	22.5 ± 1	3.8 ± 0.7	39 ± 0.7	33 ± 0.9	24 ± 1	13.9 ± 4.8	37.4 ± 1.6	29.7 ± 1.4	19.7 ± 2

¹Significantly different from unexposed sample ($P < 0.05$, two tailed t -test)

4. 5. 3. Single cell gel electrophoresis

The genotoxic effects of the selected drugs were quantified by alkaline comet assay. Exponentially growing cells were treated with different drug concentrations for one hour and embedded in low melting agarose gel. Samples were spotted on comet slides, lysed and electrophorized. As DNA is a charged molecule, during electrophoresis the fragmented DNA moves out of the nucleus and runs towards anode giving the cells a comet like shape. At higher DNA damage, more DNA fragments will migrate in the tail region. Slides were stained with SYBR-green and comets produced by each treatment were analyzed with 'Komet 4' (a semi-automated system). An olive tail moment was calculated for each comet and tail moments relative to unexposed samples were used as a measure of DNA damage. The average tail moment of unexposed samples in all experiments was GM01310 0.86 ± 0.37 , GM10902 0.54 ± 0.33 , and XP3BE 0.54 ± 0.28 , respectively.

4. 5. 3. 1. Ascaridol

DNA damage caused by ascaridol was tested at three different doses (0.1, 0.5 and 1.0 $\mu\text{g/ml}$). Exposure to 1.0 $\mu\text{g/ml}$ ascaridol produced a relative tail moment of 3.38 ± 0.74 in GM01310, 6.88 ± 0.78 in GM10902 and 6.5 ± 0.34 in XP3BE.

Ascaridol produced DNA damage in a dose-dependent manner (Figure.4.13). NER deficient cells were highly sensitive to ascaridol even at the lowest dose (0.1 $\mu\text{g/ml}$) used in the experiments. A significant increase in DNA damage was observed for GM10902 (4.41 ± 0.14) and XP3BE (4.63 ± 1.3) where as GM01310 (1.57 ± 0.41) did not show any significant DNA damage at this concentration. The difference was around three times, thus ascaridol produced DNA damage in NER deficient cells at a dose not genotoxic to the normal cells.

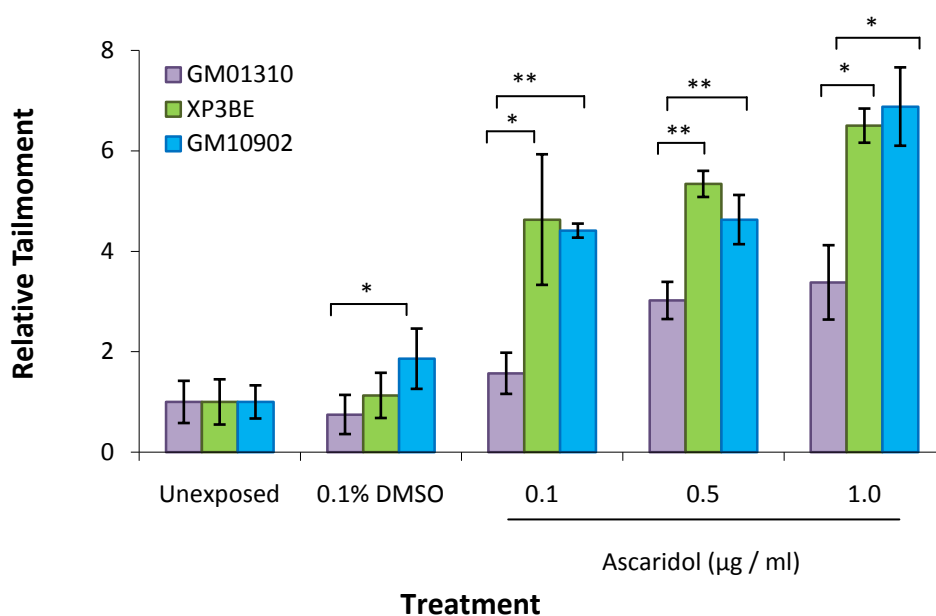


Figure.4.13. DNA damage in GM1310, GM10902 and XP3BE samples after treatment with ascaridol (0.1, 0.5, 1.0 µg/ml) and measured by comet assay.

Exponentially growing cells were treated with the respective drug concentrations for one hour. Unexposed and DMSO (solvent) exposed samples were included as controls. Tail moment (median \pm std error) relative to unexposed samples was used as a measure of DNA damage. * $P < 0.05$, ** $P < 0.01$ (two tailed t -test).

4. 5. 3. 2. Arsenic trioxide

DNA damage caused by arsenic trioxide was tested at three different doses (0.22, 0.73, 2.2 µg/ml). Exposure to 2.2 µg/ml of arsenic trioxide produced a relative tail moment of 2.66 ± 0.38 in GM01310, 6.19 ± 0.41 in GM10902 and 5.17 ± 0.46 in XP3BE.

An increase in DNA damage was observed in the three cell lines even at the low dose (0.22 µg/ml) of arsenic trioxide (Figure.4.14). In GM10902 and XP3BE, arsenic trioxide produced DNA damage in a dose-dependent manner. In GM01310, the increased DNA damage remained stable at higher doses of arsenic trioxide. 0.22 µg/ml arsenic trioxide produced significantly higher DNA damage in GM10902

when compared to GM01310. At higher doses difference between GM01310 and NER deficient cell lines was even stronger.

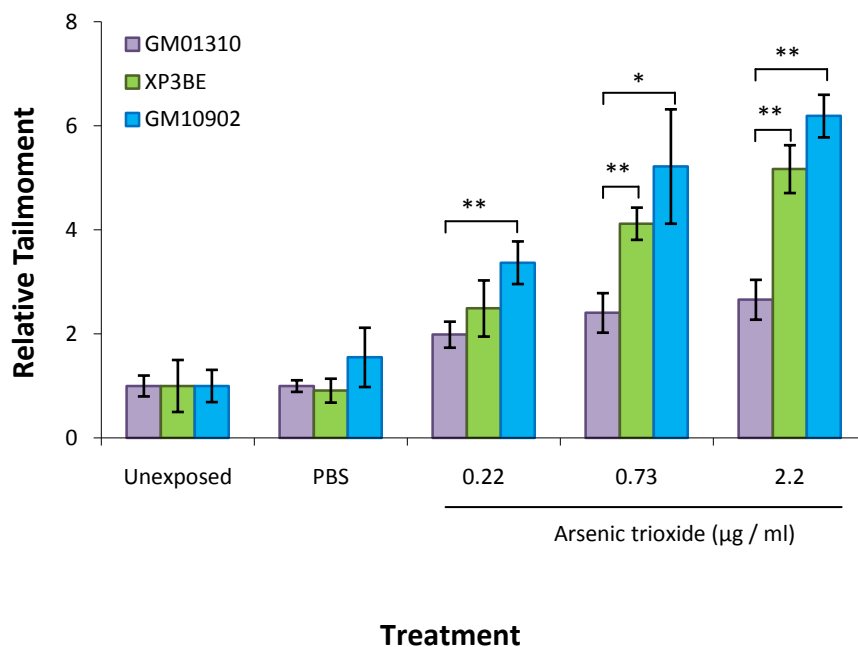


Figure.4.14. DNA damage in GM1310, GM10902 and XP3BE samples after treatment with Arsenic trioxide (0.22, 0.73, 2.2 µg/ml) as measured by alkaline comet assay. Unexposed and PBS (solvent) exposed samples were included as controls. Tail moment (median \pm std error) relative to unexposed samples was taken as a measure of DNA damage. * $P < 0.05$, ** $P < 0.01$ (two tailed t -test).

4. 5. 3. 3. TCM-25-RAB

DNA damage caused by TCM-25-RAB was tested at two different doses (5, 10 µg/ml). At 10 µg/ml TCM-25-RAB produced a relative tail moment of 5.37 ± 0.51 in GM10902 and 3.13 ± 1.08 in XP3BE whereas GM01310 had a relative tail moment of 1.58 ± 0.11 . TCM-25-RAB (Figure.4.15-a) produced DNA damage in a dose-dependent manner. A significant increase in DNA damage was observed in drug treated GM10902 and XP3BE samples, producing more damage to GM10902 cells. GM01310 did not show any significant DNA damage at any concentration.

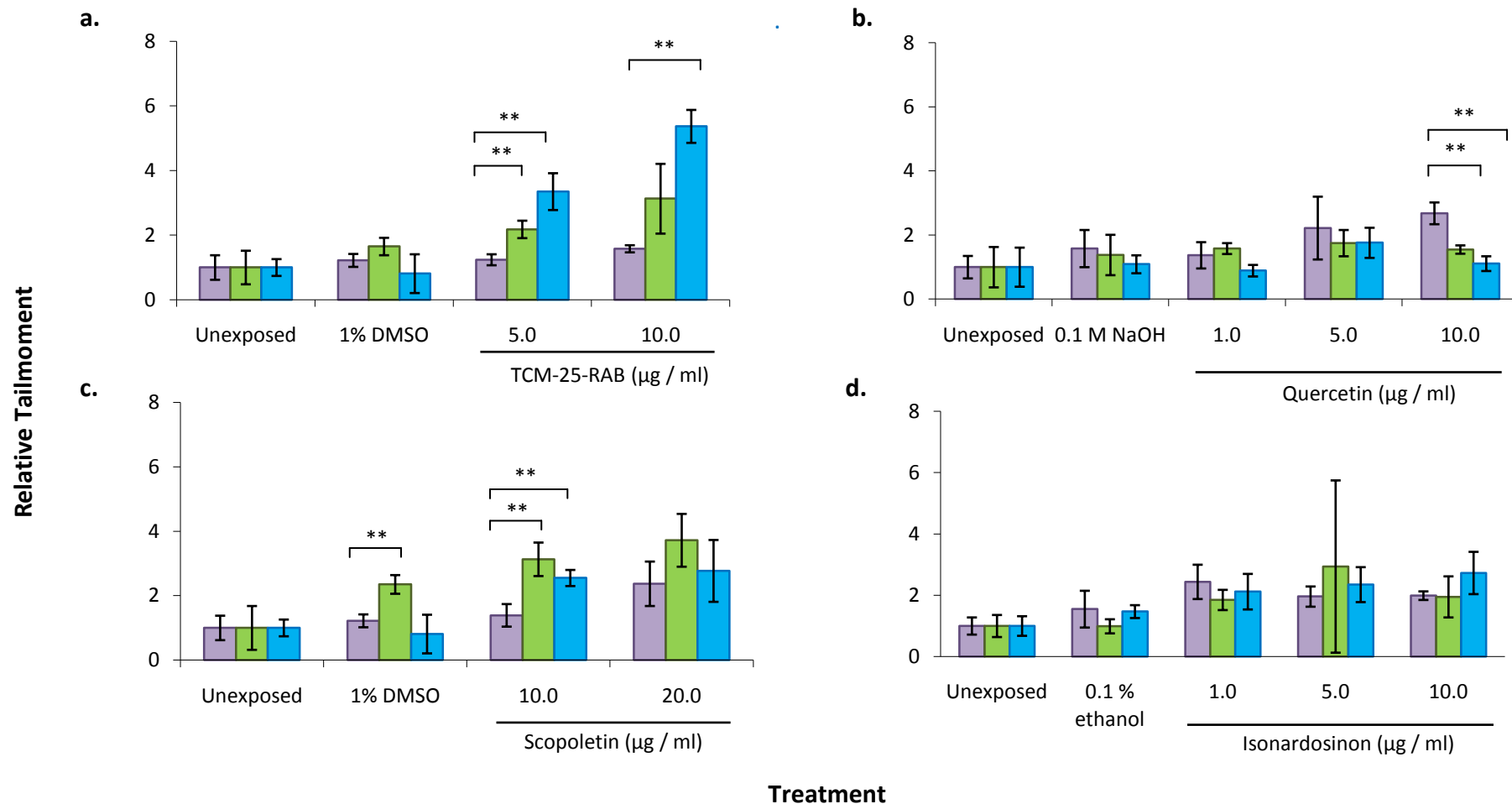


Figure.4.15. DNA damage in GM01310 (■), XP3BE (■) and GM10902 (■) after treatment with different TCM drugs and measured by comet assay. Tail moment relative to unexposed samples was used as a measure of DNA damage. **a.** Isonardosinon, **b.** Quercetin, **c.** Scopoletin and **d.** TCM-25-RAB. * $P < 0.05$, ** $P < 0.01$ (two tailed t -test).

4. 5. 3. 4. *Quercetin, Scopoletin and Isonardosinon*

Quercetin (Figure.4.15-b) was tested for its genotoxic effects at two different doses (5, 10 $\mu\text{g/ml}$). 5 $\mu\text{g/ml}$ quercetin had a similar effect on all the three cell lines. At 10 $\mu\text{g/ml}$, GM01310 cells showed significantly higher DNA damage than XP3BE and GM10902.

DNA damage caused by scopoletin (Figure.4.15-c) was tested at two different doses (10, 20 $\mu\text{g/ml}$). 10 $\mu\text{g/ml}$ of scopoletin caused a significant increase in DNA damage in XP3BE as well as GM10902 cells however at 20 $\mu\text{g/ml}$ scopoletin the three cell lines did not have a significant difference.

Isonardosinon (Figure.4.15-d) caused a slight increase in DNA damage in the three cell lines, but there was no significant difference between the cell lines.

In summary, these results show that ascaridol, arsenic trioxide and TCM-25-RAB induce significant DNA damage. This DNA damage is higher in NER deficient cells (GM10902, XP3BE) than NER proficient cells (GM01310).

4. 5. 4. **Quantification of AP sites (Arp assay)**

Next step was to investigate the type of DNA damage these drugs induce. Regarding the chemical formulas of drugs (Table.4.4), oxidative DNA damage would be probable. One method to measure oxidative damage is by counting apurinic / apyrimidinic (AP) sites in the samples after treatment. AP sites are one of the major types of lesions in DNA. These sites can generate either spontaneously or as an intermediate in base excision repair (Boiteux & Guillet, 2004).

Exponentially growing cultures were treated with drugs and their solvents for 24hrs, cells were harvested and their DNA was extracted. AP sites in the DNA samples were counted by using the 'DNA damage quantification assay-AP site counting'. It is an ELISA-like assay that uses avidin-biotin complex conjugated with horseradish peroxidase as an indicator enzyme for the detection of AP sites. The assay constitutes of ARP (aldehyde reactive probe) reagent that specifically tags the

aldehyde group in the ring opened AP site with a biotin residue. The number of AP sites (per 10^5 base pairs) was quantified by using standard ARP labeled DNA solutions and AP sites in the drug exposed samples were measured relative to the solvent control. The standard has a known amount of AP sites, ranging from 0 to 40 per 1×10^5 base pairs of calf thymus DNA. Each experiment was performed twice with two independent replicates.

Results are given in Figure.4.16. Treatment with Arsenic trioxide (2.2 $\mu\text{g/ml}$), ascaridol (0.1 $\mu\text{g/ml}$) and TCM-25-RAB (5 $\mu\text{g/ml}$) did not cause significant increase ($p > 0.05$) in AP sites in GM01310, GM10902 and XP3BE. Scopoletin (10 $\mu\text{g/ml}$) and Quercetin (1 $\mu\text{g/ml}$) exposure produced increased amount of AP sites but because of large variations, results were not significant.

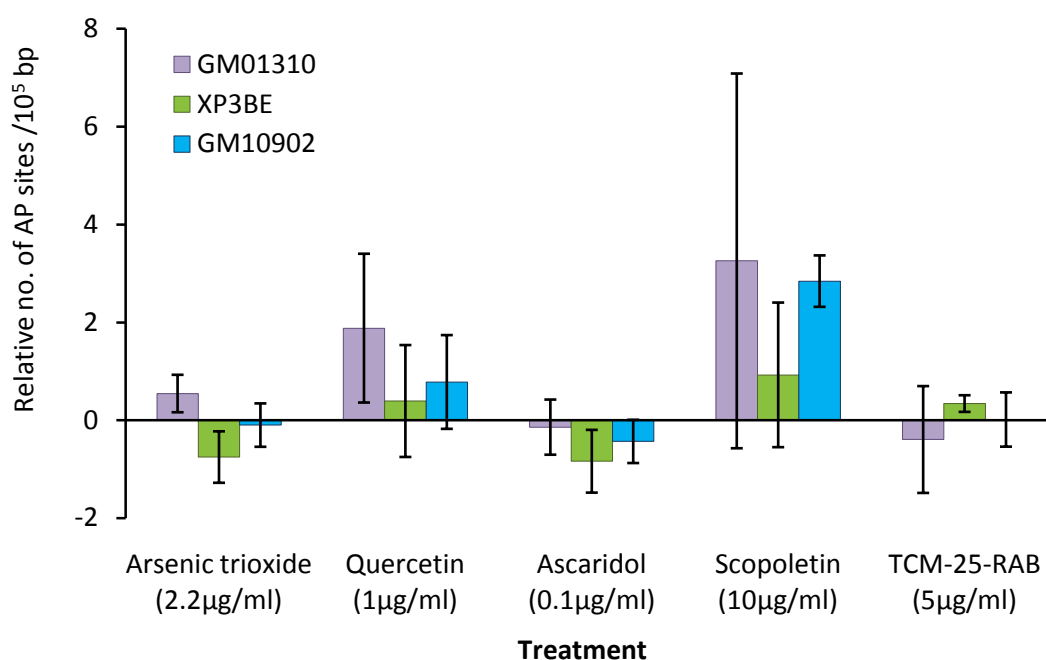


Figure.4.16. Number of AP sites / 10^5 base pairs caused by selected TCM drugs in GM01310, GM10902 and XP3BE. Results shown are relative to the solvent control of each drug. PBS is the solvent for Arsenic trioxide, 0.1M NaOH for quercetin, 1% DMSO for Ascaridol, scopoletin and TCM-25-RAB. Number of AP sites in solvents: PBS 4.19 ± 0.59 , 3.051 ± 0.733 and 3.732 ± 0.321 , 0.1M NaOH 5.317 ± 0.392 , 4.952 ± 0.539 and 4.422 ± 0.608 , 1% DMSO 4.377 ± 0.373 , 2.843 ± 0.169 and 3.086 ± 0.157 , in GM01310, GM10902 and XP3BE cells respectively. The results are from two experiments with duplicate samples for each treatment.

4. 6. Validation of results obtained for ascaridol

Ascaridol was the most promising TCM compound in our study. The drug killed NER deficient cells very efficiently and at doses that were apparently nontoxic to the normal cells. To prove that the results obtained in the previous experiments are because of NER (*XPC* and *ERCC6*) deficiencies, cytotoxicity and DNA damage caused by ascaridol were measured in a different cell model. As a model for *XPC* mutation a pair of *XPC* cell lines (XP4PA and XP4PA-SE2) was picked. The pair has the same genetic background but XP4PA is deficient in *XPC* whereas XP4PA-SE2 is the fully corrected version of the cell line by stable transfection using pXPC-3 plasmid (Legerski & Peterson, 2002). As a model for *ERCC6* mutation, the gene was silenced in XP4PA-SE2 cells using ON-TARGETplus SMARTpool siRNA and the Luciferase siRNA exposed cultures (negative control for gene silencing) were considered as repair competent control.

4. 6. 1. Determination of IC₅₀ values

To determine IC₅₀ value of ascaridol, confluent cultures of XP4PA, XP4PA-SE2, and ERCC6-silenced XP4PA-SE2 cells and Luciferase siRNA exposed cultures were exposed to different concentrations of the drug for 24 hours and relative % viabilities were measured.

For the measurement of relative % viabilities, conditions for '**The LIVE/DEAD® Viability/Cytotoxicity assay**' (Invitrogen) were optimized. The assay comprises of two fluorescent dyes, Calcein AM (excitation: 485nm, emission: 520nm) and Ethidium Homodimer (excitation: 520nm, emission: 620nm) for detecting live cells and dead cells, respectively. Ethidium Homodimer could not be optimized for these cell lines. A possible explanation is that XP4PA and XP4PA-SE2 are adherent cells and washing step removed all the dead cells from the culture. For these cell lines relative viabilities were measured by Calcein AM only (Calcein assay). Table.4.2 gives the optimum concentrations of the dyes used for the cell lines.

Relative viability curves were generated by plotting relative viability (%) against drug concentrations and IC₅₀ values were calculated. As a control, solvent exposed

and unexposed samples were included. Experiments were performed twice with three replicates for each treatment.

4. 6. 1. 1. Effect of ascaridol on paired XPC cell lines

As the Figure.4.17 demonstrates, XP4PA (*XPC*-deficient) cells ($IC_{50} = 0.013 \mu\text{g/ml}$) were very sensitive to ascaridol exposure. At $0.01 \mu\text{g/ml}$ ascaridol exposure, relative viability was only $53.3 \pm 6.7 \%$ and $1 \mu\text{g/ml}$ ascaridol killed all the cells. XP4PA-SE2 (*XPC*-proficient) cells ($IC_{50} = 2.19 \mu\text{g/ml}$) were not as sensitive as XP4PA.

There was a 165 fold difference in the sensitivity of the two cell lines to ascaridol exposure. The result confirms our previous finding '*XPC* deficient cells are more sensitive to ascaridol exposure'.

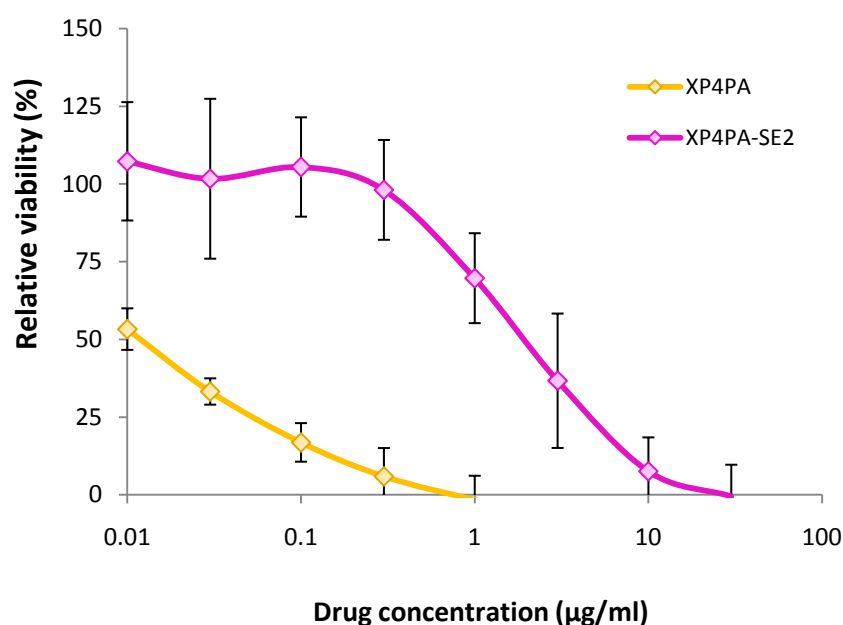


Figure.4.17. Determination of IC_{50} values for ascaridol in XP4PA and XP4PA-SE2.

Exponentially growing cells were exposed to different concentrations of ascaridol for 24 hrs and percent viability (mean \pm std.dev) relative to the unexposed sample as calculated by Calcein assay. The IC_{50} values for XP4PA = $0.013 \mu\text{g/ml}$ and XP4PA-SE2 = $2.19 \mu\text{g/ml}$. Mean values of two independent experiments with three replicates for each treatment are shown.

4. 6. 1. 2. Effect of ascaridol on ERCC6 silenced cells

As Figure.4.18 demonstrates, ERCC6 silenced cells ($IC_{50} = 0.095 \mu\text{g/ml}$) were more sensitive to ascaridol exposure than Luciferase siRNA exposed cells ($IC_{50} = 3.0 \mu\text{g/ml}$). There was a difference of 32 folds in the sensitivity of the two cell types to ascaridol exposure. This confirms our previous finding that *ERCC6* deficient cells are more sensitive to ascaridol exposure. Moreover, the Luciferase siRNA exposed cells ($IC_{50} = 3.0 \mu\text{g/ml}$) have similar sensitivity as XP4PA-SE2 ($IC_{50} = 2.19 \mu\text{g/ml}$).

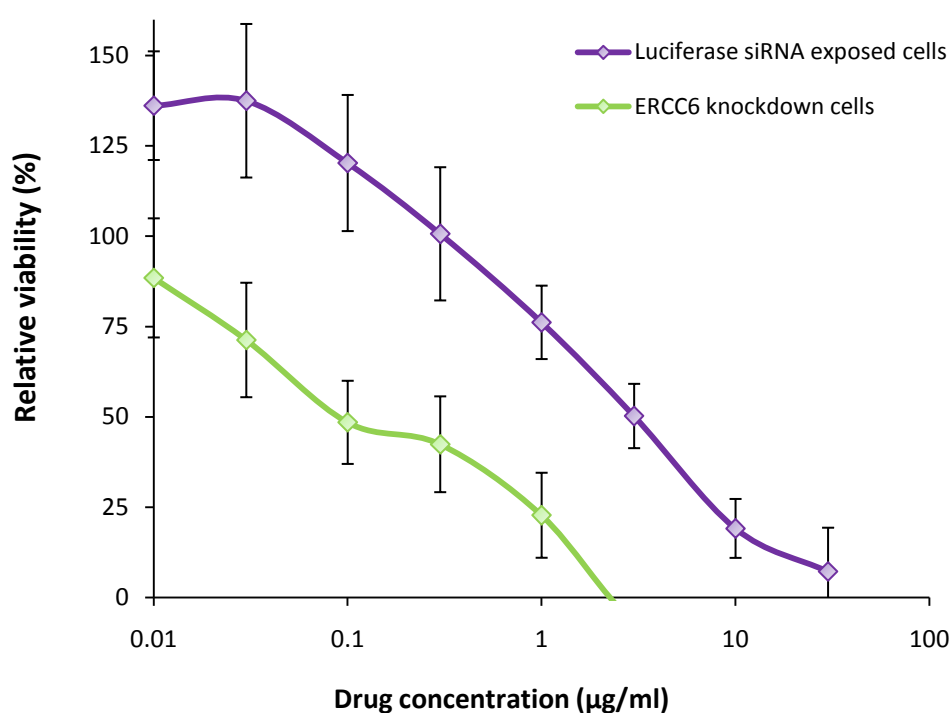


Figure.4.18. Viability curves. Relative resistance to ascaridol determined in ERCC6 silenced and Luciferase siRNA exposed (negative control) cells. Exponentially growing cells were exposed to different concentrations of ascaridol for 24hrs and percent viabilities (mean \pm std.dev) relative to the unexposed sample were calculated by Calcein assay. The IC_{50} values are ERCC6 silenced cells = $0.095 \mu\text{g/ml}$ and Luciferase siRNA exposed cells = $3.0 \mu\text{g/ml}$. Mean values of two independent experiments with three replicates for each treatment are shown.

4. 6. 2. Single cell gel electrophoresis

4. 6. 2. 1. Genotoxic effects of Ascaridol on paired XPC cell lines

DNA damage caused by ascaridol was tested at three different doses (0.1, 0.5 1.0 $\mu\text{g/ml}$). The average tail moment of unexposed samples was XP4PA = 2.94 ± 0.67 and XP4PA-SE2 = 2.95 ± 1.33 . Figure.4.19 demonstrates that ascaridol produced DNA damage in XP4PA and XP4PA-SE2 in a dose-dependent manner. 0.1 $\mu\text{g/ml}$ ascaridol caused a very strong effect on XP4PA (relative tail moment = 12.95 ± 1.29) compared with XP4PA (relative tail moment = 6.79 ± 1.41). Exposure to 1 $\mu\text{g/ml}$ ascaridol produced a relative tail moment of 15.40 ± 0.85 in XP4PA and 11.63 ± 1.50 in XP4PA-SE2. XP4PA cells had higher DNA damage compared to XP4PA-SE2 at all concentrations.

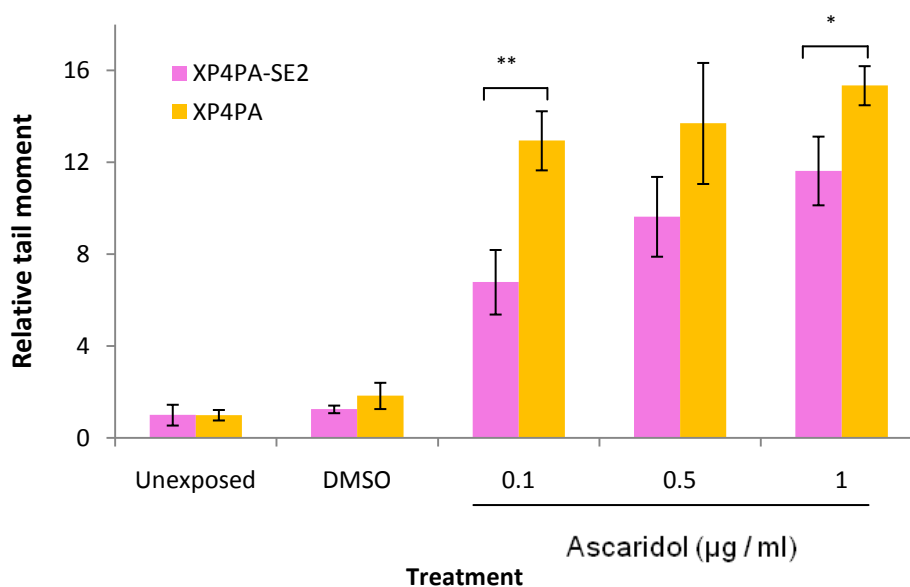


Figure.4.19. DNA damage caused by Ascaridol (0.1, 0.5, 1.0 $\mu\text{g/ml}$) in XP4PA and XP4PA-SE2 cells as measured by alkaline comet assay. Exponentially growing cells were treated with the respective drug concentrations for one hour. Unexposed and DMSO (solvent) exposed samples were included as controls. Tail moment (median \pm std error) relative to unexposed samples was used as a measure of DNA damage. * $P < 0.05$, ** $P < 0.01$ (two tailed t -test).

4. 6. 2. 2. Genotoxic effects of Ascaridol on ERCC6 silenced cells

DNA damage caused by ascaridol was tested at three different doses (0.1, 0.5, 1.0 $\mu\text{g/ml}$). The average tail moment of unexposed samples in ERCC6 silenced cells was 5.73 ± 0.49 and in the Luciferase siRNA exposed cells was 6.76 ± 1.66 . Figure.4.20 shows that ascaridol produced DNA damage in ERCC6 silenced cells in a dose-dependent manner.

At higher doses the effect was stronger and exposure to 1 $\mu\text{g/ml}$ ascaridol produced a relative tail moment of 6.30 ± 0.22 in ERCC6 silenced cells and 2.28 ± 0.40 in Luciferase siRNA exposed cells. ERCC6 silenced cells accumulated more DNA

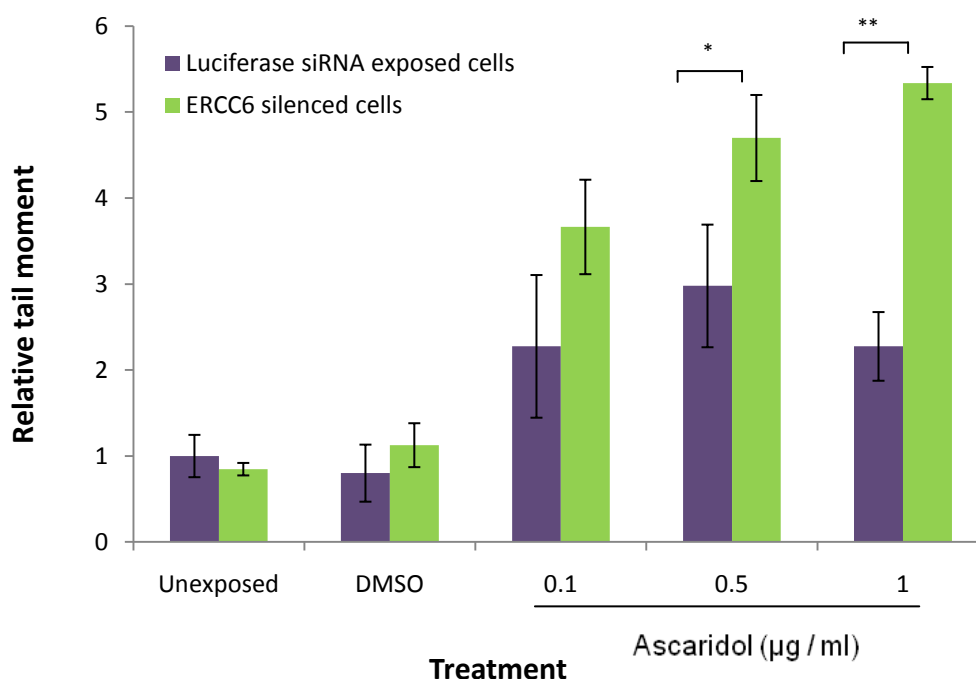


Figure.4.20. DNA damage caused by Ascaridol (0.1, 0.5, 1.0 $\mu\text{g/ml}$) in ERCC6 silenced XP4PA-SE2 cells and negative control as measured by alkaline comet assay. Exponentially growing cells were treated with the respective drug concentrations for one hour. Unexposed and DMSO (solvent) exposed samples were included as controls. Tail moment (median \pm std error) relative to unexposed samples was used as a measure of DNA damage. Negative control is Luciferase siRNA treated XP4PA-SE2 cells.* $P < 0.05$, ** $P < 0.001$ (two tailed t-test).

damage compared to repair competent cells.

XP4PA-SE2 cells were more sensitive to ascaridol compared with Luciferase siRNA exposed cells. As the results are from different experiments and involve electrophoresis, high background in paired XPC cell lines can be attributed as experimental variation.

4. 7. Mode of action of Ascaridol

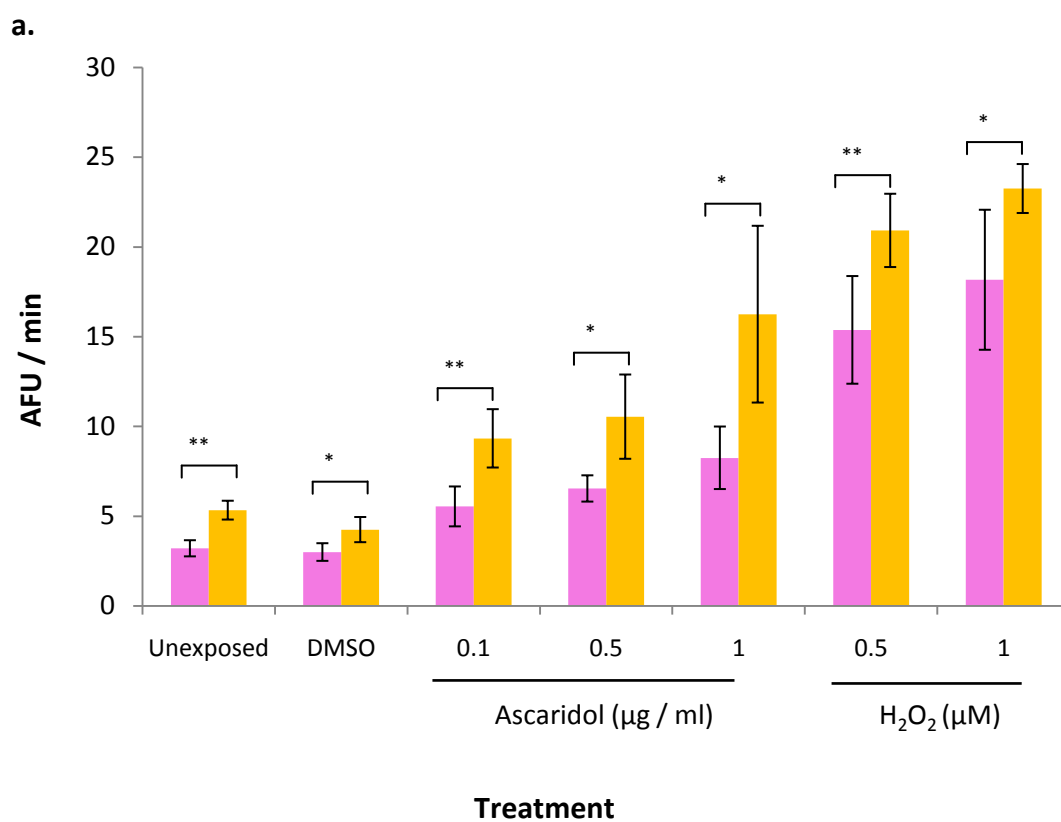
Although ascaridol was the first peroxide discovered and has been used as a medicine for centuries (Dembitsky, 2008), yet little is known about its mode of action. Our data show that the drug produces DNA damage, this damage is higher in NER deficient cells when compared to NER proficient cells. As the structure (Table.4.4) suggests, the drug contains an endoperoxide bridge and therefore may produce oxidative damage. ARP assay performed earlier did not reveal much information, therefore more direct methods like the production of reactive oxygen species by ascaridol and quantification of 8-oxodG sites by Fpg-modified comet assay were used to investigate how the drug actually works.

4. 7. 1. 2',7'-dichlorofluorescein diacetate (H₂DCFDA) assay

The intracellular production of ROS after ascaridol treatment was measured by H₂DCFDA assay. H₂DCFDA was added to XP4PA and XP4PA-SE2 cells growing in 96 well plates and samples were treated with different concentrations of ascaridol (0.1, 0.5, 1 µg/ml) and DMSO. Two concentrations of H₂O₂ were included as positive controls for ROS production. The Rate_{ROS} in the cells was measured by CytoFlour multi well plate reader, series 4000 at Ex / Em : 485 / 520 nm. The RR_{ROS} was calculated with reference to the unexposed samples.

Figure.4.21 demonstrates that the unexposed XP4PA cells (Rate_{ROS} = 5.3 ± 0.52) had a significantly higher (P < 0.001) intracellular peroxide levels compared to XP4PA-SE2 cells (Rate_{ROS} = 3.2 ± 0.45). A dose-dependent significant (P < 0.001) increase in intracellular peroxide levels was observed in ascaridol treated cells. Although XP4PA had higher basal intracellular peroxide levels compared to XP4PA-SE2, the

RR_{ROS} after treatment did not differ in both the cell lines. RR_{ROS} was 1.75 ± 0.30 , 1.98 ± 0.44 , 3.05 ± 0.92 and 1.73 ± 0.35 , 2.04 ± 0.23 , 2.57 ± 0.54 at 0.1, 0.5, 1 $\mu\text{g}/\text{ml}$ in XP4PA and XP4PA-SE2 cells, respectively. 1% DMSO exposure had no significant effect on ROS production in our cells (XP4PA RR_{ROS} = 0.8 ± 0.13 , and XP4PA-SE2 RR_{ROS} = 0.94 ± 0.15).



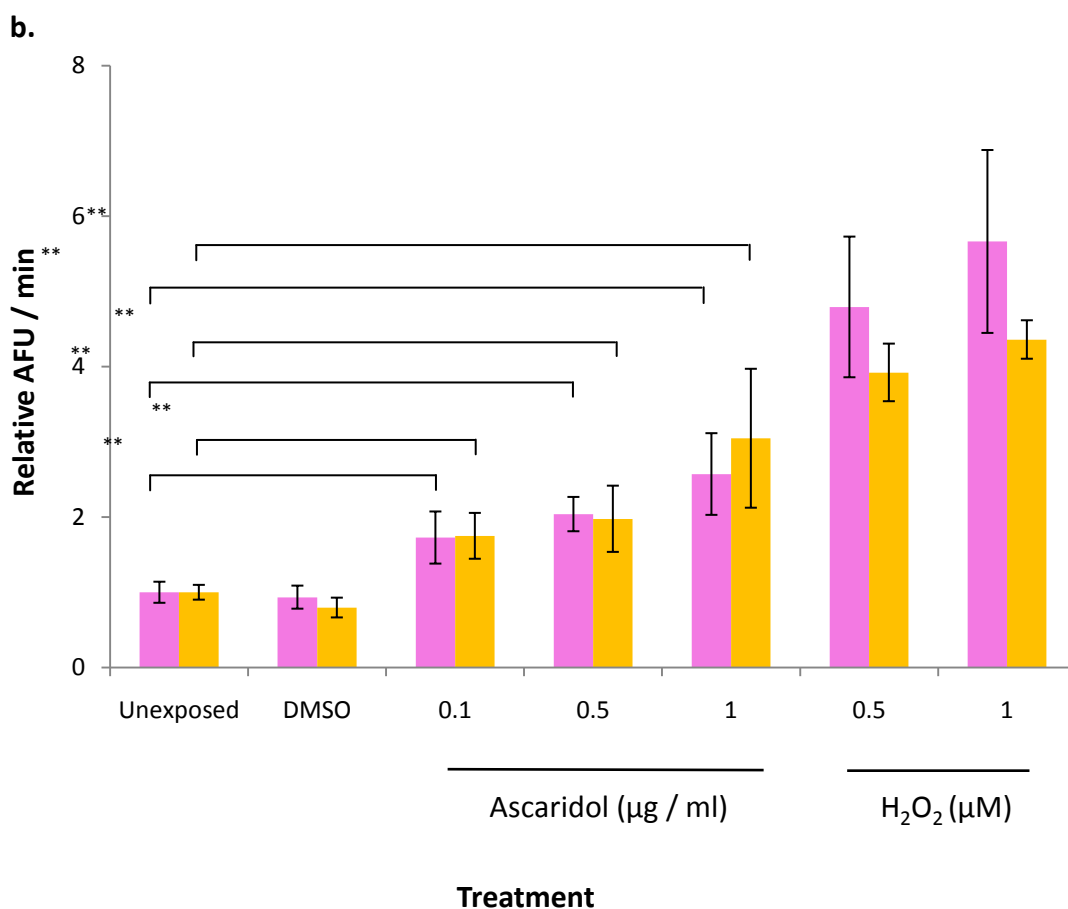


Figure.4.21. Production of reactive oxygen species (ROS) after ascaridol (0.1, 0.5, 1 µg/ml) treatment in (■) XP4PA and (■) XP4PA-SE2 cells measured by H₂DCFDA (25 µM) assay. Exponentially growing cultures were treated with ascaridol and fluorescence was measured for 40 min starting immediately. Samples treated with H₂O₂ (0.5, 1 µM) were included as positive controls. **a.** Rate of ROS (AFU/min) production. **b.** Relative Rate of ROS (relative AFU/min) production (Rate_{ROS} in unexposed XP4PA = 5.3 ± 0.52 and XP4PA-SE2 = 3.2 ± 0.45). The results are from two independent experiments with three replicates per treatment. AFU = arbitrary fluorescence units. * $P < 0.05$, ** $P < 0.001$ (two tailed t -test)

4. 7. 2. Quantification of 8-oxodG sites by Fpg-modified comet assay

Exponentially growing cell cultures were treated with different concentrations of ascaridol and DMSO for one hour, cells were harvested and embedded in agarose and spotted on comet slides. After lysis overnight samples were treated with Fpg enzyme or NEBuffer 1 for 50 min. Samples were electrophorized and comets produced were scored with Comet 4. Olive tail moments were taken as a measure of DMA damage. To differentiate the oxidized bases from single strand breaks, olive tail moment of buffer treated samples representing single strand breaks and alkali-labile sites was subtracted from Fpg treated sample (enzyme induced breaks).

4. 7. 2. 1. Effect of ascaridol on XPC deficient and proficient cell line

Oxidative DNA damage caused by ascaridol was tested at three different doses (0.1, 0.5 1.0 $\mu\text{g/ml}$). For XP4PA, the average tail moment of NEBuffer 1 treated-unexposed samples was 17.69 ± 0.80 and Fpg treated-unexposed samples was 15.62 ± 0.64 . For XP4PA-SE2, the NEBuffer 1 treated-unexposed sample was missing and the average tail moment of Fpg treated-unexposed samples was 7.31 ± 0.36 . Figure.4.22-a demonstrates that ascaridol (1 $\mu\text{g/ml}$) produced a highly significant increase in oxidized bases in XP4PA (Fpg sensitive lesions 13.78 ± 1.72 , $p = < 0.0001$) cells. XP4PA-SE2 did not show such an increase.

4. 7. 2. 2. Effect of ascaridol on ERCC6 silenced and Luciferase siRNA exposed (repair competent control) cells

Oxidative DNA damage caused by ascaridol was tested at three different doses (0.1, 0.5 1.0 $\mu\text{g/ml}$). For ERCC6 silenced cells, the average tail moment of NEBuffer 1 treated-unexposed samples was 16.69 ± 0.87 and Fpg treated-unexposed samples was 17.54 ± 1.37 . For Luciferase siRNA exposed cells, the average tail moment of NEBuffer 1 treated-unexposed samples was 15.46 ± 1.28 and Fpg treated-unexposed samples was 16.53 ± 0.90 . Figure.4.22-b demonstrates that ascaridol produced a highly significant increase in oxidized bases in ERCC6 silenced cells (Fpg sensitive lesions 19.84 ± 1.1 and 19.33 ± 1.2 at 0.5 and 1 $\mu\text{g/ml}$, respectively, $p = <$

0.0001) after ascaridol treatment. Such an increase was not observed in Luciferase siRNA exposed cells.

These results show that ascaridol is mediating DNA damage by oxidative stress and NER deficient cells are sensitive to oxidative damage compared to NER proficient cells.

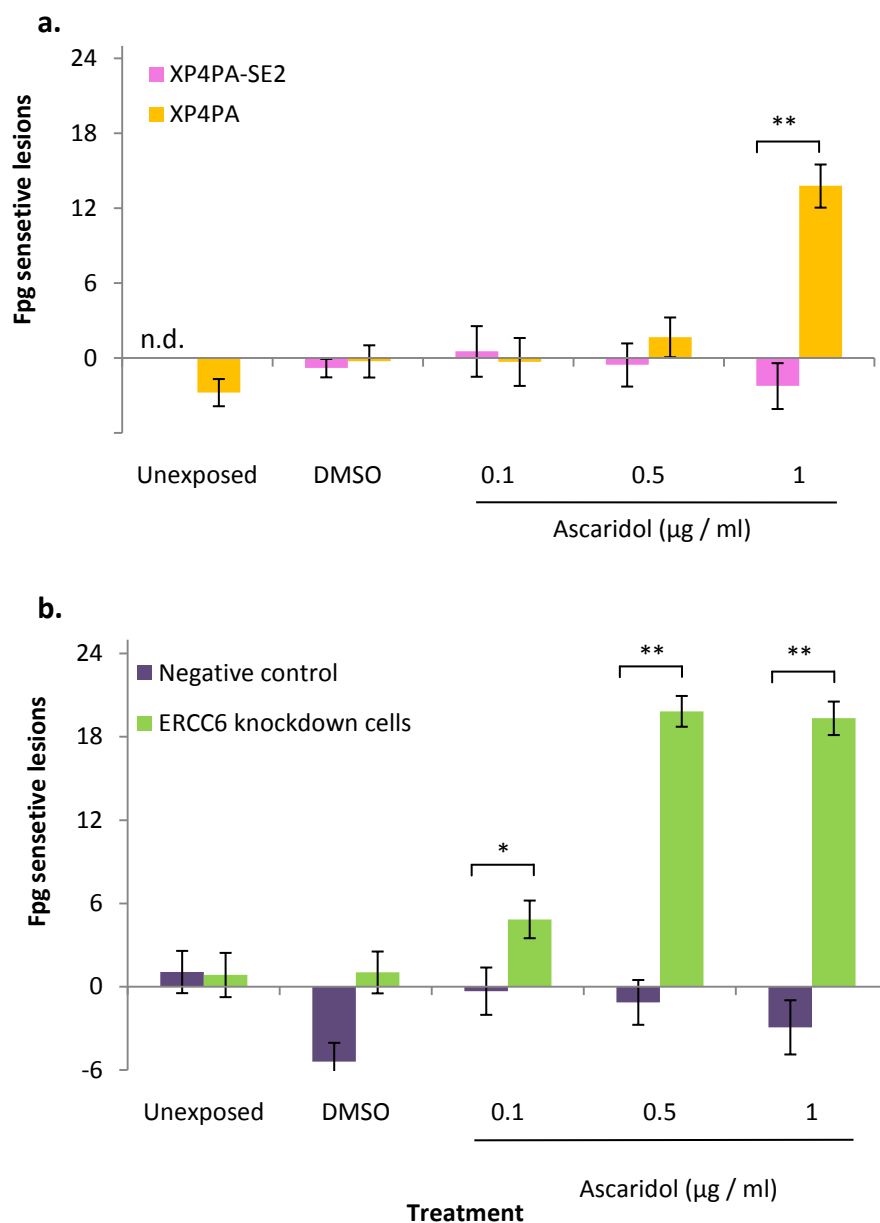


Figure.4.22. Oxidative DNA damage. Fpg sensitive lesions (mean ± std error) after treatment with different concentrations of ascaridol. Unexposed and DMSO exposed samples were included as experimental controls. **a.** XP4PA and XP4PA-SE2 cells **b.** ERCC6 silenced XP4PA-SE2 cells and negative control (luciferase siRNA treated) samples. 153 cells were scored for each treatment. * $P < 0.05$, ** $P < 0.0001$ (two tailed t -test)



5. Discussion, NER and cancer Risk

5. 1. Genotype analysis

We investigated 11 SNPs present in seven NER genes (*XPC*, *ERCC1*, *ERCC2*, *ERCC4*, *ERCC5*, *ERCC6* and *RAD23B*) in a cohort of laryngeal cancer patients and matched controls. Allele frequencies observed were similar to frequencies given for the European Caucasian population reported by the NCBI Reference Assembly (NCBI, 2007). Using multivariate logistic regression analysis, three of the investigated SNPs, *ERCC6* Arg1230Pro, *ERCC5* Asp1104His, and *RAD23B* Ala249Val, showed a significant association with laryngeal cancer risk in the overall population and in individuals with high tobacco and/or alcohol consumption. For all other SNPs, no significant associations were determined.

Some of the 11 SNPs were also investigated in two further studies in patients with squamous cell carcinoma of the head and neck. Studies included a separate analysis for laryngeal cancer in 157 non-Hispanic, white patients (An *et al.*, 2007) and in 326 Europeans (Hall *et al.*, 2007). Both studies did not find a statistically significant association for any of the SNPs and laryngeal cancer, even when considering smoking and alcohol consumption in the regression model.

5. 2. ERCC6

The *ERCC6/CSB* protein is part of the damage recognition complex of the transcription-coupled branch of the NER pathway (Fousteri & Mullenders, 2008). Larynx cancer risk of the *ERCC6* 1230Pro allele carriers was found to be only half as high as the risk of carriers of the more frequent wild type allele. As the polymorphism is encoding an amino acid change, we suggest that the 1230Pro variant strengthens the *ERCC6* protein or enhances its function, and thus protects against larynx cancer. Cockayne syndrome was not found to be a cancer predisposing condition, which could be explained by the fact that the Cockayne syndrome cells are especially sensitive to apoptosis, thereby preventing them from

tumorigenesis. However, it has been shown that *ERCC6*-disrupted mice had an increased susceptibility to skin cancer (van der Horst *et al.*, 1997). To our best knowledge, data on laryngeal cancer risk are missing for this *ERCC6* 1230Pro SNP. In breast, bladder or colon cancer patients, no statistically significant associations were reported (Berndt *et al.*, 2006; Garcia-Closas *et al.*, 2006; Huang *et al.*, 2006; Mechanic *et al.*, 2006).

5. 3. *ERCC5*

ERCC5 encodes the 3'-endonuclease *XPG* involved in the excision step of NER. Our data indicate that the *ERCC5* 1104His allele might contribute to laryngeal cancer risk in heterozygous patients. This result is not supported by other studies on laryngeal or head and neck cancer which did not report a significant association for this SNP (An *et al.*, 2007; Cui *et al.*, 2006). The mixed ethnicities in one study and the small sample size (90 and 152 patients) could be reasons for this result. Regarding other cancer types, Kumar *et al.*, (2003) found an increase in risk in breast cancer patients for His allele carriers whereas Sanyal *et al.*, (2004) reported a protective effect of this allele (homozygous His) in bladder cancer. Studies on bladder, breast, endometrial or colorectal cancer did not find an association for the *ERCC5* Asp1104His SNP in Caucasian populations (Berndt *et al.*, 2006; Garcia-Closas *et al.*, 2006; Huang *et al.*, 2006; Mechanic *et al.*, 2006; Weiss *et al.*, 2005).

5. 4. *Exogenic risk factors for larynx cancer and NER genotypes*

Smoking and alcohol consumption are among the major exogenic risk factors of laryngeal cancer (Hashibe *et al.*, 2007; IARC, 2002; La *et al.*, 2008; Ramroth *et al.*, 2004; Talamini *et al.*, 2002). Both exposures cause DNA damage such as bulky DNA adducts and oxidation products. This DNA damage has to be repaired to preserve genomic stability, and NER is one of the main pathways involved. The repair gene polymorphisms studied here were selected because of their believed effects on protein function. For assessing their contribution to cancer risk, it must, however, be noted that the tested polymorphisms are defined as low penetrance variations

that might alter the protein functions only slightly. But even a slight reduction of repair capacity might still be sufficient for complete repair with low exposure conditions. With high and longer exposure, however, DNA repair might not be sufficient any more. Thus, effects of repair gene polymorphisms should preferentially become perceptible in individuals with strong exposure to DNA damaging agents from smoking and alcohol.

We therefore stratified our data for light and heavy tobacco and alcohol consumption and analyzed the risk modifying effect of the genotype in both groups. These analyses reflected the protective effect of the *ERCC6* 1230Pro allele found in the overall evaluation in individuals with strong tobacco or/and alcohol consumption. In patients with low tobacco exposure, this protective association was already observed, despite no statistical significance. As a whole, this finding seems to strengthen the role of the *ERCC6* 1230Pro allele in the etiology of larynx cancer. The stratified analysis revealed further a moderately increased risk for *ERCC5* Asp1104His heterozygotes in heavy smokers, and a more than two fold risk increase in these individuals with medium alcohol intake which was also visible in the medium exposure group when both exposures were considered. Although statistically not significant, these data might indicate an increasing risk effect of the allele in exposed individuals.

We could not establish a dose-response effect for alcohol consumption. The strongest effects were detected in the group with an intermediate exposure of 25-50 g alcohol per day. A possible explanation could be that our risk estimates could be biased by the fact that our data on alcohol as well as tobacco consumption were derived from a questionnaire. Self-reports on lifestyle factors are subject to a different recall bias for cases and controls, although we tried to thwart this bias by trained interviewers for data acquisition. Nevertheless, our results support the results of the overall analysis and underline that gene-smoking and gene-alcohol interactions may modify laryngeal cancer risk.

Furthermore, an exposure dependent risk effect of the *RAD23B* 249Val polymorphism was found which was not apparent in the overall analysis. Regarding

the combined exposure with smoking and alcohol, 249Val carriers showed no risk effect in the low exposure group but a 2.6 fold increase in risk with high exposure. The contribution of the *RAD23B* 249Val variant to laryngeal cancer risk was reflected in the gene-gene interaction analysis, an effect similar to those reported previously by Shen *et al.*, (2005) in lung cancer. The *RAD23B* and *XPC* proteins work together as a complex in DNA damage identification in the GGR pathway. The presence of three risk alleles resulted in a 2.1 fold increased risk of larynx cancer, a level much higher than that conferred by the individual genetic variants.

Interestingly, the genetic variants of *ERCC6/CSB* and *RAD23B* are both located in genes encoding proteins involved in damage recognition, *ERCC6/CSB* in transcription coupled NER and *RAD23B/XPC* in global genome repair (Shuck *et al.*, 2008; Fousteri & Mullenders, 2008). DNA lesions not correctly recognized cannot be processed in time suggesting that this early step in NER might be rate-limiting and that a variant protein with reduced function at this critical step of the pathway might confer genomic instability and cancer.

5. 5. Limitations of our study

Our study is limited by its relatively small number of cases. Especially the analysis of gene-environment and gene-gene interactions was restricted by limited statistical power. Further analyses regarding occupational exposure or important clinical markers (such as location of the tumor in relation to the glottis) were not possible. However, in comparison to lung or breast cancer, laryngeal cancer is a rare disease and establishing large cohorts is a time-consuming and expensive task. Therefore, we improved the power of our study by increasing the number and quality of controls, and established a population-based case-control study with three healthy controls matched for age and gender for each case. As to be expected considering the strong risk factors for this type of cancer, a matching for the high risk factors smoking and alcohol consumption was not possible. As these habits are correlated with educational status, cases and controls also differed in this feature. The enrolled controls showed a higher education profile than the larynx cancer cases. It

could thus be hypothesized that controls probably had a healthier lifestyle and higher health standards (higher pattern of fruits and vegetables consumption, physical activity, attendance to health services, or health-related practices). This might also influence enzymatic mechanisms, such as DNA repair. Therefore, we cannot exclude that our data analysis, even after adjusting for education, could reflect such overall differences among cases and controls. At present, our study is among the larger studies published involving European laryngeal cancer patients (Hopkins *et al.*, 2008). Further validation of our results in larger populations is however required.

We cannot rule out the possibility of false-positive associations. When correcting our estimates for multiple testing according to Bonferroni (Silicon Genetics, 2003), a very low P value is required for statistical significance since a large number of comparisons were made. Using this stringent criterion, no odds ratio, even of the *ERCC6* Arg1230Pro SNP, would show significance in the overall analysis. The contribution of the *ERCC6* Arg1230Pro polymorphism to laryngeal cancer risk is nevertheless supported by haplotype analysis which showed a significant association for the 1213Arg-1230Pro haplotype. We can, however, not exclude that there are still other variants linked with this gene which actually determine genetic susceptibility. However, the three gene variants which we have identified to contribute to laryngeal cancer risk show their effects in more than one test, the overall analysis and the gene-environment or the gene-gene interaction analysis. Most of the associations found in our study are additionally supported by associations with cancer risk described in other studies although a clear functional impact of the polymorphisms was not shown up to now.

5. 6. Conclusion

In conclusion, our results suggest that the presence of 'risk alleles' of *ERCC6*, *ERCC5*, and *RAD23B* may result in compromised damage recognition and repair of smoking and alcohol induced DNA bulky adducts, leading to more DNA damage and higher laryngeal cancer risk. This risk modification is especially observed in

individuals that are exposed to heavy smoking or high alcohol intake. As we do not know about the biological impact of these polymorphisms, additional studies evaluating their functional significance are needed.

6. Discussion, NER and cancer therapy

Seventy two TCM drugs were screened for their cytotoxic effects on NER deficient cell lines, XP3BE and GM10902, and a normal cell line GM01310. XP3BE is deficient in *XPC* and GM10902 is deficient in *ERCC6*. Thirteen of the 72 drugs (18%) showed a differential activity against at least one of the mutant cell lines. Of these quercetin and scopoletin were specifically active against XP3BE only, TCM-25-RAB was active against GM10902 only and 10 drugs (14%) including arsenic trioxide, ascaridol, isonardosinon, TCM-22-RAB, TCM-23-RAB, TCM-44-RAB, TCM-47-RAB, TCM-48-RAB, TCM-50-RAB and TCM-54-RAB killed the two NER deficient cell lines more efficiently when compared with the normal cells, whereas a majority of the TCM drugs had no differential effect on the three cell lines. Depending on the amount available, 6 of these drugs; ascaridol, arsenic trioxide, isonardosinon, TCM-25-RAB, quercetin and scopoletin were picked for further analyses. Selected drugs were studied for their effects on cell cycle distribution and genotoxicity.

6. 1. Cell models

XPC with a molecular weight of 125 kDa has 940 amino acids (Masutani *et al.*, 1994). The XP3BE / GM02248 cell line is deficient in XPC and carries an 83bp insertion following codon Lys90. This generates a pre-mature stop codon and a truncated protein (Li *et al.*, 1993). In our experiments we confirmed the mutation reported for the cell line by PCR amplification and detected a very low amount of the XPC protein. XPC has a HR23B binding domain (amino acid 495 to 734) at the C-terminal end that overlaps with the DNA binding domain (amino acid 606 to 742) of XPC (Bernardes de Jesus *et al.*, 2008; Park & Choi, 2006). The very end of the C-terminus of XPC carries a TFIIH interaction domain (amino acid 816 to 940). XPC interacts with TFIIH through ERCC3 and p62 subunits (Uchida *et al.*, 2002). All these domains are missing in our cells. We could show that the cell line had a normal p53 expression and was more sensitive to UV exposure than normal cells. The cells are

also reported to be much more sensitive to UV light and repair DNA damage much slower than normal cells (Chavanne *et al.*, 2000).

ERCC6 is a member of SW12/SNF2-family of DNA-dependent ATPases. It has a molecular weight of 168 kDa and 1493 amino acids (Stevnsner *et al.*, 2008; Wong *et al.*, 2007). ERCC6 has an acidic domain, a glycine-rich region, two putative nuclear localization signal (NLS) sequences and 7 ATPase motifs. GM10902 cells harbor a point mutation (C2282T) in *ERCC6* gene in ATPase domain IV, generating a premature stop codon and a truncated protein (734 amino acids) (Colella *et al.*, 2000). The resulting protein lacks ATPase domains V and VI and one putative nuclear localization signal (NLS) sequence. We could confirm the mutation reported for the cell line by sequencing. Low amounts of the ERCC6 protein and normal levels of p53 expression were detected in the cells. The cell line was found to be more sensitive to UV exposure than normal cells. The result is supported by other studies as well (Itoh *et al.*, 1995; Greenhaw *et al.*, 1992). After UV exposure cells show a reduced level of RNA synthesis but normal levels of unscheduled DNA synthesis (Itoh *et al.*, 1996; Greenhaw *et al.*, 1992). GM10902 cells are defect in transcription (Kim *et al.*, 1997).

6. 2. Ascaridol

Ascaridol (also known as ascaridole, ascarisin, 1,4-epidioxy-*p*-menth-2-ene) is a bicyclic monoterpene that has an unusual bridging peroxide functional group (Dembitsky *et al.*, 2008). Our data showed that ascaridol was highly cytotoxic to NER deficient cells. GM10902 and XP3BE cells were over 1000 times more sensitive to the drug compared to GM01310 cells. Ascaridol was apparently non-toxic to normal cells. No data was found in the literature regarding the cytotoxicity of ascaridol in the NER deficient cells. Efferth *et al.*, (2002b) reported its antineoplastic activity as it is active against multi drug resistant cancer cell lines. Recently Bezerra *et al.*, (2009) showed ascaridol exhibits antitumor activity in leukemia (HL-60), melanoma (MDA-MB-435), brain (SF-295) and colon (HCT-8) cancer cell lines and in a sarcoma 180 murine model. However ascaridol did not

show any bioactivity in NCI *in vivo* antitumor screening (pubchem.ncbi.nlm.nih.gov, 2008). Cell cycle analysis showed a remarkable specificity for the effect of ascaridol. The G1 phase decreased in all three cell lines at concentrations between 0.05 to 1.0 µg/ml. In GM10902 cells, the G2/M phase increased at 0.05 and 0.1 µg/ml and then decreased at 0.5, 1.0 µg/ml. In XP3BE cells, The G2/M phase remained unchanged at 0.05 and 0.1 µg/ml and decreased at 0.5 and 1.0 µg/ml of ascaridol. In normal cells (GM01310), G2/M phase remained unchanged. In GM01310, an increase in S phase was also observed at all the concentrations. Ascaridol also caused an increase in the apoptotic peak (sub-G1 phase) in the three cell lines. GM10902 showed a dose-dependent increase in subG1, reaching up to 28% at 1.0 µg/ml and XP3BE had around 27% subG1 at all the concentrations. At all the concentrations, ascaridol produced 13 to 20% subG1 phase in GM01310. Ascaridol induced DNA damage in a dose-dependent manner and produced two to three times more DNA damage in NER deficient cells compared to the normal cells. Data regarding the effect of ascaridol on cell cycle distribution and induction of DNA damage are not available in literature.

Ascaridol is a naturally occurring compound and is a component of many plants (Holm *et al.*, 1993; Johnson & Croteau, 1984; Jardim *et al.*, 2008). Ascaridol is commercially available as a mixture of herbs (www.ghchealth.com, 2009) and also as a pure compound by some Chinese companies (www.chemexper.com, 2008). Since long ascaridol has been used as an anti-helminth drug and nematicide (Vanfleteren & Roets, 1972). The drug has also shown anti-malarial (Pollack *et al.*, 1990), antifungal (Jardim *et al.*, 2008) and trypanocidal (Kiuchi *et al.*, 2002) activities. Overdose of ascaridol can lead to death (DeStefano, 2001). However it did not show any toxic side effects, at the concentrations tested by Bezerra *et al.*, (2009). In a recent study (Tietze & Blomeke, 2008) aimed at dendritic cells and skin sensitization by contact allergens, ascaridol augmented expression of CD86 in monocyte leukemia cell line THP-1 and monocyte-derived dendritic cells.

6. 3. Arsenic trioxide

Arsenic trioxide is an established cytostatic drug. It has been used as a medicine for thousands of years and is known to induce cell apoptosis, DNA damage and to affect cell cycle. As it is a well studied compound (Gazitt & Akay, 2005; Miller, Jr. *et al.*, 2002), arsenic trioxide was selected as a positive control for our experiments. Our data showed that arsenic trioxide was 3 to 5.5 times more effective on NER deficient cells than the normal cells. Flow cytometry data showed arsenic trioxide treatment blocked cells from all the three cell lines at G2/M phase. Lower concentration (0.22 $\mu\text{g/ml}$) of the drug was required to induce this blockade in GM10902 and XP3BE cells compared to the normal cells (0.73 $\mu\text{g/ml}$). We measured sub-G1 phase as marker for DNA decay and apoptosis and found that 0.22 $\mu\text{g/ml}$ of arsenic trioxide caused twice as much of NER deficient cells to enter this phase compared to normal cells. A lot of data on apoptosis caused by arsenic trioxide is available in literature. Zhu *et al.*, (1999) reported apoptosis and growth inhibition in malignant lymphocytes after treatment with arsenic trioxide at clinically achievable concentrations. Low concentrations (0.25 – 2.0 μM) of arsenic trioxide inhibit growth of human leukemia/lymphoma cell lines HL-60, RL and K562 by inducing apoptosis (Zhu, 2003). Shao *et al.*, (2005) reported that arsenic trioxide treatment induces apoptosis and cell cycle arrest at G2/M phase in human gastric cancer cells. It also induces apoptosis and inhibits cellular growth in cisplatin sensitive and resistant ovarian cancer (Kong *et al.*, 2005) and colon cancer cells (Nakagawa *et al.*, 2002). Arsenic trioxide induces apoptosis in acute promyelocytic leukemia cells (Shao *et al.*, 1998) and is used in treatment of acute promyelocytic leukemia (Shen *et al.*, 1997; Soignet *et al.*, 1998). These studies provide support to our findings. Data from comet assay shows that arsenic trioxide leads to around three times more DNA damage in GM10902 and XP3BE than GM01310 cells. Similar findings were reported by Yedjou & Tchounwou, (2007) in human leukemia (HL-60) cells.

6. 4. Other TCM drugs

Quercetin and scopoletin are used as antioxidants (Shaw *et al.*, 2003; Lamson & Brignall, 2000). Our data showed that both these drugs were specifically cytotoxic to XP3BE cells only with little or no effect on GM10902 and GM01310 cells. Both these compounds exhibit cancer chemopreventive properties (Jang *et al.*, 2004) and are potential anti-cancer drugs (van Erk *et al.*, 2005; Bhattacharyya *et al.*, 2009). Quercetin (10 µg/ml) caused a decrease in S phase in XP3BE cells and an increase in the subG1 phase. However literature shows Quercetin caused a G0/G1 phase arrest in colon (Ranelletti *et al.*, 1992), bladder (Ma *et al.*, 2006) and breast cancer cells (Jeong *et al.*, 2009) whereas Yang *et al.*, (2006) reported G2/M phase arrest and apoptosis in lung cancer cells. Different cell types could be a reason for this result. We did not find a significant effect of quercetin on DNA damage in our cells. Scopoletin (20 µg/ml) exposure caused an increase in G1 phase in GM01310 and XP3BE cells. Kim *et al.*, (2005) reports that scopoletin induces apoptosis in promyelocytic cells. We also found a significant increase in DNA damage in XP3BE as well as GM10902 cells at lower concentration of scopoletin (10 µg/ml), however at a higher concentration (20 µg/ml), the three cell lines did not have a significant difference.

TCM-25-RAB is so far an unidentified TCM drug. It killed GM10902 cells more specifically than XP3BE and GM01310 cells. TCM-25-RAB slightly increased the G1 phase in GM10902 cells. It also increased subG1 phase by 20% in these cells but did not have any effect on cell cycle distribution of the other two cell lines. TCM-25-RAB induced dose-dependent DNA damage in GM10902 cells. This was twice as much as in XP3BE and 5 times as in GM01310. The drug did not cause any significant DNA damage in GM01310 cells at the concentrations tested.

Isonardosinon was active against both the NER deficient cell lines. It was around 10 to 15 times more cytotoxic to NER deficient cells than normal cells. Isonardosinon did not cause any significant effect on DNA damage and cell cycle distribution.

6. 5. Validation of results

Ascaridol was the most promising compound in our study. Results obtained for ascaridol were validated in a second cell model carrying *XPC* and *ERCC6* deficiencies. As a model for *XPC* mutation a pair of *XPC* cell lines, XP4PA and XP4PA-SE2 was picked. XP4PA cells harbor a dinucleotide (TG) deletion at position 1483-1484 of *XPC* causing a frameshift at codon Val431 and a premature stop codon (Li *et al.*, 1993) whereas XP4PA-SE2 is the fully corrected version of the cell line by stable transfection using pXPC-3 plasmid (Emmert *et al.*, 2000; Legerski & Peterson, 1992). As a model for *ERCC6* mutation, the gene was silenced in XP4PA-SE2 cells using ON-TARGETplus SMARTpool siRNA and the Luciferase siRNA exposed cultures (negative control for gene silencing) were considered as repair competent control.

The cytotoxicity screening revealed XP4PA cells were 165 times more sensitive to ascaridol exposure than XP4PA-SE2 cells and *ERCC6* silenced cells were 32 times more sensitive to ascaridol exposure than Luciferase siRNA exposed cells. Ascaridol caused DNA damage in these cells in a dose-dependent manner. At 1 µg/ml ascaridol exposure, XP4PA cells gathered around 1.5 times more DNA damage than XP4PA-SE2. The *ERCC6* silenced cells accumulated around 3 times more DNA damage than Luciferase siRNA exposed cells. These results confirm our previous findings that following ascaridol treatment, NER deficient cells have higher DNA damage compared to repair proficient cells.

6. 6. Mode of action of ascaridol

How ascaridol exactly works is not well understood. Ascaridol undergoes a concerted dissociative reduction by a nonadiabatic electron transfer of the O-O bond (Donkers & Workentin, 2001). Monzote *et al.*, (2009) showed that ascaridol formed carbon-centered radicals in the presence of Fe²⁺ and reduced hemin. This mechanism is very similar to another endoperoxide artemisinin, which is another anti-malarial and potent anticancer drug (Efferth *et al.*, 2002b; Golenser *et al.*, 2006; Balint, 2001). From these descriptions, we speculated that ascaridol creates oxidative stress and investigated the production of reactive oxygen species by

ascaridol. Furthermore, we quantified 8-oxodG sites by the Fpg-modified comet assay.

The production of reactive oxygen species by ascaridol in XP4PA and XP4PA-SE2 cells was measured by the 2',7'-dichlorofluorescein diacetate (H₂DCFDA) assay. Overall XP4PA cells had higher intracellular peroxide levels compared to XP4PA-SE2 cells. A dose-dependent increase in intracellular peroxide levels was observed in ascaridol treated cells. The RR_{ROS} after treatment did not differ in both the cell lines. Quantification of 8-oxodG sites by Fpg-modified comet assay showed that XP4PA cells exhibit a strong increase in oxidized bases than XP4PA-SE2 cells, after treatment with 1 µg/ml ascaridol. Similarly, *ERCC6* silenced cells exhibit a highly significant increase in Fpg sensitive lesions compared to luciferase siRNA exposed cells after ascaridol treatment. All of these findings are consistent with a role of ascaridol in mediating DNA damage by oxidative stress.

6. 7. Role of NER proteins in the repair of oxidative damage

The main pathway for the repair of oxidative DNA damage is BER (Mitra *et al.*, 1997; Seeberg *et al.*, 1995). However recent studies have identified proteins which are involved in repair of oxidative DNA damage but which belong to other repair pathways especially the NER pathway. NER is involved in the removal of 8-oxodG (Reardon *et al.*, 1997). Langie *et al.*, (2007) reported an increase in expression of NER genes including *XPC* in the presence of oxidative stress after H₂O₂ exposure. Mutations in *XPC* disturb both NER and BER (Bernardes de Jesus *et al.*, 2008). D'Errico *et al.*, (2006) reported that *XPC* deficient keratinocytes and fibroblasts were hypersensitive to DNA-oxidizing agents and re-introduction of *XPC* in these cells reduced their sensitivity. In the absence of *XPC*, a decrease in repair of 8-oxodG was observed. XPC-HR23B complex acted as a cofactor for repair of 8-oxodG by stimulating Ogg1. An XPC protein completely lacking its C-terminus does not stimulate the glycosylase activity of Ogg1 while wild type XPC shows this activity. Mutations in the N-terminal part of XPC also reduced the XPC-Ogg1 interaction, leading to reduced BER activity (Bernardes de Jesus *et al.*, 2008). Okamoto *et al.*,

(2008) found a significantly increased accumulation of 8-oxodG adducts in the liver of *XPC*-knockout mice.

ERCC6 also plays a role in the repair of oxidative DNA damage. The ATPase domains V and VI of *ERCC6* are important for the repair of 8-oxodG lesions (Tuo *et al.*, 2001) and ATPase domain VI is important for the repair of 8-oxoA lesions (Tuo *et al.*, 2002a). *ERCC6* Protein in GM10902 cells lacks both these domains. In *ERCC6* mutated cells, hOgg1 is down-regulated, causing accumulation of 8-oxodG (Dianov *et al.*, 1999; Tuo *et al.*, 2002b). The same authors (Tuo *et al.*, 2003) report accumulation of oxidative damage in *ERCC6* deficient cells. The unrepaired 8-oxodG blocks transcription by stalling RNA pol II and *ERCC6* may start TCR at this site (Slupphaug *et al.*, 2003). Sensitivity of *XPC* and *ERCC6* deficient cells to oxidative damaging agents observed in our study also highlights the involvement of these genes in oxidative damage repair.

6. 8. Other possible mechanisms

Overall, the data support the role of oxidative DNA damage as the underlying reason for the anticancer effect of ascaridol. The fact that this drug is active towards NER deficient cells at much lower concentrations than the concentrations required for normal cells hints for the involvement of other possible mechanisms.

6. 8. 1. Formation of DNA adducts

One possible mechanism is, ascaridol may bind to DNA strands leading to DNA adducts that are directly repaired by NER. Deficiency of the pathway leads to excessive DNA damage and cell death. However nothing is known about it.

6. 8. 2. Synthetic lethal interactions

Another possibility is that ascaridol targets other repair-specific gene or gene products, thus causing a synthetic lethal effect. Synthetic lethal interaction between two genes is defined as a situation when absence of either gene has no effect but when both the genes are missing, the condition becomes fatal (Dobzhansky, 1946). Ascaridol might be targeting a gene having synthetic lethal

interactions with XPC and/or ERCC6. So far such interactions of NER genes are not known (Helleday *et al.*, 2008). The concept of synthetic lethal interactions has been implicated in cancer therapy (Ashworth, 2008; Kaelin, Jr., 2005). One such example is the interaction of poly (ADP-ribose) polymerase and *BRCA1* and *BRCA2* genes (Drew & Calvert, 2008). PARP is an enzyme involved in base excision repair and *BRCA1* and *BRCA2* are important for double strand break repair (Hoeijmakers, 2001b). PARP inhibitors selectively kill *BRCA1/2* deficient cancer cells but are not toxic to normal cells (Bryant *et al.*, 2005; Farmer *et al.*, 2005). Currently clinical studies testing PARP inhibitors as single agents in *BRCA1/2* deficient tumors are ongoing (Fong *et al.*, 2009; Drew & Calvert, 2008). *ERCC6* deficient cell lines also demonstrate hypersensitivity to *PARP-1* inhibition (Thorslund *et al.*, 2005). *ERCC6* and *PARP-1* bind and relocate to the damaged site both *in vitro* as well as *in vivo*, in response to oxidative stress (Lan *et al.*, 2004). The concept of synthetic lethal interactions in cancer therapy is fairly new yet it provides a novel basis for cancer treatment. The exact mechanism by which ascaridol causes DNA damage and cell death needs therefore to be further explored.

6. 9. Limitations of the study

Although we controlled our experiments carefully, our study is limited by the fact that it was conducted *in vitro*. Although *in vitro* characterization of the potential drug helps forecast its activity *in vivo* (Jayat & Ratinaud, 1993), yet experiments in animal models are required. The cell lines included in the study were checked for the reported mutations and cultures were tested for contaminations at regular intervals. Each experiment included solvent exposed and unexposed samples. Multiple replicates for each treatment were included and experiments were performed at least twice.

6. 10. Conclusion

There is no question that the ability for improved cancer therapy by targeting DNA repair defects is extremely attractive, as many tumors show defects in DNA repair

genes such as those involved in NER. NER defects in tumors can be exploited intelligently.

We identified 13 out of 72 TCM drugs that are selectively killing NER deficient cells. Ascaridol was the most efficient TCM drug targeting the NER deficient cells. Ascaridol was up to 1000 fold more active in NER deficient cells compared to normal cells. Exquisitely high sensitivity of NER deficient cells to ascaridol is novel. We also show, for the first time that ascaridol is mediating DNA damage by oxidative stress. DNA-damaging agents still represent the most effective drugs for a large fraction of human malignancies. The growing knowledge on cell response to DNA damage and DNA repair is providing the rationale for the development of new therapies. Our data demonstrates the sensitivity of *XPC* and *ERCC6* cells to ascaridol. Defects in both these genes affect the early damage recognition steps. As most of the other NER genes are involved in both of the NER sub-pathways (GGR and TCR), we suggest that cells / tumors deficient in other NER genes are also sensitive to ascaridol. We suggest it can be used for treating NER deficient tumors and provide a rationale for the development of new therapies. Elucidation of involved mechanisms in tumor models *in vivo* is still needed.

7. Reference List

1. Adimoolam S, & Ford JM (2003). p53 and regulation of DNA damage recognition during nucleotide excision repair. *DNA Repair (Amst)* **2**, 947-954.
2. American Cancer Society (2006). Laryngeal & Hypopharyngeal Cancer. Available from: URL: www.cancer.org
3. An J, Liu Z, Hu Z, Li G, Wang LE, Sturgis EM, El-Naggar AK, Spitz MR, & Wei Q (2007). Potentially functional single nucleotide polymorphisms in the core nucleotide excision repair genes and risk of squamous cell carcinoma of the head and neck. *Cancer Epidemiol Biomarkers Prev* **16**, 1633-1638.
4. Andressoo JO, Hoeijmakers JH, & Mitchell JR (2006). Nucleotide excision repair disorders and the balance between cancer and aging. *Cell Cycle* **5**, 2886-2888.
5. Ashworth A (2008). A synthetic lethal therapeutic approach: poly(ADP) ribose polymerase inhibitors for the treatment of cancers deficient in DNA double-strand break repair. *J Clin Oncol* **26**, 3785-3790.
6. Au WW (2006). Heritable susceptibility factors for the development of cancer. *J Radiat Res (Tokyo)* **47** Suppl B, B13-B17.
7. Azqueta A, Shaposhnikov S, & Collins AR (2009). DNA oxidation: investigating its key role in environmental mutagenesis with the comet assay. *Mutat Res* **674**, 101-108.
8. Balint GA (2001). Artemisinin and its derivatives: an important new class of antimalarial agents. *Pharmacol Ther* **90**, 261-265.
9. Bartsch H, & Hietanen E (1996). The role of individual susceptibility in cancer burden related to environmental exposure. *Environ Health Perspect* **104**, 569-577.
10. Bartsch H, Dally H, Popanda O, Risch A, & Schmezer P (2007). Genetic risk profiles for cancer susceptibility and therapy response. *Recent Results Cancer Res* **174**, 19-36.
11. Batzler WU, Giersiepen K, Hentschel S, Husmann G, Kaatsch P, Katalinic A, Kieschke J, Kraywinkel K, Meyer M, Stabenow R, Stegmaier C, Bertz J, Haberland J, & Wolf U

- (2008). Krebs in Deutschland, 2003 - 2004, Häufigkeiten und Trends. www.gekid.de 42-45.
12. Becher H, Ramroth H, Ahrens W, Risch A, Schmezer P, & Dietz A (2005). Occupation, exposure to polycyclic aromatic hydrocarbons and laryngeal cancer risk. *Int J Cancer* **116**, 451-457.
13. Beenken S, Urist M, & Casiano R (2009). Laryngeal Cancer (Cancer of the larynx). Armenian Health Network. Available from: URL: <http://www.health.am/cr/laryngeal-cancer/>.
14. Bernardes de Jesus BM, Bjoras M, Coin F, & Egly JM (2008). Dissection of the molecular defects caused by pathogenic mutations in the DNA repair factor XPC. *Mol Cell Biol* **28**, 7225-7235.
15. Berndt SI, Platz EA, Fallin MD, Thuita LW, Hoffman SC, & Helzlsouer KJ (2006). Genetic variation in the nucleotide excision repair pathway and colorectal cancer risk. *Cancer Epidemiol Biomarkers Prev* **15**, 2263-2269.
16. Bezerra DP, Marinho Filho JD, Alves AP, Pessoa C, de Moraes MO, Pessoa OD, Torres MC, Silveira ER, Viana FA, & Costa-Lotufo LV (2009). Antitumor activity of the essential oil from the leaves of *Croton regelianus* and its component ascaridole. *Chem Biodivers* **6**, 1224-1231.
17. Bhattacharyya SS, Paul S, Mandal SK, Banerjee A, Boujedaini N, & Khuda-Bukhsh AR (2009). A synthetic coumarin (4-methyl-7 hydroxy coumarin) has anti-cancer potentials against DMBA-induced skin cancer in mice. *Eur J Pharmacol* **614**, 128-136.
18. Boiteux S, & Guillet M (2004). Abasic sites in DNA: repair and biological consequences in *Saccharomyces cerevisiae*. *DNA Repair (Amst)* **3**, 1-12.
19. Brabec V, & Kasparkova J (2002). Molecular aspects of resistance to antitumor platinum drugs. *Drug Resist Updat* **5**, 147-161.
20. Bradford MM (1976). A rapid and sensitive method for the quantitation of microgram quantities of protein utilizing the principle of protein-dye binding. *Anal Biochem* **72**, 248-254.

-
-
21. Brooks PJ, & Theruvathu JA (2005). DNA adducts from acetaldehyde: implications for alcohol-related carcinogenesis. *Alcohol* **35**, 187-193.
 22. Brose MS, Smyrc T, Weber BL, & Lynch HT (2003). Genetic Predisposition to Cancer. In *Cancer Medicine*, [eds]. Holland JF, Frei EI, Bast RCJr, Kufe DW, Pollock RE, & Weichselbaum RR, pp. 168-184. B.C. Decker, Hamilton.
 23. Bryant HE, Schultz N, Thomas HD, Parker KM, Flower D, Lopez E, Kyle S, Meuth M, Curtin NJ, & Helleday T (2005). Specific killing of BRCA2-deficient tumours with inhibitors of poly(ADP-ribose) polymerase. *Nature* **434**, 913-917.
 24. Buschta-Hedayat N, Buterin T, Hess MT, Missura M, & Naegeli H (1999). Recognition of nonhybridizing base pairs during nucleotide excision repair of DNA. *Proc Natl Acad Sci U S A* **96**, 6090-6095.
 25. Campbell NA, Reece JB, & Taylor MR (2009). *Biology concepts and connections*. 6th edn. San Francisco, Calif. u.a., Pearson Education.
 26. Castro MA, Mombach JC, de Almeida RM, & Moreira JC (2007). Impaired expression of NER gene network in sporadic solid tumors. *Nucleic Acids Res* **35**, 1859-1867.
 27. Chavanne F, Broughton BC, Pietra D, Nardo T, Browitt A, Lehmann AR, & Stefanini M (2000). Mutations in the XPC Gene in Families with Xeroderma Pigmentosum and Consequences at the Cell, Protein, and Transcript Levels. *Cancer Res* **60**, 1974-1982.
 28. Chen P, Wiencke J, Aldape K, Kesler-Diaz A, Miike R, Kelsey K, Lee M, Liu J, & Wrensch M (2000). Association of an ERCC1 polymorphism with adult-onset glioma. *Cancer Epidemiol Biomarkers Prev* **9**, 843-847.
 29. Chen Z, Yang J, Wang G, Song B, Li J, & Xu Z (2007). Attenuated expression of xeroderma pigmentosum group C is associated with critical events in human bladder cancer carcinogenesis and progression. *Cancer Res* **67**, 4578-4585.
 30. Cheng L, Spitz MR, Hong WK, & Wei Q (2000). Reduced expression levels of nucleotide excision repair genes in lung cancer: a case-control analysis 3. *Carcinogenesis* **21**, 1527-1530.

Reference List

31. Cleaver JE (1968). Defective repair replication of DNA in xeroderma pigmentosum. *Nature* **218**, 652-656.
32. Colella S, Nardo T, Botta E, Lehmann AR, & Stefanini M (2000). Identical mutations in the CSB gene associated with either Cockayne syndrome or the DeSanctis-cacchione variant of xeroderma pigmentosum. *Hum Mol Genet* **9**, 1171-1175.
33. Collins AR, Dusinska M, Horvathova E, Munro E, Savio M, & Stetina R (2001). Inter-individual differences in repair of DNA base oxidation, measured *in vitro* with the comet assay. *Mutagenesis* **16**, 297-301.
34. Collins AR, Duthie SJ, & Dobson VL (1993). Direct enzymic detection of endogenous oxidative base damage in human lymphocyte DNA. *Carcinogenesis* **14**, 1733-1735.
35. Compton S J, & Jones CG (1985). Mechanism of dye response and interference in the Bradford protein assay. *Anal Biochem Bd* **151**, 369-374.
36. Cui Y, Morgenstern H, Greenland S, Tashkin DP, Mao J, Cao W, Cozen W, Mack TM, & Zhang ZF (2006). Polymorphism of Xeroderma Pigmentosum group G and the risk of lung cancer and squamous cell carcinomas of the oropharynx, larynx and esophagus. *Int J Cancer* **118**, 714-720.
37. Dabholkar M, Vionnet J, Bostick-Bruton F, Yu JJ, & Reed E (1994). Messenger RNA levels of XPAC and ERCC1 in ovarian cancer tissue correlate with response to platinum-based chemotherapy. *J Clin Invest* **94**, 703-708.
38. Dabholkar MD, Berger MS, Vionnet JA, Egwuagu C, Silber JR, Yu JJ, & Reed E (1995). Malignant and nonmalignant brain tissues differ in their messenger RNA expression patterns for ERCC1 and ERCC2. *Cancer Res* **55**, 1261-1266.
39. Dabholkar MD, Berger MS, Vionnet JA, Overton L, Thompson C, Bostick-Bruton F, Yu JJ, Silber JR, & Reed E (1996). Comparative analyses of relative ERCC3 and ERCC6 mRNA levels in gliomas and adjacent non-neoplastic brain. *Mol Carcinog* **17**, 1-7.
40. Damia G, & D'Incalci M (2007). Targeting DNA repair as a promising approach in cancer therapy. *Eur J Cancer* **43**, 1791-1801.

-
-
41. Dembitsky V, Shkrob I, & Hanus LO (2008). Ascaridole and related peroxides from the genus *Chenopodium*. *Biomed Pap Med Fac Univ Palacky Olomouc Czech Repub* **152**, 209-215.
 42. Dembitsky VM (2008). Bioactive peroxides as potential therapeutic agents. *Eur J Med Chem* **43**, 223-251.
 43. D'Errico M, Parlanti E, Teson M, de Jesus BM, Degan P, Calcagnile A, Jaruga P, Bjoras M, Crescenzi M, Pedrini AM, Egly JM, Zambruno G, Stefanini M, Dizdaroglu M, & Dogliotti E (2006). New functions of XPC in the protection of human skin cells from oxidative damage. *EMBO J* **25**, 4305-4315.
 44. DeStefano A (2001). *Latino Folk Medicine: Healing Herbal Remedies from an Ancient Tradition*, 1 ed. Random House, Incorporated.
 45. Di PA, Danesi R, & Del TM (2004). Pharmacogenetics of neoplastic diseases: new trends. *Pharmacol Res* **49**, 331-342.
 46. Dianov G, Bischoff C, Sunesen M, & Bohr VA (1999). Repair of 8-oxodGuanine in DNA is deficient in Cockayne syndrome group B cells. *Nucleic Acids Res* **27**, 1365-1368.
 47. Ding YS, Zhang L, Jain RB, Jain N, Wang RY, Ashley DL, & Watson CH (2008). Levels of tobacco-specific nitrosamines and polycyclic aromatic hydrocarbons in mainstream smoke from different tobacco varieties. *Cancer Epidemiol Biomarkers Prev* **17**, 3366-3371.
 48. Dobzhansky T (1946). Genetics of Natural Populations. Xiii. Recombination and Variability in Populations of *Drosophila Pseudoobscura*. *Genetics* **31**, 269-290.
 49. Domijan AM, Zeljezić D, Kopjar N, & Peraica M (2006). Standard and Fpg-modified comet assay in kidney cells of ochratoxin A- and fumonisin B(1)-treated rats. *Toxicology* **222**, 53-9.
 50. Donkers RL, & Workentin MS (2001). Kinetics of dissociative electron transfer to ascaridole and dihydroascaridole-model bicyclic endoperoxides of biological relevance. *Chemistry* **7**, 4012-4020.
 51. Drew Y, & Calvert H (2008). The potential of PARP inhibitors in genetic breast and ovarian cancers. *Ann N Y Acad Sci* **1138**, 136-145.

52. Efferth T, Davey M, Olbrich A, Rucker G, Gebhart E, & Davey R (2002a). Activity of drugs from traditional Chinese medicine toward sensitive and. *Blood Cells Mol Dis* **28**, 160-168.
53. Efferth T, Kahl S, Paulus K, Adams M, Rauh R, Boechzelt H, Hao X, Kaina B, & Bauer R (2008). Phytochemistry and pharmacogenomics of natural products derived from traditional Chinese medicine and Chinese materia medica with activity against tumor cells. *Mol Cancer Ther* **7**, 152-161.
54. Efferth T, Olbrich A, Sauerbrey A, Ross DD, Gebhart E, & Neugebauer M (2002b). Activity of ascaridol from the anthelmintic herb *Chenopodium anthelminticum* L. against sensitive and multidrug-resistant tumor cells. *Anticancer Res* **22**, 4221-4224.
55. Efferth T, Rauh R, Kahl S, Tomicic M, Bochzelt H, Tome ME, Briehl MM, Bauer R, & Kaina B (2005). Molecular modes of action of cantharidin in tumor cells. *Biochem Pharmacol* **69**, 811-818.
56. Eiberger W, Volkmer B, Amouroux R, Dhérin C, Radicella JP, & Epe B (2008). Oxidative stress impairs the repair of oxidative DNA base modifications in human skin fibroblasts and melanoma cells. *DNA Repair (Amst)* **7**, 912-21.
57. Emmert S, Kobayashi N, Khan SG, & Kraemer KH (2000). The xeroderma pigmentosum group C gene leads to selective repair of cyclobutane pyrimidine dimers rather than 6-4 photoproducts. *Proc Natl Acad Sci U S A* **97**, 2151-2156.
58. Farmer H, McCabe N, Lord CJ, Tutt AN, Johnson DA, Richardson TB, Santarosa M, Dillon KJ, Hickson I, Knights C, Martin NM, Jackson SP, Smith GC, & Ashworth A (2005). Targeting the DNA repair defect in BRCA mutant cells as a therapeutic strategy. *Nature* **434**, 917-921.
59. Fong PC, Boss DS, Yap TA, Tutt A, Wu P, Mergui-Roelvink M, Mortimer P, Swaisland H, Lau A, O'Connor MJ, Ashworth A, Carmichael J, Kaye SB, Schellens JH, & de Bono JS (2009). Inhibition of poly(ADP-ribose) polymerase in tumors from BRCA mutation carriers. *N Engl J Med* **361**, 123-134.
60. Fousteri M, & Mullenders LH (2008). Transcription-coupled nucleotide excision repair in mammalian cells: molecular mechanisms and biological effects. *Cell Res* **18**, 73-84.

-
-
61. Frank SA (2004). Genetic predisposition to cancer - insights from population genetics. *Nat Rev Genet* **5**, 764-772.
 62. Furuta T, Ueda T, Aune G, Sarasin A, Kraemer KH, & Pommier Y (2002). Transcription-coupled nucleotide excision repair as a determinant of cisplatin sensitivity of human cells. *Cancer Res* **62**, 4899-4902.
 63. Garavello W, Lucenteforte E, Bosetti C, Talamini R, Levi F, Tavani A, Franceschi S, Negri E, & La VC (2009). Diet diversity and the risk of laryngeal cancer: a case-control study from Italy and Switzerland. *Oral Oncol* **45**, 85-89.
 64. Garcia-Closas M, Malats N, Real FX, Welch R, Kogevinas M, Chatterjee N, Pfeiffer R, Silverman D, Dosemeci M, Tardon A, Serra C, Carrato A, Garcia-Closas R, Castano-Vinyals G, Chanock S, Yeager M, & Rothman N (2006). Genetic variation in the nucleotide excision repair pathway and bladder cancer risk. *Cancer Epidemiol Biomarkers Prev* **15**, 536-542.
 65. Gazitt Y & Akay C (2005). Arsenic trioxide: an anticancer missile with multiple warheads. *Hematology* **10**, 205-213.
 66. Goldenberg DP, & Creighton TE (1984). Gel electrophoresis in studies of protein conformation and folding. *Anal Biochem* **138**, 1-18.
 67. Golenser J, Waknine JH, Krugliak M, Hunt NH, & Grau GE (2006). Current perspectives on the mechanism of action of artemisinins. *Int J Parasitol* **36**, 1427-1441.
 68. Greenhaw GA, Hebert A, Duke-Woodside ME, Butler IJ, Hecht JT, Cleaver JE, Thomas GH, and Horton WA (1992). Xeroderma pigmentosum and Cockayne syndrome: overlapping clinical and biochemical phenotypes. *Am J Hum Genet* **50**, 677-689.
 69. Hall J, Hashibe M, Boffetta P, Gaborieau V, Moullan N, Chabrier A, Zaridze D, Shangina O, Szeszenia-Dabrowska N, Mates D, Janout V, Fabianova E, Holcatova I, Hung RJ, McKay J, Canzian F, & Brennan P (2007). The association of sequence variants in DNA repair and cell cycle genes with cancers of the upper aerodigestive tract. *Carcinogenesis* **28**, 665-671.
 70. Han J (1988). Traditional Chinese medicine and the search for new antineoplastic drug. *J Ethnopharmacol* **24**, 1-17.

Reference List

71. Hashibe M, Boffetta P, Zaridze D, Shangina O, Szeszenia-Dabrowska N, Mates D, Fabianova E, Rudnai P, & Brennan P (2007). Contribution of tobacco and alcohol to the high rates of squamous cell carcinoma of the supraglottis and glottis in Central Europe. *Am J Epidemiol* **165**, 814-820.
72. Hecht SS (2001). Carcinogen biomarkers for lung or oral cancer chemoprevention trials. *IARC Sci Publ* **154**, 245-255.
73. Helleday T, Petermann E, Lundin C, Hodgson B, & Sharma RA (2008). DNA repair pathways as targets for cancer therapy. *Nat Rev Cancer* **8**, 193-204.
74. Heng HH, Bremer SW, Stevens JB, Ye KJ, Liu G, & Ye CJ (2009). Genetic and epigenetic heterogeneity in cancer: a genome-centric perspective. *J Cell Physiol* **220**, 538-547.
75. Hoeijmakers JH (2001a). DNA repair mechanisms. *Maturitas* **38**, 17-22.
76. Hoeijmakers JH (2001b). Genome maintenance mechanisms for preventing cancer. *Nature* **411**, 366-374.
77. Holm Y, Laakso I, Harmaja H, & Hiltunen R (1993). The essential oils of *Ledum palustre* L.: an ascaridol chemotype. *24th International Symposium on Essential Oils* Technische Universität Berlin, Berlin, (Poster).
78. Hoogervorst EM, van SH, & de VA (2005). Nucleotide excision repair- and p53-deficient mouse models in cancer research. *Mutat Res* **574**, 3-21.
79. Hopkins J, Cescon DW, Tse D, Bradbury P, Xu W, Ma C, Wheatley-Price P, Waldron J, Goldstein D, Meyer F, Bairati I, & Liu G (2008). Genetic polymorphisms and head and neck cancer outcomes: a review. *Cancer Epidemiol Biomarkers Prev* **17**, 490-499.
80. Huang WY, Berndt SI, Kang D, Chatterjee N, Chanock SJ, Yeager M, Welch R, Bresalier RS, Weissfeld JL, & Hayes RB (2006). Nucleotide excision repair gene polymorphisms and risk of advanced colorectal adenoma: XPC polymorphisms modify smoking-related risk. *Cancer Epidemiol Biomarkers Prev* **15**, 306-311.
81. IARC (2002). Tobacco Smoke and Involuntary Smoking. IARC Monographs on the Evaluation of Carcinogenic Risks to Humans. *IACR* **83**.

-
-
82. Itin PH, Sarasin A, & Pittelkow MR (2001). Trichothiodystrophy: update on the sulfur-deficient brittle hair syndromes. *J Am Acad Dermatol* **44**, 891-920.
 83. Itoh T, Cleaver JE, & Yamaizumi M (1996). Cockayne syndrome complementation group B associated with xeroderma pigmentosum phenotype. *Hum Genet* **97**, 176-179.
 84. Itoh T, Fujiwara Y, Ono T, & Yamaizumi M (1995). UVs syndrome, a new general category of photosensitive disorder with defective DNA repair, is distinct from xeroderma pigmentosum variant and rodent complementation group I. *Am J Hum Genet* **56**, 1267-1276.
 85. Jang DS, Cuendet M, Pawlus AD, Kardono LB, Kawanishi K, Farnsworth NR, Fong HH, Pezzuto JM, & Kinghorn AD (2004). Potential cancer chemopreventive constituents of the leaves of *Macaranga triloba*. *Phytochemistry* **65**, 345-350.
 86. Jardim CM, Jham GN, Dhingra OD, & Freire MM (2008). Composition and antifungal activity of the essential oil of the Brazilian *Chenopodium ambrosioides* L. *J Chem Ecol* **34**, 1213-1218.
 87. Jayat C, & Ratinaud MH (1993). Cell cycle analysis by flow cytometry: principles and applications. *Biol Cell* **78**, 15-25.
 88. Jeong JH, An JY, Kwon YT, Rhee JG, & Lee YJ (2009). Effects of low dose quercetin: cancer cell-specific inhibition of cell cycle progression. *J Cell Biochem* **106**, 73-82.
 89. Johnson MA, & Croteau R (1984). Biosynthesis of ascaridole: iodide peroxidase-catalyzed synthesis of a monoterpene endoperoxide in soluble extracts of *Chenopodium ambrosioides* fruit. *Arch Biochem Biophys* **235**, 254-266.
 90. Kaelin WG, Jr. (2005). The concept of synthetic lethality in the context of anticancer therapy. *Nat Rev Cancer* **5**, 689-698.
 91. Kasum CM, Jacobs DR, Jr., Nicodemus K, & Folsom AR (2002). Dietary risk factors for upper aerodigestive tract cancers. *Int J Cancer* **99**, 267-272.
 92. Kim EK, Kwon KB, Shin BC, Seo EA, Lee YR, Kim JS, Park JW, Park BH, & Ryu DG (2005). Scopoletin induces apoptosis in human promyeloleukemic cells, accompanied by activations of nuclear factor kappaB and caspase-3. *Life Sci* **77**, 824-836.

Reference List

93. Kim N, Kage K, Matsuda F, Lefranc MP, & Storb U (1997). B lymphocytes of xeroderma pigmentosum or Cockayne syndrome patients with inherited defects in nucleotide excision repair are fully capable of somatic hypermutation of immunoglobulin genes. *J Exp Med* **186**, 413-419.
94. Kim SH, Choi SJ, Kim YC, & Kuh HJ (2009). Anti-tumor activity of noble indirubin derivatives in human solid tumor models *in vitro*. *Arch Pharm Res* **32**, 915-922.
95. Kiuchi F, Itano Y, Uchiyama N, Honda G, Tsubouchi A, Nakajima-Shimada J, & Aoki T (2002). Monoterpene hydroperoxides with trypanocidal activity from *Chenopodium ambrosioides*. *J Nat Prod* **65**, 509-512.
96. Kiyohara C, & Yoshimasu K (2007). Genetic polymorphisms in the nucleotide excision repair pathway and lung cancer risk: a meta-analysis. *Int J Med Sci* **4**, 59-71.
97. Kong B, Huang S, Wang W, Ma D, Qu X, Jiang J, Yang X, Zhang Y, Wang B, Cui B, & Yang Q (2005). Arsenic trioxide induces apoptosis in cisplatin-sensitive and -resistant ovarian cancer cell lines. *Int J Gynecol Cancer* **15**, 872-877.
98. Konkimalla VB, & Efferth T (2008). Anti-cancer natural product library from traditional chinese medicine. *Comb Chem High Throughput Screen* **11**, 7-15.
99. Kumar R, Hoglund L, Zhao C, Forsti A, Snellman E, & Hemminki K (2003). Single nucleotide polymorphisms in the XPG gene: determination of role in DNA repair and breast cancer risk. *Int J Cancer* **103**, 671-675.
100. La VC, Zhang ZF, & Altieri A (2008). Alcohol and laryngeal cancer: an update. *Eur J Cancer Prev* **17**, 116-124.
101. Laemmli UK (1970). Cleavage of structural proteins during the assembly of the head of bacteriophage T4. *Nature* **227**, 680-685.
102. Lake SL, Lyon H, Tantisira K, Silverman EK, Weiss ST, Laird NM, and Schaid DJ (2003). Estimation and tests of haplotype-environment interaction when linkage phase is ambiguous. *Hum Hered* **55**, 56-65.
103. Lamson DW, & Brignall MS (2000). Antioxidants and cancer, part 3: quercetin. *Altern Med Rev* **5**, 196-208.

-
-
104. Lan L, Hayashi T, Rabeya RM, Nakajima S, Kanno S, Takao M, Matsunaga T, Yoshino M, Ichikawa M, Riele H, Tsuchiya S, Tanaka K, & Yasui A (2004). Functional and physical interactions between ERCC1 and MSH2 complexes for resistance to cis-diamminedichloroplatinum(II) in mammalian cells. *DNA Repair (Amst)* **3**, 135-143.
 105. Langie SA, Knaapen AM, Houben JM, van Kempen FC, de Hoon JP, Gottschalk RW, Gottschalk RW, & van Schooten FJ (2007). The role of glutathione in the regulation of nucleotide excision repair during oxidative stress. *Toxicol Lett* **168**, 302-309.
 106. Legerski R, & Peterson C (1992). Expression cloning of a human DNA repair gene involved in xeroderma pigmentosum group C. *Nature* **359**, 70-73.
 107. Leibel D, Laspe P, & Emmert S (2006). Nucleotide excision repair and cancer. *J Mol Histol* **37**, 225-238.
 108. Li L, Bales ES, Peterson CA, & Legerski RJ (1993). Characterization of molecular defects in xeroderma pigmentosum group C. *Nat Genet* **5**, 413-417.
 109. Liang Y, Lin SY, Brunicardi FC, Goss J, & Li K (2009). DNA damage response pathways in tumor suppression and cancer treatment. *World J Surg* **33**, 661-666.
 110. Lindahl T, Karran P, & Wood RD (1997). DNA excision repair pathways. *Curr Opin Genet Dev* **7**, 158-169.
 111. Lindl T (2002). Zell- und Gewebekultur. Spektrum Akademischer Verlag ed.
 112. Liu G, Zhou W, Yeap BY, Su L, Wain JC, Poneris JM, Nishioka NS, Lynch TJ, & Christiani DC (2007). XRCC1 and XPD polymorphisms and esophageal adenocarcinoma risk. *Carcinogenesis* **28**, 1254-1258.
 113. Lobo R, Prabhu KS, Shirwaikar A, & Shirwaikar A (2009). Curcuma zedoaria Rosc. (white turmeric): a review of its chemical, pharmacological and ethnomedicinal properties. *J Pharm Pharmacol* **61**, 13-21.
 114. Lockett KL, Snowwhite IV, & Hu JJ (2005). Nucleotide-excision repair and prostate cancer risk. *Cancer Lett* **220**, 125-135.
 115. Lorence A, & Nessler CL (2004). Camptothecin, over four decades of surprising findings. *Phytochemistry* **65**, 2735-2749.

Reference List

116. Luk JM, Wang X, Liu P, Wong KF, Chan KL, Tong Y, Hui CK, Lau GK, & Fan ST (2007). Traditional Chinese herbal medicines for treatment of liver fibrosis and cancer: from laboratory discovery to clinical evaluation. *Liver Int* **27**, 879-890.
117. Ma L, Feugang JM, Konarski P, Wang J, Lu J, Fu S, Ma B, Tian B, Zou C, & Wang Z (2006). Growth inhibitory effects of quercetin on bladder cancer cell. *Front Biosci* **11**, 2275-2285.
118. Maki CG (1999). Oligomerization is required for p53 to be efficiently ubiquitinated by MDM2. *J Biol Chem* **274**, 16531-16535.
119. Manuguerra M, Saletta F, Karagas MR, Berwick M, Veglia F, Vineis P, & Matullo G (2006). XRCC3 and XPD/ERCC2 single nucleotide polymorphisms and the risk of cancer: a HuGE review. *Am J Epidemiol* **164**, 297-302.
120. Martin SA, Lord CJ, & Ashworth A (2008). DNA repair deficiency as a therapeutic target in cancer. *Curr Opin Genet Dev* **18**, 80-86.
121. Masutani C, Sugasawa K, Yanagisawa J, Sonoyama T, Ui M, Enomoto T, Takio K, Tanaka K, van der Spek PJ, Bootsma D, & . (1994). Purification and cloning of a nucleotide excision repair complex involving the xeroderma pigmentosum group C protein and a human homologue of yeast RAD23. *EMBO J* **13**, 1831-1843.
122. Matakidou A, el GR, Webb EL, Rudd MF, Bridle H, Eisen T, & Houlston RS (2007). Genetic variation in the DNA repair genes is predictive of outcome in lung cancer. *Hum Mol Genet* **16**, 2333-2340.
123. Matullo G, Guarrera S, Sacerdote C, Polidoro S, Davico L, Gamberini S, Karagas M, Casetta G, Rolle L, Piazza A, & Vineis P (2005). Polymorphisms/haplotypes in DNA repair genes and smoking: a bladder cancer case-control study. *Cancer Epidemiol Biomarkers Prev* **14**, 2569-2578.
124. Mechanic LE, Millikan RC, Player J, de Cotret AR, Winkel S, Worley K, Heard K, Heard K, Tse CK, & Keku T (2006). Polymorphisms in nucleotide excision repair genes, smoking and breast cancer in African Americans and whites: a population-based case-control study. *Carcinogenesis* **27**, 1377-1385.
125. Miller WH, Jr., Schipper HM, Lee JS, Singer J, & Waxman S (2002). Mechanisms of action of arsenic trioxide. *Cancer Res* **62**, 3893-3903.

-
-
126. Millikan RC, Hummer A, Begg C, Player J, de Cotret AR, Winkel S, Mohrenweiser H, Thomas N, Armstrong B, Krickler A, Marrett LD, Gruber SB, Culver HA, Zanetti R, Gallagher RP, Dwyer T, Rebbeck TR, Busam K, From L, Mujumdar U, & Berwick M (2006). Polymorphisms in nucleotide excision repair genes and risk of multiple primary melanoma: the Genes Environment and Melanoma Study. *Carcinogenesis* **27**, 610-618.
 127. Mitra S, Hazra TK, Roy R, Ikeda S, Biswas T, Lock J, Boldogh I, & Izumi T (1997). Complexities of DNA base excision repair in mammalian cells. *Mol Cells* **7**, 305-312.
 128. Miyashita H, Mori S, Tanda N, Nakayama K, Kanzaki A, Sato A, Morikawa H, Motegi K, Takebayashi Y, & Fukumoto M (2001). Loss of heterozygosity of nucleotide excision repair factors in sporadic oral squamous cell carcinoma using microdissected tissue. *Oncol Rep* **8**, 1133-1138.
 129. Mohandas KM (2001). Genetic predisposition to cancer. *Current Science* **81**, 482-489.
 130. Monzote L, Stamberg W, Staniek K, & Gille L (2009). Toxic effects of carvacrol, caryophyllene oxide, and ascaridole from essential oil of *Chenopodium ambrosioides* on mitochondria. *Toxicol Appl Pharmacol*.
 131. Nakagawa Y, Akao Y, Morikawa H, Hirata I, Katsu K, Naoe T, Ohishi N, & Yagi K (2002). Arsenic trioxide-induced apoptosis through oxidative stress in cells of colon cancer cell lines. *Life Sci* **70**, 2253-2269.
 132. NCBI (2007). European Caucasian population NCBI Reference Assembly, CEU_GENO_PANEL. Available from: URL: www.ncbi.nlm.nih.gov
 133. Okamoto Y, Chou PH, Kim SY, Suzuki N, Laxmi YR, Okamoto K, Liu X, Matsuda T, & Shibutani S (2008). Oxidative DNA damage in XPC-knockout and its wild mice treated with equine estrogen. *Chem Res Toxicol* **21**, 1120-1124.
 134. Olausson KA, Dunant A, Fouret P, Brambilla E, Andre F, Haddad V, Taranchon E, Filipits M, Pirker R, Popper HH, Stahel R, Sabatier L, Pignon JP, Tursz T, Le CT, & Soria JC (2006). DNA repair by ERCC1 in non-small-cell lung cancer and cisplatin-based adjuvant chemotherapy. *N Engl J Med* **355**, 983-991.

Reference List

135. Olive PL, Banath JP, & Durand RE (1990). Heterogeneity in radiation-induced DNA damage and repair in tumor and normal cells measured using the "comet" assay. *Radiat Res* **122**,86-94.
136. Orr N, & Chanock S (2008). Common genetic variation and human disease. *Adv Genet* **62**, 1-32.
137. Ott J (2006). User's Guide to the EH program. Available from: URL: <http://www.genemapping.cn/eh.htm>
138. Park CJ, & Choi BS (2006). The protein shuffle. Sequential interactions among components of the human nucleotide excision repair pathway. *FEBS J* **273**, 1600-1608.
139. Platt KL, Aderhold S, Kulpe K, & Fickler M (2008). Unexpected DNA damage caused by polycyclic aromatic hydrocarbons under standard laboratory conditions. *Mutat Res* **650**, 96-103.
140. Pollack Y, Segal R, & Golenser J (1990). The effect of ascaridole on the *in vitro* development of Plasmodium falciparum. *Parasitol Res* **76**, 570-572.
141. Popanda O, Ebbeler R, Twardella D, Helmbold I, Gotzes F, Schmezer P, Thielmann HW, von Fournier D, Haase W, Sautter-Bihl ML, Wenz F, & Bartsch H (2003). Radiation-induced DNA damage and repair in lymphocytes from breast cancer patients and their correlation with acute skin reactions to radiotherapy. *Int J Radiat Biol* **55**, 1216-1225.
142. Popanda O, Schattenberg T, Phong CT, Butkiewicz D, Risch A, Edler L, Kayser K, Dienemann H, Schulz V, Drings P, Bartsch H, & Schmezer P (2004). Specific combinations of DNA repair gene variants and increased risk for non-small cell lung cancer. *Carcinogenesis* **25**, 2433-2441.
143. Pubchem NCBI (2008). NCI *In Vivo* Screening Data; P388 Leukemia (intraperitoneal) in CD2F1 (CDF1) mice. URL: <http://pubchem.ncbi.nlm.nih.gov/>. Downloaded on: 11-8-0009.
144. Qadeer MA, Colabianchi N, & Vaezi MF (2005). Is GERD a risk factor for laryngeal cancer? *Laryngoscope* **115**, 486-491.

-
-
145. Rajaei-Behbahani N, Schmezer P, Ramroth H, Burkle A, Bartsch H, Dietz A, & Becher H (2002). Reduced poly(ADP-ribosyl)ation in lymphocytes of laryngeal cancer patients: results of a case-control study. *Int J Cancer* **98**, 780-784.
 146. Ramroth H, Dietz A, & Becher H (2004). Interaction effects and population-attributable risks for smoking and alcohol on laryngeal cancer and its subsites. A case-control study from Germany. *Methods Inf Med* **43**, 499-504.
 147. Ranelletti FO, Ricci R, Larocca LM, Maggiano N, Capelli A, Scambia G, edetti-Panici P, Mancuso S, Rumi C, & Piantelli M (1992). Growth-inhibitory effect of quercetin and presence of type-II estrogen-binding sites in human colon-cancer cell lines and primary colorectal tumors. *Int J Cancer* **50**, 486-492.
 148. Reardon JT, Bessho T, Kung HC, Bolton PH, & Sancar A (1997). *In vitro* repair of oxidative DNA damage by human nucleotide excision repair system: possible explanation for neurodegeneration in xeroderma pigmentosum patients. *Proc Natl Acad Sci U S A* **94**, 9463-9468.
 149. Risch A, Ramroth H, Raedts V, Rajaei-Behbahani N, Schmezer P, Bartsch H, Becher H, & Dietz A (2003). Laryngeal cancer risk in Caucasians is associated with alcohol and tobacco consumption but not modified by genetic polymorphisms in class I alcohol dehydrogenases ADH1B and ADH1C, and glutathione-S-transferases GSTM1 and GSTT1. *Pharmacogenetics* **13**, 225-230.
 150. Rosell R, Felip E, & Paz-Ares L (2007). How could pharmacogenomics help improve patient survival? *Lung Cancer* **57 Suppl 2**, S35-S41.
 151. Rubbi CP, & Milner J (2003). p53 is a chromatin accessibility factor for nucleotide excision repair of DNA damage. *EMBO J* **22**, 975-986.
 152. Salaspuro V, & Salaspuro M (2004). Synergistic effect of alcohol drinking and smoking on *in vivo* acetaldehyde concentration in saliva. *Int J Cancer* **111**, 480-483.
 153. Sanyal S, Festa F, Sakano S, Zhang Z, Steineck G, Norming U, Wijkstrom H, Larsson P, Kumar R, & Hemminki K (2004). Polymorphisms in DNA repair and metabolic genes in bladder cancer. *Carcinogenesis* **25**, 729-734.
 154. Sapkota A, Gajalakshmi V, Jetly DH, Roychowdhury S, Dikshit RP, Brennan P, Hashibe M, & Boffetta P (2008). Indoor air pollution from solid fuels and risk of

- hypopharyngeal/laryngeal and lung cancers: a multicentric case-control study from India. *Int J Epidemiol* **37**, 321-328.
155. Schnke M, Schulte E, Schumacher U, & Voll M (2005). *Hals und Innere Organe, 78 Tabellen*, pp. 24-25. Thieme, Stuttgart {u.a.
156. Seeberg E, Eide L, & Bjoras M (1995). The base excision repair pathway. *Trends Biochem Sci* **20**, 391-397.
157. Selvakumaran M, Pisarcik DA, Bao R, Yeung AT, & Hamilton TC (2003). Enhanced cisplatin cytotoxicity by disturbing the nucleotide excision repair pathway in ovarian cancer cell lines. *Cancer Res* **63**, 1311-1316.
158. SenGupta S, & Harris CC (2005). p53: traffic cop at the crossroads of DNA repair and recombination. *Nat Rev Mol Cell Biol* **6**, 44-55.
159. Shao QS, Ye ZY, Ling ZQ, & Ke JJ (2005). Cell cycle arrest and apoptotic cell death in cultured human gastric carcinoma cells mediated by arsenic trioxide. *World J Gastroenterol* **11**, 3451-3456.
160. Shao W, Fanelli M, Ferrara FF, Riccioni R, Rosenauer A, Davison K, Lamph WW, Waxman S, Pelicci PG, Lo CF, Avvisati G, Testa U, Peschle C, Gambacorti-Passerini C, Nervi C, & Miller WH, Jr. (1998). Arsenic trioxide as an inducer of apoptosis and loss of PML/RAR alpha protein in acute promyelocytic leukemia cells. *J Natl Cancer Inst* **90**, 124-133.
161. Shaw CY, Chen CH, Hsu CC, Chen CC, & Tsai YC (2003). Antioxidant properties of scopoletin isolated from *Sinomonium acutum*. *Phytother Res* **17**, 823-825.
162. Shen M, Berndt SI, Rothman N, Demarini DM, Mumford JL, He X, Bonner MR, Tian L, Yeager M, Welch R, Chanock S, Zheng T, Caporaso N, & Lan Q (2005). Polymorphisms in the DNA nucleotide excision repair genes and lung cancer risk in Xuan Wei, China. *Int J Cancer* **116**, 768-773.
163. Shen ZX, Chen GQ, Ni JH, Li XS, Xiong SM, Qiu QY, Zhu J, Tang W, Sun GL, Yang KQ, Chen Y, Zhou L, Fang ZW, Wang YT, Ma J, Zhang P, Zhang TD, Chen SJ, Chen Z, & Wang ZY (1997). Use of arsenic trioxide (As₂O₃) in the treatment of acute promyelocytic leukemia (APL): II. Clinical efficacy and pharmacokinetics in relapsed patients. *Blood* **89**, 3354-3360.

-
-
164. Shuck SC, Short EA, & Turchi JJ (2008). Eukaryotic nucleotide excision repair: from understanding mechanisms to influencing biology. *Cell Res* **18**, 64-72.
 165. Silicon Genetics (2003). Multiple Testing Corrections. URL: <http://www.silicongenetics.com>
 166. Singh NP, McCoy MT, Tice RR, & Schneider EL (1988). A simple technique for quantitation of low levels of DNA damage in individual cells. *Exp Cell Res* **175**,184-191.
 167. Sinha S, Singh RK, Alam N, Roy A, Roychoudhury S, & Panda CK (2008). Alterations in candidate genes PHF2, FANCC, PTCH1 and XPA at chromosomal 9q22.3 region: pathological significance in early- and late-onset breast carcinoma. *Mol Cancer* **7**, 84.
 168. Slupphaug G, Kavli B, & Krokan HE (2003). The interacting pathways for prevention and repair of oxidative DNA damage. *Mutat Res* **531**, 231-251.
 169. Smith CJ, Fischer TH, & Sears SB (2000). Environmental tobacco smoke, cardiovascular disease, and the nonlinear dose-response hypothesis. *Toxicol Sci* **54**, 462-472.
 170. Soignet SL, Maslak P, Wang ZG, Jhanwar S, Calleja E, Dardashti LJ, Corso D, DeBlasio A, Gabrilove J, Scheinberg DA, Pandolfi PP, & Warrell RP, Jr. (1998). Complete remission after treatment of acute promyelocytic leukemia with arsenic trioxide. *N Engl J Med* **339**, 1341-1348.
 171. Starmer HM, Tippett DC, & Webster KT (2008). Effects of laryngeal cancer on voice and swallowing. *Otolaryngol Clin North Am* **41**, 793-818, vii.
 172. Stein S, Lao Y, Yang IY, Hecht SS, & Moriya M (2006). Genotoxicity of acetaldehyde- and crotonaldehyde-induced 1,N2-propanodeoxyguanosine DNA adducts in human cells. *Mutat Res* **608**, 1-7.
 173. Stephens M, & Donnelly P (2003). A comparison of bayesian methods for haplotype reconstruction from population genotype data. *Am J Hum Genet* **73**, 1162-1169.

-
-
174. Stevnsner T, Muftuoglu M, Aamann MD, & Bohr VA (2008). The role of Cockayne Syndrome group B (CSB) protein in base excision repair and aging. *Mech Ageing Dev* **129**, 441–448.
 175. Sturgis EM, Dahlstrom KR, Spitz MR, & Wei Q (2002). DNA repair gene ERCC1 and ERCC2/XPD polymorphisms and risk of squamous cell carcinoma of the head and neck. *Arch Otolaryngol Head Neck Surg* **128**, 1084-1088.
 176. Sugawara K (2008). Xeroderma pigmentosum genes: functions inside and outside DNA repair. *Carcinogenesis* **29**, 455-465.
 177. Takebayashi Y, Nakayama K, Kanzaki A, Miyashita H, Ogura O, Mori S, Mutoh M, Miyazaki K, Fukumoto M, & Pommier Y (2001). Loss of heterozygosity of nucleotide excision repair factors in sporadic ovarian, colon and lung carcinomas: implication for their roles of carcinogenesis in human solid tumors. *Cancer Lett* **174**, 115-125.
 178. Talamini R, Bosetti C, La VC, Dal ML, Levi F, Bidoli E, Negri E, Pasche C, Vaccarella S, Barzan L, & Franceschi S (2002). Combined effect of tobacco and alcohol on laryngeal cancer risk: a case-control study. *Cancer Causes Control* **13**, 957-964.
 179. Tan KY, Liu CB, Chen AH, Ding YJ, Jin HY, & Seow-Choen F (2008). The role of traditional Chinese medicine in colorectal cancer treatment. *Tech Coloproctol* **12**, 1-6.
 180. Thorslund T, von KC, Harrigan JA, Indig FE, Christiansen M, Stevnsner T, & Bohr VA (2005). Cooperation of the Cockayne syndrome group B protein and poly(ADP-ribose) polymerase 1 in the response to oxidative stress. *Mol Cell Biol* **25**, 7625-7636.
 181. Tietze C, & Blomeke B (2008). Sensitization assays: monocyte-derived dendritic cells versus a monocytic cell line (THP-1). *J Toxicol Environ Health A* **71**, 965-968.
 182. Tuo J, Chen C, Zeng X, Christiansen M, & Bohr VA (2002a). Functional crosstalk between hOgg1 and the helicase domain of Cockayne syndrome group B protein. *DNA Repair (Amst)* **1**, 913-927.
 183. Tuo J, Jaruga P, Rodriguez H, Bohr VA, & Dizdaroglu M (2003). Primary fibroblasts of Cockayne syndrome patients are defective in cellular repair of 8-hydroxyguanine and 8-hydroxyadenine resulting from oxidative stress. *FASEB J* **17**, 668-674.

-
-
184. Tuo J, Jaruga P, Rodriguez H, Dizdaroglu M, & Bohr VA (2002b). The cockayne syndrome group B gene product is involved in cellular repair of 8-hydroxyadenine in DNA. *J Biol Chem* **277**, 30832-30837.
 185. Tuo J, Muftuoglu M, Chen C, Jaruga P, Selzer RR, Brosh RM, Jr., Rodriguez H, Dizdaroglu M, & Bohr VA (2001). The Cockayne Syndrome group B gene product is involved in general genome base excision repair of 8-hydroxyguanine in DNA. *J Biol Chem* **276**, 45772-45779.
 186. Uchida A, Sugasawa K, Masutani C, Dohmae N, Araki M, Yokoi M, Ohkuma Y, & Hanaoka F (2002). The carboxy-terminal domain of the XPC protein plays a crucial role in nucleotide excision repair through interactions with transcription factor IIH. *DNA Repair (Amst)* **1**, 449-461.
 187. van der Horst GT, van Steeg H, Berg RJ, van Gool AJ, de WJ, Weeda G, Morreau H, Beems RB, van Kreijl CF, de Gruijl FR, Bootsma D, & Hoeijmakers JH (1997). Defective transcription-coupled repair in Cockayne syndrome B mice is associated with skin cancer predisposition. *Cell* **89**, 425-435.
 188. van Erk MJ, Roepman P, van der Lende TR, Stierum RH, Aarts JM, van Bladeren PJ, & van OB (2005). Integrated assessment by multiple gene expression analysis of quercetin bioactivity on anticancer-related mechanisms in colon cancer cells *in vitro*. *Eur J Nutr* **44**, 143-156.
 189. Vanfleteren J, & Roets D (1972). The Influence of Some Anthelmintic Drugs On the Population Growth of the Free-Living Nematodes *Caenorhabditis Briggsae* and *Turbatrix Aceti* (Nematoda : Rhabditida). *Nematologica* **18**, 325-338.
 190. Vogel U, Hedayati M, Dybdahl M, Grossman L, & Nexo BA (2001). Polymorphisms of the DNA repair gene XPD: correlations with risk of basal cell carcinoma revisited. *Carcinogenesis* **22**, 899-904.
 191. Volker M, Mone MJ, Karmakar P, van HA, Schul W, Vermeulen W, Hoeijmakers JH, van DR, van Zeeland AA, & Mullenders LH (2001). Sequential assembly of the nucleotide excision repair factors *in vivo*. *Mol Cell* **8**, 213-224.
 192. Wall ME, & Wani MC (1996). Camptothecin. Discovery to clinic. *Ann N Y Acad Sci* **803**, 1-12.

Reference List

193. Wang MW, Hao X, & Chen K (2007). Biological screening of natural products and drug innovation in China. *Philos Trans R Soc Lond B Biol Sci* **362**, 1093-1105.
194. Weiss JM, Weiss NS, Ulrich CM, Doherty JA, Voigt LF, & Chen C (2005). Interindividual variation in nucleotide excision repair genes and risk of endometrial cancer. *Cancer Epidemiol. Biomarkers Prev* **14**, 2524-2530.
195. Welsh C, Day R, McGurk C, Masters JR, Wood RD, & Koberle B (2004). Reduced levels of XPA, ERCC1 and XPF DNA repair proteins in testis tumor cell lines. *Int J Cancer* **110**, 352-361.
196. Wen SX, Tang PZ, Zhang XM, Zhao D, Guo YL, Tan W, & Lin DX (2006). [Association between genetic polymorphism in xeroderma pigmentosum G gene and risks of laryngeal and hypopharyngeal carcinomas]. *Zhongguo Yi Xue Ke Xue Yuan Xue Bao* **28**, 703-706.
197. Wong HK, Muftuoglu M, Beck G, Imam SZ, Bohr VA, & Wilson III DM (2007). Cockayne syndrome B protein stimulates apurinic endonuclease 1 activity and protects against agents that introduce base excision repair intermediates. *Nucleic Acids Research* **35**, 4103–4113.
198. Wood RD, Mitchell M, Sgouros J, & Lindahl T (2001). Human DNA repair genes. *Science* **291**, 1284-1289.
199. Wu X, Gu J, & Spitz MR (2007a). Mutagen sensitivity: a genetic predisposition factor for cancer. *Cancer Res* **67**, 3493-3495.
200. Wu YH, Cheng YW, Chang JT, Wu TC, Chen CY, & Lee H (2007b). Reduced XPC messenger RNA level may predict a poor outcome of patients with nonsmall cell lung cancer. *Cancer* **110**, 215-223.
201. Wu YH, Tsai Chang JH, Cheng YW, Wu TC, Chen CY, & Lee H (2007c). Xeroderma pigmentosum group C gene expression is predominantly regulated by promoter hypermethylation and contributes to p53 mutation in lung cancers. *Oncogene* **26**, 4761-4773.
202. www.chemexper.com/. 2008.
203. www.ghchealth.com. (2009). Available at URL: <http://www.globalhealingcenter.com/paratrex.php>.

-
-
204. Yang JH, Hsia TC, Kuo HM, Chao PD, Chou CC, Wei YH, & Chung JG (2006). Inhibition of lung cancer cell growth by quercetin glucuronides via G2/M arrest and induction of apoptosis. *Drug Metab Dispos* **34**, 296-304.
 205. Yedjou CG, & Tchounwou PB (2007). In-vitro cytotoxic and genotoxic effects of arsenic trioxide on human leukemia (HL-60) cells using the MTT and alkaline single cell gel electrophoresis (Comet) assays. *Mol Cell Biochem* **301**, 123–130.
 206. Yin J, Li J, Ma Y, Guo L, Wang H, & Vogel U (2005). The DNA repair gene ERCC2/XPD polymorphism Arg 156Arg (A22541C) and risk of lung cancer in a Chinese population. *Cancer Lett* **223**, 219-226.
 207. Yin J, Vogel U, Ma Y, Qi R, Sun Z, & Wang H (2007). A haplotype encompassing the variant allele of DNA repair gene polymorphism ERCC2/XPD Lys751Gln but not the variant allele of Asp312Asn is associated with risk of lung cancer in a northeastern Chinese population. *Cancer Genet Cytogenet* **175**, 47-51.
 208. Yin Y, Stephen CW, Luciani MG, & Fahraeus R (2002). p53 Stability and activity is regulated by Mdm2-mediated induction of alternative p53 translation products. *Nat Cell Biol* **4**, 462-467.
 209. Yu F, Takahashi T, Moriya J, Kawaura K, Yamakawa J, Kusaka K, Itoh T, Morimoto S, Yamaguchi N, & Kanda T (2006a). Traditional Chinese medicine and Kampo: a review from the distant past for the future. *J Int Med Res* **34**, 231-239.
 210. Yu J, Mallon MA, Zhang W, Freimuth RR, Marsh S, Watson MA, Goodfellow PJ, & McLeod HL (2006b). DNA repair pathway profiling and microsatellite instability in colorectal cancer. *Clin Cancer Res* **12**, 5104-5111.
 211. Zheng W, Blot WJ, Shu XO, Gao YT, Ji BT, Ziegler RG, & Fraumeni JF, Jr. (1992). Diet and other risk factors for laryngeal cancer in Shanghai, China. *Am J Epidemiol* **136**, 178-191.
 212. Zhou W, Liu G, Miller DP, Thurston SW, Xu LL, Wain JC, Lynch TJ, Su L, & Christiani DC (2002). Gene-environment interaction for the ERCC2 polymorphisms and cumulative cigarette smoking exposure in lung cancer. *Cancer Res* **62**, 1377-1381.
 213. Zhu J (2003). The molecular mechanism of arsenic trioxide-induced apoptosis and oncosis in leukemia/lymphoma cell lines. *Acta Haematol* **110**, 1-10.

Reference List

214. Zhu XH, Shen YL, Jing YK, Cai X, Jia PM, Huang Y, Tang W, Shi GY, Sun YP, Dai J, Wang ZY, Chen SJ, Zhang TD, Waxman S, Chen Z, & Chen GQ (1999). Apoptosis and growth inhibition in malignant lymphocytes after treatment with arsenic trioxide at clinically achievable concentrations. *J Natl Cancer Inst* **91**, 772-778.
215. Zienolddiny S, Campa D, Lind H, Ryberg D, Skaug V, Stangeland L, Phillips DH, Canzian F, & Haugen A (2006). Polymorphisms of DNA repair genes and risk of non-small cell lung cancer. *Carcinogenesis* **27**, 560-567.

8. Appendix

8.1. Genotypes of the larynx cancer case-control study participants

Table.8.1. Genotypes of the larynx cancer case-control study participants

Lab	ERCC1	ERCC1	ERCC1	ERCC2	ERCC4	ERCC5	ERCC5	ERCC6	ERCC6	RAD23B	XPC
no.	Asn118Asn	C8092A	IVS5+33	Arg156Arg	Arg415Gln	Asp1104His	His46His	Arg1213Gly	Arg1230Pro	Ala249Val	Lys939Gln
1	CT	CA	CC	AC	GG	GG	TC	AA	GG	CC	AC
2	CC	AA	CC	CC	GG	GG	TC	AA	GG	CC	CC
3	CT	CA	CC	CC	GA	GC	CC	AA	GG	CT	AC
4	CC	AA	CC	CC	GG	GG	CC	AA	GG	CC	CC
5	CT	CA	CC	CC	GG	GG	CC	AA	GG	CC	AC
6	CT	CC	CA	AC	GG	GG	CC	AG	GG	CC	AC
7	CT	CC	CA	AC	GG	GC	CC	AG	GG	CC	CC
8	CT	CC	CA	AC	GG	GC	TC	AA	GG	CC	AC
9	CT	CA	CC	CC	GG	GG	TC	AG	GG	CC	AC
10	TT	CC	CC	AC	GG	GG	CC	AG	GG	CC	CC
11	TT	CC	CC	CC	GG	GG	CC	AA	GG	CC	AA
12	TT	CC	CC	AC	GA	GG	CC	AA	GC	CC	CC
13	CT	CC	CA	AC	GG	GC	TC	AA	GG	CC	AC
14	TT	CC	CC	AC	GG	GG	TT	AA	GG	CT	AA
15	TT	CC	CC	CC	GG	GG	CC	AA	GG	CC	AC
16	CT	CA	CC	CC	GG	GC	TC	AG	GG	CT	AC
18	CT	CC	CA	CC	GG	GG	TC	AG	GG	CC	CC
19	CT	CC	CA	AC	GG	GG	TC	AA	GG	CC	AC
20	CT	CC	CA	CC	GA	GG	TC	AG	GG	CT	AC
21	CT	CA	CC	AC	GA	GC	CC	AA	GG	CT	AC
22	CC	CA	CA	AC	GA	GC	TC	AG	GG	TT	AC
23	CC	AA	CC	AC	GG	GG	CC	AG	GG	CT	AA
24	TT	CC	CC	AC	GG	GG	CC	AA	GC	CT	AC
25	CC	AA	CC	AC	GG	GG	TC	AA	GG	CC	AC
26	CC	AA	CC	AA	GG	GG	TC	AA	GC	CT	AC
27	CT	CA	CC	CC	GG	GC	TT	AG	GG	CC	AC
28	CT	CC	CA	AC	GG	GG	CC	AA	GG	CC	AC
30	TT	CC	CC	CC	GA	GC	TT	AG	GG	CT	AA
31	TT	CC	CC	AC	GG	GG	TC	AA	GG	CC	CC
32	TT	CC	CC	AC	GG	GG	TC	AG	GG	CC	CC
33	CT	CA	CC	AC	GG	GC	CC	AG	GG	CT	AC
34	CT	CA	CC	AC	GG	GG	CC	AA	GG	CC	AA

Appendix

Lab	ERCC1	ERCC1	ERCC1	ERCC2	ERCC4	ERCC5	ERCC5	ERCC6	ERCC6	RAD23B	XPC
no.	Asn118Asn	C8092A	IVS5+33	Arg156Arg	Arg415Gln	Asp1104His	His46His	Arg1213Gly	Arg1230Pro	Ala249Val	Lys939Gln
35	TT	CC	CC	AA	GA	GG	CC	AA	GG	CT	AC
36	CT	CC	CC	AA	GG	GG	CC	AA	GG	CT	CC
37	CT	CA	CC	AC	GG	GG	CC	AG	GC	CT	AC
39	CT	CC	CA	AC	GA	GG	TC	GG	GG	CC	AC
40	CT	CA	CC	AC	GA	GG	TC	AA	GG	CT	CC
41	CC	AA	CC	CC	GG	GG	CC	AA	GG	CC	AC
42	CT	CA	CC	AC	GA	GG	TC	AA	GG	CC	AA
43	TT	CC	CC	AC	GG	GC	TC	AA	GG	CT	AA
44	TT	CC	CC	AA	GG	GC	TC	AA	GC	CC	AA
45	TT	CC	CC	AC	GG	GG	CC	AG	GG	CC	AA
46	TT	CC	CC	AC	GG	GG	TC	AA	GG	CC	AC
47	CT	CA	CC	AC	GG	GG	CC	AG	GC	CC	AC
48	CC	CC	AA	CC	GG	GC	CC	AA	GG	CC	AC
49	CC	AA	CC	CC	GG	GG	CC	AA	GG	CC	AA
50	CT	CC	CA	CC	GG	GG	CC	AA	GG	CC	AC
51	CT	CC	CA	AC	GG	GC	TC	AG	GG	CT	AC
52	TT	CC	CC	CC	GG	GC	CC	AA	GG	CC	AA
53	CC	AA	CC	CC	GG	GG	TC	AA	GG	CC	AC
54	CC	CC	AA	CC	GG	GC	TT	AA	GG	CT	AC
55	TT	CC	CC	AA	GG	GG	CC	AA	GG	CC	AA
56	CT	CA	CC	AC	GG	GC	TC	AG	GG	CT	AC
57	TT	CC	CC	AA	GG	GC	TT	AG	GG	CC	AC
58	CT	CA	CC	AC	GG	GG	CC	GG	GG	CC	AC
59	TT	CC	CC	AC	GG	GG	CC	AA	GG	TT	AC
60	CC	CC	AA	CC	GG	GG	CC	AA	GG	CC	AC
62	TT	CC	CC	AC	GG	GC	TC	AA	GG	CC	AA
63	TT	CC	CC	AC	GG	GC	TC	AA	GG	CC	AC
64	CT	CA	CC	AA	GA	GC	TC	AA	GG	CC	AC
65	CT	CC	CA	AC	GG	GC	TC	AA	GG	CC	AA
67	TT	CC	CC	AC	GG	GC	TC	AA	GG	CT	AC
68	CT	CC	CA	AA	GG	GG	TC	AG	GC	CT	AC
69	CT	CA	CC	AC	GG	GG	CC	AG	GG	CC	AA
70	TT	CC	CC	AC	GG	GG	TC	AG	GG	CC	AA
71	TT	CC	CC	AA	GG	GG	TC	AG	GG	CC	AA
72	TT	CC	CC	AC	GG	GG	CC	AA	GG	CC	AC
73	CC	CA	CA	CC	GG	GG	CC	AA	GG	CC	AC
76	TT	CC	CC	AA	GG	GC	TT	AG	GG	CC	CC
77	CT	CA	CC	AC	GG	GC	TT	AA	GG	CC	AC
78	CT	CA	CC	AC	GG	GC	TC	AA	GG	CC	AA
79	CT	CC	CA	CC	GG	GG	CC	AA	GC	CC	CC
80	CT	CA	CC	AC	GG	GG	TC	AG	GG	CC	CC
82	CT	CA	CC	CC	GG	GG	CC	AG	GG	CT	AC
83	CT	CA	CC	AA	GG	GC	TT	AG	GG	CC	AA

Lab	ERCC1	ERCC1	ERCC1	ERCC2	ERCC4	ERCC5	ERCC5	ERCC6	ERCC6	RAD23B	XPC
NO.	Asn118Asn	C8092A	IVS5+33	Arg156Arg	Arg415Gln	Asp1104His	His46His	Arg1213Gly	Arg1230Pro	Ala249Val	Lys939Gln
84	TT	CC	CC	AA	GG	GC	TC	AG	GG	CC	AC
85	CT	CA	CA	CC	GG	GC	TT	AG	GG	CC	AA
86	CT	CC	CA	AC	GG	GG	TC	AA	GG	CT	CC
87	CT	CC	CA	CC	GG	GC	TC	AG	GG	CT	AC
88	CT	CA	CC	CC	GG	GC	TC	AA	GG	TT	AA
89	TT	CC	CC	AC	GG	GG	TC	AA	GC	CC	AA
90	TT	CC	CC	AC	GG	GG	CC	AG	GG	CC	AC
91	CT	CA	CC	AC	GG	GC	CC	AA	GG	CC	AC
92	CT	CC	CA	CC	GG	GC	TC	AA	GG	CC	AC
93	TT	CC	CC	AC	GG	GG	CC	AA	GG	CT	AA
94	TT	CC	CC	AA	GG	GC	TC	AA	GG	CC	AC
95	TT	CC	CC	AC	GG	GG	TC	AG	GG	CC	AC
96	CC	CC	AA	AC	GA	GG	TC	AA	CC	CC	AA
97	CT	CA	CC	CC	GG	GC	TT	AA	GG	CC	AC
98	TT	CC	CC	AC	GG	GG	TT	AA	GG	CC	AC
99	CT	CC	CA	CC	GG	GG	CC	AA	GG	CT	AC
100	CC	AA	CC	CC	GG	GG	TC	AG	GG	CC	CC
101	TT	CC	CC	AC	GG	CC	TC	AG	GC	CT	AA
102	CC	CA	CA	CC	GG	GG	TC	AG	GC	CC	AA
103	CC	CA	CA	CC	GG	GG	CC	AG	GG	CT	AC
104	TT	CC	CC	AC	GG	GG	TC	AA	GG	CC	AC
105	CT	CA	CC	AC	GG	GG	CC	AA	GC	CC	AC
106	CC	AA	CC	AC	GG	GG	TC	AG	GG	CT	AC
107	CT	CA	CC	AC	GG	GG	TC	AA	GG	CT	CC
108	CT	CC	CA	AC	GG	GG	TC	AG	GG	CT	AC
109	CT	CA	CC	AA	GG	GG	TC	AA	GG	CT	AA
111	CT	CC	CA	AC	GG	GG	CC	AA	GG	CC	AC
113	TT	CC	CC	CC	GG	GC	TC	AA	GC	CT	AA
114	CT	CA	CC	AA	GG	GC	TC	AG	GG	CC	CC
115	CT	CC	CA	AC	GA	GC	TC	AG	GG	CC	AC
116	CT	CA	CC	AC	GG	GG	TT	AA	GC	TT	CC
117	TT	CC	CC	CC	GA	GC	TT	AA	GG	CC	AC
118	CT	CA	CC	AC	GG	GG	CC	AA	GG	CT	AC
119	TT	CC	CC	AC	GA	GG	CC	AG	GC	CC	AC
120	TT	CC	CC	CC	GG	GG	CC	AA	GC	CC	AC
122	TT	CC	CC	AA	GG	GG	CC	AG	GC	CC	AC
124	CT	CC	CA	CC	GA	GG	TC	AA	GG	CC	AC
125	TT	CC	CC	CC	GG	GC	TC	AA	GG	CT	AA
126	CT	CA	CC	CC	GG	GC	TT	AG	GG	CT	AC
128	CT	CA	CC	AC	GG	GG	TC	AG	GG	CC	AC
129	CC	CA	CC	CC	GG	GC	TC	AG	GG	CC	AC

Appendix

Lab	ERCC1	ERCC1	ERCC1	ERCC2	ERCC4	ERCC5	ERCC5	ERCC6	ERCC6	RAD23B	XPC
no.	Asn118Asn	C8092A	IVS5+33	Arg156Arg	Arg415Gln	Asp1104His	His46His	Arg1213Gly	Arg1230Pro	Ala249Val	Lys939Gln
130	TT	CC	CC	AC	GG	GC	TC	AA	GG	CC	AC
131	CC	AA	CC	CC	GG	GG	TT	AA	GC	CC	AA
132	TT	CC	CC	AC	GG	GC	TT	AG	GG	CC	AC
133	TT	CC	CC	AA	GA	GC	CC	GG	GG	TT	AC
134	TT	CC	CC	AC	GG	GG	TC	GG	GG	CC	AC
135	CT	CA	CC	AC	GG	GG	TC	AA	GG	CC	AC
136	TT	CC	CC	AA	GA	GG	CC	AG	GG	CC	AC
138	TT	CC	CC	AC	GG	GG	TC	AG	GC	CC	AA
139	TT	CA	CC	CC	GG	GG	TC	AA	GG	CC	AC
140	CT	CC	CA	CC	GG	GG	TC	AG	GG	CC	AC
141	TT	CC	CC	AC	GG	GC	TC	AA	GG	CC	AC
142	TT	CC	CC	AC	GG	GG	CC	GG	GG	CC	CC
143	CT	CC	CA	CC	GG	GC	TC	AA	GG	CC	AC
144	CT	CA	CC	AC	GG	GC	TC	AG	GG	CC	CC
145	CT	CA	CC	AC	GG	GG	CC	AA	GG	CT	AC
146	CT	CC	CA	AC	GG	GC	TT	AA	GG	CC	CC
147	CT	CC	CA	AA	GG	GG	TC	GG	GG	CC	AC
148	CC	AA	CC	CC	GA	GG	CC	AG	GG	CC	AC
149	CT	CA	CC	AC	GG	GG	TT	AA	GG	CC	AA
151	CT	CC	CA	CC	GG	GC	TT	AA	GC	CC	AC
152	TT	CC	CC	AC	GG	GG	TC	AA	CC	TT	AC
153	CT	CC	CA	CC	GG	GG	CC	AA	GG	CT	AC
154	CC	AA	CC	AC	GA	GG	CC	AA	GG	CC	AA
155	TT	CC	CC	AC	GG	CC	TT	AA	GG	CC	AA
156	CT	CC	CA	AC	GA	GC	TC	AA	GG	CT	AC
157	TT	CC	CC	CC	GG	GG	CC	AG	GG	CT	AC
159	CT	CC	CA	AC	GG	GC	TC	AA	GC	CT	AA
160	TT	CC	CC	AC	GG	GG	CC	AG	GG	CC	CC
161	CT	CA	CC	AC	GG	GC	TC	GG	GG	CT	AA
162	CT	CC	CA	CC	GA	GG	TC	AA	GG	CT	AA
163	CT	CC	CC	AA	GG	GG	CC	AG	GG	CC	CC
165	TT	CC	CC	AA	GA	GG	TC	AA	GG	CC	AA
166	CT	CA	CC	AC	GA	CC	TT	AA	GG	CC	AC
167	CT	CA	CC	CC	GG	GG	CC	AG	GG	CC	AC
168	CC	CA	CA	CC	GG	GC	TC	AA	GG	CT	AC
170	CC	AA	CC	AC	GG	GG	CC	AG	GG	CT	AC
171	CC	AA	CC	CC	GG	GC	TC	AA	GG	CT	AC
174	TT	CC	CC	AC	GG	GC	TT	AA	GG	CC	AA
175	TT	CC	CC	AA	GG	GG	CC	AG	GC	CT	AC
176	TT	CC	CC	AC	GG	GG	CC	AA	GG	CC	AC
177	CC	CA	CA	CC	GG	GC	CC	AA	GG	CT	AC
178	TT	CC	CC	AC	GG	GC	TC	AA	GG	CC	CC
179	CC	AA	CC	AC	GG	GC	TC	AG	GG	CC	AC

Lab	ERCC1	ERCC1	ERCC1	ERCC2	ERCC4	ERCC5	ERCC5	ERCC6	ERCC6	RAD23B	XPC
NO.	Asn118Asn	C8092A	IVS5+33	Arg156Arg	Arg415Gln	Asp1104His	His46His	Arg1213Gly	Arg1230Pro	Ala249Val	Lys939Gln
180	TT	CC	CC	CC	GG	GG	TT	AA	GG	CC	AA
181	CT	CA	CC	AC	GG	GG	TC	AG	GG	CC	AC
182	TT	CC	CC	AC	GG	CC	CC	AA	GG	CC	AC
183	CT	CA	CC	AA	GG	GG	TC	AG	GG	CC	AC
184	CC	AA	CC	AC	GG	GC	TC	AA	GG	CC	AC
185	CT	CA	CC	CC	GG	GC	TC	AA	GC	TT	AA
186	CT	CC	CA	CC	GG	GG	CC	AG	GG	CC	AC
187	CT	CA	CC	CC	GG	GG	CC	AG	GG	CT	AA
189	TT	CC	CC	AC	GG	CC	TT	AA	GG	CC	AC
190	TT	CC	CC	AC	GG	GG	TC	AA	GC	CC	AC
191	CC	AA	CC	CC	GG	GG	CC	AG	GG	CC	AC
192	CT	CC	CA	CC	GG	CC	TT	GG	GG	CC	AA
193	TT	CC	CC	AC	GG	CC	TT	AA	GG	CC	CC
194	TT	CC	CC	AC	GG	GC	TC	AG	GC	CC	AA
195	TT	CC	CC	AC	GG	GC	TT	AG	GG	CC	AA
196	TT	CC	CC	AA	GG	GC	TT	AG	GG	CC	CC
197	CT	CA	CC	CC	GG	GG	TT	AG	GC	TT	AA
198	TT	CC	CC	CC	GG	GG	CC	AG	GG	CT	AC
199	TT	CC	CC	CC	GG	GG	CC	AG	GG	CT	AC
200	TT	CC	CC	AA	GG	GG	TC	AA	GG	CT	AA
201	TT	CC	CC	AC	GG	GG	TC	AA	GC	CT	AC
202	CT	CC	CA	AA	GG	GG	TC	AA	GG	CC	AC
203	CT	CA	CC	AC	GA	GC	CC	AA	GG	CT	AC
204	CT	CA	CC	AC	GG	GG	CC	AA	GG	CT	AC
205	CT	CA	CC	AC	GG	GG	TC	AG	GG	TT	AC
206	CT	CA	CC	AC	GG	GG	TC	AG	GG	CC	AA
207	CT	CA	CC	CC	GA	GG	CC	AG	GG	CC	AA
209	TT	CC	CC	AC	GG	GG	TT	AA	GC	TT	AA
211	TT	CC	CC	AA	GG	GC	TT	AG	GG	CC	AA
212	CC	AA	CC	AC	GG	GG	TC	AA	GG	CC	CC
213	TT	CC	CC	AA	GG	GC	TC	AA	GG	CC	AC
214	TT	CC	CC	AA	GG	GG	TC	AG	GG	CT	AA
215	CT	CA	CC	AC	AA	GG	CC	AA	GC	CC	AC
216	CC	CA	CA	CC	GG	GC	TC	AA	GG	CT	AC
218	TT	CC	CC	CC	GG	GG	TC	AA	GG	CT	AC
219	CT	CC	CA	CC	GA	GC	TT	AA	GG	CT	AC
220	CT	CA	CC	AC	GG	GG	CC	AA	GC	CC	CC
222	CC	AA	CC	AC	GG	GG	TC	AA	GG	CC	CC
223	CT	CA	CC	AC	GG	GC	TT	AA	GG	CT	AC
224	TT	CC	CC	AC	GG	GC	TC	AA	GG	CC	CC
225	TT	CC	CC	CC	GG	GC	TC	AG	GG	CT	AA

Appendix

Lab	ERCC1	ERCC1	ERCC1	ERCC2	ERCC4	ERCC5	ERCC5	ERCC6	ERCC6	RAD23B	XPC
no.	Asn118Asn	C8092A	IVS5+33	Arg156Arg	Arg415Gln	Asp1104His	His46His	Arg1213Gly	Arg1230Pro	Ala249Val	Lys939Gln
226	CT	CA	CC	AC	GG	GC	TT	AG	GG	TT	AA
227	TT	CC	CC	AC	GG	GG	TC	AG	GG	CC	CC
228	TT	CC	CC	CC	GG	GC	TC	AA	GG	CT	CC
229	TT	CC	CC	AA	GA	GG	CC	AA	GG	CT	CC
230	CT	CC	CC	CC	GA	GC	TC	AA	GC	CC	AC
231	CT	CC	CA	AC	GG	CC	TT	AG	GG	CC	AC
232	TT	CC	CC	AC	GG	GG	CC	AG	GC	CC	CC
233	CT	CA	CC	AC	GG	GG	TC	AG	GC	CT	AC
234	CT	CC	CA	AC	GA	GG	CC	AA	GG	CC	AC
235	TT	CC	CC	AC	GG	GC	CC	GG	GG	CC	AC
236	CT	CC	CA	CC	GG	GC	TC	AG	GG	CC	AC
237	CT	CA	CC	AC	GG	GG	CC	AA	GC	CT	AA
238	CT	CA	CC	AC	GG	GC	TC	AA	GC	CC	AA
239	TT	CC	CC	AA	GG	GC	CC	AA	GG	CC	AC
240	CT	CA	CC	CC	GG	GG	TC	AA	GC	CT	AC
241	CT	CA	CC	AA	GG	GC	TC	AA	GG	CC	CC
242	CT	CA	CC	AA	GG	GC	TC	AG	GG	CC	AC
243	TT	CC	CC	AC	GG	GG	CC	AA	GG	CC	AC
244	TT	CC	CC	AA	GG	GC	TC	AA	GC	CC	CC
246	TT	CC	CC	CC	GG	GG	TT	AG	GG	CC	AC
247	TT	CC	CC	AA	GG	CC	TC	AA	GG	TT	AC
248	CT	CA	CC	AC	GG	GG	CC	AA	GG	CC	AC
249	CT	CC	CA	AC	GG	GG	CC	AA	GG	CT	AC
250	CT	CA	CC	AC	GG	GG	TT	AA	GG	CC	AA
251	TT	CC	CC	AC	GG	GG	CC	AA	GC	CC	CC
252	CT	CA	CC	CC	GG	GC	TC	AA	GG	TT	AC
253	CT	CC	CA	AA	GG	GG	TT	AA	GG	CC	AA
254	TT	CC	CC	AC	GG	GG	TC	AA	GG	CT	CC
255	TT	CC	CC	AC	GG	GC	TT	AA	GG	CC	AC
257	TT	CC	CC	AC	GA	GG	CC	AA	GG	CC	AA
258	CC	CA	CA	AC	GG	GG	TC	AA	GG	CC	AA
259	TT	CC	CC	CC	GA	GC	TC	AA	GG	CC	AA
260	CT	CA	CC	CC	GG	GG	TC	AA	GG	CC	CC
261	CT	CC	CA	CC	GG	GC	TT	GG	GG	CC	AA
262	CC	CA	CA	CC	GA	GG	TT	AG	GG	CC	AC
264	CT	CA	CC	CC	GA	GG	CC	AG	GG	CT	AA
265	TT	CC	CC	AC	GG	GG	CC	AA	GG	CT	AA
266	TT	CC	CC	CC	GG	GC	TC	AA	GG	CC	AC
267	CT	CA	CC	AC	GG	GG	TT	AA	GC	CC	AA
268	CT	CA	CC	CC	GG	GG	CC	AA	GG	CC	AA
269	TT	CC	CC	AC	GG	GG	CC	AG	GG	CC	AA
270	CT	CC	CA	AC	GG	GC	TC	AA	GG	CC	AC
271	TT	CC	CC	AC	GG	GC	TC	AA	GG	CC	AC

Lab	ERCC1	ERCC1	ERCC1	ERCC2	ERCC4	ERCC5	ERCC5	ERCC6	ERCC6	RAD23B	XPC
NO.	Asn118Asn	C8092A	IVS5+33	Arg156Arg	Arg415Gln	Asp1104His	His46His	Arg1213Gly	Arg1230Pro	Ala249Val	Lys939Gln
272	TT	CC	CC	AC	GG	GG	CC	AA	GG	CC	AC
274	TT	CC	CC	AA	GA	GG	TC	AA	GG	CC	AA
275	TT	CC	CC	CC	GG	GG	TC	AA	GC	TT	AA
276	CT	CC	CA	AA	GG	GG	TC	AG	GG	CC	CC
278	CT	CA	CC	AC	GG	GG	TC	AA	GC	CC	CC
280	TT	CC	CC	CC	GG	GG	CC	AA	GG	CT	AA
282	TT	CC	CC	AC	GA	CC	TT	AA	GG	CC	AC
283	CC	CA	CA	AC	GA	GC	TC	AA	GG	CC	AC
285	TT	CC	CC	AC	GG	GG	TT	AA	GG	CT	AA
286	CT	CA	CC	AA	GG	GG	CC	AA	GG	CC	AC
287	TT	CC	CC	AA	GG	GG	TC	AG	GG	CC	AA
289	TT	CC	CC	CC	GG	GG	CC	AA	GG	CC	AA
290	CT	CA	CC	AA	GG	GC	TC	GG	GG	CT	CC
291	TT	CC	CC	AC	GG	GC	TT	AA	GC	CC	AA
292	TT	CC	CC	CC	GA	GG	CC	AG	GG	CT	CC
293	CT	CA	CC	CC	GA	GC	TC	AA	GG	CC	AA
294	TT	CC	CC	AC	GG	GG	CC	AA	GG	CT	AC
295	CT	CA	CC	AC	GG	GG	CC	AG	GG	CC	AC
296	CT	CA	CC	CC	GG	GG	TC	AG	GG	CT	AC
297	CT	CA	CC	AC	GG	GG	TC	AA	GG	CT	CC
298	TT	CC	CC	AC	GG	GG	TC	AG	GG	CT	AC
299	CT	CA	CC	CC	GG	GG	TC	AG	GG	CT	CC
301	CC	AA	CC	CC	GG	CC	TT	AA	GG	CT	AC
302	TT	CC	CC	AC	GA	GC	TC	AA	GG	CT	AA
303	CT	CC	CA	AC	GG	GG	TC	GG	GG	CC	AC
304	CT	CC	CA	AA	GG	GG	TT	AA	GG	CT	AA
305	CT	CC	CC	CC	GG	GC	CC	AA	GG	CC	CC
306	TT	CC	CC	CC	GG	GG	CC	AG	GG	CC	CC
307	TT	CC	CC	AA	GG	GG	CC	AG	GG	CC	AC
308	CT	CA	CC	CC	GG	GC	TC	AG	GG	CT	CC
309	TT	CC	CC	AA	GA	GC	CC	AA	GG	CT	AC
310	TT	CC	CC	AC	GG	GG	TC	AG	GG	CT	CC
311	TT	CC	CC	AC	GG	GC	TC	AA	GG	CC	AA
312	TT	CC	CC	CC	GG	GG	CC	AA	CC	CT	AA
313	CC	AA	CC	AC	GA	CC	TT	AG	GG	CC	AC
314	TT	CC	CC	AC	GG	GC	TC	AA	GG	CC	AC
315	TT	CC	CC	AC	GG	GC	TC	AA	GC	CC	AC
316	CT	CC	CA	AC	GG	CC	TT	AA	GC	CC	AC
318	TT	CC	CC	AA	GG	GG	TC	AA	GG	CT	AA
319	CC	CA	CA	CC	GG	CC	TC	AA	GG	CC	AA
320	TT	CC	CC	AC	GG	GC	TC	AA	GG	CC	AA

Appendix

Lab	ERCC1	ERCC1	ERCC1	ERCC2	ERCC4	ERCC5	ERCC5	ERCC6	ERCC6	RAD23B	XPC
no.	Asn118Asn	C8092A	IVS5+33	Arg156Arg	Arg415Gln	Asp1104His	His46His	Arg1213Gly	Arg1230Pro	Ala249Val	Lys939Gln
323	TT	CA	CC	CC	GG	GG	CC	AA	GG	CC	AA
326	CT	CA	CC	AC	GG	CC	TT	AA	GG	CC	AC
329	TT	CC	CC	CC	GG	GG	TC	GG	GG	CC	AA
330	CT	CC	CC	AC	GG	GG	CC	AA	GG	CC	AA
331	CC	AA	CC	AC	GG	GG	TC	AA	GC	CC	AC
332	TT	CC	CC	AA	GG	GC	TC	AG	GG	CC	CC
333	CT	CC	CA	CC	GG	GG	TC	AG	GG	CC	CC
334	CT	CC	CA	CC	GG	GC	TC	AG	GG	CC	AA
335	TT	CC	CC	AA	GG	GG	CC	AA	GG	CT	AC
336	TT	CC	CC	AC	GG	GC	TC	AA	GG	TT	AC
337	TT	CC	CC	AA	GG	GG	CC	GG	GG	CC	AC
338	CT	CC	CA	CC	GG	GG	CC	AA	GG	CT	AC
339	TT	CC	CC	AA	GG	GC	TC	AG	GG	CC	AC
340	CC	CA	CA	CC	GG	GC	TC	AA	GG	CT	AC
341	CC	CA	CA	CC	GG	GG	TC	AA	GG	CC	AA
342	TT	CC	CC	AA	GG	GG	CC	GG	GG	CC	AA
343	CT	CA	CC	AA	GG	GG	TC	AA	GG	TT	AA
344	CC	CA	CC	CC	GA	GG	TC	AG	GG	TT	AC
345	TT	CC	CC	AA	GG	GG	TC	AA	GC	CC	AA
346	TT	CC	CC	AA	GG	GG	TC	AA	GG	CC	AC
347	TT	CC	CC	AC	GA	GG	TC	AG	GG	CT	AC
348	TT	CC	CC	CC	GA	GC	TC	AA	GC	CC	AC
349	CT	CC	CA	AC	GA	GG	CC	AG	GG	CT	AC
350	CT	CA	CC	AC	GG	GG	CC	AG	GG	CC	AA
352	TT	CC	CC	AA	GG	GG	TC	AA	GC	CC	AC
353	CT	CC	CA	AC	GG	GC	TC	AA	GG	CC	AA
354	TT	CC	CC	AC	GG	GC	TT	AA	GG	CC	AA
355	TT	CC	CC	AA	GA	GC	TC	AA	GC	CC	AA
356	TT	CC	CC	AC	GG	GC	CC	AG	GC	CT	AC
357	CC	CA	CA	AC	GG	GG	TT	AA	GG	CC	AC
359	CT	CA	CC	AC	GG	GC	CC	AG	GG	CC	AC
360	TT	CA	CC	AC	GG	GC	TC	AA	GG	CC	AC
361	CT	CC	CA	CC	GG	GC	TT	GG	GG	CT	AC
362	CT	CA	CC	AC	GA	GG	TC	AA	GG	CT	AC
364	CT	CC	CA	AC	GG	GG	CC	AG	GC	CC	CC
365	TT	CC	CC	CC	GG	GG	CC	AA	GG	CC	AC
366	TT	CC	CC	AC	GA	GG	CC	AG	GG	CT	AC
367	CT	CC	CA	AC	GG	GC	TC	AA	GG	CT	AA
368	TT	CC	CC	CC	GG	GG	CC	AA	GG	CC	AC
370	TT	CC	CC	AC	GG	GG	CC	AA	GG	CT	AA
371	CT	CA	CC	AA	AA	GC	TC	AA	GG	CC	CC
373	CT	CC	CA	AC	GG	GG	TT	AA	GG	CT	AA
374	CT	CC	CA	CC	GG	GG	CC	AG	GC	CT	AA

Lab	ERCC1	ERCC1	ERCC1	ERCC2	ERCC4	ERCC5	ERCC5	ERCC6	ERCC6	RAD23B	XPC
NO.	Asn118Asn	C8092A	IVS5+33	Arg156Arg	Arg415Gln	Asp1104His	His46His	Arg1213Gly	Arg1230Pro	Ala249Val	Lys939Gln
375	TT	CC	CC	AC	GA	GG	CC	AG	GG	CT	CC
376	CT	CA	CC	AC	GG	GC	TT	AA	GG	CC	AA
377	TT	CC	CC	AA	GG	GG	TC	AG	GG	CC	CC
378	TT	CC	CC	AC	GA	GC	TC	AA	GG	CC	AC
379	TT	CC	CC	AC	GG	GG	CC	AA	GG	CC	AA
382	TT	CC	CC	AC	GG	GC	TC	AG	GG	CC	AA
383	CT	CC	CA	AC	GG	GC	TT	AG	GG	CT	AA
384	CT	CA	CC	AC	GG	GC	TC	AA	GG	TT	AC
385	CT	CA	CC	CC	GG	GG	CC	AG	GG	CT	AC
387	CC	AA	CC	AA	GG	GG	CC	AG	GG	CT	AA
388	TT	CC	CC	CC	GG	GG	TC	AG	GG	CC	CC
389	TT	CC	CC	CC	GG	GG	CC	AA	GG	CC	AC
390	TT	CC	CC	AC	GA	GG	CC	AA	GC	CT	AA
391	CC	CA	CA	AC	GG	GG	TC	AA	GC	CC	CC
392	CT	CA	CC	CC	GG	GG	TC	AA	GC	CT	AA
393	TT	CC	CC	AC	GG	GG	CC	AG	GG	CC	AA
394	TT	CC	CC	AA	GG	GG	TC	AG	GG	CC	AC
395	CT	CA	CC	AC	GG	CC	TC	AA	GG	CC	AC
396	TT	CC	CC	AA	GG	GG	CC	AA	GC	CC	AA
397	CT	CA	CC	AC	GG	GC	TC	GG	GG	TT	AC
398	TT	CC	CC	AC	GA	GC	TC	AA	GC	CT	AC
399	TT	CC	CC	AC	GG	GG	CC	AA	GC	CC	AA
400	TT	CC	CC	CC	GG	GG	TT	AG	GG	CT	AC
401	TT	CC	CC	CC	GG	GC	CC	AA	GG	CC	AA
402	CT	CA	CC	CC	GG	GC	TC	AG	GG	CC	AC
404	CT	CC	CC	AA	GG	GG	CC	AA	GG	CC	AA
405	TT	CC	CC	CC	GG	GG	TT	AA	GG	CC	AA
407	CT	CC	CA	CC	GA	GG	TC	AA	GC	CC	AA
408	CT	CA	CC	AC	GA	GG	TC	AG	GG	CC	AA
410	CC	CA	CC	CC	GG	GC	TT	AG	GG	CC	AC
411	TT	CC	CC	AC	GG	GG	TC	AA	GG	CC	AA
412	CT	CC	CA	CC	GG	GC	TT	AA	GG	CC	AC
414	CC	AA	CC	CC	GA	CC	TT	AG	GG	CC	CC
415	TT	CC	CC	AC	GG	GC	TT	AG	GG	CC	AC
416	CT	CA	CC	CC	GG	GG	CC	AG	GG	CC	CC
417	CT	CA	CC	CC	GG	CC	TC	AA	GG	CC	CC
418	TT	CC	CC	AC	GG	GG	CC	AG	GC	CT	AA
420	CT	CA	CC	AA	GG	GG	TC	AA	GG	CT	AC
421	CT	CC	CA	AC	GA	GG	CC	AG	GG	CC	CC
422	CT	CC	CA	AA	GG	GG	TC	AG	GG	CT	AA
423	TT	CC	CC	AA	GG	GG	TC	AA	GG	CT	AC

Appendix

Lab	ERCC1	ERCC1	ERCC1	ERCC2	ERCC4	ERCC5	ERCC5	ERCC6	ERCC6	RAD23B	XPC
no.	Asn118Asn	C8092A	IVS5+33	Arg156Arg	Arg415Gln	Asp1104His	His46His	Arg1213Gly	Arg1230Pro	Ala249Val	Lys939Gln
424	CT	CC	CA	CC	GG	GG	CC	AA	GC	CC	AC
425	CT	CC	CC	CC	GG	GG	TC	GG	GG	CC	AC
426	TT	CC	CC	AC	GG	GG	CC	GG	GG	CC	AC
427	TT	CC	CC	AA	GG	GG	TC	AG	GG	CT	AA
428	CC	AA	CC	CC	GG	GG	CC	AG	GG	CC	AA
429	CC	AA	CC	AC	GG	GG	TT	AA	GG	CT	CC
431	TT	CC	CC	AA	GA	GG	CC	AA	GG	CC	AC
432	CT	CA	CC	CC	GG	GC	TC	GG	GG	CC	AA
434	TT	CC	CC	AA	GG	GG	CC	AA	GG	TT	AA
435	TT	CC	CC	AA	GG	GG	CC	AG	GC	CC	CC
437	CT	CA	CC	AC	GG	GC	TC	AG	GG	CC	AA
438	TT	CC	CC	AC	GG	GG	CC	AA	GG	CC	AA
439	CT	CA	CC	AC	GG	GG	CC	AA	GC	CC	AC
440	TT	CC	CC	AA	GG	GC	TC	AG	GG	CT	AC
441	TT	CC	CC	CC	GG	GG	CC	GG	GG	CC	CC
442	CT	CC	CA	CC	GG	GC	TC	AG	GG	CC	AA
443	TT	CC	CC	CC	GG	GG	TC	AG	GG	CC	AA
444	TT	CC	CC	AA	GG	GC	TT	AG	GG	CT	AC
445	CT	CA	CC	CC	GG	GG	TT	AG	GG	CC	CC
447	CT	CA	CC	AC	GG	GC	TC	AA	GG	CC	AC
448	TT	CC	CC	AA	GG	GG	CC	AA	GG	TT	CC
449	CT	CA	CC	AA	GG	GC	TC	AA	GG	CC	AC
450	TT	CC	CC	AC	GG	GG	TT	AG	GG	CC	AA
451	CT	CA	CC	CC	GG	GG	TT	AA	GG	CT	AA
453	TT	CC	CC	CC	GG	GG	TC	AA	GG	CC	AC
454	CT	CA	CC	AC	GA	GG	TC	AA	GG	CC	AA
455	CC	AA	CC	AA	GG	GG	CC	GG	GG	CC	AC
456	CT	CA	CC	AC	GG	GG	TT	AA	GC	CT	AA
457	CC	AA	CC	CC	GG	GG	CC	AG	GG	CC	AA
458	TT	CC	CC	AA	GG	GG	CC	AA	GG	CC	AC
459	CT	CA	CC	AA	GA	GG	TC	AA	GG	CT	CC
460	CT	CA	CC	CC	GG	GC	TC	AA	GG	CC	AC
461	TT	CC	CC	AC	GG	GG	CC	GG	GG	CC	AC
462	TT	CC	CC	CC	GG	GG	CC	AA	GG	CT	AC
463	CT	CC	CA	CC	GG	GG	CC	AG	GG	CC	AA
464	TT	CC	CC	AA	GG	GG	CC	AG	GG	CC	AC
465	CT	CC	CA	AC	GA	GG	CC	AA	GG	CC	AA
467	CC	CC	AA	CC	GG	GC	TC	AA	GG	CT	AC
468	TT	CC	CC	AC	GG	GC	TC	AA	GG	CC	AA
469	TT	CA	CC	AC	GG	GC	CC	AG	GG	CC	CC
470	CT	CC	CA	AC	GG	GG	TC	AA	GG	CC	AC
471	CT	CC	CA	AC	GG	GG	TC	AG	GG	CC	AC
472	CT	CA	CC	AC	GG	GC	TC	AA	GG	CT	AA

Lab	ERCC1	ERCC1	ERCC1	ERCC2	ERCC4	ERCC5	ERCC5	ERCC6	ERCC6	RAD23B	XPC
NO.	Asn118Asn	C8092A	IVS5+33	Arg156Arg	Arg415Gln	Asp1104His	His46His	Arg1213Gly	Arg1230Pro	Ala249Val	Lys939Gln
473	CT	CA	CC	AC	GG	GC	TC	AA	GC	CT	AC
474	CT	CA	CC	CC	GG	GG	TC	AA	GG	CT	AC
475	TT	CC	CC	AA	GG	GC	TC	AA	GG	CC	AC
476	TT	CC	CC	CC	GG	CC	TC	AA	GG	CC	AA
477	CT	CC	CA	CC	GG	GG	CC	AA	GG	CT	AA
478	CT	CA	CC	CC	GG	GG	TC	AA	GG	CC	AC
479	TT	CC	CC	AC	GG	GC	TC	AA	CC	CC	AA
481	CC	CC	AA	AC	GG	GG	CC	AA	GC	CT	AA
482	CC	CC	AA	AC	GG	GG	CC	AA	GG	CC	AA
483	CT	CA	CC	CC	GG	GG	CC	AA	GC	CC	CC
484	TT	CC	CC	AC	GG	GG	TC	AA	GG	CC	AC
486	TT	CC	CC	AC	GG	GC	CC	AA	GG	CC	AA
487	CT	CC	CA	AC	GG	GC	TC	AA	GC	CC	AC
489	CT	CC	CA	AA	GG	GG	CC	AG	GG	CC	AC
490	CC	CC	AA	AA	GG	GC	TT	AA	GG	CT	AC
491	CC	CA	CA	AC	GG	GG	TC	AA	GG	CC	AA
492	CT	CA	CC	AA	GG	GG	TC	AA	GG	TT	AA
495	CT	CA	CC	AC	GA	GC	TT	GG	GG	CT	CC
496	CC	CA	CA	CC	GG	GC	TC	AG	GG	CC	AA
498	TT	CC	CC	AA	GG	GG	TC	AA	GG	CC	AC
499	TT	CC	CC	AC	GG	GC	TC	GG	GG	CC	AA
500	CT	CC	CA	AA	GG	GC	TC	AA	GG	CT	AC
501	TT	CC	CC	AC	GG	GG	TC	AA	GG	CC	AC
502	TT	CC	CC	AA	GG	GG	TC	AA	GC	CT	AC
504	CT	CC	CA	AA	GG	GG	CC	AA	GG	CT	AA
505	CT	CA	CC	AA	GG	GC	TT	AG	GC	CC	AA
506	TT	CC	CC	AC	GA	GC	TT	AA	GG	CC	AC
507	CT	CA	CC	AC	GG	GC	TC	AA	GG	CC	AC
508	CC	AA	CC	CC	GG	GC	TC	AA	GG	TT	AC
509	TT	CC	CC	AC	GG	GG	TC	AG	GG	CT	AC
510	TT	CC	CC	CC	GA	GC	TC	AA	GC	CC	AA
511	CT	CA	CC	AC	GG	GG	CC	AG	GG	CT	AA
512	CT	CA	CC	CC	GG	GG	CC	AA	GG	CC	AC
513	TT	CC	CC	CC	GA	GG	TC	AA	GG	CC	AC
514	TT	CC	CC	CC	GA	GG	CC	AA	GG	TT	CC
515	CC	AA	CC	AC	GG	GG	TC	AA	GC	CC	AC
516	CC	CA	CA	CC	GG	GG	CC	AA	GG	CC	AA
517	TT	CC	CC	CC	GG	GG	TT	AG	GG	CC	AA
518	TT	CC	CC	CC	GG	GC	TT	AA	GG	CC	CC
519	CT	CA	CC	AC	GA	GG	TT	AA	GC	CC	AC
520	TT	CC	CC	AC	GG	GG	TT	AA	GG	CC	AC

Appendix

Lab	ERCC1	ERCC1	ERCC1	ERCC2	ERCC4	ERCC5	ERCC5	ERCC6	ERCC6	RAD23B	XPC
no.	Asn118Asn	C8092A	IVS5+33	Arg156Arg	Arg415Gln	Asp1104His	His46His	Arg1213Gly	Arg1230Pro	Ala249Val	Lys939Gln
521	CC	CC	AA	CC	GG	GG	TT	AA	GG	CC	CC
522	CC	AA	CC	CC	GG	GG	CC	AA	GG	CC	CC
523	TT	CC	CC	AC	GG	GG	CC	AG	GG	CC	AC
524	CT	CC	CC	AC	AA	GC	TC	AA	GG	CT	AC
526	TT	CC	CC	AA	GG	GC	TC	AA	GG	CC	AA
527	TT	CC	CC	AC	GG	GG	TC	AA	GC	CC	AA
528	TT	CC	CC	AC	GG	GC	CC	AA	GC	CT	CC
529	CT	CA	CC	AC	GG	GC	CC	AA	GC	CT	AA
530	TT	CC	CC	AC	GG	GG	CC	AG	GG	TT	AA
532	TT	CC	CC	AA	GG	GG	TC	AG	GG	CC	AA
533	CT	CC	CA	CC	GG	GG	CC	AA	GG	CC	AC
534	TT	CC	CC	AC	GG	GC	TC	AA	CC	CC	AA
535	TT	CC	CC	AC	GG	GC	TC	AA	GG	CT	CC
536	TT	CC	CC	AC	GA	GG	CC	GG	GG	CT	AC
537	CT	CC	CC	AC	GG	GG	CC	AG	GG	CT	AC
538	CT	CA	CC	AA	GG	GC	TT	AA	GG	CT	AA
541	CT	CC	CA	AC	GG	GC	TC	AA	GC	CC	AC
542	CT	CA	CC	CC	GG	GG	CC	AA	GG	CC	AC
543	CC	CC	AA	CC	GG	GG	CC	AA	GG	CT	AC
544	TT	CC	CC	AC	GG	GG	CC	AA	GG	CC	AC
545	TT	CC	CC	AC	GG	GC	TC	AG	GG	CT	AA
546	CT	CA	CC	AC	GG	GC	TC	AG	GC	TT	CC
547	TT	CC	CC	AC	GG	GC	TT	AA	GC	CT	AC
548	TT	CC	CC	AA	GA	GG	CC	GG	GG	CT	AA
549	TT	CC	CC	AC	GG	GG	TC	AA	GG	CT	AA
550	CT	CC	CA	AA	GG	GG	TC	AG	GG	CT	AC
551	CT	CC	CA	CC	GG	GC	CC	AG	GG	CC	AA
552	CT	CA	CC	AA	GG	GG	TT	AG	GG	CT	AC
554	TT	CC	CC	AC	GG	GC	TT	AG	GG	CC	AC
555	TT	CC	CC	AC	GG	GG	TC	AA	GC	CC	AA
556	TT	CC	CC	AC	GG	GC	TT	AG	GG	CT	AA
557	CT	CC	CA	CC	GG	GC	TC	AG	GG	CC	AC
558	CT	CA	CC	CC	GG	GG	CC	AG	GG	CC	AC
559	TT	CC	CC	AA	GG	GG	TC	AA	GG	CC	AA
560	TT	CC	CC	CC	GA	GG	TC	AG	GC	CC	AA
561	CT	CC	CC	AC	GG	GC	TC	AA	GC	CT	AA
562	CC	AA	CC	AA	GG	GC	TC	AG	GG	TT	AC
564	TT	CC	CC	AA	GG	GG	CC	AA	GG	CC	AC
565	CC	CA	CA	AC	GG	GG	TC	AG	GG	CC	AC
566	CT	CC	CA	AC	GA	GG	TC	AA	GG	CT	AC
567	TT	CC	CC	AC	GG	GG	TC	AG	GG	CC	AC
568	TT	CC	CC	AC	GG	GC	TT	AA	GG	CC	AA
569	TT	CC	CC	AA	GG	GC	TC	AA	GG	CT	AC

Lab	ERCC1	ERCC1	ERCC1	ERCC2	ERCC4	ERCC5	ERCC5	ERCC6	ERCC6	RAD23B	XPC
NO.	Asn118Asn	C8092A	IVS5+33	Arg156Arg	Arg415Gln	Asp1104His	His46His	Arg1213Gly	Arg1230Pro	Ala249Val	Lys939Gln
570	CT	CA	CC	AC	GG	CC	TT	AA	GG	CT	AC
572	TT	CC	CC	AC	GG	CC	CC	AA	GG	CC	AC
574	CT	CA	CC	AC	GG	GC	TT	GG	GG	CT	AC
575	TT	CC	CC	AC	GA	CC	TT	AG	GG	TT	AC
576	TT	CC	CC	CC	GG	GG	CC	AA	GG	CT	AC
577	CT	CA	CC	AC	GG	GC	TT	AA	GG	TT	AC
578	TT	CC	CC	AA	GG	CC	TT	AA	GG	CC	AC
580	CC	AA	CC	CC	GA	GG	TC	AG	GG	CC	AA
582	CC	AA	CC	CC	GG	GG	CC	AA	GG	CC	AA
583	CT	CC	CA	AA	GG	GG	CC	AA	GG	CC	AA
584	CT	CA	CA	AA	GG	GG	TC	AG	GG	CT	AC
585	CT	CA	CC	CC	GG	GG	TC	AA	GG	CC	AC
586	TT	CC	CC	AC	GG	GC	TC	GG	GG	CC	AC
589	CT	CA	CC	AC	GG	GG	CC	AG	GG	CC	AC
590	TT	CC	CC	AC	GG	GC	TT	AA	GG	CC	AA
591	TT	CC	CC	AA	GG	GC	TT	AG	GG	CT	AA
592	CT	CC	CA	AC	GG	GG	TC	GG	GG	CT	AA
593	CT	CA	CC	AC	GG	GG	CC	GG	GG	CC	AA
594	CT	CA	CC	AC	GA	GC	TC	AA	GG	CC	AC
595	CT	CC	CA	AC	GG	GC	CC	AG	GG	CC	AC
596	CT	CA	CA	CC	GG	GG	CC	AA	GG	CC	AA
597	CT	CA	CC	AC	GA	GC	TT	AA	GG	CT	CC
598	CT	CC	CA	AC	GA	GC	TC	AA	CC	CC	AA
599	TT	CC	CC	AA	GG	GC	TC	AG	GG	CC	AA
600	TT	CC	CC	AA	GG	GG	TC	AA	GG	CC	AC
601	CC	CC	AA	AC	GG	GC	TC	AA	GC	CT	AA
602	TT	CC	CC	CC	GG	GG	TT	AG	GG	CC	AC
603	TT	CC	CC	AC	GG	GG	TC	AA	GG	TT	AC
604	TT	CC	CC	AA	GG	GG	TC	AA	GG	CC	AA
605	TT	CC	CC	AC	GG	GC	TT	AA	GG	CC	AA
606	CT	CC	CA	AC	GA	GC	TC	AG	GG	CC	AC
607	TT	CC	CC	AA	GG	GG	TC	AG	GG	CC	CC
608	CT	CA	CC	CC	GG	GG	CC	AG	GC	CC	AC
609	CT	CC	CA	AA	GG	GG	TC	AA	GC	CT	AC
610	TT	CC	CC	CC	GG	GC	TT	AG	GC	CC	AC
611	CT	CC	CA	AC	GG	GG	TC	AA	GG	CC	AA
612	TT	CC	CC	AC	GG	GC	TC	AG	GG	CT	AC
613	CT	CC	CA	AC	GG	GG	CC	AG	GG	CC	AA
615	CT	CA	CC	AA	GG	GG	CC	AG	GG	CT	AC
616	CC	CA	CA	CC	GG	GG	TT	AA	GG	CC	AC
617	CT	CC	CA	AC	GG	CC	TT	AA	GC	CC	AC

Appendix

Lab	ERCC1	ERCC1	ERCC1	ERCC2	ERCC4	ERCC5	ERCC5	ERCC6	ERCC6	RAD23B	XPC
no.	Asn118Asn	C8092A	IVS5+33	Arg156Arg	Arg415Gln	Asp1104His	His46His	Arg1213Gly	Arg1230Pro	Ala249Val	Lys939Gln
619	CT	CA	CC	AC	GG	GC	TT	AA	GG	CT	AC
620	CT	CC	CA	AC	GG	GG	CC	AG	GG	CT	AA
621	TT	CC	CC	AC	GG	GG	TT	AG	GG	CT	AC
622	CT	CA	CC	AC	GG	GC	TC	AA	GG	CT	CC
623	CT	CA	CC	CC	GG	GG	TT	AA	GG	CC	AA
624	CT	CA	CC	CC	GG	GC	TC	AA	GG	CT	AA
625	TT	CC	CC	AA	GG	GG	TC	AA	GG	CC	AC
626	TT	CC	CC	AA	GG	GG	TC	AA	GG	TT	AC
628	TT	CC	CC	AC	GG	GC	TC	GG	GG	CC	AC
629	CT	CA	CC	CC	GG	GG	CC	AA	GG	CC	CC
630	TT	CC	CC	AC	GG	GC	TC	GG	GG	CT	AA
631	TT	CC	CC	AC	GG	GC	TC	AA	GG	CC	AC
632	TT	CA	CC	AC	GG	GC	TC	AG	GG	CT	AC
633	CT	CA	CC	AA	GG	GC	TT	AA	GG	CC	AA
634	CT	CA	CC	AC	GG	GC	TT	AG	GG	CC	AC
635	CT	CC	CA	AC	GG	GC	TC	AG	GG	TT	AC
637	CT	CC	CA	AC	GG	GG	TC	AA	GG	CC	AC
638	CT	CA	CC	AC	GG	GC	TC	AG	GC	CC	AC
639	TT	CC	CC	AC	GA	GC	TT	AA	GC	CC	AA
642	CT	CA	CC	AC	GG	GG	TC	AG	GG	CC	AC
643	CT	CC	CA	AA	GG	GC	TC	AG	GC	CC	AA
645	CT	CA	CC	AC	GG	GG	CC	AA	GG	CC	AC
646	CT	CC	CA	AC	GG	GG	TC	AA	GG	CT	AC
647	CT	CA	CC	AC	GG	GC	TT	AA	GG	CC	AA
648	CT	CC	CA	AC	GG	GG	CC	AA	GG	CC	AC
649	CC	CC	AA	CC	GG	GC	TC	AA	GG	CC	AA
650	CT	CA	CC	AC	GA	GG	TC	AA	GG	CC	AC
652	TT	CC	CC	AC	GA	CC	TT	AA	GG	CT	AC
653	CT	CA	CC	CC	GA	GG	TC	AA	GG	CC	AC
655	CC	AA	CC	CC	GG	GG	TC	AG	GG	CT	AA
656	TT	CC	CC	CC	GA	GG	TC	AA	GG	CC	AA
657	TT	CC	CC	AC	GG	GC	TC	AG	GG	CC	AA
658	CT	CC	CA	AC	GG	GG	CC	AA	GG	CC	AC
659	TT	CC	CC	CC	GG	GG	CC	AA	GG	CT	AA
661	TT	CC	CC	AC	GG	GC	TC	AG	GC	CT	AC
662	TT	CC	CC	AC	GA	GG	CC	AA	GC	CC	CC
663	CT	CC	CA	AC	GG	CC	TT	AG	GG	CC	AA
664	CC	CA	CA	AC	GG	GC	TC	AG	GC	CC	AC
665	CC	CA	CA	CC	GG	GG	TC	AA	GC	CT	AA
666	TT	CC	CC	CC	GG	GG	TC	AG	GG	CC	AC
668	CT	CA	CC	AA	GG	GG	TC	GG	GG	CC	AC
669	CT	CC	CA	CC	GG	GC	TC	AA	GC	CT	AA
670	TT	CC	CC	AC	GA	GC	TC	AA	GG	CC	AA

Lab	ERCC1	ERCC1	ERCC1	ERCC2	ERCC4	ERCC5	ERCC5	ERCC6	ERCC6	RAD23B	XPC
NO.	Asn118Asn	C8092A	IVS5+33	Arg156Arg	Arg415Gln	Asp1104His	His46His	Arg1213Gly	Arg1230Pro	Ala249Val	Lys939Gln
671	CT	CC	CA	AC	GA	GG	CC	AA	GG	CC	AC
672	TT	CC	CC	AA	GG	GG	CC	AA	GG	CC	AA
673	CT	CA	CC	AA	GG	GG	CC	AA	GC	CC	CC
674	CC	AA	CC	CC	GG	GG	TC	AG	GC	CC	AA
675	TT	CC	CC	CC	GG	GG	CC	AA	GG	CT	AA
678	CT	CA	CC	AA	GG	GG	TC	AA	GG	TT	CC
679	CC	CA	CA	AC	GG	GG	TC	AA	GG	CC	AC
680	CT	CA	CC	CC	GG	GG	TT	AG	GG	CC	CC
681	CT	CA	CC	AA	GG	GG	TC	GG	GG	CC	AA
682	TT	CC	CC	AC	GA	GG	TC	AG	GC	CC	AC
683	CT	CC	CA	AC	GG	GG	TC	AG	GG	TT	CC
684	TT	CC	CC	CC	GA	CC	TC	AA	GC	CT	AC
685	TT	CC	CC	AC	GG	GC	TC	GG	GG	CC	AC
686	CT	CA	CC	AC	GG	GG	TC	AA	CC	CC	AA
687	TT	CC	CC	AA	GG	GG	TC	AG	GG	CT	AC
688	TT	CC	CC	CC	GG	GG	TT	AG	GG	CC	AA
689	TT	CC	CC	AC	GG	GG	TC	AG	GG	CC	AA
690	CT	CC	CA	AA	GG	GG	TC	AA	GG	CC	CC
692	CT	CA	CC	AA	GG	GC	TC	AA	GG	TT	CC
693	TT	CC	CC	CC	GG	GC	TC	AG	GG	CC	AC
694	CC	AA	CC	CC	GG	GC	TT	AA	GC	CC	AA
695	TT	CC	CC	AC	GG	GG	TT	AA	GG	CC	CC
696	CT	CC	CA	AA	GG	GC	TC	AG	GG	CC	AC
697	TT	CC	CC	AC	GG	GG	CC	GG	GG	CT	CC
698	CT	CA	CC	CC	GG	GG	CC	GG	GG	CC	AA
699	CT	CA	CC	CC	GG	GC	TC	AG	GG	CC	AA
700	TT	CC	CC	AC	GG	GG	CC	AG	GG	CC	AA
701	TT	CC	CC	AC	GG	GG	CC	AA	GG	CC	AC
702	TT	CC	CC	AA	GG	GG	CC	AG	GG	TT	AC
705	CT	CC	CC	AC	GG	GC	TC	AA	GG	CC	AC
706	CT	CC	CA	CC	GG	GG	CC	AA	GG	CC	CC
707	CT	CC	CA	AA	GG	GC	TT	AG	GG	CC	AC
708	CT	CA	CC	CC	GA	GC	CC	AA	GG	CC	AA
710	CT	CA	CC	CC	GG	GG	CC	AG	GG	CT	AC
711	CC	CC	AA	CC	GG	GC	TC	AA	CC	CC	AA
712	TT	CC	CC	AC	GG	GC	TC	AG	GG	CC	AA
713	TT	CC	CC	CC	GG	GG	TC	AG	GG	CT	AC
714	TT	CC	CC	AA	GG	GG	TC	AA	GC	CC	AC
715	CC	CA	CA	AC	GG	GG	TC	AA	GC	CT	AC
716	CC	CA	CA	AC	GG	GG	TC	AA	GG	CC	AA
717	CC	CA	CC	AC	GA	GG	TT	AA	GG	CT	AA

Appendix

Lab	ERCC1	ERCC1	ERCC1	ERCC2	ERCC4	ERCC5	ERCC5	ERCC6	ERCC6	RAD23B	XPC
no.	Asn118Asn	C8092A	IVS5+33	Arg156Arg	Arg415Gln	Asp1104His	His46His	Arg1213Gly	Arg1230Pro	Ala249Val	Lys939Gln
718	CT	CA	CC	AA	GG	GG	CC	AG	GG	CC	AC
720	CT	CA	CC	AC	GG	GG	CC	AA	GG	CT	AC
721	TT	CC	CC	AC	GG	GG	CC	AG	GG	CC	CC
722	CC	CC	AA	CC	GG	GG	CC	AA	GC	CC	AC
723	CT	CA	CC	AA	GG	GG	CC	AA	GG	CT	AA
726	CT	CA	CC	CC	GA	GC	TC	GG	GG	CC	AC
728	TT	CC	CC	AA	GG	GG	TC	AA	GG	TT	AC
729	CT	CA	CC	AC	GG	GG	CC	AA	GG	CT	AC
730	TT	CC	CC	AC	GG	GC	TC	AA	GG	CT	AA
731	TT	CC	CC	CC	GG	GG	CC	AG	GG	CC	CC
732	CT	CA	CC	CC	GG	GG	TC	AG	GG	CC	AC
734	CT	CA	CC	AC	GG	GC	TT	AG	GG	CC	AA
736	CC	CA	CA	CC	GG	GC	TT	AA	GG	CT	CC
738	CT	CA	CC	CC	GG	GG	TT	AG	GC	CT	AA
739	CT	CA	CC	AC	GG	GC	TT	AA	GG	CC	AC
740	CT	CA	CC	AA	GG	GG	TT	AA	GC	CC	CC
741	TT	CC	CC	CC	GG	GG	CC	AA	GG	CC	AC
742	CT	CA	CC	CC	GG	GG	CC	AA	GG	CC	AA
743	CC	CC	AA	AC	GG	GG	TC	AA	GG	CT	AC
744	TT	CC	CC	AC	GG	GG	TC	AA	GC	CC	AC
745	CC	CA	CA	CC	GG	GC	TC	AA	GG	CC	AC
746	CT	CA	CC	AA	GG	GG	CC	AA	GG	CC	AA
747	CT	CA	CC	CC	GG	GC	TC	AA	GG	CC	AA
748	CT	CA	CC	AC	GG	CC	TT	AG	GG	CT	AC
749	TT	CC	CC	AC	GA	CC	TC	AA	GC	CC	AA
750	CT	CA	CC	AC	GA	GG	CC	AG	GG	CC	AC
751	TT	CC	CC	AC	GA	GC	TC	AA	GG	CC	AC
752	CT	CC	CA	CC	GG	GG	TC	AG	GG	CC	AC
753	CT	CA	CC	AC	GG	GC	TC	AG	GG	CC	CC
754	TT	CC	CC	AC	GG	GG	CC	AA	GG	CC	AC
757	TT	CC	CC	AA	GG	GG	TC	AA	GG	CC	AA
758	CT	CC	CA	CC	GG	GG	CC	AA	GG	CC	AA
760	TT	CC	CC	AA	GG	GC	TC	GG	GG	CC	AC
761	TT	CC	CC	AC	GA	GC	TC	AA	GG	CT	AC
762	CC	AA	CC	AC	GG	GC	TC	AG	GG	CT	CC
763	CT	CA	CC	AC	GG	CC	TC	AG	GG	CC	AC
765	TT	CC	CC	AA	GA	GC	CC	AA	GC	CT	AC
766	TT	CC	CC	AC	GA	GG	CC	AA	CC	CC	CC
767	TT	CC	CC	AC	GA	GG	CC	AA	GG	TT	AC
769	CT	CA	CC	AC	GA	GC	TC	AG	GG	CT	CC
772	CC	AA	CC	CC	GG	GC	TC	AA	GC	CC	AA
774	TT	CC	CC	AA	GG	GG	CC	AA	GG	CT	AA
775	CT	CA	CC	CC	GG	GG	TC	AA	GG	CC	AC

Lab	ERCC1	ERCC1	ERCC1	ERCC2	ERCC4	ERCC5	ERCC5	ERCC6	ERCC6	RAD23B	XPC
NO.	Asn118Asn	C8092A	IVS5+33	Arg156Arg	Arg415Gln	Asp1104His	His46His	Arg1213Gly	Arg1230Pro	Ala249Val	Lys939Gln
776	TT	CC	CC	AC	GG	GC	TC	AA	GG	CC	AC
777	CT	CC	CA	AA	GG	GC	TT	AA	GG	CT	CC
778	CT	CA	CC	AC	GG	GC	TT	AA	GG	CT	AA
779	TT	CC	CC	AC	GG	GG	TC	AA	GG	CT	AC
780	CT	CC	CA	AC	GG	GG	TC	GG	GG	CT	AC
781	CT	CA	CC	CC	GG	GG	TC	AG	GG	CC	AC
782	CT	CC	CA	AC	GG	GG	TC	AA	GG	CC	AC
783	TT	CC	CC	AA	GG	GG	CC	GG	GG	CC	AA
784	CT	CA	CC	AC	GG	GC	TT	AG	GC	CT	AC
785	TT	CC	CC	AC	GG	GC	TC	AA	GC	CT	AC
786	TT	CC	CC	AA	GG	GC	TT	AA	GG	CC	AA
788	TT	CC	CC	CC	GG	GG	CC	AG	GG	CC	AC
789	CT	CC	CA	AC	GA	GG	CC	AA	GG	CC	AA
791	CT	CA	CC	CC	GG	CC	TC	AG	GG	CT	AA
792	CT	CA	CC	AC	GG	GC	TC	AA	GG	CC	CC
793	TT	CC	CC	CC	GG	GG	TC	AA	GG	CC	AA
794	CT	CC	CA	AA	GG	GG	TT	AG	GG	CC	AA
795	TT	CC	CC	CC	GA	GC	TC	AA	GG	CC	AC
796	CC	CA	CA	CC	GG	GC	TC	GG	GG	CT	AA
797	CT	CA	CC	AC	GG	CC	TT	AA	GG	CC	AC
798	CC	CA	CA	AC	GA	GC	CC	AA	GG	CT	AC
802	TT	CC	CC	AA	GG	GG	TC	AG	GG	CC	AC
803	CT	CA	CC	AA	GG	CC	TT	AA	GG	CT	AC
804	CC	AA	CC	AC	GA	GG	CC	AG	GG	CC	AA
805	CT	CA	CC	CC	GA	GC	TC	AG	GG	TT	AC
807	TT	CC	CC	CC	GG	GG	TC	AA	GG	CT	AC
808	TT	CC	CC	AA	GA	GG	CC	AG	GG	CC	AC
809	TT	CC	CC	CC	GG	GG	CC	AG	GG	CC	AC
810	TT	CC	CC	AC	GG	GG	TC	AG	GG	CT	AA
812	CT	CC	CA	AC	GG	GC	TT	AA	GC	CT	AC
813	TT	CC	CC	AC	GG	GG	CC	AA	GG	CC	AC
814	CT	CA	CC	CC	GG	CC	TT	AA	GC	CC	AA
816	TT	CC	CC	CC	GG	GC	TT	AG	GG	CC	CC
818	CT	CC	CA	AC	GA	CC	TT	AA	GC	CT	AC
819	TT	CC	CC	AA	GG	GG	CC	AG	GG	CT	AA
821	TT	CC	CC	AA	GG	GC	TC	AA	GG	CC	AA
822	CT	CA	CC	AC	GG	GG	TC	AA	GG	CC	AA
823	CT	CC	CA	AA	GG	GC	CC	AG	GG	CT	AC
824	CC	AA	CC	CC	GG	GC	CC	AG	GG	CT	AA
826	TT	CC	CC	AA	GG	GC	TC	AA	GG	CC	AA
827	CT	CC	CA	AC	GG	GC	TC	AA	GG	CC	CC

Appendix

Lab	ERCC1	ERCC1	ERCC1	ERCC2	ERCC4	ERCC5	ERCC5	ERCC6	ERCC6	RAD23B	XPC
no.	Asn118Asn	C8092A	IVS5+33	Arg156Arg	Arg415Gln	Asp1104His	His46His	Arg1213Gly	Arg1230Pro	Ala249Val	Lys939Gln
829	CC	CA	CA	CC	GG	CC	TT	AA	GC	CC	AC
830	CT	CC	CA	CC	GG	GC	TC	AA	GG	CC	AC
831	TT	CC	CC	AA	AA	GC	TT	AG	GG	CC	AA
833	CT	CA	CC	AA	GG	GC	CC	AG	GG	CC	AC
834	CT	CC	CA	AA	GG	GC	CC	AA	GG	CC	AC
835	CT	CC	CA	AC	GA	GC	TC	AG	GG	CC	AC
842	CC	CA	CA	CC	GG	GG	CC	AG	GG	CC	AA
843	CC	CA	CA	CC	GG	GG	TC	AA	GG	CC	CC
844	CT	CA	CC	AC	GG	GG	CC	AG	GG	CC	AC
845	TT	CC	CC	AC	GG	GG	TC	AA	GG	CC	AC
846	CT	CA	CC	AC	GG	GG	TC	AA	GC	CT	AA
847	TT	CC	CC	CC	GG	GC	TC	AA	GG	CC	AA
848	CT	CA	CC	AC	GG	GG	CC	AA	GG	CT	AC
849	CT	CA	CC	AC	GG	GG	CC	AA	GG	CC	AC
850	TT	CC	CC	CC	GG	GG	TT	GG	GG	CC	AC
852	CT	CA	CC	CC	GG	GG	CC	AA	GC	CT	AA
853	TT	CC	CC	CC	GG	GG	CC	AG	GG	TT	AC
854	TT	CC	CC	CC	GG	GG	CC	AG	GC	CT	AA
855	CT	CC	CA	AC	GG	GG	TC	AA	GG	TT	AC
856	CT	CC	CA	AA	GG	GG	CC	GG	GG	CC	AA
857	TT	CC	CC	AC	GG	GC	TC	AA	GG	CC	AA
861	TT	CC	CC	AA	GG	GG	CC	AG	GG	CT	AA
863	CT	CA	CC	AA	GA	GG	TC	AG	GC	CC	AC
864	CT	CA	CC	AA	GG	GC	TT	AA	GG	CC	AC
865	TT	CC	CC	AA	GG	GG	TC	AA	GC	CC	AC
866	CT	CC	CA	CC	GG	GG	TC	AA	GG	CT	AC
867	TT	CC	CC	AC	GG	GC	TT	AG	GC	CC	AC
868	CT	CC	CA	AC	GG	GC	TC	AA	GG	CT	CC
870	TT	CA	CC	CC	GG	GG	TC	AG	GG	CC	AC
871	TT	CC	CC	AC	GG	GG	CC	AG	GG	TT	AA
873	TT	CC	CC	CC	GG	GG	CC	AG	GG	CC	AC
875	TT	CC	CC	AC	GG	GG	TC	AA	GG	CC	AC
876	CT	CA	CC	AC	GG	GC	TC	AA	GC	CT	AC
877	CT	CA	CC	AA	GG	GG	TC	GG	GG	CC	CC
878	CT	CA	CC	CC	GA	GG	TC	AA	GG	CC	AA
879	CT	CA	CC	AC	GA	GG	TC	AA	GG	CC	AC
881	CT	CC	CA	AC	GG	GG	CC	AA	GC	CT	AA
882	TT	CC	CC	AC	GG	GC	TC	GG	GG	CC	AA
883	TT	CC	CC	AA	GG	GC	TC	AA	GG	CT	AC
884	CC	AA	CC	AC	GG	GG	CC	GG	GG	CC	AA
885	CT	CA	CC	AA	GG	GC	TC	AA	GG	CC	AA
886	TT	CC	CC	AC	GG	GG	CC	AA	GG	CT	AC
887	CT	CA	CC	AC	GG	GC	TC	AA	GG	CC	CC

Lab	ERCC1	ERCC1	ERCC1	ERCC2	ERCC4	ERCC5	ERCC5	ERCC6	ERCC6	RAD23B	XPC
NO.	Asn118Asn	C8092A	IVS5+33	Arg156Arg	Arg415Gln	Asp1104His	His46His	Arg1213Gly	Arg1230Pro	Ala249Val	Lys939Gln
888	TT	CC	CC	AC	GG	GG	CC	AG	GG	CT	AC
889	TT	CC	CC	CC	GG	GC	TC	AA	GG	CC	AA
891	CT	CC	CA	AC	GA	GG	TC	AA	GG	CT	CC
892	TT	CC	CC	AC	GG	GG	TC	AA	GC	CT	AC
893	CT	CA	CC	AC	GG	GC	TC	AA	GC	CT	AC
894	CC	AA	CC	CC	GA	GG	TC	AA	GC	CC	AC
895	CC	CA	CA	CC	GG	GC	CC	AG	GC	CT	AC
897	CT	CC	CA	CC	GG	GG	CC	AG	GG	CC	AC
898	CT	CA	CC	AC	GG	GC	TT	AG	GG	TT	AC
902	TT	CC	CC	AC	GG	GC	TC	AA	GG	CC	AC
904	TT	CC	CC	CC	GG	GC	TC	AG	GG	CC	AC
905	CT	CA	CC	CC	GG	GC	TC	AG	GG	CC	CC
906	TT	CC	CC	AA	GG	GG	CC	AG	GG	CC	CC
907	CT	CC	CC	AC	GG	GG	TC	AA	GC	CC	AC
908	CT	CA	CC	AC	GG	GG	CC	AA	GG	CT	AA
909	TT	CC	CC	CC	GG	GG	TC	AG	GG	CC	CC
910	CT	CA	CC	CC	GG	GC	CC	AA	GG	CC	AA
911	TT	CC	CC	AA	GG	CC	TT	AA	GG	CC	AC
912	TT	CC	CC	AA	GG	GC	TC	AG	GC	CC	AC
913	TT	CC	CC	AA	GG	GG	TT	AG	GG	CT	CC
914	TT	CC	CC	AA	GG	GG	TT	AA	GG	CC	AA
915	TT	CA	CC	AC	GG	GG	CC	AA	GG	CT	AA
916	TT	CC	CC	CC	GA	GG	CC	AA	CC	CC	AA
917	TT	CC	CC	AC	GG	GC	TT	AG	GG	CT	AC
918	TT	CC	CC	AC	GG	GC	TC	AA	GG	CT	AC
919	CC	CA	CA	CC	GG	GC	TC	GG	GG	CT	AC
920	TT	CC	CC	AA	GG	GC	TT	AA	GG	CT	AC
921	TT	CC	CC	CC	GG	GG	TC	AA	GG	CT	AA
922	TT	CC	CC	AC	GG	GG	TC	AG	GG	CC	AA
923	TT	CC	CC	CC	GG	GG	TT	AG	GG	CC	AC
924	CT	CA	CC	AC	GG	GC	TC	AA	GG	CC	AA
926	CT	CA	CC	AA	GG	GG	CC	AA	GG	CC	AA
927	CT	CA	CC	AA	GG	GG	TT	AG	GG	CC	AA
928	CC	AA	CC	AC	GG	GG	TC	AA	GG	CC	AC
929	CT	CA	CC	AC	GA	GC	TC	GG	GG	CC	AA
931	CT	CA	CC	AC	GG	GC	TC	AA	GG	CC	AC
932	TT	CC	CC	AC	GG	GG	TC	AG	GG	CT	AA
933	TT	CC	CC	AA	GG	GG	CC	AG	GG	CC	AA
934	CC	CA	CA	AC	GG	GC	TC	AA	GG	CC	AC
935	CC	AA	CC	CC	GG	GG	TC	AA	GG	CC	AC
936	CT	CA	CC	AC	GG	GG	CC	AG	GG	CC	AC

Appendix

Lab	ERCC1	ERCC1	ERCC1	ERCC2	ERCC4	ERCC5	ERCC5	ERCC6	ERCC6	RAD23B	XPC
no.	Asn118Asn	C8092A	IVS5+33	Arg156Arg	Arg415Gln	Asp1104His	His46His	Arg1213Gly	Arg1230Pro	Ala249Val	Lys939Gln
937	CT	CC	CC	CC	GG	GG	CC	AA	GG	CT	AA
939	CT	CC	CA	AA	GA	GG	TT	AA	GG	CT	AC
940	TT	CC	CC	CC	GG	GC	TC	AG	GG	CT	AC
941	CT	CA	CC	AC	GG	CC	TT	AG	GC	CC	AC
942	CC	AA	CC	AC	GG	GC	TC	AG	GG	CT	AA
943	CT	CA	CC	AC	GG	GC	TC	AA	GC	CT	AA
944	TT	CC	CC	AC	GG	GC	TC	AA	GG	CC	CC
945	CT	CA	CC	AC	GG	GC	TC	AG	GG	CT	CC
946	CT	CA	CC	AC	GG	GC	TT	AG	GC	TT	CC
947	CT	CA	CC	AC	GG	GG	CC	AA	GG	CC	AA
949	TT	CC	CC	AA	GG	GG	TC	AA	GG	CC	AA
950	CC	CA	CA	CC	GG	GC	TC	AA	GG	CT	AA
954	CT	CA	CC	AC	GG	GC	TC	AG	GG	CC	CC
955	CT	CA	CC	CC	GG	GG	TC	AA	GG	CC	AA
956	CT	CA	CC	CC	GA	GC	TC	AG	GG	CT	AA
961	CT	CC	CA	AC	GG	CC	TT	AA	GG	CC	AC
962	TT	CC	CC	AA	GA	GC	TT	AA	GG	CC	AC
963	CT	CA	CC	AC	GG	GC	TC	AA	GG	CC	AA
966	TT	CC	CC	AC	GG	GG	TC	AG	GG	CC	CC
969	CT	CC	CA	AC	GA	GG	TC	AG	GG	CT	AA
970	CT	CA	CC	AC	GG	GG	CC	AA	GG	CT	AA
971	TT	CC	CC	AC	GG	GC	TC	AA	GG	CC	AC
972	TT	CC	CC	CC	GG	GC	TC	AG	GC	CC	AC
973	CT	CA	CC	CC	GG	GC	TC	AA	GG	CC	AA
974	TT	CC	CC	AC	GA	GC	TC	AG	GC	CT	AC
975	CT	CA	CC	AC	GG	GC	CC	AG	GG	CC	AA
976	TT	CC	CC	AC	GG	GG	CC	AA	GG	CC	AA
978	CC	CA	CA	AC	GG	CC	TT	AA	GG	CC	AC
981	CT	CA	CC	AC	GA	CC	TT	AA	GC	CC	AA
982	TT	CC	CC	AA	GG	GC	TC	AA	GG	CT	CC
983	CC	AA	CC	CC	GG	GG	CC	AA	GC	CC	AC
984	CT	CA	CC	AC	GG	CC	CC	AA	GG	CC	CC
986	TT	CC	CC	AC	GA	GG	CC	AA	GG	CC	AC
987	CT	CA	CC	CC	GG	CC	TT	AG	GG	CC	AA
988	TT	CC	CC	AC	GG	GG	CC	AA	GC	CT	AC
989	TT	CC	CC	AC	GG	GG	CC	AA	GG	TT	CC
990	CC	AA	CC	CC	GG	GC	TC	AA	GC	CC	AC
991	CT	CA	CC	AC	GG	GC	TC	AA	GG	CC	AA
992	CT	CA	CC	CC	GG	GG	TC	AG	GG	CT	AA
993	CC	CC	AA	AC	GG	CC	TT	AA	GG	CC	CC
994	TT	CC	CC	AA	GG	GG	TC	AA	GC	CC	AA
995	TT	CC	CC	AC	GA	GC	TC	AA	GG	CC	CC
996	CT	CA	CC	AA	GG	GG	CC	AA	GG	TT	AC

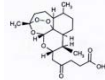
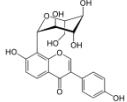
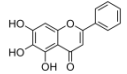
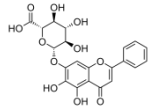
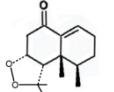
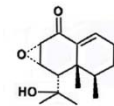
Lab	ERCC1	ERCC1	ERCC1	ERCC2	ERCC4	ERCC5	ERCC5	ERCC6	ERCC6	RAD23B	XPC
NO.	Asn118Asn	C8092A	IVS5+33	Arg156Arg	Arg415Gln	Asp1104His	His46His	Arg1213Gly	Arg1230Pro	Ala249Val	Lys939Gln
997	CT	CA	CC	AC	GG	GG	TC	AA	GG	CC	AC
998	CT	CA	CC	CC	GA	GC	TT	AA	GG	CC	CC
999	CT	CC	CA	AC	GG	GG	TC	AA	GC	CT	AC
1000	TT	CA	CC	AC	GG	GG	CC	AG	GG	CT	AC
1001	CT	CC	CA	CC	GG	GG	CC	AA	GG	CT	AC
1002	CC	CA	CA	CC	GA	GC	TT	AA	GG	CC	AA
1003	TT	CC	CC	AA	GG	GC	TC	AA	GG	CC	AA
1004	CT	CA	CC	AC	GG	GG	TC	AA	GG	CT	CC
1005	CT	CA	CC	CC	GG	GC	TC	AG	GC	TT	AC
1006	CT	CC	CA	AC	GG	GC	TC	AA	GG	CC	AA
1008	CT	CC	CA	AC	GG	GC	CC	AA	GG	CT	AC
1009	CT	CA	CC	AC	GG	GG	TC	GG	GG	CC	AA
1010	CT	CA	CC	AA	GG	GC	CC	AA	GG	CT	AC
1011	TT	CC	CC	CC	GG	GC	TC	AG	GG	CC	CC
1012	TT	CC	CC	CC	GG	GC	TC	AA	GG	CT	AA
1013	CC	CC	AA	CC	GA	CC	TC	AA	GG	CT	AC
1014	CT	CC	CC	AC	GG	GG	TT	AG	GG	CC	CC
1015	TT	CC	CC	AC	GA	GG	TC	AG	GC	CC	AC
1016	CT	CC	CA	AC	GG	GC	TC	AA	GG	CT	AC
1017	TT	CC	CC	AC	GG	GG	CC	AG	GG	CT	AC
1018	CT	CA	CC	AC	GG	GG	CC	AG	GG	CT	AA
1019	CT	CA	CC	AC	GG	GG	CC	AA	GC	CC	AA
1020	CT	CC	CA	AC	GG	GC	TC	AA	GG	CC	AA
1022	CC	AA	CC	AC	GG	GG	TC	AA	GG	CT	AC
1023	TT	CC	CC	AC	GG	GG	TC	AG	GG	TT	AC
1024	CC	CA	CA	AA	GG	GG	CC	AA	GG	CC	AC
1025	TT	CC	CC	AC	GG	GG	CC	AG	GG	CC	AA
1026	CT	CC	CA	CC	GG	GG	CC	AA	GG	CC	AC
1027	CT	CA	CC	AA	GA	GC	TC	AA	GG	CC	AC
1028	CT	CA	CC	AC	GG	GG	CC	AG	GG	CC	AA
1029	CC	CA	CA	CC	GG	GG	TC	AA	GG	CT	AA
1031	CT	CA	CC	AC	GG	GG	CC	AA	GG	CC	AC
1032	TT	CC	CC	CC	GA	GC	TC	AG	GC	CC	AC
1033	CT	CA	CC	CC	GG	GG	CC	AA	GC	TT	AA
1034	CT	CC	CA	AA	GG	GG	TC	AG	GG	CT	AC
1035	CT	CA	CC	CC	GG	GG	CC	AA	CC	CC	CC
1036	TT	CC	CC	AA	GG	GC	TC	AA	GG	CC	AC
1037	TT	CC	CC	CC	GG	GC	TC	AG	GC	CC	AA
1038	CT	CA	CC	AC	GG	GG	CC	AG	GG	CC	AA
1039	CT	CC	CA	AA	GG	GG	TT	AA	GC	CC	CC
1040	TT	CC	CC	AC	GG	GG	TC	AA	GG	TT	AC

Appendix

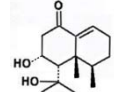
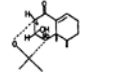
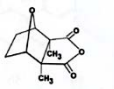
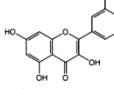
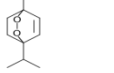
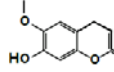
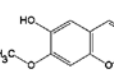
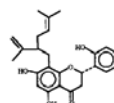
Lab	ERCC1	ERCC1	ERCC1	ERCC2	ERCC4	ERCC5	ERCC5	ERCC6	ERCC6	RAD23B	XPC
no.	Asn118Asn	C8092A	IVS5+33	Arg156Arg	Arg415Gln	Asp1104His	His46His	Arg1213Gly	Arg1230Pro	Ala249Val	Lys939Gln
1041	CC	CA	CA	AC	GG	GG	CC	AA	GG	CC	AA
1042	TT	CC	CC	AC	GG	GC	TC	AA	GG	CC	AA
1043	TT	CC	CC	AA	GA	GC	TC	AG	GG	CC	AC
1044	CC	AA	CC	CC	GG	GG	TC	AA	GC	CC	CC
1045	CT	CA	CC	AA	GA	GG	CC	AA	GG	CC	CC
1048	TT	CC	CC	AC	GG	GC	TC	AA	GG	CC	AA
1050	CC	CC	AA	CC	GG	GG	CC	AG	GG	CT	AC
1051	CT	CA	CC	CC	GG	GC	TT	AA	GC	CC	AC
1052	TT	CC	CC	AA	GG	GG	TC	AA	GG	CC	AC
1053	CT	CC	CA	AA	GA	GC	TC	AG	GG	CC	AC
1054	CT	CA	CC	CC	GG	GC	TT	AA	GG	CT	AC
1056	TT	CC	CC	AC	GG	GG	CC	AA	GG	CC	AA
1057	TT	CC	CC	AA	GG	GC	TC	AA	GG	CC	AA
1058	CC	CA	CA	CC	GG	GC	TC	AA	GG	CC	AC
1061	CT	CC	CA	CC	GG	GG	TC	AA	GC	CC	CC
1062	CT	CA	CC	CC	GG	GC	TC	AG	GG	CC	AC
1063	CC	CA	CA	AC	GG	GG	CC	AG	GG	CC	CC
1064	CT	CC	CA	CC	GA	GC	TT	AG	GC	CC	CC
1065	CC	AA	CC	CC	GG	GC	TT	AA	GG	CT	AC
1066	CT	CA	CC	CC	GA	GG	TC	AG	GG	CC	AA
1071	TT	CC	CC	AA	GG	GG	TC	AG	GG	TT	AA
1072	TT	CC	CC	AC	GA	GG	CC	AG	GG	CT	AA
1073	CT	CC	CA	CC	GA	GC	TC	AG	GG	CC	AA

8. 2. Traditional Chinese medicine compounds

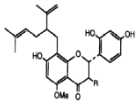
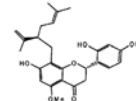
Table.8.2. TCM drugs and their solvents.

No.	code	Name/code from another project	CAS-no.	mole mass (g/mol)	Chemical formula	Molecular structure	Stock solution / solubility
1	TCM-1-RAB	Artesunate	83507-69-1	384	C ₁₉ H ₂₈ O ₈		2 mg in 500 µl DMSO, then add 500 µl water
2	TCM-2-RAB	Puerarin	3681-99-0	416	C ₂₁ H ₂₀ O ₉		2 mg in 1 ml water under heating
3	TCM-4-RAB	Baicalein	491-67-8	270	C ₁₅ H ₁₀ O ₅		2 mg in 1ml EtOH under heating, then add 1 ml water
4	TCM-5-RAB	Baicalin	21967-41-9	446	C ₂₁ H ₁₈ O ₁₁		2 mg in 1ml EtOH under heating, then add 1 ml water
5	TCM-6-RAB	Nardosinon	23720-80-1	250	C ₁₅ H ₂₂ O ₃		2 mg in 100 µl EtOH under heating, then add 900 µl water
6	TCM-7-RAB	Isonardosinon	27062-01-7	250	C ₁₅ H ₂₂ O ₃		2 mg in 100 µl EtOH under heating, then add 900 µl water

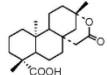
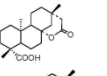
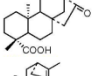
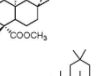
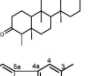
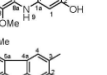
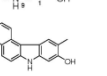
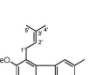
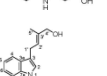
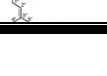
Appendix

No.	code	Name/code from another project	CAS-no.	mole mass (g/mol)	Chemical formula	Molecular structure	Stock solution / solubility
7	TCM-8-RAB	Tetrahydronardosin on	-	252	C ₁₅ H ₂₄ O ₃		2 mg in 100 µl EtOH under heating, then add 900 µl water
8	TCM-9-RAB	Nardofuran	42438-76-6	250	C ₁₅ H ₂₂ O ₃		2 mg in 500 µl DMSO, then add 500 µl water
9	TCM-11-RAB	Cantharidin	56-25-7	196	C ₁₀ H ₁₂ O ₄		2 mg in 500 µl DMSO, then add 500 µl water
10	TCM-12-RAB	Arsenic trioxide	1327-53-3	198	As ₂ O ₃		1 mg / ml PBS
11	TCM-13-RAB	Quercetin	117-39-5	338	C ₁₅ H ₁₀ O ₇		2 mg in 100 µl NaOH under heating, then add 900 µl water
12	TCM-15-RAB	Ascaridol	512-85-6	168	C ₁₀ H ₁₆ O ₂		1 mg / ml DMSO
13	TCM-16-RAB	Scopoletin	92-61-5	193	C ₁₀ H ₈ O ₄		2 mg / ml DMSO
14	TCM-17-RAB	Isoscopoletin	776-86-3	193	C ₁₀ H ₈ O ₄		2 mg / ml DMSO
15	TCM-19-RAB	Sophoraflavon G	-	424	C ₂₅ H ₂₈ O ₆		2 mg / ml DMSO

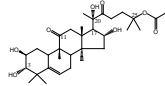
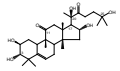
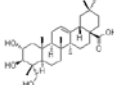
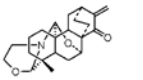
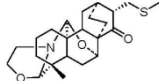
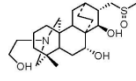
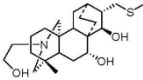
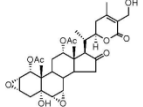
Appendix

No.	code	Name/code from another project	CAS-no.	mole mass (g/mol)	Chemical formula	Molecular structure	Stock solution / solubility
16	TCM-20-RAB	Kushenol I	99119-69-4	438	C ₂₅ H ₂₆ O ₇		2 mg / ml DMSO
17	TCM-21-RAB	Kurarion	34981-26-5	438	C ₂₆ H ₃₀ O ₆		2 mg / ml DMSO
18	TCM-22-RAB	Norkurarinol	-	424	C ₂₅ H ₂₈ O ₇		2 mg / ml DMSO
19	TCM-23-RAB	2'-Methoxykurarinone	-	452	C ₂₇ H ₃₂ O ₆		2 mg / ml DMSO
20	TCM-24-RAB	TCM-221B	-	-	-	Under investigation	1 mg / ml DMSO
21	TCM-25-RAB	TCM-222B	-	-	-	Under investigation	1 mg / ml DMSO
22	TCM-26-RAB	TCM-224B	-	-	-	Under investigation	1 mg / ml DMSO
23	TCM-27-RAB	TCM-225B	-	-	-	Under investigation	1 mg / ml DMSO
24	TCM-29-RAB	TCM-227B	-	-	-	Under investigation	1 mg / ml DMSO
25	TCM-30-RAB	TCM-228B	-	-	-	Under investigation	1 mg / ml DMSO
26	TCM-31-RAB	TCM-229B	-	-	-	Under investigation	1 mg / ml DMSO

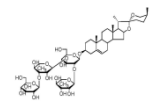
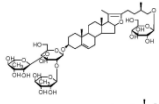
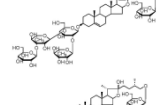
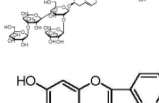
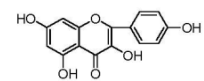
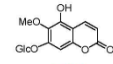
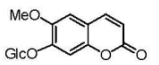
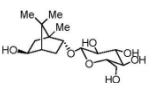
Appendix

No.	code	Name/code from another project	CAS-no.	mole mass (g/mol)	Chemical formula	Molecular structure	Stock solution / solubility
27	TCM-32-RAB	TCM-230B	-	-	-	Under investigation	1 mg / ml DMSO
28	TCM-33-RAB	TCM-231B	-	-	-	Under investigation	1 mg / ml DMSO
29	TCM-34-RAB	KIB-LIU-001	-	334	C ₂₀ H ₃₀ O ₄		12 mg / ml DMSO
30	TCM-35-RAB	KIB-LIU-002	-	334	C ₂₀ H ₃₀ O ₄		12 mg / ml DMSO
31	TCM-38-RAB	KIB-LIU-005	-	318	C ₂₀ H ₃₀ O ₃		12 mg / ml DMSO
32	TCM-41-RAB	KIB-LIU-008	-	316	C ₂₁ H ₃₂ O ₂		4 mg / ml DMSO
33	TCM-42-RAB	HGM1	-	426	C ₃₀ H ₅₀ O		1 mg / ml DMSO
34	TCM-44-RAB	HGM3	-	227	C ₁₄ H ₁₃ NO ₂		0.5 mg / ml DMSO
35	TCM-47-RAB	HGM4	-	227	C ₁₄ H ₁₃ NO ₂		12 mg / ml DMSO
36	TCM-48-RAB	HGM5	-	279	C ₁₈ H ₁₇ NO ₂		12 mg / ml DMSO
37	TCM-49-RAB	HGM7	-	295	C ₁₉ H ₂₁ NO ₂		12 mg / ml DMSO
38	TCM-50-RAB	HGM8	-	269	C ₁₈ H ₂₃ NO		12 mg / ml DMSO

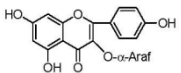
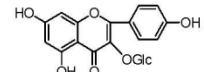
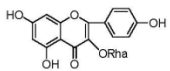
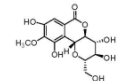
Appendix

No.	code	Name/code from another project	CAS-no.	mole mass (g/mol)	Chemical formula	Molecular structure	Stock solution / solubility
39	TCM-51-RAB	25-O-Acetyl-23,24-dihydrocucurbitacin F	-	560	C ₃₂ H ₄₇ O ₈		2 mg / ml DMSO
40	TCM-52-RAB	23,24-Dihydrocucurbitacin F	-	521	C ₃₀ H ₄₈ O ₇		2 mg / ml DMSO
41	TCM-53-RAB	Arjunolic acid	465-00-9	489	C ₃₀ H ₄₈ O ₅		2 mg / ml DMSO
42	TCM-54-RAB	KIB-LIU9	-	335	C ₂₂ H ₂₉ NO ₃		4 mg / ml DMSO
43	TCM-55-RAB	KIB-LIU10	-	403	C ₂₃ H ₃₃ NO ₃ S		4 mg / ml DMSO
44	TCM-56-RAB	KIB-LIU11	-	425	C ₂₃ H ₃₉ NO ₄ S		4 mg / ml DMSO
45	TCM-57-RAB	KIB-LIU12	-	409	C ₂₃ H ₃₉ NO ₃ S		2 mg / ml DMSO
46	TCM-58-RAB	KIB-LIU13	-	602	C ₃₂ H ₄₂ O ₁₁		2 mg / ml DMSO

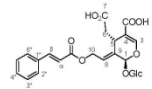
Appendix

No.	code	Name/code from another project	CAS-no.	mole mass (g/mol)	Chemical formula	Molecular structure	Stock solution / solubility
47	TCM-59-RAB	KIB-LIU14	-	1030	C ₅₁ H ₈₂ O ₂₁		2 mg / ml DMSO
48	TCM-60-RAB	KIB-LIU15	-	1030	C ₅₁ H ₈₂ O ₂₁		2 mg / ml DMSO
49	TCM-61-RAB	KIB-LIU16	-	1192	C ₅₇ H ₉₂ O ₂₆		2 mg / ml DMSO
50	TCM-62-RAB	KIB-LIU17	-	1210	C ₅₇ H ₉₄ O ₂₇		4 mg / ml DMSO
51	TCM-71-RAB	WYF-1	-	-	-		2 mg / ml DMSO
52	TCM-72-RAB	WYF-3	-	-	-		2 mg / ml DMSO
53	TCM-73-RAB	WYF-5	-	-	-		2 mg / ml DMSO
54	TCM-74-RAB	WYF-6	-	-	-		2 mg / ml DMSO

Appendix

No.	code	Name/code from another project	CAS-no.	mole mass (g/mol)	Chemical formula	Molecular structure	Stock solution / solubility
55	TCM-75-RAB	WYF-7	-	-	-		2 mg / ml DMSO
56	TCM-77-RAB	WYF-9	-	-	-		2 mg / ml DMSO
57	TCM-78-RAB	WYF-10	-	-	-		2 mg / ml DMSO
58	TCM-79-RAB	WYF-11	-	-	-		2 mg / ml DMSO
59	TCM-81-RAB	WYF-13	The <i>n</i> -BuOH fraction of EtOH extract from <i>Ardisia Solanacea</i>				2.5 mg / 1.25 ml DMSO
60	TCM-83-RAB	LGF-1	-	-	-	Under investigation	2 mg / ml DMSO
61	TCM-84-RAB	LGF-2	-	-	-	Under investigation	2 mg / ml DMSO
62	TCM-85-RAB	LGF-3	-	-	-	Under investigation	2 mg / ml DMSO
63	TCM-86-RAB	LGF-4	-	-	-		2 mg / ml DMSO

Appendix

No.	code	Name/code from another project	CAS-no.	mole mass (g/mol)	Chemical formula	Molecular structure	Stock solution / solubility
64	TCM-87-RAB	LGF-5	-	-	-		2 mg / ml DMSO
65	TCM-88-RAB	LGF-6	-	-	-	Under investigation	2 mg / ml DMSO
66	TCM-89-RAB	LGF-7	-	-	-		2 mg / ml DMSO
67	TCM-90-RAB	LGF-9	-	-	-		2 mg / ml DMSO
68	TCM-91-RAB	LGF-10	-	-	-	Under investigation	2 mg / ml DMSO
69	TCM-92-RAB	LGF-11	-	-	-	Under investigation	2 mg / ml DMSO
70	TCM-93-RAB	LGF-12	-	-	-	Under investigation	2 mg / ml DMSO
71	TCM-94-RAB	LGF-13	-	-	-		2 mg / ml DMSO
72	TCM-95-RAB	LGF-14	The <i>n</i> -BuOH fraction of EtOH extract from <i>Homalomena occulta</i>				1.3 mg / 650 μ l DMSO
73	TCM-S1-RAB	water					
74	TCM-S2-RAB	PBS					
75	TCM-S3-RAB	DMSO					
76	TCM-S4-RAB	10% NaOH					
77	TCM-S5-RAB	50% DMSO					

Appendix

No.	code	Name/code from another project	CAS-no.	mole mass (g/mol)	Chemical formula	Molecular structure	Stock solution / solubility
78	TCM-S6-RAB	50% EtOH					
79	TCM-S7-RAB	10% EtOH					
80	TCM-S8-RAB	30% EtOH					



Acknowledgements

I'm grateful to Almighty ALLAH for helping and enabling me to complete the thesis.

I would like to appreciate and thank PD Dr. Odilia Popanda and Dr. Peter Schmezer for their guidance throughout my PhD. Without their help and support I would not have been able to organize and complete this thesis. I am also thankful to Prof. Thomas Efferth for giving me the opportunity to work on this interesting project as well as for his guidance and help.

I also thank Dr. Christoph Plass for providing me with the opportunity to work on my PhD thesis in the Division of Epigenomics and Cancer Risk Factors at Deutsches Krebsforschungszentrum (DKFZ) in Heidelberg.

I am also thankful to PD Dr. Rajiv Kumar (Division of Molecular Genetic Epidemiology, DKFZ) and Prof. Dr. Michael Wink (Institut für Pharmazie und Molekulare Biotechnologie, Abteilung Biologie, University of Heidelberg) for their keen interest and valuable comments.

Special thanks to Maria Timofeeva, Julia Strathmann, Karin Klimo and Sabine Behrens (Division of Cancer Epidemiology, DKFZ) for their help in experimental and statistical analysis.

I am also grateful to all the participants of larynx cancer case control study. I am grateful to Prof. H. Becher and Dr. H. Ramroth (Department of Tropical Hygiene and Public Health, University of Heidelberg) for their help with the larynx cancer study and the statistical analysis. I would also like to mention Prof. A. Dietz, Prof. Dr. H. Weidauer, Prof. Dr. P. Plinkert, Prof. Dr. K. Hörmann, Prof. Dr. K. Reck, Prof. Dr. K.-W. Delank, Prof. Dr. C. Naumann and Prof. Dr. B. Lippert for their participation in larynx cancer study. Our collaborator for TCM project was Prof. X. Hao (Kunming Institute of Botany, the Chinese Academy of Sciences, Kunming, China).

I acknowledge support by the Higher Education Commission (HEC), Pakistan and DAAD.

I also wish to thank my lab fellows, Jitti, Sebastian, Lea, Céline, Peter, Otto, Reini, Claudia, Katrin and Andreas (DNA Repair and Epigenomics, DKFZ) for their excellent

moral and technical support. Special thanks to Christine for the help with Zusammenfassung.

I would like to express gratitude to my family. Special thanks to my parents from the depth of my heart for all their love and prayers, my brothers Mann, Mohib and Navid for the support, my sweet nieces Guria, Marium and Muniba for filling my life with color and hubby dear Nafees for all the understanding and care. I want to thank my Grandma, my in-laws, my aunts, uncles, all my cousins and Sobia for their wishes. Thanks to all my friends Nusrat, Azima, Behjat, Uzma, Saba, Kiran, to name some of them.

At the end, I would also like to remember my old friends who are long gone, for they helped me to become what I am today.

جزاك الله خير

'May Allah grant you goodness'

Curriculum Vitae

Personal Information

Name	Rashda Abbasi
Father's name	Ejaz Ahmad Abbasi
Date of birth	2 nd July 1976
Marital status	Married
NIC #	37405-3586115-0
Nationality	Pakistani

Honors and Awards:

- ✚ **2nd Best poster** prize, PhD retreat 2008, Weil der Stadt, Germany.
- ✚ **Overseas Scholarships Scheme for PhD in Selected Fields in Germany** by DAAD-HEC.
- ✚ First position in faculty of sciences in M.Sc. (1997 - 1999) **Silver Medal**.
- ✚ First position in department of Zoology (M. Sc.) in University of Arid Agriculture.
- ✚ Won the Fauji Foundation academic distinction award, 2000.

Education and Research Experience

- ✚ **2006 - 2009**, Division of Epigenomics and Cancer Risk Factors, Deutsches Krebsforschungszentrum (DKFZ) in the Helmholtz Association. **PhD candidate**, Thesis title 'Nucleotide excision repair pathway modulating both cancer risk and therapy'. First supervisor: Prof. Dr. T. Efferth. Worked under the supervision of Prof. Dr. O. Popanda, Dr. P. Schmezer and Prof. Dr. Christoph Plass.
- ✚ **2002 - 2005**, As **Scientific Officer** in Biomedical and Genetic Engineering Division, KRL, Islamabad, Pakistan.

- ✚ **2001 - 2002**, worked as senior section **teacher** in Bismah Army Public School, Hamza Camp, Rawalpindi, Pakistan.
- ✚ **1999 - 2001**, Quaid-i-Azam Uni. Islamabad, Pakistan. **M. Phil scholar**, Dissertation title 'Study of Genetic Disorders in Pakistani Families (Deafness)'. Supervisor: Dr. SA. Shami, external supervisor: Dr. R. Qamar, BnGE Div. KRL Islamabad, Pakistan. 'CGPA 4.1/5.00'.
- ✚ **1997 - 1999**, University of Arid Agriculture, Rawalpindi, Pakistan. **MSc student**, Report title 'Effect of Genotype on quality of Bovine Semen'. Supervisor: Dr. Z. Hussain, external supervisor: Dr. N. Ahmad, NARC, Islamabad, Pakistan 'CGPA 3.94/4.00'.
- ✚ **1995 - 1997**, Govt. College for Women, 6th road, Rawalpindi. **BSc student**. Subjects: Zoology, Botany, Chemistry.
- ✚ **1992 - 1995**, Govt. College for Women, 6th road, Rawalpindi. Higher Secondary School (**HSSC**). Subjects: Pre-Medical.
- ✚ **Before 1992**, Rawalpindi Grammar School, Rawalpindi. Secondary School (**SSC**). Subjects: Science.

Previous publications

- ✚ Forshew T, Johnson CA, Khaliq S, Pasha S, Willis C, **Abbasi R**, Tee L, Smith U, Trembath RC, Mehdi SQ, Moore AT, Maher ER. Locus heterogeneity in autosomal recessive congenital cataracts: linkage to 9q and germline HSF4 mutations. Hum Genet. 2005 Sep;117(5):452-9. Epub 2005 Jun 16.
- ✚ **Abbasi R**, Shami SA, Qamar R, Ayub Q, Khaliq S. A Pakistani family with Autosomal recessive sensorineural hearing loss linked to DFNB7/11. (2001). American Journal of Medical Genetics (Abstract).

Conferences / retreats attended.

- ✚ 10th Biennial Meeting of the Deutsche Gesellschaft für DNA-Reparaturforschung (2nd to 5th September 2008), Berlin.
- ✚ Heidelberg Forum for young life scientists (10th to 11th September 2009), Heidelberg, Germany.

✚ PhD retreat 2007, Weil der Stadt, Germany.

✚ PhD retreat 2008, Weil der Stadt, Germany.

Social activities

✚ Member of the **PhD retreat committee 2008** held in Weil der Stadt, Germany

✚ Member of German DNA repair society '**Deutsche Gesellschaft für DNA-Reparaturforschung (DGDR)**'.



Publications from thesis

- ✚ **Abbasi R**, Ramroth H, Becher H, Dietz A, Schmezer P, & Popanda O (2009). Laryngeal cancer risk associated with smoking and alcohol consumption is modified by genetic polymorphisms in ERCC5, ERCC6, and RAD23B but not by polymorphisms in five other nucleotide excision repair genes. *Int J Cancer* **125**, 1431-1439.
- ✚ **Abbasi R**, Ramroth H, Becher H, Dietz A, Schmezer P, & Popanda O (**Poster**). Laryngeal cancer risk associated with smoking and alcohol consumption is modified by genetic polymorphisms in the nucleotide excision repair genes ERCC6 and RAD23B. *10th Biennial Meeting of the Deutsche Gesellschaft für DNA-Reparaturforschung*, 2nd to 5th September 2008, Berlin, Germany.
- ✚ **Abbasi R**, Ramroth H, Becher H, Dietz A, Schmezer P, & Popanda O (**Poster**). Laryngeal cancer risk associated with smoking and alcohol consumption is modified by genetic polymorphisms in the nucleotide excision repair genes ERCC6 and RAD23B. *Heidelberg Forum for young life scientists*, 10th to 11th September 2009, Heidelberg, Germany.
- ✚ R. Abbasi, H. Ramroth, H. Becher, A. Dietz, P. Schmezer and O. Popanda, (**Poster**). Laryngeal cancer risk associated with smoking and alcohol consumption is modified by genetic polymorphisms in the nucleotide excision repair genes ERCC6 and RAD23B. *PhD Retreat*, 24th to 27th July 2008, Weil der Stadt, Germany.
- ✚ **Abbasi R**, Becher H, Ramroth H, Dietz A, Popanda O, & Schmezer P (**Talk**). Nucleotide excision repair as an important pathway influencing laryngeal cancer risk. *PhD Retreat*, 22nd to 24th July 2007, Weil der Stadt, Germany.





